

## University of Southampton Research Repository

Copyright © and Moral Rights for this thesis and, where applicable, any accompanying data are retained by the author and/or other copyright owners. A copy can be downloaded for personal non-commercial research or study, without prior permission or charge. This thesis and the accompanying data cannot be reproduced or quoted extensively from without first obtaining permission in writing from the copyright holder/s. The content of the thesis and accompanying research data (where applicable) must not be changed in any way or sold commercially in any format or medium without the formal permission of the copyright holder/s.

When referring to this thesis and any accompanying data, full bibliographic details must be given, e.g.

Thesis: Author (Year of Submission) "Full thesis title", University of Southampton, name of the University Faculty or School or Department, PhD Thesis, pagination.

Data: Author (Year) Title. URI [dataset]



UNIVERSITY OF SOUTHAMPTON  
FACULTY OF SOCIAL SCIENCES  
SOUTHAMPTON BUSINESS SCHOOL

# Essays on Memory and Dynamics of Connectedness in Bitcoin Markets

by  
Ahmad Maaitah

A thesis submitted for the degree of  
Doctor of Philosophy in Management Science

August 2020



UNIVERSITY OF SOUTHAMPTON  
FACULTY OF SOCIAL SCIENCES  
SOUTHAMPTON BUSINESS SCHOOL

# Essays on Memory and Dynamics of Connectedness in Bitcoin Markets

by

Ahmad Maaitah

Main Supervisor: Professor Tapas Mishra  
Supervisor: Professor Simon Wolfe

A thesis submitted for the degree of  
Doctor of Philosophy in Business Studies and Management

August 2020



UNIVERSITY OF SOUTHAMPTON

## Abstract

FACULTY OF SOCIAL SCIENCES  
SOUTHAMPTON BUSINESS SCHOOL

Doctor of Philosophy

by Ahmad Maaitah

This thesis sheds new light on the exogenous and endogenous determinants of volatility in Bitcoin prices across many major countries around the globe. Different empirical strategies are proposed to investigate and understand the complex behaviour of volatility, its movements and significant persistence. Chapter Two identifies and characterises the ‘givers and receivers’ of volatility in cross-market Bitcoin prices and discusses international diversification strategies in this context. Using both time and frequency domain mechanisms, we provide estimates of outward and inward spillover effects. These have implications for (weak-form) cross-market inefficiency. In our setting, we treat a high degree of spillover as an indicator of weak-form inefficiency, because investors can utilise information on the dynamic spillover effects to produce best long-run predictions of the market. Our results show that Bitcoin prices depict strong (dynamic) spillover in volatility, especially during episodes of high uncertainty. The Bitcoin-USD exchange rate possesses net predictive power, mirrored by the tendency of the Bitcoin-EURO market as a net receiver relative to other markets. Robustness exercise generally supports our claim. The overall implication is that during episodes of high uncertainty, Bitcoin markets depict greater dynamic inefficiency, instrumenting the role of asymmetric information in the path-dependence and predictive power of Bitcoin prices in an interdependent market.

Chapter Three investigates the endogenous growth mechanisms of Bitcoin prices aligned with empirical tests designed to show whether persistence is a product of such a model. However, characterising learning in the Bitcoin market is exceedingly complex, as it is frequently affected by news and/or economic/financial dynamics. Sudden arrival of a shock (for instance, Brexit) can break the cycle of endogenous persistence generating mechanisms. We propose a variant of ARFIMA Markov Switching, with endogenous switch governing the internal dynamics of Bitcoin prices or volatility system. This MS-ARFIMA (endogenous) is synchronised with different mechanisms and shows the credible role of policy on containing volatility persistence. Our model and empirical strategies are new, and our results show the significance of true memory under episodes of structural breaks.

Chapter Four studies Bitcoin prices/volatility during cyber attacks and identifies how they can be seriously manipulated in some markets. In the meantime, exchange rate differentials across markets offer investors the opportunity to enhance portfolio returns. Under these scenarios, it is expected that price volatility on one particular Bitcoin-to-currency exchange market (e.g. Bitcoin-USD) can flow to other markets and can also be acquired from others. Any quantitative information on the centrality or relative isolation of some Bitcoin-to-currency markets can actually help investors to better anticipate their complex dynamic behaviour and exploit potential for forecast-able gain. These premises are rigorously tested in the current paper, using daily price data on six major Bitcoin-to-currency exchange rates. We show the net predictive power and the net receiver of volatility during different cyber attacks. Eventually, such tendencies could help investors design trending strategies to systematically beat the market, hedging and diversifying their investment to maximise profit with the lowest associated risk, and speculating on the behaviour of the market in future attacks.

# Contents

<b>Abstract</b>	<b>v</b>
<b>List of Figures</b>	<b>xi</b>
<b>List of Tables</b>	<b>xv</b>
<b>Declaration of Authorship</b>	<b>xix</b>
<b>Acknowledgements</b>	<b>xxi</b>
<b>1 Introduction</b>	<b>1</b>
1.1 Research context . . . . .	2
1.2 Research aims . . . . .	4
1.3 Research objectives . . . . .	5
1.4 General Literature Review and Contributions . . . . .	6
1.5 A schematic representation of the thesis . . . . .	9
<b>2 Giver and the Receiver: Understanding Spillover Effects and Predictive Power in Cross-market Bitcoin Prices</b>	<b>11</b>
2.1 Introduction . . . . .	12
2.2 Literature review . . . . .	14
2.2.1 The volatility Spillover definition . . . . .	14
2.2.2 Volatility Spillover theories . . . . .	15
2.2.2.1 Heat waves and Meteor showers . . . . .	15
2.2.3 Empirical review . . . . .	17
2.2.4 Critical evaluation of research strategies . . . . .	22
2.2.4.1 GARCH model . . . . .	22
2.2.4.2 Vector Auto-regression (VAR) method . . . . .	23
2.2.4.3 Conclusion . . . . .	24
2.3 Data and summary statistics . . . . .	24
2.4 Methodology . . . . .	29
2.5 Results . . . . .	32
2.5.1 Volatility spillovers . . . . .	32
2.5.1.1 Directional connectedness (static spillovers): Time domain analysis . . . . .	33
2.5.1.2 Frequency domain analysis of static spillovers . . . . .	34
2.5.1.3 Dynamic spillover effects: Rolling window estimates . . . . .	35
2.5.2 Returns spillovers . . . . .	40

2.5.2.1	Directional connectedness (static spillovers): Time domain analysis . . . . .	40
2.5.2.2	Frequency domain analysis of static spillovers . . . . .	41
2.5.2.3	Rolling windows analysis (dynamic spillover plots) . . . . .	43
2.5.3	Robustness . . . . .	48
2.5.3.1	Sensitivity to forecast horizon and window size for static and dynamic spillover system . . . . .	48
2.5.3.2	Alternative measures of volatility . . . . .	48
2.5.3.3	VAR model Stability . . . . .	51
2.6	Conclusions . . . . .	53
<b>3</b>	<b>The Relevance of Memory and Efficiency in Endogenously Switching Cross-market Bitcoin Prices</b>	<b>63</b>
3.1	Introduction . . . . .	64
3.2	Literature review. . . . .	67
3.2.1	Modelling the breakpoints in Moving average process . . . . .	69
3.2.2	Modelling the breakpoints in Auto-regressive model AR . . . . .	71
3.2.3	Modelling the long memory (Fractional integration) . . . . .	73
3.2.4	Modelling structural breaks with ARFIMA process . . . . .	75
3.2.5	Review of the Cryptocurrency literature . . . . .	78
3.3	Empirical Methodology . . . . .	80
3.3.1	Markov Switching Auto-regressive Model MS-AR . . . . .	80
3.3.2	Markov Switching Auto-regressive moving Average MS-ARMA . .	82
3.3.3	Markov-Switching Auto-regressive Fractional Integral Moving Average MS-ARFIMA . . . . .	83
3.4	Data and estimation results . . . . .	85
3.4.1	Data . . . . .	85
3.4.2	Summary statistics . . . . .	86
3.4.3	Stationarity and the presence of long memory . . . . .	88
3.5	Discussion of results . . . . .	89
3.5.1	Structural Breaks . . . . .	90
3.5.2	Fractional Integration . . . . .	92
3.5.3	MS-ARFIMA model . . . . .	97
3.5.4	Robustness . . . . .	104
3.6	Conclusions . . . . .	109
<b>4</b>	<b>Dynamic Co-movements and Cyberattacks in Cross-market Bitcoin Prices: Spillover and Variance Decomposition of Network Topology</b>	<b>111</b>
4.1	Introduction . . . . .	113
4.2	Literature review . . . . .	115
4.3	Data and summary statistics . . . . .	118
4.4	Methodology . . . . .	121
4.5	Results . . . . .	124
4.5.1	Static connectedness . . . . .	124
4.5.2	Dynamic connectedness . . . . .	125
4.5.3	Network Analysis of variance decomposition . . . . .	128
4.5.4	Robustness . . . . .	133

4.5.4.1	VAR model Stability . . . . .	133
4.6	Conclusions . . . . .	134
<b>5</b>	<b>Conclusions</b>	<b>137</b>
5.1	Conclusion and Policy Implications . . . . .	138
5.2	Future Research Directions . . . . .	139
<b>A</b>	<b>Supplement to Chapter 2</b>	<b>141</b>
<b>B</b>	<b>Supplement to Chapter 3</b>	<b>173</b>
<b>C</b>	<b>Supplement to Chapter 4</b>	<b>191</b>



# List of Figures

2.1	Exchange rate returns . . . . .	27
2.2	Exchange rate volatility . . . . .	28
2.3	Overall volatility spillovers (dynamic plot) and Economic Policy Uncertainty Index . . . . .	36
2.4	Volatility spillovers to others: Dynamic plot . . . . .	37
2.5	Volatility spillovers from others: Dynamic plot . . . . .	38
2.6	Net volatility spillovers: Dynamic plot . . . . .	39
2.7	Overall returns spillovers (dynamic plot) and Economic Policy Uncertainty Index . . . . .	43
2.8	Returns spillovers to others, dynamic plot . . . . .	45
2.9	Returns spillovers from others, dynamic plot . . . . .	46
2.10	Net returns spillovers, dynamic plot . . . . .	47
2.11	Overall returns spillovers (dynamic plot – 15-day ahead forecast) and Economic Policy Uncertainty Index . . . . .	49
2.12	Overall returns spillovers (dynamic plot – 60-day ahead forecast) and Economic Policy Uncertainty Index . . . . .	50
2.13	Overall volatility spillovers (dynamic plot – 15-day ahead forecast) and Economic Policy Uncertainty Index . . . . .	51
2.14	Overall volatility spillovers (dynamic plot – 60-day ahead forecast) and Economic Policy Uncertainty Index . . . . .	52
2.15	Comparison of GK and Parkinson Volatility Plots . . . . .	55
2.16	Overall volatility spillovers (dynamic plot): Garman-Klass volatility measure . . . . .	57
2.17	Volatility spillovers from others, dynamic plot: Garman-Klass volatility measure . . . . .	58
2.18	Volatility spillovers to others, dynamic plot: Garman-Klass volatility measure . . . . .	59
2.19	Net volatility spillovers, dynamic plot . . . . .	60
3.1	Bitcoin daily volatility of five markets . . . . .	87
3.2	Estimated breaks in the volatility of Bitcoin exchange markets (Bai and Perron) . . . . .	93
3.3	The rolling windows of estimated "d" in Bitcoin markets. . . . .	96
3.4	Bitcoin exchange rates and the path of estimated switching in the mean of volatility . . . . .	100
3.5	Bitcoin Exchange rates volatility and the estimated value of ARFIMA process . . . . .	102
3.6	Bitcoin Exchange rates volatility and the estimated values of MS-ARFIMA model . . . . .	103

---

3.7	The Bitcoin daily return-volatility of the five markets . . . . .	105
3.8	Estimated breaks in the daily return volatility of Bitcoin ex- change markets (Bai and Perron) . . . . .	106
3.9	Bitcoin exchange rates and the path of estimated switching in the mean of return volatility . . . . .	107
4.1	Volatility Exchange Rates . . . . .	120
4.2	Net pairwise directional networks. . . . .	123
4.3	Overall volatility spillovers (dynamic plot) . . . . .	127
4.4	Directional-volatility connectedness network, 22/06/2015 . . . . .	129
4.5	Directional-volatility connectedness network, 02/08/2016 . . . . .	130
4.6	Directional-volatility connectedness network, 06/12/2017 . . . . .	131
4.7	Directional-volatility connectedness network, 20/09/2018 . . . . .	132
4.8	Directional-volatility connectedness network, 07/05/2019 . . . . .	132
A.1	. . . . .	171
A.2	. . . . .	172
B.1	The Rolling Windows of the estimated "d" parameter and the rolling windows of "rolled d " in BTC/USD market . . . . .	173
B.2	The Rolling Windows of the estimated "d" parameter and the rolling windows of "rolled d " in BTC/EUR market . . . . .	174
B.3	The Rolling Windows of the estimated "d" parameter and the rolling windows of "rolled d " in BTC/GBP market . . . . .	175
B.4	The Rolling Windows of the estimated "d" parameter and the rolling windows of "rolled d " in BTC/AUD market . . . . .	176
B.5	The Rolling Windows of the estimated "d" parameter and the rolling windows of "rolled d " in BTC/CAD market . . . . .	177
B.6	BTC/USD Exchange rates return volatility and the estimated values of ARFIMA model . . . . .	184
B.7	BTC/EUR Exchange rates return volatility and the estimated values of ARFIMA model . . . . .	185
B.8	BTC/GBP Exchange rates return volatility and the estimated values of ARFIMA model . . . . .	186
B.9	BTC/AUD Exchange rates return volatility and the estimated values of ARFIMA model . . . . .	187
B.10	BTC/CAD Exchange rates return volatility and the estimated values of ARFIMA model . . . . .	188
B.11	BTC/USD Exchange rates return volatility and the estimated values of MS-ARFIMA model . . . . .	188
B.12	BTC/EUR Exchange rates return volatility and the estimated values of MS-ARFIMA model . . . . .	189
B.13	BTC/GBP Exchange rates return volatility and the estimated values of MS-ARFIMA model . . . . .	189
B.14	BTC/AUD Exchange rates return volatility and the estimated values of MS-ARFIMA model . . . . .	190
B.15	BTC/CAD Exchange rates return volatility and the estimated values of MS-ARFIMA model . . . . .	190

---

C.1	Overall volatility spillovers (dynamic plot), 15-120-Day Rolling Window	193
C.2	Overall volatility spillovers (dynamic plot), 15-150-Day Rolling Window	194
C.3	Overall volatility spillovers (dynamic plot), 15-180-Day Rolling Window	195
C.4	Overall volatility spillovers (dynamic plot), 30-150-Day Rolling Window	196
C.5	Overall volatility spillovers (dynamic plot), 30-180-Day Rolling Window	197
C.6	Overall volatility spillovers (dynamic plot), 60-120-Day Rolling Window	198
C.7	Overall volatility spillovers (dynamic plot), 60-150-Day Rolling Window	199
C.8	Overall volatility spillovers (dynamic plot), 60-180-Day Rolling Window	200
C.9	Volatility spillovers to others, dynamic plot	201
C.10	Volatility spillovers from others, dynamic plot	202
C.11	Net Volatility spillovers, dynamic plot	203
C.12	Directional-volatility connectedness network, 22/05/2015	204
C.13	Directional-volatility connectedness network, 15/02/2016	204
C.14	Directional-volatility connectedness network, 13/10/2016	205
C.15	Directional-volatility connectedness network, 26/04/2017	205
C.16	Directional-volatility connectedness network, 17/05/2017	206
C.17	Directional-volatility connectedness network, 18/12/2017	206
C.18	Directional-volatility connectedness network, 26/12/2017	207
C.19	Directional-volatility connectedness network, 07/01/2018	207
C.20	Directional-volatility connectedness network, 15/02/2018	208
C.21	Directional-volatility connectedness network, 04/03/2018	208
C.22	Directional-volatility connectedness network, 12/04/2018	209
C.23	Directional-volatility connectedness network, 21/12/2018	209
C.24	Directional-volatility connectedness network, 27/12/2018	210
C.25	Directional-volatility connectedness network, 26/01/2019	210
C.26		211



# List of Tables

2.1	Summary statistics, exchange rate returns and volatility . . . . .	26
2.2	Volatility spillovers across five selected exchange rates in time domain . . . . .	33
2.3	Volatility spillovers across five selected exchange rates in frequency domain . . . . .	34
2.4	Returns spillovers across five selected exchange rates . . . . .	41
2.5	Returns spillovers across five selected exchange rates - Frequency domain analysis . . . . .	42
2.6	Different Volatility measures across five selected exchange rates .	54
2.7	Volatility spillovers across five selected exchange rates: Garman-Klass measure . . . . .	56
2.8	Volatility spillovers across five selected exchange rates - Frequency domain analysis: Garman-Klass Measure of Volatility . .	56
2.9	Multivariate Qu and Perron Test for Structural Changes in VAR model . . . . .	61
2.10	ADF Test for the VAR Coefficients' Residuals . . . . .	61
3.1	Summary statistics, exchange rate volatility . . . . .	87
3.2	ADF and KPSS unit root tests, exchange rate volatility . . . . .	89
3.3	Narayan and Popp (2010) Unit Root Test with Multiple Break Points for The Five Bitcoin Markets . . . . .	89
3.4	Estimated breaks in the volatility of Bitcoin exchange markets, (Bai and Perron) test . . . . .	91
3.5	Hansen 1992's Test for Stability of Bitcoin Markets . . . . .	92
3.6	Estimates of Local Whittle (LW) for the volatility of the five BTC markets . . . . .	95
3.7	Estimates of Exact Local Whittle (ELW) for the volatility of the five BTC markets . . . . .	95
3.8	Estimates of Feasible Exact Local Whittle (FELW) for the volatility of the five BTC markets . . . . .	95
3.9	Estimates of Two-step Exact Local Whittle (TSELW) for the volatility of the five BTC markets) . . . . .	95
3.10	Hansen Linearity Test . . . . .	98
3.11	Estimates of MS-ARFIMA model of volatility across the five Bitcoin markets . . . . .	99
3.12	Estimates of Feasible Exact Local Whittle (FELW) for the return volatility of the five BTC markets . . . . .	105
3.13	Estimates of Two-step Exact Local Whittle (TSELW) for the return volatility of the five BTC markets . . . . .	106

3.14	Estimates of MS-ARFIMA model of volatility return across the five Bitcoin markets . . . . .	108
4.1	Summary statistics, exchange rate volatility . . . . .	118
4.2	Connectedness table . . . . .	121
4.3	Volatility spillovers across six selected exchange rates in time domain – 30-day ahead forecast . . . . .	127
4.4	Cyberattcks in Bitcoin Markets . . . . .	129
4.5	Multivariate Qu and Perron Test for Structural Changes in VAR model . . . . .	135
4.6	ADF Test for the VAR Coefficients' Residuals . . . . .	135
A.1	ADF and Phillips-Perron unit root tests, exchange rate returns .	141
A.2	ADF and Phillips-Perron unit root tests, exchange rate volatility	142
A.3	Returns spillovers across five selected exchange rates – 7-day ahead forecast . . . . .	143
A.4	Returns spillovers across five selected exchange rates – 10-day ahead forecast . . . . .	143
A.5	Returns spillovers across five selected exchange rates – 60-day ahead forecast . . . . .	144
A.6	Volatility spillovers across five selected exchange rates – 7-day ahead forecast . . . . .	145
A.7	Volatility spillovers across five selected exchange rates – 10-day ahead forecast . . . . .	145
A.8	Volatility spillovers across five selected exchange rates – 60-day ahead forecast . . . . .	146
A.9	Returns spillovers across five selected exchange rates – Frequency domain analysis with 4-day frequency band and 7-day ahead forecast . . . . .	147
A.10	Returns spillovers across five selected exchange rates – Frequency domain analysis with 16-day frequency band and 7-day ahead forecast . . . . .	148
A.11	Returns spillovers across five selected exchange rates – Frequency domain analysis with 30-day frequency band and 7-day ahead forecast . . . . .	149
A.12	Returns spillovers across five selected exchange rates – Frequency domain analysis with 4-day frequency band and 10-day ahead forecast . . . . .	150
A.13	Returns spillovers across five selected exchange rates – Frequency domain analysis with 16-day frequency band and 10-day ahead forecast . . . . .	151
A.14	Returns spillovers across five selected exchange rates – Frequency domain analysis with 30-day frequency band and 10-day ahead forecast . . . . .	152
A.15	Returns spillovers across five selected exchange rates – Frequency domain analysis with 4-day frequency band and 30-day ahead forecast (baseline estimates) . . . . .	153

A.16 Returns spillovers across five selected exchange rates – Frequency domain analysis with 16-day frequency band and 30-day ahead forecast . . . . .	154
A.17 Returns spillovers across five selected exchange rates – Frequency domain analysis with 30-day frequency band and 30-day ahead forecast . . . . .	155
A.18 Returns spillovers across five selected exchange rates – Frequency domain analysis with 4-day frequency band and 60-day ahead forecast . . . . .	156
A.19 Returns spillovers across five selected exchange rates – Frequency domain analysis with 16-day frequency band and 60-day ahead forecast . . . . .	157
A.20 Returns spillovers across five selected exchange rates – Frequency domain analysis with 30-day frequency band and 60-day ahead forecast . . . . .	158
A.21 Volatility spillovers across five selected exchange rates – Frequency domain analysis with 4-day frequency band and 7-day ahead forecast . . . . .	159
A.22 Volatility spillovers across five selected exchange rates – Frequency domain analysis with 16-day frequency band and 7-day ahead forecast . . . . .	160
A.23 Volatility spillovers across five selected exchange rates – Frequency domain analysis with 30-day frequency band and 7-day ahead forecast . . . . .	161
A.24 Volatility spillovers across five selected exchange rates – Frequency domain analysis with 4-day frequency band and 10-day ahead forecast . . . . .	162
A.25 Volatility spillovers across five selected exchange rates – Frequency domain analysis with 16-day frequency band and 10-day ahead forecast . . . . .	163
A.26 Volatility spillovers across five selected exchange rates – Frequency domain analysis with 30-day frequency band and 10-day ahead forecast . . . . .	164
A.27 Volatility spillovers across five selected exchange rates – Frequency domain analysis with 4-day frequency band and 30-day ahead forecast (baseline estimates) . . . . .	165
A.28 Volatility spillovers across five selected exchange rates – Frequency domain analysis with 16-day frequency band and 30-day ahead forecast . . . . .	166
A.29 Volatility spillovers across five selected exchange rates – Frequency domain analysis with 30-day frequency band and 30-day ahead forecast . . . . .	167
A.30 Volatility spillovers across five selected exchange rates – Frequency domain analysis with 4-day frequency band and 60-day ahead forecast . . . . .	168
A.31 Volatility spillovers across five selected exchange rates – Frequency domain analysis with 16-day frequency band and 60-day ahead forecast . . . . .	169

A.32 Volatility spillovers across five selected exchange rates – Frequency domain analysis with 30-day frequency band and 60-day ahead forecast . . . . .	170
B.1 Estimates of BTC/USD market volatility under different specifications of MS-ARFIMA process . . . . .	178
B.2 Estimates of BTC/EUR market volatility under different specifications of MS-ARFIMA process . . . . .	178
B.3 Estimates of BTC/GBP market volatility under different specifications of MS-ARFIMA process . . . . .	179
B.4 Estimates of BTC/AUD market volatility under different specifications of MS-ARFIMA process . . . . .	179
B.5 Estimates of BTC/CAD market volatility under different specifications of MS-ARFIMA process . . . . .	180
B.6 Estimates of BTC/USD market return volatility under different specifications of MS-ARFIMA process . . . . .	181
B.7 Estimates of BTC/EUR market return volatility under different specifications of MS-ARFIMA process . . . . .	181
B.8 Estimates of BTC/GBP market return volatility under different specifications of MS-ARFIMA process . . . . .	182
B.9 Estimates of BTC/AUD market return volatility under different specifications of MS-ARFIMA process . . . . .	182
B.10 Estimates of BTC/CAD market return volatility under different specifications of MS-ARFIMA process . . . . .	183
C.1 Volatility spillovers across six selected exchange rates in time domain – 60-day ahead forecast . . . . .	191
C.2 Volatility spillovers across six selected exchange rates in time domain – 90-day ahead forecast . . . . .	192
C.3 Volatility spillovers across six selected exchange rates in time domain – 120-day ahead forecast . . . . .	192

## Declaration of Authorship

I, Ahmad Maaitah , declare that this thesis titled, 'Essays on Memory and Dynamics of Connectedness in Bitcoin Markets' and the work presented in it are my own. I confirm that:

- This work was done wholly or mainly while in candidature for a research degree at this University.
- Where any part of this thesis has previously been submitted for a degree or any other qualification at this University or any other institution, this has been clearly stated.
- Where I have consulted the published work of others, this is always clearly attributed.
- Where I have quoted from the work of others, the source is always given. With the exception of such quotations, this thesis is entirely my own work.
- I have acknowledged all main sources of help.
- Where the thesis is based on work done by myself jointly with others, I have made clear exactly what was done by others and what I have contributed myself.
- Part of this work has been published as:

Gillaizeau, M., Jayasekera, R., Maaitah, A., Mishra, T., Parhi, M., & Volokitina, E.(2019). Giver and the receiver: Understanding spillover effects and predictive powerin cross-market bitcoin prices. International Review of Financial Analysis.

Signed : \_\_\_\_\_

Date : \_\_\_\_\_



## **Acknowledgements**

I would like to take this opportunity to express my heartfelt gratitude to all those who helped me through my PhD journey.

First and foremost, I owe a deep debt of gratitude to my astonishing supervisor, Professor Tapas Mishra for his endless support and priceless encouragement. This thesis would never have been written without his guidance and valuable comments. An ocean of thanks for his boundless lessons, precious advice and enjoyable talks. I would like to extend my thanks and appreciation to my second supervisor, Professor Simon Wolfe for his help and insightful advice through my PhD journey. I am extremely thankful and grateful to my parents, Qasim Maaitah and Zainab Kafaween, as well as my siblings for helping, supporting and encouraging me during my Master's and PhD journey. Their attention, concern and prayers are very much appreciated. All the good moments and enjoyable times that I have spent with my friends and Soton family will be lasting and impenetrable memories - big thanks to you all.

Ahmad Qasim Maaitah

17/05/2020 Southampton.



*To my beloved parents Qasim and Zainab . . .*



*“No memory is ever alone; it’s at the end of a trail of memories, a dozen trails that each have their own associations . . .”*

*Louis L’Amour*

*Soton, Highfield Campus, Office 2/6019, Out of Hours Working  
Authorisation ...*



# Chapter 1

## Introduction

## 1.1 Research context

During the last century, the move towards a digital world began to increase rapidly, particularly in the financial industry. The arrival of the global financial crisis in 2008 was the straw that broke the camel's back and the starting spark of a new financial era. The first state-of-the-art, well-developed digital currency was introduced on 31 Oct 2008 by the pseudonymous "Satoshi Nakamoto" to tackle all the restrictions and disadvantages of fiat currencies, and facilitate movement and exchange around the world at very low cost, and highly secure system (Nakamoto, 2008). Indeed, trading and transferring of cryptocurrencies (Bitcoin) does not need a central authority or financial institution to verify and transfer the transaction among users <sup>1,2</sup>.

*"You will not find a solution to political problems in cryptography. Yes, but we can win a major battle in the arms race and gain a new territory of freedom for several years. Governments are good at cutting off the heads of a centrally controlled networks like Napster, but pure P2P networks like Gnutella and Tor seem to be holding their own."*

*Satoshi Nakamoto* <sup>3</sup>.

The peer-to-peer electronic cash system is completely decentralised, which enables users to totally control the ownership of currency and prevent double spending (reversal) transactions. Thus, on the one hand, the Bitcoin has bypassed the financial turmoil of 2008 by decentralising the system and becoming an unrestricted and independent digital currency, unlike others. On the other hand, the novelty of Bitcoin and block-chain technology has created a status of uncertainty and ambiguity around the globe in the absence of strict monetary and financial regulations.

After the white paper of Bitcoin was introduced at the end of 2008, Satoshi Nakamoto released the first block (the Genesis block) on Jan 3, 2009, as the first transaction in the history of Bitcoin, under the following title, "The Times 03/Jan/2009 Chancellor on brink of second bailout for banks". To date, that is until midnight, Feb 12, 2020, the number of blocks that have been generated over the last 11 years is 616,996 blocks with market capitalisation exceeding \$ 185 billion and circulating supply around BTC 18 million. However, the circulating supply should approach BTC 21 million by the end of 2140 <sup>4,5,6,7</sup>.

In spite of the market capitalisation of the cryptocurrencies market (more than 2000 digital currencies) exceeding \$ 290 billion, the Bitcoin market still the most important one;

---

<sup>1</sup>To review the history of digital currency before 2008, see (Chuen, 2015)

<sup>2</sup>1 Satoshi = 0.00000001 BTC

<sup>3</sup>Metzdowd.com

<sup>4</sup>Thetimes.co.uk

<sup>5</sup>Btc.com

<sup>6</sup>Coinmarketcap (Feb 11, 2020)

<sup>7</sup>Mining the rest of Bitcoins will be progressively slower because the block reward is halving every 210,000 blocks (approximately each four years) and reduce new bitcoin supply by 50 percent.

hence its market share is around 63%. Therefore, huge contributions from this market are participating directly and indirectly through different channels in the global financial markets. Consequently, investigating and studying the Bitcoin markets furnishes us with a deeper understanding of market behaviour and connectedness with other markets, providing insights for investors and policy makers. Broadly, we can divide the research into three main areas, allowing us to scrutinise the Bitcoin market critically and systematically, and providing valuable information to interested agents by: firstly, studying the static and dynamics of Bitcoin prices in both the short and long-run domains; secondly, studying the endogenous dynamics of Bitcoin prices and assessing the volatility persistence in such a system; thirdly, studying the technological aspects of Bitcoin, such as cyber securities, and identifying their major impact on the Bitcoin markets.

The issue of spillover effects is very important nowadays as globalisation strengthens the connectedness between the markets around the globe. Thus, volatility spillover is more profound when market interdependence is high, especially during financial crisis and episodes of economy-wide uncertainty. Information on a *within-market* transmission of shocks possesses high policy value because viable policy interventions can limit the possible proliferation of shocks beyond certain acceptable bounds. Some studies such as Corbet et al. (2018) shed light on the spillover effects of volatility from a ‘cryptocurrency market’ to ‘other asset markets’ (such as stock and gold), Cheah et al. (2018) demonstrating the importance of cross-market dynamic interdependence of Bitcoin prices by estimating a system-wide long-memory.

However, *memory* is logically imperishable during the lifespan of a boundedly rational agent. The only characteristic one can note about the existence of memory is whether it is small or big, and concerns the long or short ‘trail’ of associations it inherently defines over a period of time - just as Louis L’Amour (an American author) has famously quoted. In the case of cryptocurrency, a similar strand of research has begun to emerge (see for instance, (Bariviera, 2017)) barring some exceptions (viz. Cheah et al., 2018) where some directions of the source of long-memory are discussed.

From a technical point of view, cyber criminality in the cryptocurrency market is a very serious matter, and extensive efforts from legislators and decision-makers are being made to create an efficient environment with flexible boundaries to restrict or frustrate manipulation across cryptocurrency markets(Böhme, Christin, Edelman, & Moore, 2015; Dwyer, 2015; Gandal, Hamrick, Moore, & Oberman, 2018). The impact of cyber attacks on the return of cryptocurrencies has caused the system to be highly volatile, and the increasing number of attacks appearing to have a major impact on the volatility market.

## 1.2 Research aims

The aim of this thesis is to study and investigate the cross-market dynamics of Bitcoin prices by employing a spillover effects index, long-memory measures and network topology from an empirical perspective. The thesis sheds light on a new alternative investment, proposing credible empirical strategies to help investors, policy makers and researchers to make crucial decisions and build coherent future investment plans.

The aims of each chapter are as follows:

Chapter Two provides a comprehensive study of the *cross-market* spillovers of volatility in Bitcoin prices and the predictive power each market possesses relative to others. Essentially, the chapter sheds light on the net receivers and prime givers of volatility across markets to help investors design trending strategies to systematically beat the market.

Chapter Three aims to detect the volatility persistence in the Bitcoin cross-market and identify the true long memory within the market, so as to have a deeper understanding of the endogenous dynamics in the system, and how the market frequently reacts to news and economic events. Indeed, the presence of *true* long memory could enable investors to capture speculative profits via market timing, and policy makers could introduce circuit breakers to stop trading in Bitcoin cross-markets when the market switches abruptly to a high-volatility regime.

The aim of Chapter Four is to study the reaction of Bitcoin prices during cyber attack episodes, and how volatility can seriously flow across markets. Indeed, quantitative information on the centrality or relative isolation of some Bitcoin-to-currency markets could actually help investors to better anticipate their complex dynamic behaviour and exploit potential of forecastable gains.

### 1.3 Research objectives

The research objectives for each chapter of the thesis are as follows:

The research objectives in Chapter Two are:

- To empirically quantify the volatility spillover effects in cross-market Bitcoin prices through generalised variance decomposition process.
- To identify the net receiver and prime giver of volatility across Bitcoin markets and manage the shocks within a dynamic/static system.
- To examine the co-movement of uncertainty index and total directional volatility spillover across Bitcoin markets.
- To detect the volatility spillover in the short-run and long-run horizon.

The research objectives in Chapter Three are:

- To detect the true long memory properties within Bitcoin markets and distinguish between structural breaks and long-range dependence.
- To empirically estimate an endogenous switch led ARFIMA model, which allows 'memory' co-moves with 'switches' endogenously to detect the true persistence pattern across markets.
- To quantify and detect the speed of adjustment behaviour of long-memory properties within the markets.

The research objectives in Chapter Four are:

- To empirically examine the impact of cyber attacks on the Bitcoin financial system.
- To design weighted directed networks of Bitcoin prices volatilities during episodes of hacking events.
- To detect the connectedness between Bitcoin markets statistically and dynamically under a series of cyber attacks.

## 1.4 General Literature Review and Contributions

Cryptocurrency literature has been subject to an astounding amount of research over the last five years. The explosion of work focuses primarily on several aspects, such as the connectedness among cryptocurrencies and other assets in a financial market, volatility persistence within the market, and the risk generated by cybercrime and hacking events.

Several studies have attempted to study the spillover phenomenon in cryptocurrency markets. Kurka (2017) investigated the interconnectedness between the cryptocurrency market and a bundle of traditional assets. Different spillover index approaches were applied to a group of financial assets, including Bitcoin, to detect the linkages between them. Interestingly, they found a very low level of linkage between Bitcoin and other assets, except for gold, which received several shocks from Bitcoin during that period. Corbet et al. (2018) employed a generalised variance decomposition method in time and frequency domains to investigate the connectedness amongst several financial assets, and three major cryptocurrencies. They found high levels of linkage among the cryptocurrencies, and very low connectedness between the cryptocurrencies and other financial assets. Their analysis suggested that the cryptocurrencies market contains its own risk which is hard to hedge against.

Bouri et al. (2018) studied the level of linkage between particular cryptocurrencies and four major financial assets<sup>8</sup> in both bear and bull market conditions through VAR-asymmetric GARCH method. The model suggested that Bitcoin and the commodities markets are not completely isolated from one another. In addition, the results clearly showed that Bitcoin was receiving shocks more than transmitting them to other markets.

Consequently, Chapter Two contributes to the literature in the following two significant ways.

- Previous studies have investigated the spillover effects between a cryptocurrency market and a conventional asset market. Hence a major contribution of the second chapter is to quantify (dynamic) spillover effects in cross-market Bitcoin prices, and to shed light on the net receiver and prime giver of volatility across markets for a single cryptocurrency (Bitcoin).
- As a further contribution, we employ Parkinson's (1980) high-low volatility measure, as well as Garman-Klass type of volatility estimates to capture dynamic movements between high and low Bitcoin prices.

---

<sup>8</sup>Equities, bonds, currencies and commodities

A wide range of empirical research also focuses on long-range persistence, cointegration and structural breaks to explain the complex behaviour and non-linear dynamics of Bitcoin prices (Alvarez-Ramirez et al., 2018; Caporale, Gil-Alana, & Plastun, 2018; Cheah et al., 2018).

Neglecting the time series properties during the analysis process could generate misleading information. Several studies have analysed the time varying behaviour of long-range dependence through different tests, such as Hurst exponent and detrended fluctuation analysis *DFA* and exact local whittle estimation with rolling windows (Alvarez-Ramirez et al., 2018; Bariviera, 2017; Bariviera, Basgall, Hasperu  , & Naiouf, 2017; Caporale et al., 2018; Cheah et al., 2018). Statistical properties may be subject to sudden changes over time, especially in the Bitcoin markets, which may leave some distortion shocks permanency; hence, structural breaks testing is crucial to validate the long-range stability process (Al-Yahyaee et al., 2018; Bouri et al., 2019; Charfeddine & Maouchi, 2019; Mensi et al., 2018, 2019). A long debate in the literature suggests that the presence of structural breaks in a time series could appear as high long-range persistence; thus, level shifts and long memory are easily confused, as Diebold and Inoue (2001) suggested.

All the aforementioned studies ignore the fact that diagnosing structural breaks and long memory individually does not clarify the problem, and provides unstable results. On the contrary, Diebold and Inoue (2001) suggested that long-range dependence and turning points should be modelled in a conquer unified framework, allowing the system to distinguish between the latter phenomena simultaneously and endogenously. The focus on a cross-market rather than a single market has significance in our context: by employing *ARFIMA* Markov Switching with endogenous switches governing the internal dynamics of Bitcoin prices or volatility system, we will be able to distinguish between the true and spurious long memory with higher accuracy. Accordingly, Chapter Three contributes to the nascent literature on the source and implications of ‘memory’ in Bitcoin markets in the following three significant ways:

- The chapter puts forward an identification strategy to demonstrate the source and implications of long memory in Bitcoin markets. It also proposes a demand-driven long memory channel for Bitcoin, showing that there are waves of Buyer initiated transactions (given a fixed supply of Bitcoin) which follow a Beta distribution with memory, by following a linear algorithm of aggregation and power distribution.
- We model the (non-)existence of long memory to an endogenous market system mechanism which might give rise to persistent shock, with or without a mean reversion. We discuss this in the light of an endogenous switch in the memory and mean of the Bitcoin price process.
- Using daily Bitcoin data for five different markets, we study the nature of persistence in Bitcoin volatility, while considering an endogenous switch in volatility. From

this, we shed light on the nature of the true long memory, and quantify to what extent true 'memory' governs the internal dynamics of the system.

Regulations, information systems and cyber criminality are very important corners in cryptocurrency markets, allowing legislators and decision-makers to design appropriate regulations and create an efficient environment with flexible boundaries to restrict the frustration and manipulation across these markets (Böhme et al., 2015; Dwyer, 2015; Gandal et al., 2018).

Abhishta et al. (2019) found that DDoS attacks have a direct negative impact on Bitcoin prices, and induce the network to be more volatile and vulnerable over time. Moreover, cyber attacks on Bitcoin (e.g. DDoS, code bugs or user errors) and the common response from users (e.g. code revision, computer security measures or temporary suspension) could diminish the value of Bitcoin and leave a serious distortion in the network. Caporale et al. (2019) investigated the impact of cyber attacks on the returns of four cryptocurrencies (e.g. Bitcoin, Stellar, Litecoin and Ethernam). The Markov switching analysis and cumulative measures suggested that cyber attacks induce the system to be highly volatile, the number of cyber attacks being positively correlated with the level of volatility. (Corbet et al., 2020) studied the relationship between cybercriminal events and cross-cryptocurrency markets. Results show very high episodes of volatility and broad co-movement in cryptocurrency markets when hijackers attempted to penetrate the network.

Consequently, Chapter Four contributes to the literature in the following two significant ways.

- We study *the network topology of Bitcoin prices volatilities* by designing several weighted directed networks during 19 major cyber attacks. Although economic and political events can generate volatilities within financial markets, cyber attacks could have a more significant impact on the cryptocurrencies market, being fully electronic and vulnerable to cyber attack. Each cryptocurrency has a unique and distinct infrastructure (network); thus focusing on the Bitcoin market rather than cryptocurrencies markets allows us to investigate the network more thoroughly and efficiently.
- We examine the impact of 19 cyber attacks on Bitcoin markets through variance decomposition method. To the best of our knowledge, there is no available financial theoretical model to justify conditioning the predictive power of an asset market on volatility in a cryptocurrency market. In this sense, a major contribution of the current chapter is to measure and identify the network connectedness between Bitcoin markets under several cyber attacks. In so doing, we aim to shed light on six Bitcoin markets under different security breaches to identify their magnitude and direction statically, dynamically and graphically.

## 1.5 A schematic representation of the thesis

**Chapter One** gives a general introduction and background on the Bitcoin markets, followed by the research aims and objectives which systematically cover the purpose of this thesis.

**Chapter Two** sheds light on the ‘givers and receivers’ of volatility in cross-market Bitcoin prices and discusses international diversification strategies in this context. In this chapter, the spillover index method is used to analyse and identify the magnitude and direction of volatility movement under a time domain and frequency domain process. A battery of robustness checks are applied to validate the conducted results.

**Chapter Three** focuses on the endogenous dynamics in cross-market Bitcoin prices. The chapter introduce a first-hand strategy to detect and identify long memory properties while quantifying the structural breaks simultaneously. An endogenous Markov switching ARFIMA mechanism with Shimotsu long memory test and Bai & Perron estimation are used to create an empirical strategy for investors and policy makers to provide a credible role of policy on containing volatility persistence across Bitcoin markets.

**Chapter Four** sheds light on the technological aspect of Bitcoin, and shows how cyber attacks can severely affect the network and leave a lengthy distorted footprint. Generalised variance decomposition approach is applied to confirm the movement of volatility across markets, then network theory with the help of rolling windows to identify the depth of impact from different types of cyber attacks.

**Chapter Five** provides a detailed conclusion, and presents the main implications of the thesis.



## Chapter 2

# Giver and the Receiver: Understanding Spillover Effects and Predictive Power in Cross-market Bitcoin Prices

### Abstract

We identify and characterise the ‘givers and the receivers’ of volatility in cross-market Bitcoin prices and discuss international diversification strategies in this context. Using both time and frequency domain mechanisms, we provide estimates of outward and inward spillover effects. These have implications for (weak-form) cross-market inefficiency. In our setting, we treat high-degree of spillover as an indicator of weak-form inefficiency because investors can utilise information on the dynamic spillover effects to produce a best long-run prediction of the market. Our results show that Bitcoin prices depict strong (dynamic) spillover in volatility, especially during episodes of high uncertainty. The Bitcoin-USD exchange rate possesses net predictive power, mirrored by the tendency of the Bitcoin-EURO market as a net receiver relative to other markets. Robustness exercise generally supports our claim. The overall implication is that during episodes of high uncertainty, Bitcoin markets depict greater dynamic inefficiency, instrumenting the role of asymmetric information in the path-dependence and predictive power of Bitcoin prices in an interdependent market.

**Keywords:** Cross-market Bitcoin prices; Return and volatility spillovers;

Uncertainty; Inefficiency; Prediction

**JEL Classification:** C1; E4; D5

## 2.1 Introduction

Since it was actively traded in 2013, Bitcoin – the biggest and most active cryptocurrency with a market capitalization over \$110<sup>1</sup> billion – has struck investors' expectations of a quick and sizeable return, like none other. In the absence of strict monetary and financial regulations, cryptocurrency investors seem to be fully exploiting this opportunity and are quickly moving from a state of despondency (due to recurrent losses from their investments in regulated financial markets) to one of hope (because, Bitcoin prices are fundamentally driven by the 'feeling and the memory' of investors at a point of time.<sup>2</sup> To investigate the nature of such type of investment decisions and help governments design adequate regulations for limiting cross-market movement of shocks, a remarkable growth of research has sprung lately.

A helicopter survey<sup>3</sup> reveals that the literature has focused on two main aspects of cryptocurrency price movements. First, conceptual designs aiming to depict potential weaknesses of this market show how the latter can subject investors to insurmountable unsystematic risks (see for instance, Cheah & Fry, 2015; Cheah et al., 2018; Gandal et al., 2018). Second, a plethora of empirical research has systematically presented state-of-the-art estimation techniques to identify, among others, informational inefficiency (viz. Urquhart, 2016), long-range persistence behavior and cointegration (viz. Alvarez-Ramirez et al., 2018; Caporale et al., 2018; Cheah et al., 2018), volatility spillovers and dynamic interactions with other financial assets (viz. Corbet et al., 2018). Thus far, the extant research has largely focused on a cross-section of cryptocurrencies and sparsely on a cross-market dynamics of a single cryptocurrency (except for the leading work of Cheah et al., 2018). This chapter aims to contribute to this nascent literature by studying volatility spillover across Bitcoin markets, exchanged in various currencies.

The issue of cross-market volatility has been studied in a macroeconomic context (for instance, Diebold & Yilmaz, 2012), where it is shown that volatility spillover is more profound when market interdependence is high, especially during financial crisis and episodes of economy-wide uncertainty (Cheah et al., 2018). Information on a *within-market* transmission of shocks possesses high policy value because viable policy interventions can limit possible proliferation of shocks beyond certain acceptable bounds. Moreover, managing shocks *within* a system is relatively easier as one can exploit the *system dynamic* features of shocks so as to monitor their movements and generate better predictive power for an asset. Although Bitcoin is traded electronically, like a huge number of assets

<sup>1</sup>coinmarketcap.com (Oct 2018)

<sup>2</sup>See Cheah et al. (2018) for details.

<sup>3</sup>Theoretical and empirical research in cryptocurrencies can be broadly divided into three important interdependent areas; viz., regulations and information system research, financial market and monetary theoretical formulation of cryptocurrency demand/supply, and development (and applications) of state-of-the-art econometric and/or statistical mechanics to understand (predictive patterns of) price movements. To minimise space and repetition of a succinct literature review, interested readers are encouraged to refer to Corbet et al. (2019) for an excellent survey.

globally, cross-economy differentials in the trading of Bitcoin reflects not only the role of macroeconomic and financial market regulations, but also represent investors' sentiment concerning an investment in a risky asset. While former studies (such as Corbet et al. (2018)) shed light on spillover effects of volatility from a 'cryptocurrency market' to 'other asset markets' (such as stock and gold), Cheah et al. (2018) demonstrated the importance of cross-market dynamic interdependence of Bitcoin prices by estimating a system-wide long-memory. The focus on a cross-market rather than a single market cryptocurrency market in the latter study holds significance in our context: by modelling directional spillover effects one creates a stock of information for investors who decide on an arbitrage value of Bitcoin traded in various markets. The investors exploit information on the predictive power of each market, such as the net receiver and net giver of volatility. Such a study is helpful in shaping robust investment strategy of a single cryptocurrency traded in various markets.

Broadly speaking, the current chapter's main aim is to improve our limited understanding of the *cross-market* spillovers of volatility in Bitcoin prices and the predictive power each market possesses relative to others. Since Gandal et al. (2018) showed that Bitcoin prices can be seriously manipulated, a thorough understanding of volatility movements across Bitcoin markets is important to gauge net predictive power of each market. Accordingly, this chapter contributes to the literature in two significant ways. First, differing from the convention, we study *spillover effects of return and volatility across markets* for a single cryptocurrency. Although study of spillover effects between a cryptocurrency market and a conventional asset market offers important insights on if and whether shocks from cryptocurrency market impact volatility in an asset market, it lacks in a directional predictive power. This is because these two markets are distinct with respect to the modes of operandi. Moreover, to the best of our knowledge there is no available financial theoretic model to justify conditioning predictive power of an asset market on the volatility in a cryptocurrency market. In this light, a major contribution of the current chapter is to quantify (dynamic) spillover effects in cross-market Bitcoin prices. By doing so, we aim to shed light on the net receiver and prime giver of volatility across markets. As a further contribution, we employ Parkinson's (1980) high-low volatility measure as well as Garman-Klass type of volatility estimates to capture dynamic movements between high and low Bitcoin. Using these volatility measure (details of which will be presented in Section 2), we show that the Bitcoin-USD exchange rate possesses net predictive power and that the Bitcoin-EURO market appears to be a net receiver of volatility relative to other markets. Eventually, such tendencies could help investors design trending strategies to systematically beat the market.

To investigate further, the rest of the chapter is planned as follows. Section 2 review the literature. Section 3 discusses data and summary statistics. section 4 discusses estimation method. Section 5 presents empirical results and robustness analyses. Section 6 concludes

and presents the main implications of our research. Section 7 displays all the necessary estimations in appendix A.

## 2.2 Literature review

Extensive research has been done on volatility spillover, because of the importance of volatility connectedness across global financial markets. Portfolio managers, traders, investors, policy makers and many others are interested in analysing the spillover of volatility across financial assets and markets. The current body of literature has identified significant contributions from the indirect effect of volatility on financial securities and Bitcoin. This section introduces the theoretical framework of volatility spillover across foreign exchange markets. Firstly, definitions and the roots of volatility connectedness will be introduced. Secondly, the theories most related to financial contagion literature will be revised. Thirdly, focusing on one stream of the literature, the exchange rate volatility spillover domain will be reviewed from 1990 until the present. Finally, the most adopted methodologies in the latter stream of the literature will be discussed.

### 2.2.1 The volatility Spillover definition

The rapid technological development in global financial markets has increased the integration and connectedness amongst economies around the world. The financial linkages have induced scholars and practitioners to investigate the effect of a particular event (e.g. economic, political, catastrophic) on a group of economies around the world and how the shocks generated flow across these economies. Different methodologies have been introduced to examine how a particular shock in a certain market could transmit the risk to another market or group of markets.

Prior to the definition of volatility spillover, the term ‘financial contagion’, was the first terminology appearing in the literature. The word ‘contagion’ is derived from medicine and describes how a particular contagious disease can spread across a patient’s surrounding environment. Similarly, financial contagion can be defined as a series of shocks which affect a range of economies at varying levels, due to the extent of their connectedness (Claessens & Forbes, 2013)<sup>4</sup>. However, among the different types of volatility, this study adopts unconditional volatility (Parkinson 1980). Volatility is a statistical measure used to study the behaviour of economic variables over time (Enders, 2008). In addition, it is considered to be an unpredictable parameter in the econometric system. Mixing all the latter terms, volatility spillover effects can be defined as a measurement tool for a particular shock(s) generated in a certain financial asset (market) with full regard to the

---

<sup>4</sup>This chapter uses the broader definition of contagion, see (Claessens & Forbes, 2013) for more definitions (e.g. the shift-contagion, etc)

linkages between the affected financial asset (market) and other assets (markets) across the world (Bollerslev & Hodrick, 2017; Engle & Susmel, 1993).

## 2.2.2 Volatility Spillover theories

The above definitions and explanation provide a clear concept of volatility linkage across financial markets. This section will revise the two main, well-known grounded theories in the volatility spillover effect literature:

### 2.2.2.1 Heat waves and Meteor showers

The first spark of financial contagion began after a long debate in the literature of efficient market hypotheses (EMH). The essence of this theory discussed how financial markets across the world react to the arrival of new information at different levels <sup>5</sup>. Based on the EMH concept, a new stream of literature started to focus on the factors that could transmit the risk from market to market, and on how to identify the direction of risk flow among economies.

Consequently, the seminal work by (Ito & Roley, 1987) was the first attempt to explore the idea of volatility spillover effect across financial markets. Their research question was: "News from the U. S. and Japan: which moves the Yen/Dollar exchange rate?". For the sake of analysis, the series of yen/dollar exchange rates from 1980 to 1985 was divided into four segments to scrutinize the behaviour of the series in each segment. Their analysis found a significant linkage in the fluctuations of the Japanese and U.S. markets.

On the same ground, a seminal study by (Engle et al., 1990) introduced two distinguishable hypotheses: "Heat Waves & Meteor Showers ". They investigated the volatility clustering of the yen/dollar series across the U.S. and Japanese markets. The results indicated that the null hypothesis of Heat Waves was significantly rejected, while the hypothesis relating to Meteor Showers was not rejected, which implies that there was significant evidence of the transmission of volatility from one market to another. To understand the general conceptual framework of both hypotheses, a small example has been provided by (Engle et al., 1990)'s paper. Firstly, the Heat Waves, or own spillover hypothesis can be explained by imagining how a hot day in London might keep the weather hot there in the following few days, but this does not necessarily make it hot in Dublin. In other words, if a particular shock increases volatility in a specific economy, this does not cause the volatility to increase in another related economy. Secondly, and in contrast, Meteor Shower, or cross spillover, implies that if meteors start falling down to Earth, London, Dublin and other cities will certainly experience some effects. Econometrically,

---

<sup>5</sup>(Fama, 1970, 1976, 1991)

if a particular shock increases the volatility of a specific market, the same shock might also increase the volatility of other markets <sup>6</sup>.

The Heat Waves and Meteor Shower hypothesis is a controversial issue in the body of literature. The location-specific auto-correlation phenomenon, or Heat Wave hypothesis, has been found to exist in almost all financial markets. The own-spillover effect might be generated by a local political or economic event and, interestingly, the shock will affect only the local economy, without any transmission to other economies. An interesting debate about the two hypotheses started after (Baillie & Bollerslev, 1991) proved that own-specific volatility is more reliable and significant than cross market volatility. For example, in 2006, Hassan et al. investigated the volatility linkages among Asian developing and developed financial markets between 1991 and 2000. Surprisingly, the null hypothesis, "Heat Waves", failed to be rejected between 1991 and 1993 in the developed markets of the Philippines, Korea and Indonesia. The latter results implied that a weak linkage existed between the developed and developing markets in Asia, and that was due to the adopted contradictory policies between both markets (Andersen & Bollerslev, 1997; Dacorogna et al., 1993; Hogan Jr & Melvin, 1994, for more details see). To illustrate the seasonality in FX volatility, (Cai et al., 2008; Engle & Susmel, 1993; Fleming & Lopez, 1999; Hassan et al., 2006; Melvin & Melvin, 2003; Melvin & Yin, 2000).

By contrast, a remarkable and growing body of literature has investigated the cross-spillover volatility or Meteor Shower hypothesis. Market interdependence is the fundamental key here, whereby a particular set of financial markets can be dominated by a specific shock, such as a monetary policy, or a political decision. By revising the volatility spillover literature it appears that the Meteor Shower hypothesis has conquered the opposite hypothesis, by introducing more empirical methodologies to prove the existence of cross-spillover volatility across financial markets (Engle et al., 1990; Fleming & Lopez, 1999; Hamao et al., 1991; Ito et al., 1992; King & Wadhwani, 1990; Lahaye & Neely, 2018; Reyes, 2001). For example, (Glosten et al., 1993; Nelson & Foster, 1994; Reyes, 2001) investigated both hypotheses with respect to the asymmetric volatility spillover in financial markets. Their results suggested that asymmetric models could generate the best forecast of volatility (Engle & Susmel, 1993) Moreover, (Lahaye & Neely, 2018) claimed that the cross-spillover hypothesis is more effective than the own-spillover hypothesis.

However, a significant stream of the literature is consistent with the seminal work of (Engle et al., 1990). The importance of this has grown gradually because of the remarkable connectedness among global financial markets around the world. The following subsection reviews the major empirical research that has investigated the volatility spillover effect.

---

<sup>6</sup>For more details see (Engle et al., 1990)

### 2.2.3 Empirical review

Volatility spillover literature has expanded gradually to cover different areas, as volatility spillover varies from country to country, market to market, and from financial asset to financial asset. Consequently, this subsection focuses chronologically on the exchange rate volatility spillover literature and endeavours to discuss the most important papers in this area.

Engle et al. (1990) investigated the volatility clustering of two exchange rates to defend their claim about financial markets linkages. Consequently, they applied a multivariate general autoregressive conditional heteroscedasticity (MGARCH) model with regard to (Bollerslev, 1986; Ito & Roley, 1987)'s empirical methodologies. They investigated whether the yen/dollar exchange rate between 1985 and 1986 actually transmitted any shocks (information) among the Tokyo and New York exchange markets. The null hypothesis Meteor Shower failed to be rejected, at a 5% significance level. Failing to reject the null hypothesis clarified that the flow of information between both international markets was significant and did exist. Econometrically, they tried to trace any possible shock in the system by dividing the volatility component into many different segments. The results of the robustness test validated the strength of their analysis and outcomes. Following this seminal work, many researchers started to scrutinize volatility spillover across financial markets.

A quick response to (Engle et al., 1990)'s research came from (Baillie & Bollerslev, 1991), who built a seasonal GARCH model to detect the volatility over time in each series and ran an LM test to capture the leptokurtosis phenomenon amongst the data set. The Japanese yen, the German deutschmark, the Swiss franc and the British pound were regressed against the U.S. dollar between Jan 1986 and July 1986 to find any cross-spillover volatility. Their results confirmed that the meteor shower phenomenon significantly existed. By contrast, interestingly, the seasonal ARCH system suggested some significant own-spillover information (local shocks) across the data. Additionally, running the robust test did not capture enough evidence in the system to support the cross-spillover hypothesis across the exchange rates. Also, in 1993, Baillie, Bollerslev, and Redfearn analysed a major group of global exchange rates against the U.S. dollar. They chose a distinguishable event, called the "Bear Squeeze", which occurred in the 1920s, to find any evidence of volatility transmission among six currencies. Indeed, they found that the Belgian and French exchange rates were transmitting volatility over the Swiss and Italian exchange rates. Their robustness check suggested a similar conclusion as the previous research. In Asia, Alba (1999) examined the period following the East Asian crisis (1990) to find some evidence of the volatility that flowed among the Asian markets. The applied model<sup>7</sup> suggested that the volatility spillover effect across the six exchange rates was only statistically significant for two exchange rates. Volatility transmission was

<sup>7</sup>proposed by (R. F. Engle & Gau, 1997).

detected in the Chinese and “Philippines and Thailand” markets. Further, a causality test concluded that the Chinese exchange rate was dominating the other two exchange rates in the sample span period.

Hereafter, scholars started to pay more attention to volatility spillover and began developing different methodologies to detect the meteor shower phenomenon in financial markets. A study by Huang and Yang (2002) investigated the extent to which the London, Tokyo and New York financial markets were linked. A causality-in-variance analysis<sup>8</sup> was applied to trace the volatility spillover between the currencies of those markets against the U.S dollar. Huang and Yang (2002) stated confidently that a causality- in- variance test was more accurate and reliable than the GARCH family models. However, many studies have supported the body of literature by fruitful analysis of the volatility spillover effect across financial markets. For more details see(Hong, 2001; Kearney & Patton, 2000; Speight & McMillan, 2001).

On the other hand, Melvin and Melvin (2003) studied the deutschmark and Japanese yen against the U.S. dollar across five regional markets<sup>9</sup> were recognized by quoting patterns analysis to find the level of interdependence between the different markets. Regional volatility models were built to find the own-region and cross-region spillover. After analysing the high frequency data, they found that the volatility spillover in both own-region and cross-region was statistically significant. By contrast, they claimed that the own-region (Heat Wave hypothesis) was economically significant and more important than the Meteor Shower hypothesis. Finally, Melvin and Melvin (2003) claimed that (Engle et al., 1990)’s research used normal daily exchange rates for the New York and Tokyo markets, and found that this data did not reflect the actual behaviour of both markets. Consequently, they based their analysis on high frequency data, simply to achieve more accurate results than(Engle et al., 1990).

In Europe, Nikkinen et al. (2006) investigated the level of linkages among the most active financial markets in Europe. The performance of the Swiss franc, the Sterling pound and the Euro exchange rates against the U.S. dollar were chosen for the period from Oct 2001 to Sep 2004 to find any inter-dependency among the three markets. A vector autoregressive (VAR) model and Granger causality were used to trace the volatility spillover across the markets. A significant volatility spillover was identified between the three exchange rates and, interestingly, the Euro was found to dominate the other exchange rates. Further, the franc and the pound did not have a remarkable impact on the Euro during the sample period. Econometrically, they stated that employing Granger causality could help researchers in detecting the number of possible lags among the direction of causalities and volatilities. Further, impulse response shock can easily trace more than one variable of volatility over time to identify the evolution after any particular shock. What is more, applying variance decomposition generated all the information that describes the amount

<sup>8</sup>The test was proposed by (Cheung & Ng, 1996)

<sup>9</sup>The distinct regions (Asia, Asia & Europe, Europe, Europe & America and America)

of contribution of each variable across the VAR system. Consequently, Nikkinen et al. (2006) claimed that adopting a VAR model provides simple and clear estimations, and has great power to forecast the volatility spillover. By contrast, the VAR model still has a controversial issue, in that reordering the variables within the system could lead to wide changes in the coefficients and residuals value and, hence, spurious results (Stock & Watson, 2001).

However, Inagaki (2007) applied a residual cross-correlation function (CCF) model<sup>10</sup> to examine the linkages between the Euro and the British pound against the U.S. dollar between Jan 1999 and Dec 2004. The results suggested that the Euro dominated the pound over the sample period, and that the pound simply received the volatility without any significant volatility transmission. Inagaki (2007) stated that applying the Granger causality test, which relies on multivariate (GARCH), could be complicated, due to the possible uncertainty in the test. By contrast, he claimed that applying residual cross-correlation function has many advantages. For instance, the model does not have simultaneous equations, as in the multivariate GARCH models, and is simple to apply.

In the same field, Kitamura (2010) and Zhang et al. (2008) studied the level of interdependency among different global exchange rates. The latter research investigated the volatility spillover in the Asian context. Both studies claimed with confidence that volatility spillover across financial markets is statistically significant and considered to be a good indicator for decision makers.

However, a seminal work by (Diebold & Yilmaz, 2009) was introduced to measure the return and volatility spillover across global equity markets. They built a simple and intuitive test to measure the level of interdependence among asset returns or volatilities. Their approach was based on the VAR model, but they used a very different method to analyse the data. A variance decomposition method associated with N-variable VAR model was employed to build "the spillover index". They analysed seven developed stock markets (France, Hong Kong, UK, Germany, Australia, U.S. and Japan) and twelve developing markets (Turkey, Chile, Argentina, Taiwan, Philippines, South Korea, Mexico, Brazil, Thailand, Singapore, Malaysia and Indonesia) between Jan 1992 and Nov 2007. Two types of results were analysed (i) static, and (ii) dynamic return/volatility spillover. Their model suggested that return/volatility spillover is statistically significant in both crisis and non-crisis episodes. Their framework is easy to apply and use and, hence, to interpret. By contrast, a remarkable limitation existed in their empirical methodology, in that the VAR model is sensitive for reordering the financial variables, which suggests possible spurious results if the variables are reordered inappropriately. Thankfully, Klößner and Wagner (2014) solved this problem by building a coherent conquering strategy to calculate all the possible orders in the VAR model. They claimed that calculating all the possible orderings for large models could take hundreds or thousands of years on modern computers, but fortunately with their algorithm, the model can be calculated in a short

---

<sup>10</sup>This model was proposed by (Cheung & Ng, 1996).

time. Unfortunately however, despite all the positive attributes of the algorithm, it still has some drawbacks as it is difficult to apply and needs high quality computers to run.

In the same research area, McMillan and Speight (2010) investigated the Euro against three currencies (the pound, yen and U.S. dollar) from Jan 2002 to April 2006 through Diebold and Yilmaz's methodology. Their results suggested a significant interdependence among the exchange returns and volatilities across the data set. The spillover index indicated that the euro-dollar was dominating the other two exchange rates, while the euro-pound and the euro-yen had a slight impact on the euro-dollar exchange rate. Nevertheless, McMillan and Speight (2010) claimed that univariate and multivariate GARCH were not fully efficient as a spillover index. For instance, the GARCH family models have several forms to detect many different characteristics in financial data, but there is no particular model that can capture most of these characteristics. Further, multivariate GARCH, for example, have a large number of parameters in the system. By contrast, McMillan and Speight (2010) stated that the spillover index approach is easy to apply and simple to interpret. Also, the VAR model and variance decomposition method allowed for gathering spillover effects across markets into a single spillover measure. Since Diebold and Yilmaz introduced their own method, many researchers have supported their approach in the literature. For more details about studying the exchange rate volatility spillover through Diebold and Yilmaz methodology, see (Antonakis, 2012; Bubák et al., 2011; Liow, 2015; Louzis, 2015). The data sets of the latter studies have covered various regions around the world, such as Asia and Europe, Europe and the G7 countries<sup>11</sup>, America and South Africa and central Europe. All the results support the volatility spillover index, particularly, and the linkages between markets, generally.

Diebold and Yilmaz (2012) developed a further version of their 2009 published work. The main limitation in their 2009 approach was the variable ordering in the VAR system. Fortunately, the gap was bridged by generalising the vector auto regressive framework. Now, forecast-error variance decompositions are invariant to the ordering problem in the VAR system. They employed the new approach to analyse the volatility spillover between four U.S. financial assets: commodities, bonds, stocks and foreign exchange. Positively, their model found significant volatility transmission across markets, and the results were more accurate and reliable than the previous research<sup>12</sup>. More details will be discussed in the methodology section.

In 2018, Baruník and Křehlík introduced a model for analysing the frequency dynamics of connectedness in financial markets, which was slightly similar to (Diebold & Yilmaz, 2012)'s approach. The main difference was that this model relied on a spectral representation of variance decomposition which calculated the model based on frequency analysis, not on impulse response shocks as Diebold and Yilmaz had done. The frequency domain enabled study of the connectedness across markets in the short-run, medium-run or

---

<sup>11</sup>G-7 countries are: Japan, USA, Germany, Italy, UK, France and Canada.

<sup>12</sup>(Diebold & Yilmaz, 2009)

long-run. They studied the intra-market linkages of seven U.S. stocks and, interestingly, the results indicated that volatility transmission was detected by the model at different levels of frequencies.

Turning to the cryptocurrencies market, Kurka (2017) investigated the interconnectedness among the cryptocurrency market and a bundle of traditional assets. (Diebold & Yilmaz, 2009, 2012) and (Baruník et al., 2016) methodologies were applied to a group of assets (Bitcoin, foreign exchange rate, commodities, stock indices and bonds) to detect the linkage between Bitcoin and other assets from Jun 2011 to Dec 2015. Interestingly, they found a very low level of linkage between Bitcoin and other assets, except gold, which received several shocks from Bitcoin during that period. They claimed that the results provided useful information to assist portfolio managers to make their diversification decisions.

In the same field, Corbet et al. (2018) investigated the linkage amongst three major cryptocurrencies and other financial assets to find a relationship between cryptocurrency and other markets. A generalised variance decomposition method (Diebold & Yilmaz, 2012) and a time domain approach (Baruník & Křehlík, 2018) were employed to investigate the connectedness amongst the assets, either through one period along the sample span or at different frequencies, respectively. Interestingly, although they found high levels of linkages among the cryptocurrencies, there was very low connectedness between the cryptocurrencies and the other financial assets. Their analysis suggested that the cryptocurrencies market contains its own risk which is hard to hedge against. In addition, Bouri et al. (2018) studied the level of linkage between particular cryptocurrencies and four major financial assets<sup>13</sup> in both bear and bull market conditions to identify the relations between Bitcoin and conventional investments. They employed a VAR-asymmetric GARCH model to analyse daily data from July 2010 to Oct 2017 in order to capture the linkages among the financial assets. Surprisingly, their analysis suggested that Bitcoin and the commodities markets were not completely isolated from one another. Also, the results clearly showed that Bitcoin was receiving shocks more than transmitting them to other markets.

Moving to energy and technology companies, Symitsi and Chalvatzis (2018) applied an asymmetric multivariate VAR-GARCH model to daily data between Aug 2011 and Feb 2018, to identify the interdependence between Bitcoin and technology companies<sup>14</sup>. Their results indicated remarkable volatility spillover in the short-run from the energy and technology markets to the Bitcoin market. By contrast, volatility spillover from the Bitcoin market to other markets was found to be significant in the long run. Consequently, they admitted that the low correlation of Bitcoin with the other assets indicated that a

---

<sup>13</sup>equities, bonds, currencies and commodities

<sup>14</sup>S&P Global Clean Energy Index (SPGCE), the MSCI World Information Technology Index (MSCIWIT), and the MSCI World Energy Index (MSCIWE)

portfolio could gain higher returns and lower risk, compared with a portfolio that did not invest in Bitcoin.

This section has shown most of literature concerned with the volatility spillover of foreign exchange rates across different regions around the world. The next section will discuss the most applied methodologies in the literature.

### **2.2.4 Critical evaluation of research strategies**

This section contains a critical evaluation of the main methodologies and approaches that have been applied in the research field. Previous studies have indicated that the VAR model and GARCH family models are the most applied methodologies with regard to volatility spillover analysis (Soriano & Climent, 2005).

#### **2.2.4.1 GARCH model**

An auto-regressive conditional heteroskedastic (ARCH) model has provided a huge advantage in forecasting financial time series. The two main characteristics of the model are that it detects “volatility clustering” easily and that the error term is assumed to be non-constant over time (Engle, 1982). A later model was developed by Taylor (1986) and Bollerslev (1986) independently to cover the shortcomings of the ARCH model. Thus, the GARCH model has been extensively employed to study volatility connectedness across markets, assets or/and countries. The main approaches are Univariate GARCH, and Multivariate GARCH.

The univariate GARCH method can be defined as a class of specifications which analyse past and current information (error term) to forecast the behaviour of financial variables (Brooks, 2014). A huge number of extensions have been developed to deal with the complexity of financial data. Specifically, spill-over volatility has been studied intensively through GARCH. For instance, T-GARCH, E-GARCH and GJR-GARCH have been employed to study the volatility connectedness across financial markets, for example, (Cheung & Ng, 1996; Hamao et al., 1991; Inagaki, 2007; Lin et al., 1994). The univariate GARCH process is claimed to be easy and simple. Moreover, the model is less complicated than multivariate models, and the computation process is more robust (Inagaki, 2007). By contrast, the main disadvantage of the univariate model is that ignoring the covariance between the series will lose lots of important information. Consequently, researchers have inclined towards multivariate GARCH to analyse the correlation among time series. The later model has proven its success in forecasting the interdependence between financial variables, and that it is better than the univariate GARCH models (Antonakakis, 2008).

The multivariate GARCH method is an n-variate process that extends from the univariate model to permit the n-dimensional conditional covariance matrix depending on the data

set (Engle & Kroner, 1995). This model has helped research to grow rapidly after solving the difficulties in the previous model. Many extensions have been employed to study the volatility interdependence among financial markets, such as (F-ARCH, CCC, VECM, DCCC and MGARCH) (Patnaik, 2013; Zhang et al., 2008). Multivariate GARCH has proven its success over univariate GARCH because of its power when dealing with multi-series and finding the correlations among them. One of the extensions, called the dynamic conditional correlation (DCC) model, is as elastic as the univariate model with less computation compared with other multivariate models (Antonakakis, 2008). By contrast, MGARCH provides some strong inference in analysing co-volatilities cases, but the model has different extensions that capture different problems in financial data, so that it is becoming more complex to employ all extensions within one case study. Moreover, using MGARCH requires a particular level of the correlation existence among financial variables; otherwise the results will be false. In this regard, researchers have tried to build a more effective and flexible model that can describe the behaviour of financial variables in a more flexible way as a vector auto-regressive model.

#### 2.2.4.2 Vector Auto-regression (VAR) method

The VAR model is considered to be a combination of models, between simultaneous equations and a univariate system that can be compressed into a particular system (Brooks, 2014). The VAR model was proposed by (Sims, 1980) to develop the VAR system regarding the correlation and interdependence amongst different variables within the system. With regard to volatility spillover across markets, the model can be analysed via three main approaches: Granger causality, variance decomposition and impulse response shock. The VAR model has been applied widely (Bubák et al., 2011; Diebold & Yilmaz, 2009; Kavli & Kotzé, 2014; Liow, 2015) and supports the results of (Sims, 1980) and many others. However, the model suffers from some disadvantages, such as the sudden growth of the unknown coefficient when the system analyses large numbers of variables (Stock & Watson, 2001). Further, the order of the variables has a huge impact on the output results, whereby changing the order of the variables could lead to spurious results. For more details see (Diebold & Yilmaz, 2009; Kilian, 1999). The model applied in this study was developed by (Diebold & Yilmaz, 2009), who significantly solved some of the aforementioned shortcomings of the VAR model. Intuitively, Diebold and Yilmaz (2012) modified their approach by generalising the vector auto regressive model to solve the variable order problem.

To summarise, Bitcoin exchange is becoming a fundamental tool in economies worldwide and has had a significant impact across financial markets. Thus, finding a coherent methodology to study the volatility spillover across financial markets is necessary, and essential to support the final decision over investing in Bitcoin or different financial assets.

### 2.2.4.3 Conclusion

To conclude, financial assets (exchange rates, stocks or bonds) play an important role in the world economies, in that they have a remarkable impact on both the hosted economy and other related economies. In the first section, the volatility spillover effect was defined, and the root of the definition was traced. Then, a brief discussion clarified the most important theory "Heat Waves and Meteor Shower" on which volatility spillover is based. In the third section, the literature was reviewed chronologically to identify the main research into the Bitcoin and exchange markets stream across different areas of the world. Finally, the two most applied methodologies in the literature, the GARCH family and the VAR model, were addressed and compared briefly.

## 2.3 Data and summary statistics

Bitcoins are traded in a number of currencies in a number of exchanges across different countries. For the purpose of our analysis, we limit our sample to 5 Bitcoin/currency pairs with less than 26 percent missing values over the sample period. That is, the U.S. dollar (USD), Australian dollar (AUD), Canadian dollar (CAD), Euro (EUR), and British pound (GBP). Although Bitcoins in USD, AUD, CAD, and EUR have started trading before December 1, 2011, Bitcoins in GBP started trading from January 1, 2012. For Bitcoin in CAD and EUR there are some missing closing prices during the early years in the sample period. Thus, the availability of the daily closing prices varies across different currencies.<sup>15</sup> Moreover, to lend comparison to the empirical results of Cheah et al. (2018) who investigate cross-market long-memory interdependency in Bitcoin prices, we limit our observation period span to March 12th 2013 to January 31st 2018. We collect data from the aggregation website Bitcoin Charts (bitcoincharts). Data prior to 25/2/2014 are collected from Mt.Gox. Subsequent to Mt. Gox closure the remaining observations were collected from other exchange platforms such as Bitstamp (the largest European Bitcoin exchange) and LocalBitcoins.<sup>16</sup>

Daily continuously compounded returns are computed by taking the first difference of log-transformed close price series. Our chosen measure of volatility is Parkinson's High-Low historical volatility (HL-HV) model.<sup>17</sup> The reasons for choosing this approach are twofold. First, the HL-HV model deals with sensitivity to trading hours more efficiently than the more intuitive close-to-close volatility model (Bennett & Gil, 2012). Second, this

<sup>15</sup>Initially, we gained price data in various currencies after considering the length of observation, the frequency of non-trading date as well as trading volume. The five exchange markets considered in our work still cover more than 80% of market trading, which can fairly represent the whole market.

<sup>16</sup>At the time of undertaking the estimation, we gathered data from various sources so as to allow us to construct a continuous time series data. It's possible that different websites report slightly different prices. Our estimation showed no significant differences in the estimates.

<sup>17</sup>Following an anonymous referee's suggestions, an alternative measure of volatility, viz., Garman-Klass measure - has been used for robustness exercise. The results are discussed in Section 4.3.2.

model generates more significant information and improves the efficiency of the volatility estimate (Parkinson, 1980). Consequently, Bennett and Gil (2012) claim that Parkinson's volatility measure is more efficient and productive than popular close-to-close volatility estimates.

Formally,  $V$  for each of our five Bitcoin to currency exchange rates is calculated as follows.

$$V = 100 \times \left( \frac{1}{4 \ln(2)} \cdot \ln \left( \frac{h}{l} \right)^2 \right) \quad (2.1)$$

where  $h$  and  $l$  are the highest and lowest exchange rates on a given trading day, respectively. The estimator above computes the daily variance, hence, the corresponding estimate of the annualised daily percent standard deviation (volatility) is computed as follows:

$$Vol = \sqrt{365 * V}$$

Given their temporal dimension, all return and volatility series are checked for stationarity with the help of Augmented Dicky Fuller (ADF) and Philips-Perron (pperron) unit root tests (Dickey & Fuller, 1979; Phillips & Perron, 1988). Results are presented in Tables A.1 and A.2 (for returns and volatility, respectively) in appendix A. Both tests suggest to systematically reject the null of the presence of a unit root with 99% confidence for every daily returns series (Table A.1), suggesting the latter are stationary. Similarly, the null is rejected at the 1% threshold for all tests carried out on exchange rate volatility series (Table A.2), and we conclude that our volatility series are also stable.

Table 2.1 provides summary statistics of the individual daily returns series (upper panel) and volatility (lower panel). The returns series are plotted in Figure 2.1. Average daily returns are similar across individual series and range from about 0.3 (BTC/USD, BTC/EUR and BTC/GBP) to around 0.34 (BTC/AUD). Median daily returns are systematically lower than average ones, hinting at potentially asymmetrically distributed series. Indeed, Bitcoin to USD (BTC/USD) and Bitcoin to GBP (BTC/GBP) exchange rates returns exhibit a small negative skew, suggesting a slightly larger concentration of observations to the right of their central tendency, while all other series are characterised by a positive third statistical moment (long right tails), although it is very close to zero for BTC/AUD and BTC/CAD returns.

All returns series display unequivocally leptokurtic behaviours with sample Kurtosis above 10 (up to 45 in the case of BTC/EUR), suggesting they have long tails representing occurrences of extreme events of highly variable magnitudes with a mass point around the central tendency. The latter observation is confirmed by the graphs presented in Figure 2.1. Overall, the BTC/USD and BTC/EUR returns series appear to be the most stable with maximum values of 30.8 and 77.3 for minima of -34.5 and -61.8, respectively, along with sample standard deviations at least twice as small as that of any other series under scrutiny. The BTC/CAD exchange rate returns exhibit the most widely spread

Table 2.1 Summary statistics, exchange rate returns and volatility

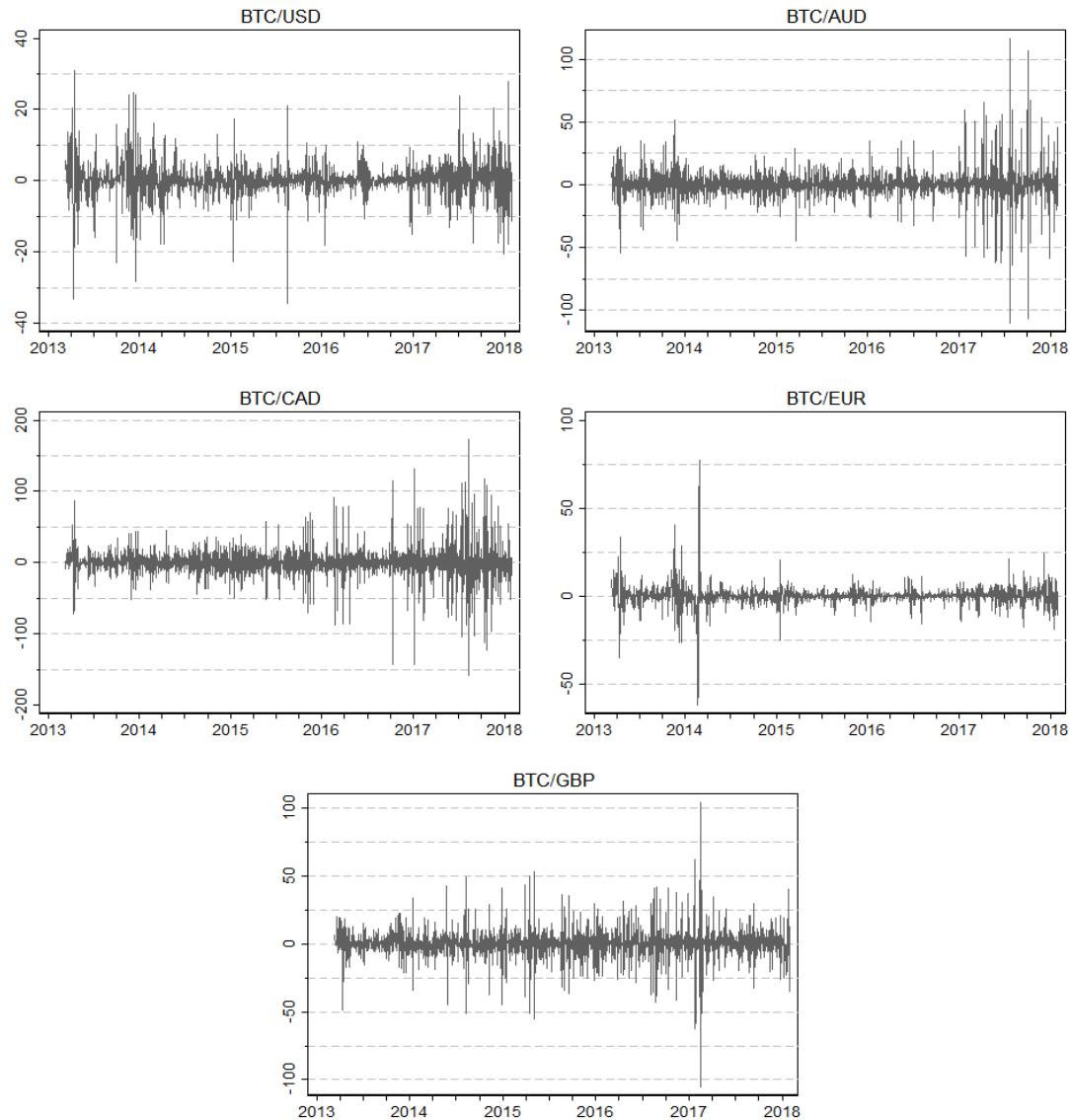
Cross-market exchange rate							
(a) Returns	Mean	St. Dev.	Median	Max	Min	Skewness	Kurtosis
BTC/USD	0.307	4.929	0.225	30.83	-34.54	-0.357	11.69
BTC/AUD	0.344	12.35	0.205	116.7	-110.6	0.0326	22.75
BTC/CAD	0.321	22.31	0.276	172.5	-157.7	0.0315	14.38
BTC/EUR	0.308	5.776	0.266	77.29	-61.84	0.763	45.55
BTC/GBP	0.304	11.30	0.301	104.3	-105.4	-0.149	16.38
(b) Volatility							
BTC/USD	0.709	1.008	0.455	20.68	0	9.086	139.2
BTC/AUD	6.091	4.467	4.426	30.67	0.105	1.499	5.329
BTC/CAD	7.248	4.681	6.284	30.01	0	1.054	4.330
BTC/EUR	0.740	0.899	0.472	11.29	0.0698	4.899	39.67
BTC/GBP	9.298	6.378	7.688	69.04	0	2.639	17.65
Number of observations	1786						

distribution (minimum return of -157.7 for a maximum of 172.5) and are also characterised by the largest standard deviation in the sample (over 22). Plots in Figure 2.1 suggest that the instability of the BTC/CAD returns series is most notably due to the large number of extreme events since early 2017, a feature that is noticeable in the BTC/AUD returns too, and also on the BTC/USD market, though to a lesser extent. At a glance, graphs in Figure 2.1 reveal frequent bouts of highly volatile returns which seem to be fairly evenly distributed on either side of their long run central tendencies, with the BTC/USD and BTC/EUR markets being the most stable.

The summary statistics of cross-market exchange rates volatility (lower panel of Table 2.1) comfort our previous intuitions. The average volatility of BTC/USD and BTC/EUR settles at around 0.7 and is smaller than that of other exchange rates by one order of magnitude (from around 6 for BTC/AUD to over 9 for BTC/GBP). Furthermore, the two aforementioned series exhibit much larger positive skews and higher Kurtosis than their counterparts, and such leptokurtic and heavily right skewed distributions suggest that these markets are less prone to unusually high levels of volatility. That is, observations concentrate to the left of the distribution close to the central tendency (recall that volatility is always positive).

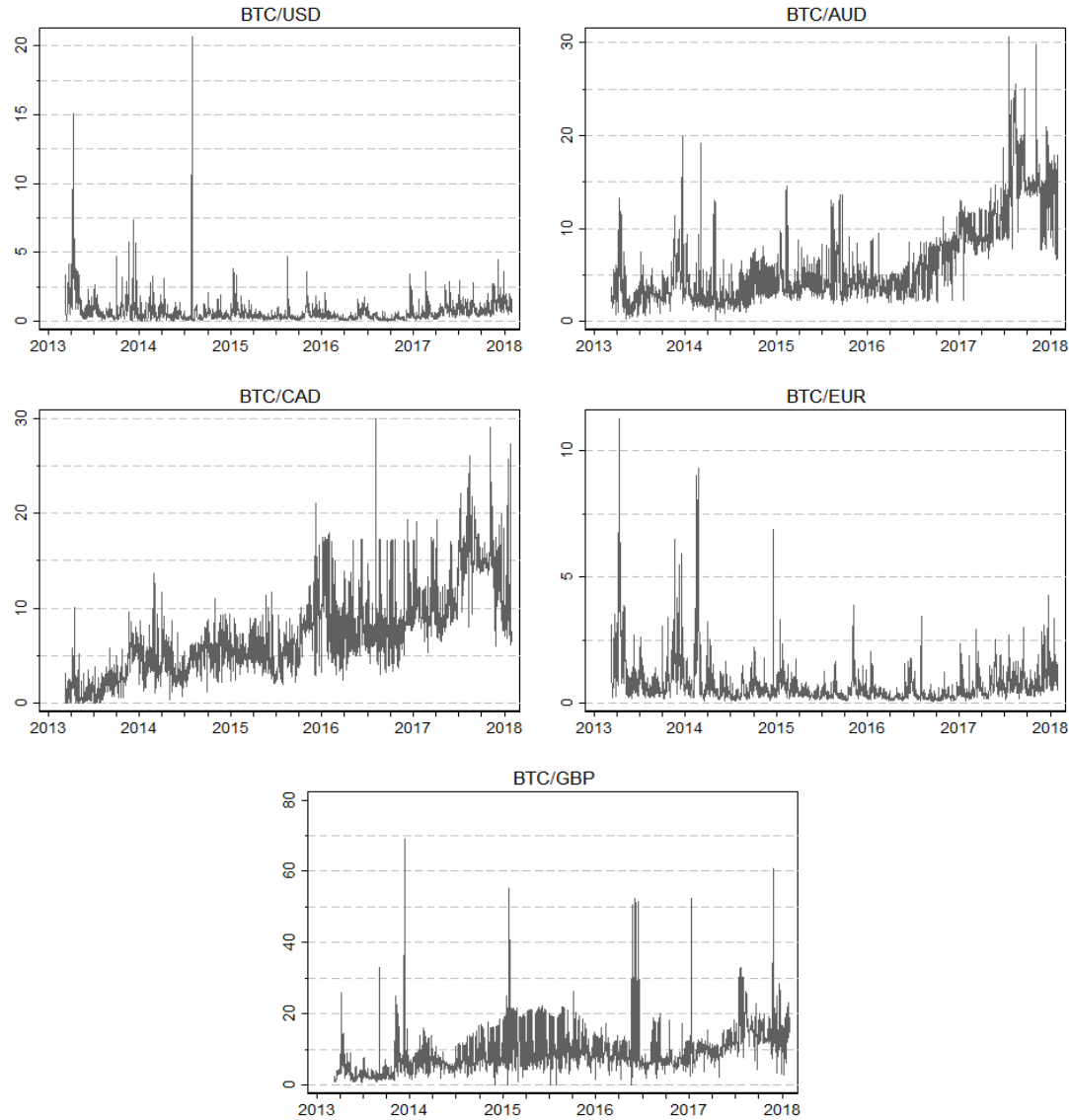
While confirming that the BTC/USD and BTC/EUR markets are the most stable over the period of study, Table 2.1 strengthens the idea that the BTC/GBP has experienced the most extreme occurrences of high uncertainty, as witnessed by the scale of the y-axis on the graph presented in Figure 2.2. Interestingly, the series plotted in Figure 2.2 show a seemingly upward trend in the volatility of BTC/CAD over time which also appears in BTC/AUD volatility from the end 2016 on. An apparent increase in average volatility also appears on the three other markets in 2017 and early 2018, although to a lesser extent.

Figure 2.1 Exchange rate returns



*Note:* Exchange rate returns series, daily. Dates on the x-axis indicate the start of the year, and ticks are quarterly.

Figure 2.2 Exchange rate volatility



*Note:* Exchange rate volatility series, daily. Dates on the x-axis indicate the start of the year, and ticks are quarterly.

## 2.4 Methodology

We follow the generalized variance decomposition approach developed in Diebold and Yilmaz (2012) in order to estimate returns and volatility spillovers across the five markets under scrutiny. This methodology provides both static and dynamic measures of spillovers, and several papers have used a similar empirical framework analyse the interconnectedness of financial markets (e.g. Corbet et al., 2018; Fernández-Rodríguez et al., 2016; Lucey et al., 2014; Yarovaya et al., 2016). However, to the best of our knowledge no previous research has analysed cross-market returns and volatility spillovers on Bitcoin to currency exchange rates.

The variance decomposition approach to measuring return and volatility spillovers (first presented in Diebold and Yilmaz (2009)) exploits Cholesky factorisation methods. This produces orthogonal innovations as is typically required for variance decompositions in Vector Auto-Regressive (VAR) models, with the main drawback of being sensitive to variable ordering (Diebold & Yilmaz, 2009). Diebold and Yilmaz (2012) propose a so-called generalised variance decomposition (GVD) that allows them to alleviate the orthogonality condition altogether and to account for correlated innovations, hence improving on their previous effort by making their measure of spillovers invariant to the order of the variables in the system (Diebold & Yilmaz, 2012; Koop et al., 1996; Pesaran & Shin, 1998). Considering our case of investigation - the five market Bitcoin price system - the estimates of spillover are based on the following covariance-stationary VAR model:

$$y_t = \sum_{i=1}^p \mu_i y_{t-i} + \epsilon_t \quad (2.2)$$

where  $y_t = (y_{1t}, y_{2t}, y_{3t}, y_{4t}, y_{5t})$  or is a  $(1 \times 5)$  random vector of endogenous variables;  $\mu$  is a  $(5 \times 5)$  coefficient matrix;  $y_{t-1}$  is the previous realisation of  $y_t$ ; and  $\epsilon_t = (\epsilon_{1t}, \epsilon_{2t}, \epsilon_{3t}, \epsilon_{4t}, \epsilon_{5t})$  is an *i.i.d.* error term with  $\epsilon_t \sim (0, \Sigma_\epsilon)$ .

The VAR model in Equation 2.2 can be re-written as a moving average process as follows:

$$y_t = \sum_{i=0}^{\infty} \delta_i \epsilon_{t-i} \quad (2.3)$$

where  $(5 \times 5)$  coefficient matrices  $\delta_i$  depend on the recursion  $\delta_i = \mu_1 \delta_{i-1} + \mu_2 \delta_{i-2} + \dots + \mu_p \delta_{i-p}$  with  $\delta_0$  an identity matrix and  $\delta_i = 0$  if  $i < 0$ .

The heart of the GVD approach is to generate the correlated shocks by using the past distribution of errors (Diebold & Yilmaz, 2012). Therefore, the h-step-ahead forecast error GVD matrix is given by:

$$\tau_{ij}^g(h) = \frac{\sigma_{ii}^{-1} \sum_{h=0}^{h-1} (e_i' \delta_h \Sigma e_j)^2}{\sum_{h=0}^{h-1} (e_i' \delta_h \Sigma \delta_h' e_j)} \quad (2.4)$$

where  $e_i$  is the selection vector with its  $i^{th}$  element equal to one and zeros otherwise;  $\delta_h$  is the coefficient matrix times the h-lagged shock vector;  $\Sigma$  is the variance matrix of the error vector  $\epsilon$ ; and  $\sigma_{ii}$  is the  $i^{th}$  diagonal element of  $\Sigma$ .

The shocks generated through Equation 2.4 are not required to be orthogonal, so the sum of forecast error variance contributions are not equal to one, i.e.  $\sum_j \tau_{ij}^g(h) \neq 1$ . Therefore, to utilise the shares available in the variance decomposition matrix with the spillover calculation, the authors propose to normalise the above variance shares as follows:

$$\tilde{\tau}_{ij}^g(h) = \frac{\tau_{ij}^g(h)}{\sum_{j=1}^N \tau_{ij}^g(h)} \quad (2.5)$$

where  $g$  is the order of the system (such as five market system as in our case),  $\sum_{j=1}^N \tilde{\tau}_{ij}^g(h) = 1$  and  $\sum_{i,j=1}^N \tilde{\tau}_{ij}^g(h) = N$ .

The quantities in equation 2.5 can then be used directly to estimate several measures of interest as follows:

- **Total spillover:**

$$S.O^g(h) = \frac{\sum_{\substack{i,j=1 \\ i \neq j}}^N \tilde{\tau}_{ij}^g(h)}{\sum_{i,j=1}^N \tilde{\tau}_{ij}^g(h)} \times 100 = \frac{\sum_{\substack{i,j=1 \\ i \neq j}}^N \tilde{\tau}_{ij}^g(h)}{N} \times 100 \quad (2.6)$$

- **Directional spillover:**

The following quantity measures the extent to which variable  $i$  is influenced by volatility shocks received from all other variables:

$$S.O_i^g(h) = \frac{\sum_{\substack{j=1 \\ j \neq i}}^N \tilde{\tau}_{ij}^g(h)}{\sum_{j=1}^N \tilde{\tau}_{ij}^g(h)} \times 100 \quad (2.7)$$

Similarly, the amount of volatility transmitted by variable  $i$  to the other variables in the system can be gauged as follows:

$$S.O_{.i}^g(h) = \frac{\sum_{j=1}^N \tilde{\tau}_{ji}^g(h)}{\sum_{j=1}^N \tilde{\tau}_{ji}^g(h)} \times 100 \quad (2.8)$$

- **Net spillover:**

Finally, subtracting volatility spillovers *from* other variables from the volatility spillovers *to* other variables gives a measure of net spillovers:

$$S.O_i^g(h) = S.O_{.i}^g(h) - S.O_{i.}^g(h) \quad (2.9)$$

In order to refine our empirical study, we also implement the methodology presented in Baruník and Křehlík (2018) that builds on a *spectral representation* of variance decompositions to identify connectedness amongst variables at various levels of frequency. That way, the authors extend the work of Diebold and Yilmaz (2012) by offering the possibility to explore the frequency dynamics in a system of variables and thus to estimate spillovers of heterogeneous magnitudes at different frequencies. In other terms, the strength of cross-market connectedness can vary across the frequency domain, i.e. the influence of idiosyncratic shocks on other variables might be limited to the short run or have a long-run impact on connected markets.

## 2.5 Results

Having discussed thus far various approaches to estimate spillover effects, in this section, we discuss results to shed light on the predictive power of each Bitcoin market. The basis for our estimation of spillovers are VAR models for daily returns and exchange rate volatility. We use Akaike's Information Criterion (AIC) to decide on the number of lags to include, and confirm its adequacy with Lagrange multiplier auto-correlation tests after VAR estimation. We chose a VAR order 17 and 7 for returns and volatility series, respectively. The Generalised Variance Decomposition is then carried out for 30-day-ahead forecasts.

We comment on the results for volatility spillovers and returns spillovers in two distinct sub-sections. Indeed, the former provide indications as to which components of the system are closely connected to each other given their sensitivity to one another's uncertainty. Returns spillovers, however, reveal more precise information regarding which components of the system are most important in *predicting* future price movements on other markets. Each set of results includes a full sample *static* analysis broken down into *directional connectedness* (from applying the method of Diebold and Yilmaz (2012)) and *frequency domain connectedness* (following Baruník and Křehlik (2018)), the latter allowing to refine the former by providing a decomposition of time-frequency dynamics of returns and volatility spillovers. However, in a full sample analysis the alternation of positive and negative extreme events typical of financial markets – some short-lived and others more persistent that can generate important downturns or speculative bubbles – tends to be smoothed over time. Therefore, we complement our results by carrying out an analysis similar to the former on a sub-sample of the data that is rolled over one day at a time to obtain a picture of *dynamic spillovers*. This methodology suggested by Diebold and Yilmaz (2012) allows to gauge how the strength of cross-market connectedness evolves over time. We use a 150-day rolling window. Finally, various robustness checks are discussed in the third sub-section.

### 2.5.1 Volatility spillovers

Table 2.2 displays results of the full sample analysis on directional, net and total spillovers for exchange rate volatility. The markets under consideration exhibit a non-trivial degree of interconnectedness with a *total spillover index* (TSI) of 15.78%. It appears that volatility shocks to the BTC/EUR and BTC/USD markets are the most influential in their contribution 'TO other' markets' volatility (24.8% and 25.9%, respectively), with BTC/AUD in third position (around 17%).

Table 2.2 Volatility spillovers across five selected exchange rates in time domain

	BTC/USD	BTC/AUD	BTC/CAD	BTC/EUR	BTC/GBP	Directional FROM others
BTC/USD	79.16	4.15	0.45	15.32	0.92	20.84
BTC/AUD	4.26	84.40	3.87	6.67	0.79	15.60
BTC/CAD	0.30	6.63	89.99	1.82	1.26	10.01
BTC/EUR	20.74	4.75	0.88	72.17	1.47	27.83
BTC/GBP	0.63	1.39	1.62	0.98	95.37	4.63
Directional TO others	25.93	16.92	6.82	24.79	4.45	<i>TSI:</i> $78.90/500 =$
Net spillovers	5.09	1.32	-3.19	-3.04	-0.18	<i>15.78%</i>

Note: Exchange rates volatility spillovers following Diebold and Yilmaz (2012). Numbers are percentages. “TSI” stands for Total Spillover Index.

### 2.5.1.1 Directional connectedness (static spillovers): Time domain analysis

Interestingly, the BTC/EUR market is also the most sensitive to uncertainty in other exchange rates (highest estimate in contribution ‘FROM others’), and the BTC/USD market the second most sensitive. In contrast, the BTC/GBP is by far the least influenced and least influential market in terms of volatility spillovers. BTC/CAD is also only loosely connected to the system, and is a bit more sensitive to other markets’ volatility than it is influential on others. Negative *net* volatility spillovers for the BTC/CAD and BTC/EUR exchange rates show that, overall, these markets tend to be net recipients of volatility. On the other hand, BTC/USD appears to be a net provider of volatility to the system, with net spillovers around 5%.

A closer look at pairwise spillovers reveals that the strongest bilateral relationship is to be found between the BTC/EUR and BTC/USD exchange rates, with volatility spillovers of about 15% from the former to the latter and little above 20% in the other direction. Both markets also display a non-trivial relationship with BTC/AUD – albeit of lesser intensity – which is almost symmetric in the case of BTC/USD (spillovers little above 4% in either direction) and slightly asymmetric in the case of BTC/EUR with its influence on BTC/AUD (around 6.7%) exceeding its sensitivity (little below 5%). Note that BTC/AUD is also a net provider of volatility to BTC/CAD – for which it is the main partner – and to BTC/GBP, although pairwise spillovers involving the latter never even reach 2%.

In sum, among the five markets under consideration BTC/EUR is the “most” connected one, with BTC/USD close second, while BTC/GBP appears to be the most isolated market. The pair BTC/EUR - BTC/USD are the most closely interlinked exchange rates, with about 15% to 20% of the forecast error variance in either variable’s volatility being explained by innovations in the other. Results also suggest that BTC/AUD might

work as an intermediary allowing volatility to circulate between the main components of the system, i.e. BTC/USD and BTC/EUR, and the more isolated markets, namely BTC/CAD and BTC/GBP.

### 2.5.1.2 Frequency domain analysis of static spillovers

Table 2.3 refines the previous empirical results by providing a decomposition of time-frequency dynamics of volatility spillovers. The top panel considers *short* horizons (less than 4 days), while the bottom panel is concerned with *long* horizons (4 days or more).

**Table 2.3 Volatility spillovers across five selected exchange rates in frequency domain**

(a) *Short horizon*

	BTC/USD	BTC/AUD	BTC/CAD	BTC/EUR	BTC/GBP	FROM others
BTC/USD	35.09	0.38	0.08	3.91	0.16	4.52
BTC/AUD	0.19	23.94	0.23	0.39	0.08	0.88
BTC/CAD	0.07	0.43	42.71	0.35	0.12	0.96
BTC/EUR	2.64	0.39	0.09	22.93	0.11	3.24
BTC/GBP	0.15	0.22	0.14	0.22	58.48	0.74
TO others	3.05	1.42	0.54	4.87	0.47	<i>TSI: 10.34/193.49 = 5.34%</i>

(b) *Long horizon*

	BTC/USD	BTC/AUD	BTC/CAD	BTC/EUR	BTC/GBP	FROM others
BTC/USD	44.07	3.77	0.37	11.41	0.77	16.32
BTC/AUD	4.08	60.46	3.64	6.28	0.71	14.71
BTC/CAD	0.23	6.20	47.28	1.47	1.14	9.05
BTC/EUR	18.09	4.36	0.79	49.25	1.35	24.59
BTC/GBP	0.48	1.17	1.48	0.75	36.89	3.89
TO others	22.88	15.50	6.27	19.92	3.98	<i>TSI: 68.55/306.51 = 22.37%</i>

*Note:* Volatility spillovers, frequency domain analysis following Baruník and Křehlík (2018). *Short* and *Long* horizons refer to ‘4 days or less’ and ‘more than 4 days’, respectively. Numbers are percentages.

The top panel of Table 2.3 shows that overall volatility spillovers in the system are around 5.3% when considering a short time horizon. In line with previous results, BTC/USD and BTC/EUR are the main providers and recipients of short-lived volatility shocks in the system, as well as each other’s most influential counterpart, although in this instance BTC/EUR (BTC/USD) is a net provider (recipient) of volatility to BTC/USD (from BTC/EUR) and to (from) the system as a whole.

The bottom panel of Table 2.3 suggests that interconnectedness in the system is much stronger in the long run, with overall volatility spillovers above 22% for volatility. The earlier pattern of results is once again repeated, and BTC/EUR and BTC/USD are by far

the most influential components of the system and each other's privileged partner, with the former a net recipient and the latter a net provider of volatility. BTC/AUD remains the second favorite counterpart for each of the two main markets – albeit spillovers are of a much smaller magnitude (well below 5%) – and the most important partner of BTC/CAD. As expected, results confirm that BTC/GBP is rather isolated from the system regarding transmissions of either short-run or long-run volatility shocks.

### 2.5.1.3 Dynamic spillover effects: Rolling window estimates

#### (a) Overall spillovers

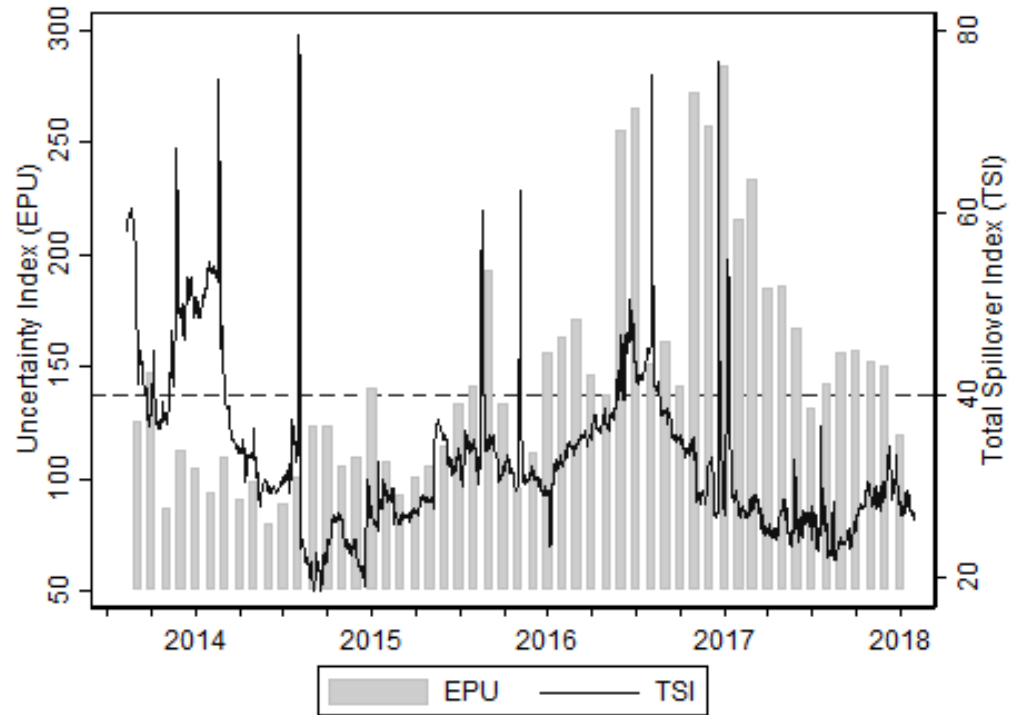
To study how volatility spillovers co-move with fluctuations in uncertainty, we plot overall volatility spillovers in the system in Figure 2.3 along with a monthly index measuring global Economic Policy Uncertainty (EPU)<sup>18</sup>. The TSI ranges between 20% and 40% throughout most of the sample period. We observe a sharp drop from above 50% to below 20% between the first and third quarters of 2014, mirroring with a few months lag the sharp decline in EPU between the summer of 2013 and the spring of 2014. The slow upward trend in TSI from late 2014 until mid-2016 also mimics the overall rise in uncertainty over the same period. The highest values of EPU are found around mid- and late 2016 and early 2017, with an extremely volatile TSI between late 2016 and early 2018.

#### (b) Spillovers FROM and TO others

Volatility spillovers transmitted to other exchange rates, received from others, and net spillovers for each of the five markets under scrutiny are plotted in Figures 2.4, 2.5 and 2.6, respectively. The top left plot of Figure 2.4 confirms the role of BTC/USD as a big provider of volatility to the system over time, with spillovers to others routinely above 10%. Spillovers from BTC/EUR typically oscillate between 2% and 10% except for a 6-month period (2013Q4 and 2014Q1) where they often reach above 15%. Volatility spillovers from BTC/AUD also range between 0 and 10% and often exceed 5%, while those from BTC/CAD typically stay between 0% and slightly above 10%. Volatility shocks to BTC/GBP explain around approximately 5% or less of volatility shocks on other markets during the sample period, except for short periods of time (in 2013Q3 and between 2016Q2 and 2016Q4) where they greatly exceed 10%.

As displayed in Figure 2.5, the sensitivity of the BTC/USD market to uncertainty shocks on other markets is highly volatile between 2013Q3 and 2014Q1 (spillovers ranging from 10% up to 20%) and more stable afterwards, with spillovers from others slowly declining

<sup>18</sup>Data gathered from <http://www.policyuncertainty.com/>.

Figure 2.3 Overall volatility spillovers (dynamic plot) and Economic Policy  
Uncertainty Index

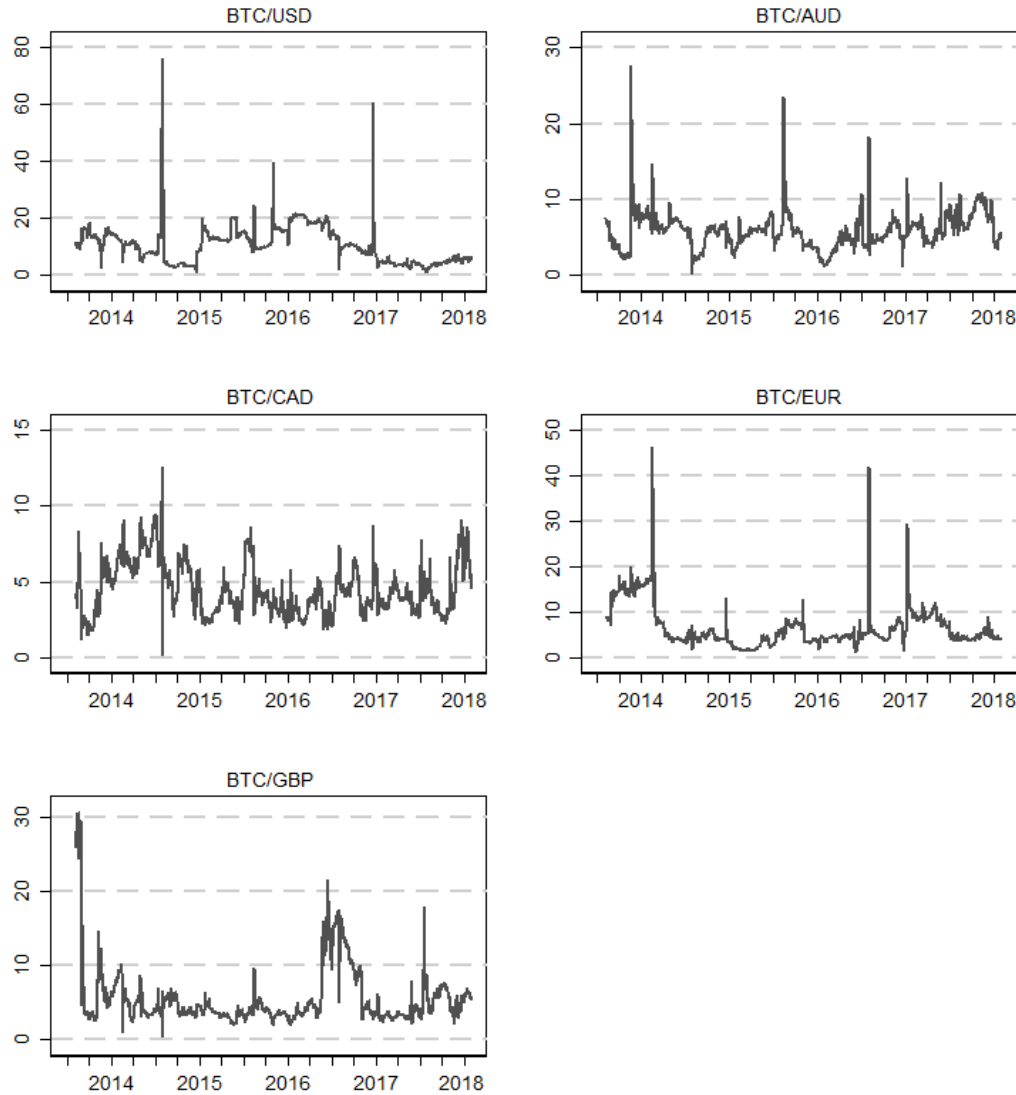
*Note:* Dynamic overall *volatility* spillovers computed following Diebold and Yilmaz (2012) with a 150-day rolling window, right scale (percentages). Monthly Global Economic Policy Uncertainty (EPU) index, left scale. The dashed line shows the median value of EPU over the sample period. Dates on the x-axis indicate the start of the year, and ticks are quarterly.

down to 2.5% in 2014Q4 and remaining between that level and approximately 7% for most of the sample period. The evolution over time of spillovers from others to BTC/AUD resembles that observed for BTC/USD but is more stable, with spillovers from others to BTC/AUD concentrating between 4% and up 6% (approximately). Spillovers to BTC/EUR, however, remain volatile throughout the period under scrutiny and routinely exceed 10% while seldom going below 6%, albeit stabilising between approximately 4% and 7% starting in 2017Q1 until the end of the sample period. Spillovers to BTC/GBP from other markets oscillate between approximately 4% and 10% throughout the sample period, ranging most often between 5% and 10%. The sensitivity of BTC/CAD to volatility shocks on other markets features a similar profile to that of BTC/GBP albeit more unstable, with spillovers seldom below 5% and reaching more often above 10%.

### (c) Net spillovers

The previously described patterns come together in Figure 2.6 to give a picture of the temporal evolution of net spillovers for each exchange rate considered in the present study. We see at a glance that net spillovers tend to oscillate around zero over time, for all

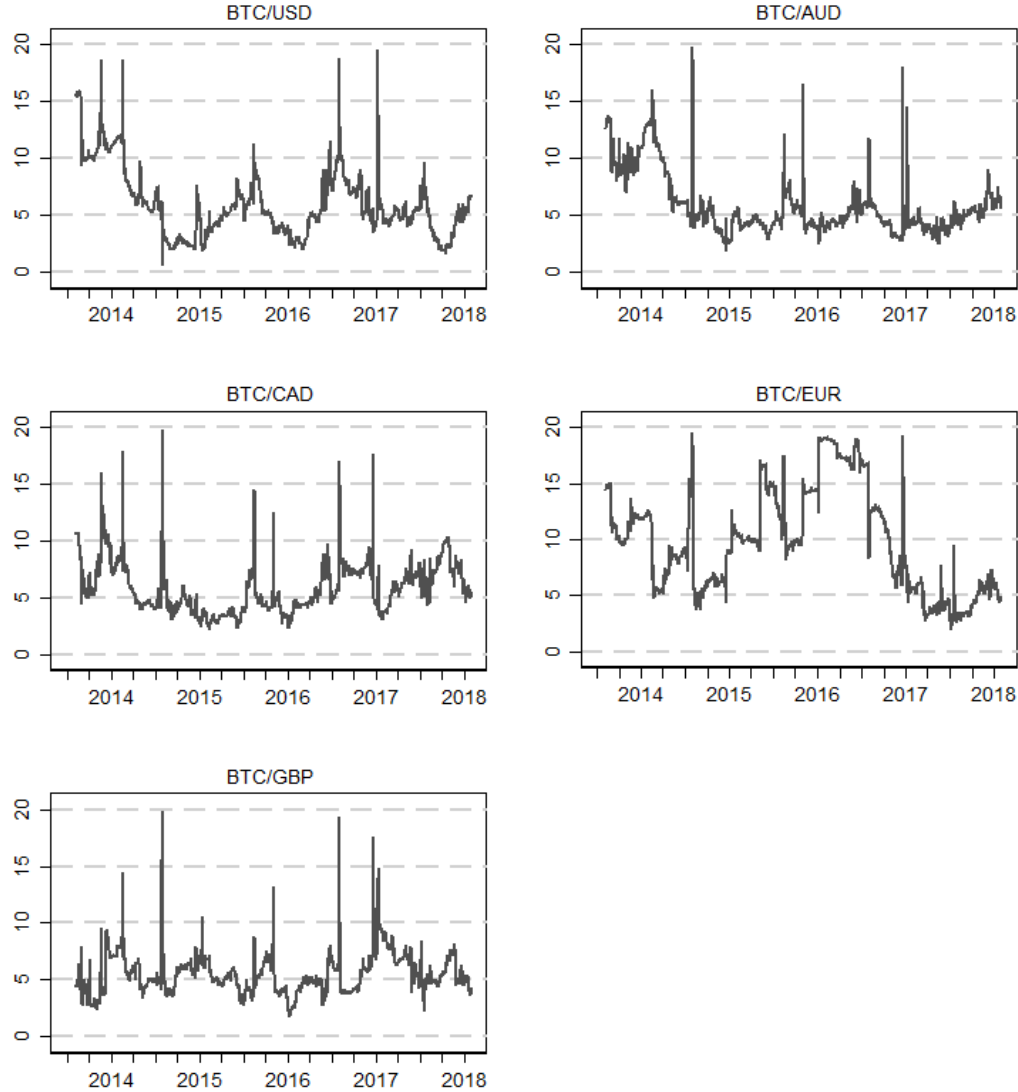
Figure 2.4 Volatility spillovers to others: Dynamic plot



*Note:* Dynamic volatility spillovers *to* others computed following Diebold and Yilmaz (2012) with a 150-day rolling window. Y-scales in percentages. Dates on the x-axis indicate the start of the year, and ticks are quarterly.

markets. Nonetheless, BTC/USD displays mostly positive net spillovers for the sample period, with a long period of exclusively positive values (from 2015Q1 to mid-2016) often around and above 15%. It tends to confirm the role of BTC/USD as a net provider of volatility to the system. Additionally, we identify three brief bouts of extremely high positive net spillovers for BTC/USD in early 2014Q3, early 2015Q4 and late 2016Q4. Interestingly, all other markets feature largely negative net spillovers during these events, making them net receivers of volatility. This observation strengthens the idea that BTC/USD is central in the system as the prime source of uncertainty, with volatility shocks on that market strongly destabilising other exchange rates.

Figure 2.5 Volatility spillovers from others: Dynamic plot

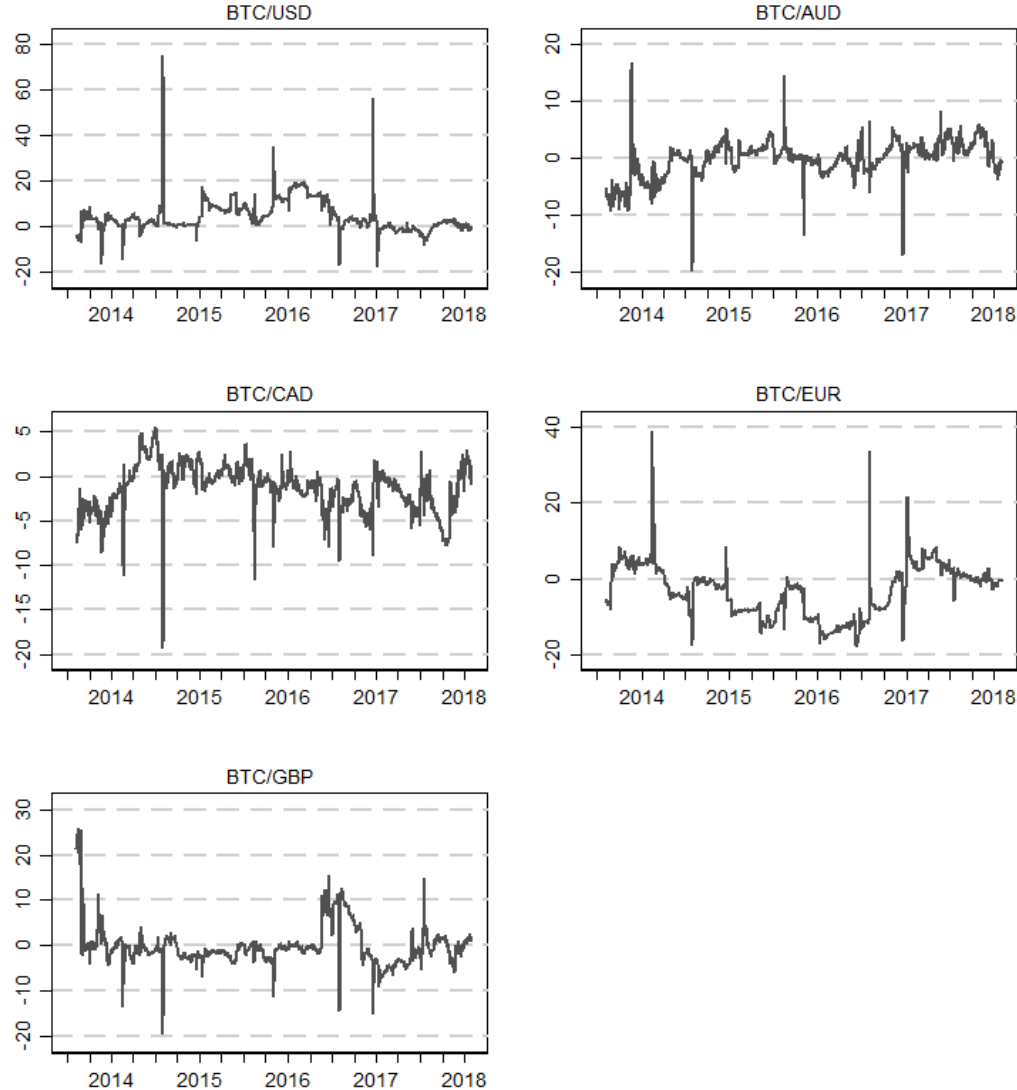


*Note:* Dynamic volatility spillovers *from* others computed following Diebold and Yilmaz (2012) with a 150-day rolling window. Y-scales in percentages. Dates on the x-axis indicate the start of the year, and ticks are quarterly.

The middle right plot of Figure 2.6 clearly shows that BTC/EUR net spillovers are typically negative over the sample period and closely mirror those observed for BTC/USD, especially so during the period identified earlier (from 2015Q1 to mid-2016) when BTC/USD (BTC/EUR) net spillovers are consistently positive (negative) and large. This dynamic spillovers plot ascertains the persistence over time of the role of BTC/EUR as a net recipient of volatility in the system, and also corroborates the “privileged” relationship between BTC/EUR and BTC/USD.

Net volatility spillovers from BTC/AUD are mostly negative between 2013, Q3 and 2014,

Figure 2.6 Net volatility spillovers: Dynamic plot



Note: Dynamic *net* volatility spillovers computed following Diebold and Yilmaz (2012) with a 150-day rolling window. Y-scales in percentages. Dates on the x-axis indicate the start of the year, and ticks are quarterly.

Q2, but this market is typically a net provider of volatility throughout the rest of the sample period. In contrast, net spillovers for BTC/CAD are mostly negative over time, with a pattern mirroring that of BTC/AUD and reminding us of the close relationship between both markets uncovered from the full sample (static) analysis. The BTC/GBP market is characterised by surprisingly high positive net spillovers at the start of the sample period, for a brief amount of time, before experiencing small negative net spillovers most of the time with the exception of the period 2016Q2 - 2016Q4 when net spillovers are again large and positive (with one brief event of extreme negative values corresponding to a bout of high volatility transmission from BTC/USD).

To summarise findings so far, it appears that connectedness between Bitcoin-to-currency exchange markets reflects overall uncertainty. Trading on Bitcoin markets depends largely on investor sentiment, and a lack of confidence eventually heightens volatility on these markets which become more intensely interlinked as investors diversify to mitigate risks pertaining to a particular market. In that respect, BTC/USD is likely a prime source of volatility for the system. Indeed, volatility to BTC/USD and BTC/EUR are the most influential in predicting the volatility of other exchange rates (Figure 2.4), and the BTC/EUR volatility tends to be the most sensitive to innovations on other markets (Figure 2.5). Additionally, the BTC/USD exchange rate is typically a net provider of volatility, which is mirrored by the tendency of the BTC/EUR market to be a net receiver in its connection to other markets, while the influences to and from others for the other three exchange rate volatility series tend to even out (Figure 2.6). Note that Figure 2.6 displays net spillovers that get notably closer to zero over 2017 and in early 2018, especially so for BTC/USD and BTC/EUR.

As was previously stated, we interpret volatility spillovers as being indicative of the *intensity* of cross-market connectedness in the system. In the next section we turn to the results pertaining to exchange rates returns spillovers that contain information on the predictive power of price movements on a given market in influencing prices on other markets.

## 2.5.2 Returns spillovers

### 2.5.2.1 Directional connectedness (static spillovers): Time domain analysis

Table 2.4 presents returns spillovers obtained from the full sample analysis using the method of Diebold and Yilmaz (2012). Returns on the markets under scrutiny feature a significant degree of interdependence reflected by an estimated TSI of 17.4%. Results confirm the predominance of BTC/USD and BTC/EUR in the system, with returns spillovers to other markets of almost 23% and above 24%, respectively. Unexpected changes in returns on the BTC/AUD and BTC/GBP markets contribute roughly the same share of explanatory power in determining forecast error variance in other markets' returns (14.2% and 16.2%, respectively). In the meantime, returns to BTC/EUR are by far the most sensitive to innovations in other markets' returns (31% spillovers from others), while returns on the BTC/USD, BTC/AUD and BTC/GBP markets exhibit about twice as little sensitivity (spillovers from others around 16%).

The above observations establish BTC/USD as having the most predictive power in the system with net spillovers above 6%, and returns to BTC/EUR as experiencing a net influence from unexpected price movements on other markets (negative net spillovers of almost 7%). Returns to BTC/GBP are altogether as influential as they are sensitive, and returns to BTC/AUD are characterised by small negative net spillovers. Note that

Table 2.4 Returns spillovers across five selected exchange rates

	BTC/USD	BTC/AUD	BTC/CAD	BTC/EUR	BTC/GBP	Directional FROM others
BTC/USD	83.58	2.36	1.69	9.60	2.77	16.42
BTC/AUD	3.17	83.97	2.82	5.73	4.32	16.03
BTC/CAD	1.82	1.87	92.54	2.15	1.63	7.46
BTC/EUR	14.26	6.49	2.89	68.92	7.44	31.08
BTC/GBP	3.73	3.50	2.10	6.72	83.95	16.05
Directional TO others	22.97	14.22	9.50	24.19	16.17	<i>TSI:</i> $87.05/500 =$
Net spillovers	6.55	-1.81	2.04	-6.89	0.12	<i>17.41%</i>

*Note:* Exchange rates returns spillovers following Diebold and Yilmaz (2012). Numbers are percentages. “TSI” stands for Total Spillover Index.

BTC/CAD displays small positive net spillovers (around 2%) but its returns are only loosely connected to the system (spillovers to and from others below 10%).

Pairwise returns spillovers show a pattern in line with volatility spillovers discussed earlier: BTC/EUR is typically the most influential partner of every other exchange rate, a fact particularly salient for the BTC/USD and BTC/GBP markets. Additionally, returns to BTC/EUR are especially sensitive to innovations in returns to BTC/USD, the latter therefore holding a net predictive power in that relationship. Other noticeable relationships are BTC/EUR - BTC/GBP – spillovers around 7% in either direction with a small (below 1%) net positive spillover for the second – and BTC/EUR - BTC/AUD – spillovers around 6% in either direction, again with a small (below 1%) net positive spillover for the second. All bilateral relationships involving BTC/CAD display pairwise spillovers below 3%.

This first glance at returns spillovers comforts the idea that the previously identified connectedness (through volatility spillovers) between BTC/USD and BTC/EUR matters, in that the former market holds a net predictive power in determining price movements on the latter. Actually, shocks to BTC/USD returns are the most influential in the system as a whole, and BTC/EUR returns are the most sensitive to shocks on other markets. Note that BTC/GBP is more strongly connected to the system in terms of returns spillovers than it is in terms of volatility. This is likely due to the range of variations in the BTC/GBP returns series being consistent with that of other markets (Figure 2.1), whereas discrepancies are more prominent in the case for volatility series (Figure 2.2).

### 2.5.2.2 Frequency domain analysis of static spillovers

Table 2.5 provides a decomposition of time-frequency dynamics for the returns spillovers presented in Table 2.4. The top panel indicates that overall returns spillovers in the

system are around 14.5% when focussing on short-term components of forecast error variances. The pattern of results is qualitatively similar to the previous case where BTC/USD and BTC/EUR are the most important providers of short-lived shocks to returns in the system, with the latter the most sensitive of such shocks. They are also each other's most influential counterpart, BTC/EUR being a net recipient of unexpected price movements from BTC/USD and from the system as a whole. We find again the previously observed almost symmetric relationships between BTC/EUR and BTC/GBP (spillovers around 5%) and between BTC/EUR and BTC/AUD (spillovers between 4% and 5%).

Table 2.5 Returns spillovers across five selected exchange rates - Frequency domain analysis

(a) *Short horizon*

	BTC/USD	BTC/AUD	BTC/CAD	BTC/EUR	BTC/GBP	FROM others
BTC/USD	64.96	1.52	1.35	5.78	1.89	10.54
BTC/AUD	2.07	81.66	2.66	4.29	3.64	12.66
BTC/CAD	1.50	1.59	90.51	1.50	1.39	5.98
BTC/EUR	9.15	4.96	2.51	53.60	5.73	22.35
BTC/GBP	2.40	2.77	1.75	4.68	81.17	11.59
TO others	15.12	10.83	8.26	16.25	12.65	<i>TSI: 63.11/435.01 = 14.51%</i>

(b) *Long horizon*

	BTC/USD	BTC/AUD	BTC/CAD	BTC/EUR	BTC/GBP	FROM others
BTC/USD	18.62	0.84	0.34	3.82	0.88	5.89
BTC/AUD	1.10	2.31	0.16	1.43	0.68	3.38
BTC/CAD	0.32	0.28	2.03	0.65	0.24	1.48
BTC/EUR	5.11	1.53	0.38	15.32	1.71	8.73
BTC/GBP	1.33	0.74	0.35	2.04	2.78	4.46
TO others	7.86	3.39	1.24	7.94	3.51	<i>TSI: 23.94/64.99 = 36.83%</i>

*Note:* Returns spillovers, frequency domain analysis following Baruník and Křehlík (2018). *Short* and *Long* horizons refer to '4 days or less' and 'more than 4 days', respectively.

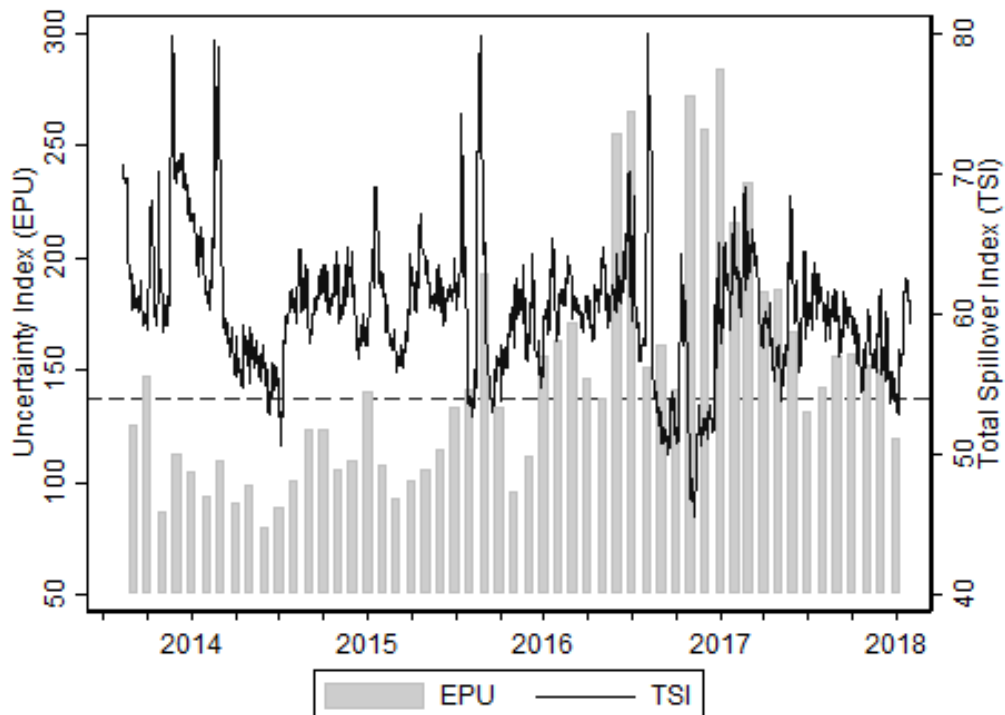
The bottom panel of Table 2.5 ascertains the interdependence of returns across the five exchange rates under scrutiny by presenting an estimated TSI of close to 37% in the long run. There again, net predictive power is held by BTC/USD with regards to BTC/EUR and to the whole system, with BTC/EUR the largest provider and recipient of returns shocks to and from other markets. BTC/AUD and BTC/GBP are the other two favourite counterparts of BTC/EUR after BTC/USD, and BTC/CAD is confirmed to be the least influenced and least influential market in terms of returns spillovers.

### 2.5.2.3 Rolling windows analysis (dynamic spillover plots)

#### (a) Overall spillovers

The total spillover index for exchange rate daily returns is depicted in Figure 2.7 along with the monthly EPU index. In spite of a certain degree of volatility with values ranging from below 50% to almost 80%, it appears that the returns TSI in the system fluctuates around 60% for most of the sample period. We observe a decline in returns connectedness across markets between 2013Q4 and 2014Q3 (from 70% to little above 50%), before the TSI stabilises around 60% for the period 2014Q3 to 2016Q2, except for a high variable TSI in 2015Q3. The dramatic plunge over the second half of 2016 is compensated for in early 2017 and the TSI again fluctuates between 55% and 65% for the remainder of the sample period.

Figure 2.7 Overall returns spillovers (dynamic plot) and Economic Policy Uncertainty Index



*Note:* Dynamic overall *returns* spillovers computed following Diebold and Yilmaz (2012) with a 150-day rolling window, right scale (percentages). Monthly Global Economic Policy Uncertainty (EPU) index, left scale. The dashed line shows the median value of EPU over the sample period. Dates on the x-axis indicate the start of the year, and ticks are quarterly.

The plot confirms the strong interdependence of returns in the system over time (TSI almost always above 50%), and shows that it is fairly stable for the duration the sample period with no evident pattern suggesting its link to overall uncertainty. Although counter-intuitive, it is not incompatible with earlier results on volatility spillovers. Indeed,

the latter were found to reflect the variations of global economic uncertainty, suggesting more strongly interconnected markets in times of high uncertainty. In spite of volatility transmitting more or less “easily” across components of the system depending on the economic climate, the capacity of returns shocks to help predict price movements on other markets remains stable over time in the system overall.

### (b) Spillovers FROM and TO others

In the spirit of Diebold and Yilmaz (2012) dynamic spillovers are broken down into directional spillovers to other markets, from other markets, and net spillovers depicted in Figures 2.8, 2.9 and 2.10, respectively.

A quick glance at individual plots in Figure 2.8 reveals that the BTC/USD exchange rate exerts the biggest influence on other variables of the system, and that this influence strengthens in 2017 and early 2018. Interestingly, the influence of BTC/EUR returns shocks on other markets shifts downwards at the end of the sample period (from early 2017 on) after fluctuating around 5% to 7% most of the time. Returns spillovers from BTC/AUD, BTC/CAD and BTC/GBP to other markets are erratic but overall range between approximately 8% and 17% throughout the period under scrutiny.

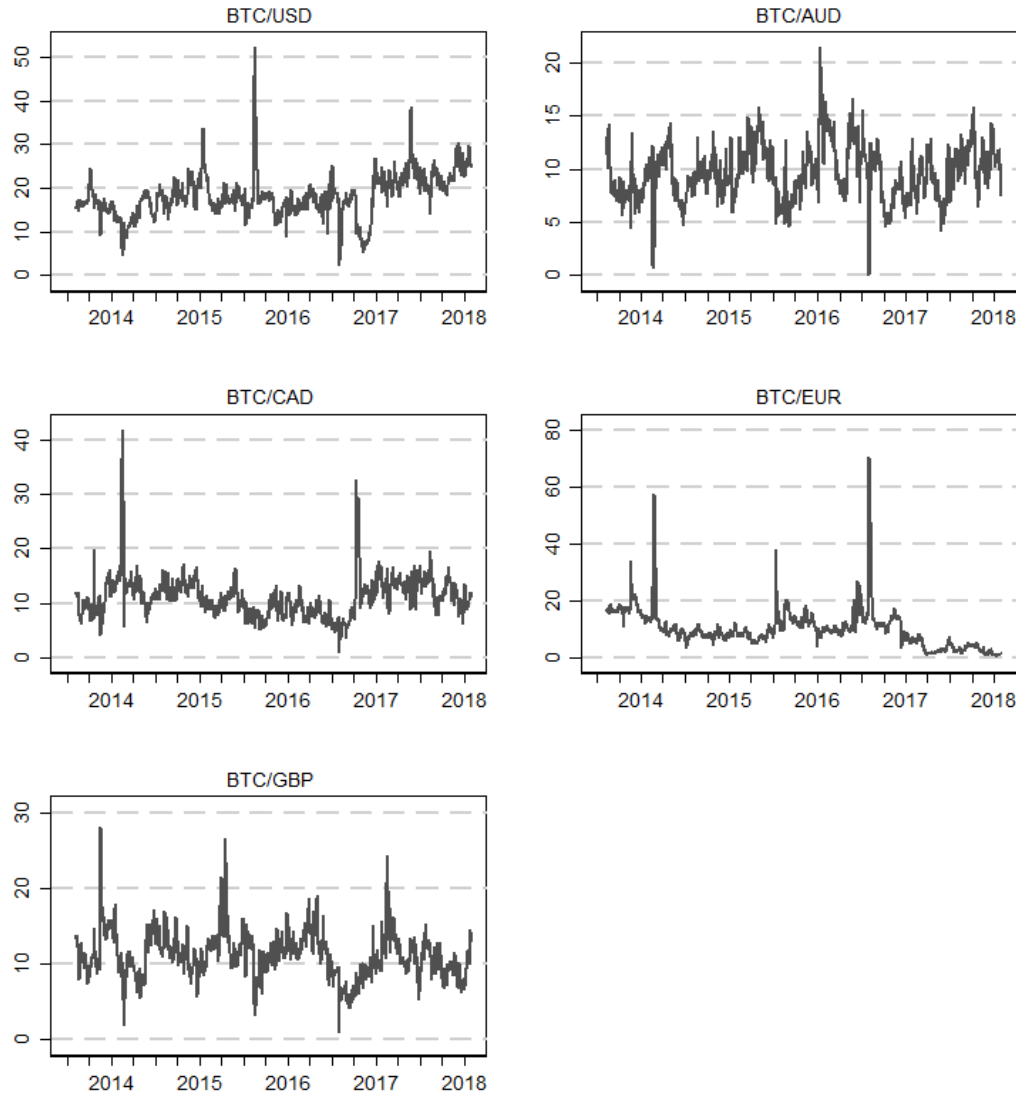
Figure 2.9 indicates that BTC/USD returns are significantly influenced by shocks from other markets in late 2013 and early 2014 with spillovers between almost 13% and approximately 16%, while the latter then steady and fluctuate mostly in the range 6% - 14%. Returns spillovers received by BTC/AUD from other exchange rates range largely between 10% and 15%, as is the case for BTC/CAD and BTC/GBP. The share of forecasting error variance of BTC/EUR returns explained by innovations in other variables is almost systematically above 10% and routinely above 15%, and even larger than 15% between 2014Q2 and mid-2015 and after 2017Q1.

### (c) Net spillovers

Dynamic net spillovers plotted in Figure 2.10 confirm the former intuition stemming from our full sample analysis. The BTC/USD exchange rate returns exhibit almost exclusively positive net spillovers – reaching above 10% starting in early 2017–, representing the predictive power of shocks on the BTC/USD market in forecasting returns on other markets. Conversely, the BTC/EUR market is strongly connected to the system as a net receiver, i.e. mostly negative net spillovers that seem to mirror the BTC/USD ones over time with a marked decline starting in 2017Q1. The net connectedness of BTC/GBP returns is very erratic over time and incessantly crosses the zero line.

A similarly changeable pattern can be discerned for BTC/AUD, although its net spillovers are typically negative, characterising that market as usually predictable. Net returns

Figure 2.8 Returns spillovers to others, dynamic plot

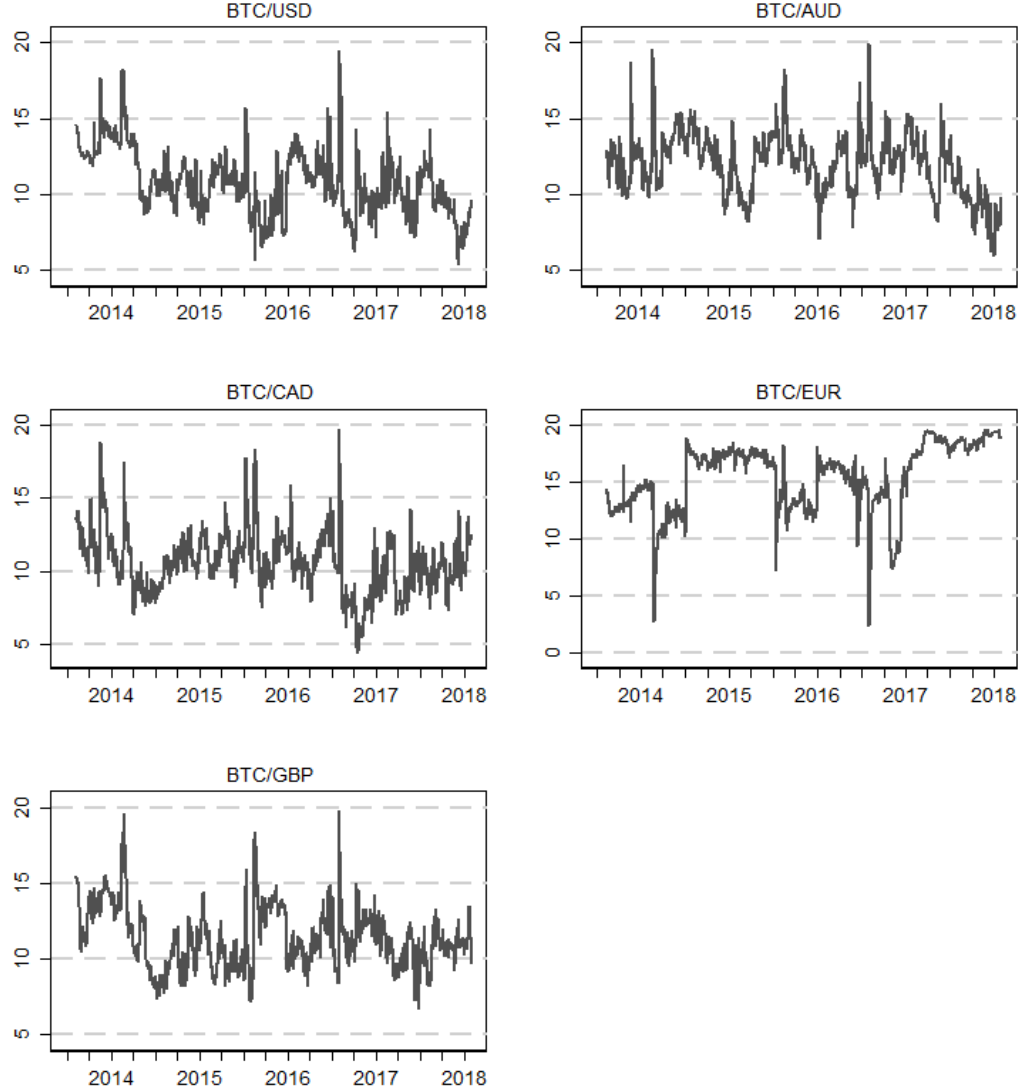


*Note:* Dynamic returns spillovers *to others* computed following Diebold and Yilmaz (2012) with a 150-day rolling window. Y-scales in percentages. Dates on the x-axis indicate the start of the year, and ticks are quarterly.

spillovers from BTC/CAD slowly evolve around zero over time in a serpent-like fashion: negative in late 2013, positive in 2014, mostly negative from 2015Q1 to 2016Q4, and mostly positive for the remainder of the sample period. Their magnitude remains fairly small in absolute terms (seldom greater than 25%), reflecting the little influence of said market in predicting returns in the system.

In sum, results from our analysis of returns spillovers seem to complement nicely those commented on volatility spillovers. The BTC/USD and BTC/EUR are confirmed in their central roles in the system. They remain the most closely interlinked markets, and

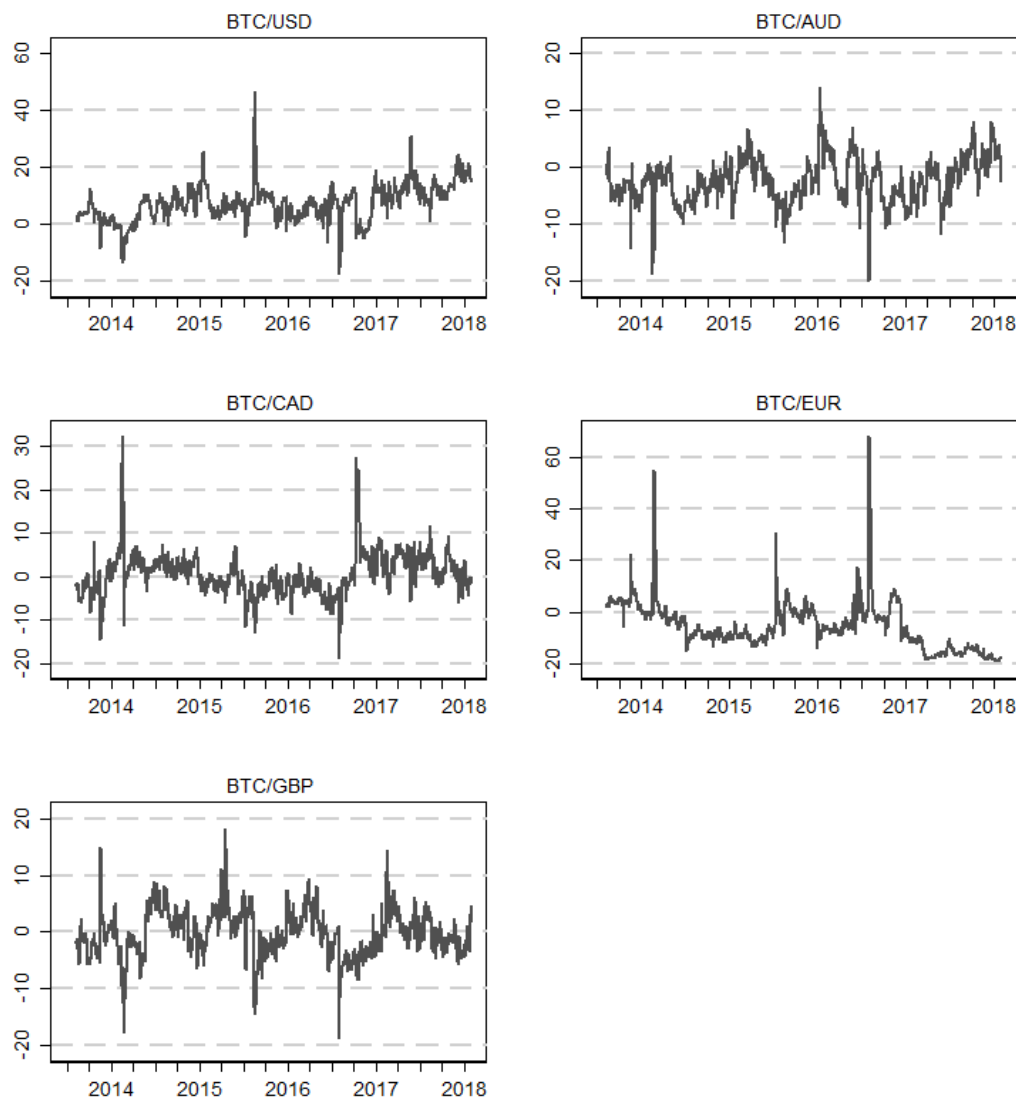
Figure 2.9 Returns spillovers from others, dynamic plot



*Note:* Dynamic returns spillovers *from* others computed following Diebold and Yilmaz (2012) with a 150-day rolling window. Y-scales in percentages. Dates on the x-axis indicate the start of the year, and ticks are quarterly.

the former holds a net predictive power with regards to the system as a whole. That is, unexpected shocks in returns to BTC/USD embed information as to probable future shocks in prices on other markets, especially so for BTC/EUR. That relationship is the only one to be so dramatically asymmetric, the one between BTC/EUR and BTC/GBP, for instance, giving only a marginal advantage to the latter in terms of predictive power.

Figure 2.10 Net returns spillovers, dynamic plot



*Note:* Dynamic *net* returns spillovers computed following Diebold and Yilmaz (2012) with a 150-day rolling window. Y-scales in percentages. Dates on the x-axis indicate the start of the year, and ticks are quarterly.

### 2.5.3 Robustness

How sensitive are our results to the choice of forecast horizon, window size, and alternative measure of volatility? In this section, we undertake robustness exercise in each aspect mentioned above.

#### 2.5.3.1 Sensitivity to forecast horizon and window size for static and dynamic spillover system

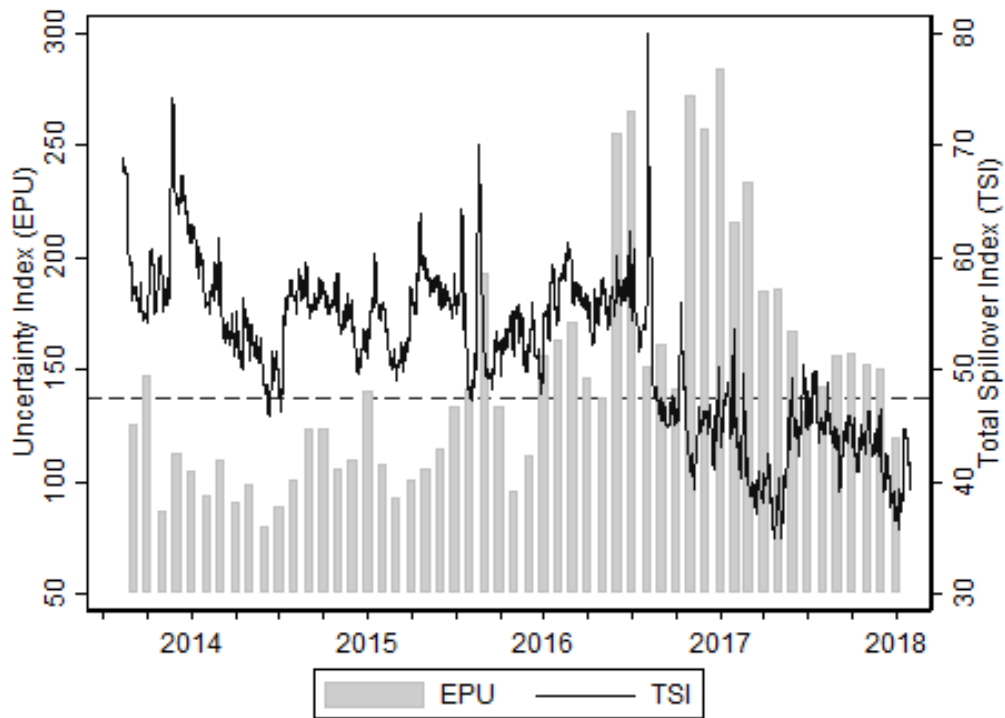
We check the robustness of our full sample analysis results to the choice of the forecast horizon and the tuning of frequency bands that identify short- and long-run components of the forecast error GVD. Recall that our results are based on 30-days-ahead forecasts and that the time-frequency domain analysis consider the short horizon to be 4 days and the long horizon to be over 4 days. We performed similar estimations with 7-, 10-, and 60-days-ahead forecasts, and using 16 and 30 days to split frequency domains. The ensuing results (reported in appendix A) corresponding to Tables 2.2, 2.3, 2.4 and 2.5 presented above produced very similar values for the estimated spillovers and yielded qualitatively identical conclusions.

Next, Figures 2.11 and 2.12 (Figures 2.13 and 2.14) plot dynamic overall returns (volatility) spillovers using 15 days and 60 days as the forecast horizon for computing the GVD, respectively. We observe that the latter graphs are strongly consistent with Figure 2.7 (for return) (and Figure 2.3 for volatility, respectively) not only in the estimated values of the total spillover index, but also in the shape of the evolution that records the same extreme events in every case.

#### 2.5.3.2 Alternative measures of volatility

Recall that our empirical analyses are based on Parkinson's High-Low historical volatility ( $HL - HV$ ) measure. This measure provides useful information regarding the future volatility than a close-to-close estimator. Garman and Klass (GK, 1980) proposed a volatility measure based on open ( $O$ ), high ( $H$ ), low ( $L$ ) and close ( $C$ ) prices to achieve better accuracy than previous estimators. Hence, as a robustness check, we use GK class of estimators and re-estimate spillover effects. The similarity between Parkinson and GK estimators are that both follow a geometric Brownian motion. However, drift and opening jumps are not treated in both models (Wiggins, 1991), but both estimators are 5 and 7 times respectively as powerful as the close-to-close measure (Garman & Klass, 1980; Parkinson, 1980). Recent studies have even gone further in extending *GK* volatility measure (among them see, for instance, Rogers-Satchell (*OHLC*) measure (Rogers & Satchell, 1991), *GK - ABD* volatility measure (Alizadeh et al., 2002) and *GK - YZ*

Figure 2.11 Overall returns spillovers (dynamic plot – 15-day ahead forecast) and Economic Policy Uncertainty Index



Note: Right scale (percentages): Dynamic overall *returns* spillovers computed following Diebold and Yilmaz (2012) with a 150-day rolling window, using a 15-day ahead forecast. Left scale: monthly Global Economic Policy Uncertainty (EPU) index. The dashed line shows the median value of EPU over the sample period. Dates on the x-axis indicate the start of the year, and ticks are quarterly.

volatility measure (Yang & Zhang, 2000)<sup>19</sup>. These measures are summarised below:

$$GK = \left\{ 0.5 \times (H_t - L_t)^2 \right\} - \left\{ (2\ln(2) - 1) \times (C_t - O_t)^2 \right\} \quad (2.10)$$

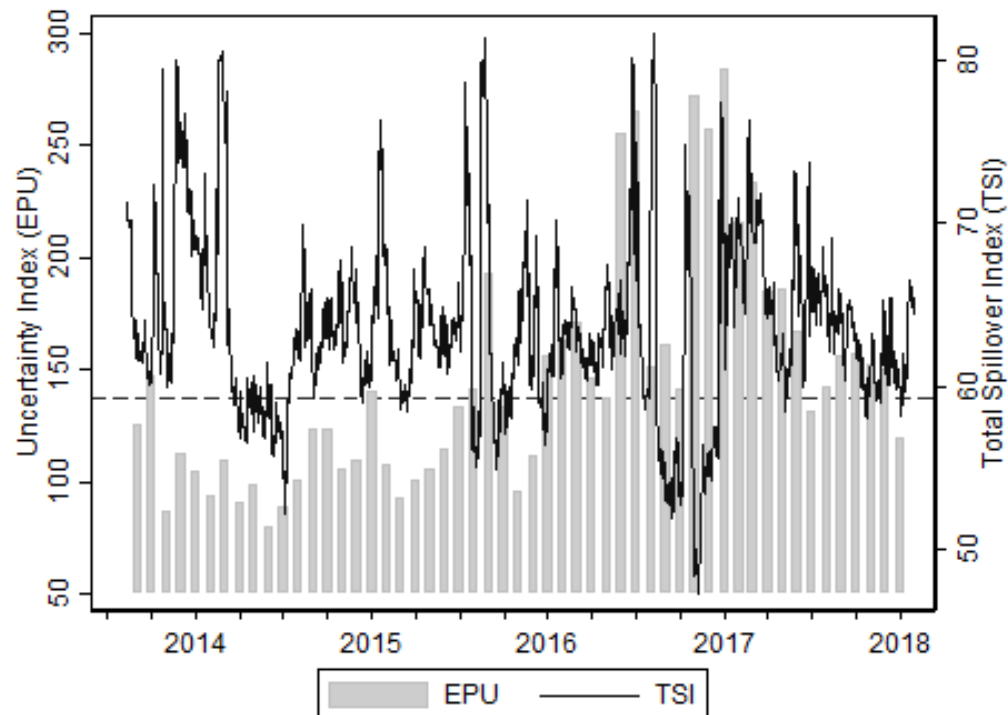
$$Rogers-Satchell = \left\{ (H_t - C_t) \times (H_t - O_t) \right\} + \left\{ (L_t - C_t) \times (L_t - O_t) \right\} \quad (2.11)$$

$$Yang-Zhang = (O_t - C_{t-1})^2 + 0.511 \times (H_t - L_t)^2 - (2\ln(2) - 1) \times (C_t - O_t)^2 \quad (2.12)$$

$$\begin{aligned} GK - ABD = & 0.511 \times (H_t - L_t)^2 - 0.019 \times \left\{ (C_t - O_t) \times (H_t + L_t - 2O_t) - 2 \right. \\ & \left. \times (H_t - O_t) \times (L_t - O_t) \right\} - 0.383 \times (C_t - O_t)^2 \end{aligned} \quad (2.13)$$

<sup>19</sup><https://www.quantshare.com/itemd-197-trading-indicator-yang-zhang-extension-of> or (Bennett & Gil, 2012)

Figure 2.12 Overall returns spillovers (dynamic plot – 60-day ahead forecast) and Economic Policy Uncertainty Index



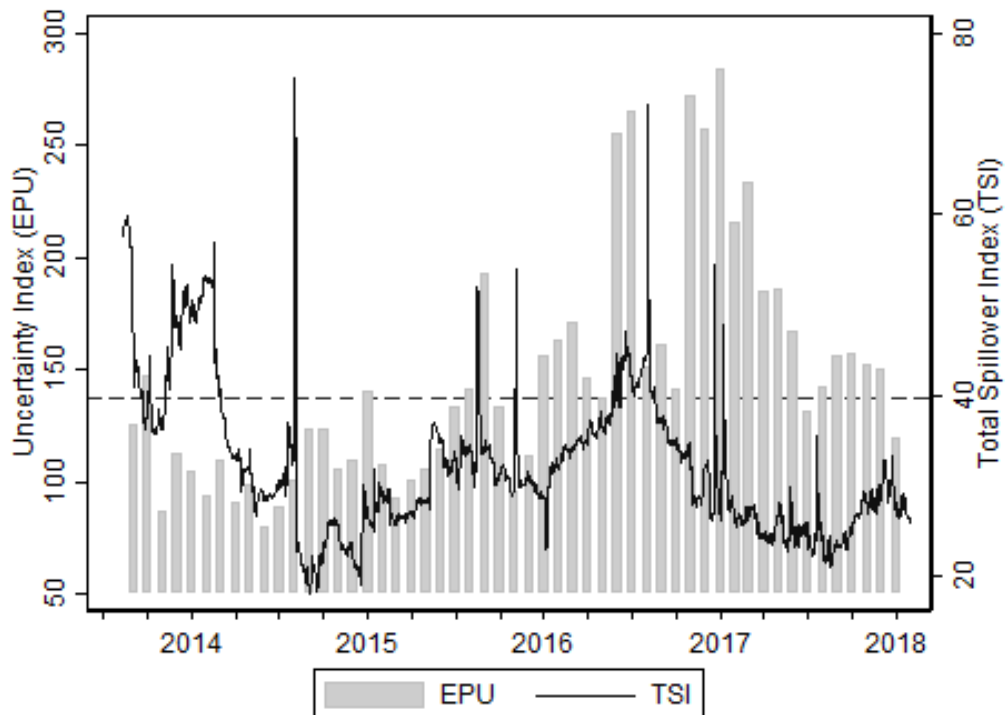
Note: Right scale (percentages): Dynamic overall *returns* spillovers computed following Diebold and Yilmaz (2012) with a 150-day rolling window, using a 60-day ahead forecast. Left scale: monthly Global Economic Policy Uncertainty (EPU) index. The dashed line shows the median value of EPU over the sample period. Dates on the x-axis indicate the start of the year, and ticks are quarterly.

The above measures compute the daily variance, so the corresponding estimate of the annualised daily percent standard deviation (volatility) is  $Vol = \sqrt{365 * Variance}$ . The summary statistics for the above measures are presented in Table 2.6.

We compute the static and dynamic volatility spillover based on Garman-Klass (GK) volatility. To begin with we compare the GK volatility measure with that of Parkinson (see Figure 2.15). As such, there is no significant differences in peaks and troughs and the fluctuations appear to co-move. In Tables 2.7 and 2.8 we have presented the overall spillover estimates from Diebold-Yilmaz and the frequency domain approach of Barunik and Krehlik, respectively based on this measure of volatility.<sup>20</sup> Figures 2.16, 2.17, 2.18, 2.19, we have presented the dynamic volatility spillover effects (overall, from, to, and net, respectively). The results are consistent with the ones derived from Parkinson's measure. Hence, our conclusions on the predictive power (giver and the net receiver) remain unchanged to the use of an alternative measure of volatility.

<sup>20</sup>We have also estimated spillover effects from other class of GK measure of volatility, such as GK-YZ, etc. The results are available with the authors upon request.

Figure 2.13 Overall volatility spillovers (dynamic plot – 15-day ahead forecast) and Economic Policy Uncertainty Index



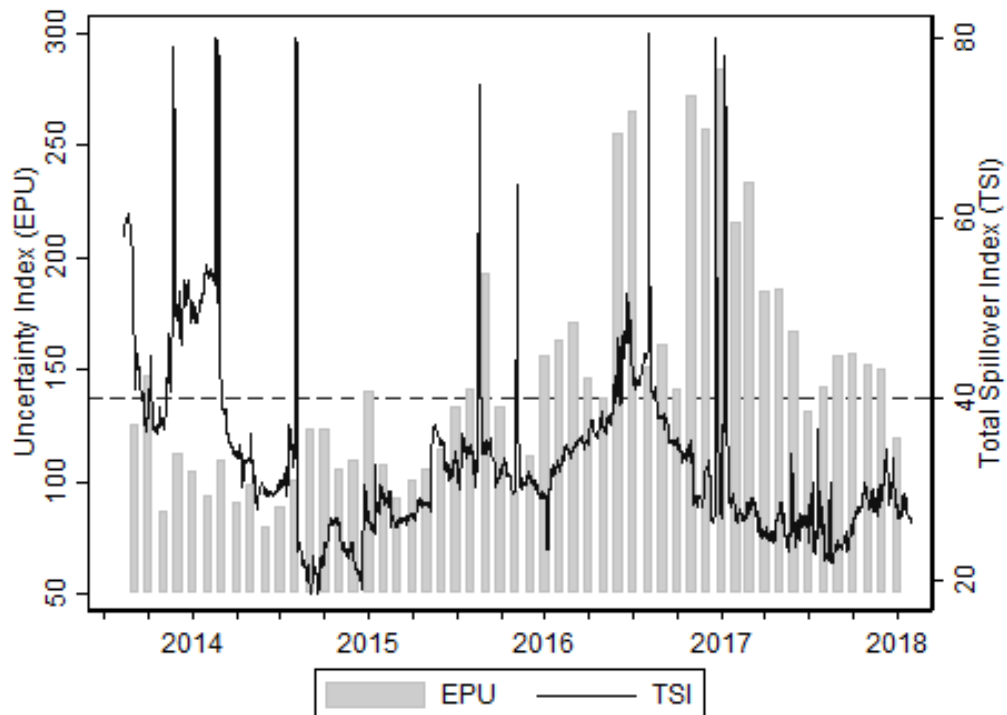
Note: Right scale (percentages): Dynamic overall *volatility* spillovers computed following Diebold and Yilmaz (2012) with a 150-day rolling window, using a 15-day ahead forecast. Left scale: monthly Global Economic Policy Uncertainty (EPU) index. The dashed line shows the median value of EPU over the sample period. Dates on the x-axis indicate the start of the year, and ticks are quarterly.

### 2.5.3.3 VAR model Stability

The spillover index measures the overall connectedness of the system. Therefore, the dynamic spillover variations (e.g. figures 2.3 and 2.7) explain the flow of information within the system, but do not clarify the extreme shocks along the dynamic overall volatility spillover. Claeys and Vašíček (2014) suggested that using (Qu & Perron, 2007) break test to detect the structural breaks in a VAR system could help to identify these significant spikes within the transmission mechanism. Following the latter work, we applied Qu and Perron test on the volatility exchange rates to investigate the potential structural breaks in the system. Indeed, detecting the sudden changes in the spillover index within these markets could help us to identify potential events that might induce the series to change its properties over time.

Table 2.9 shows the results of Qu and Perron analysis. The VAR dataset consists of the five Bitcoin markets from March 2013 to January 2018. The trimming percentage is 15% of the sample span, and the maximum breaks allowed individually for two and five respectively. The test statistics for both WD max and sequential tests exceed the critical values except for the fifth break (Seq test ( $m = 5$ )  $\sim (5 \mid 4)$ ). Thus, the null hypothesis

Figure 2.14 Overall volatility spillovers (dynamic plot – 60-day ahead forecast) and Economic Policy Uncertainty Index



Note: Right scale (percentages): Dynamic overall *volatility* spillovers computed following Diebold and Yilmaz (2012) with a 150-day rolling window, using a 60-day ahead forecast. Left scale: monthly Global Economic Policy Uncertainty (EPU) index. The dashed line shows the median value of EPU over the sample period. Dates on the x-axis indicate the start of the year, and ticks are quarterly.

of no structural breaks rejected for the WD max and indicates four (out of five) breaks, based on the sequential test. The confidence interval for the four break dates are as follows: 1- 09/01/2014. 2- 04/10/2014. 3- 23/09/2015. 4- 10/07/2016. We can link the latter dates to remarkable events that hit the cryptocurrency market. At the beginning of 2014, the largest Bitcoin exchange platform, Mt. Gox, started to have security issues; the platform was then hacked and \$ 473 million was stolen. After the middle of 2015, the administrator of Scrypt platform, Marcelo Santos, posted that the platform had been breached and hijackers had stolen several Bitcoin hot wallets. Finally, during 2016 and after the flash crash of Bitfinex platform, the Bitcoin price fell by approximately 14%. All the latter events appeared along the overall spillover dynamic plot (Figure 2.3), but it was confirmed by Qu and Perron (2007) test that the spillover spikes actually spread the volatility to other markets.

To check the VAR stability, we extract the coefficients' residuals and test their stationarity to ensure the consistency of the mean and variance of residuals over time. Table 2.10 shows that the test rejects the null of unit root for all exchange rates in both sub-tables. Further, Figures (A.1 and A.2) show the inverse roots of AR characteristic polynomial

for return and volatility lie inside the unit circle, which indicates that the VAR process is stable.

## 2.6 Conclusions

As long as economies' core are continually subject to frictions and are driven by incomplete information, it is nearly impossible to not experience spillover of shocks in some form or other. Depending on the net receiver or net dispenser of volatility, the magnitude of spillover effects represents vulnerability of a system to external shocks. The context of investigation in this chapter, thus, has intermittent link to a broad economic and financial theory: as long as investors' choice of investment is governed by relative hedging value of an asset traded in various markets, they will invariably use estimates of spillover effects as the guiding information set to predict the next best investment strategy. Moreover, spillover effects in a market can be used as an indicator of relative market inefficiency. A weak-form cross-market inefficiency requires high-degree of spillover across markets where there is a clear indication of net receiver and net giver of volatility. This way, an investor can exploit arbitrage value by embedding the dynamic features of spillover in his prediction strategy. In this chapter, we have created a first-hand information set for cryptocurrency investors by estimating spillover-effects in five markets where Bitcoin is highly traded.

A unique aspect of our research concerns estimation of volatility spillover effects (with a better measure of volatility) *across* Bitcoin markets. We have investigated how spillover effects are governed by uncertainty episodes. With an aim to capture information asymmetry through fluctuations in uncertainty, our study sheds important insights on the dynamic interdependence of spillover effects during high/low uncertainty episodes. By doing this, we capture the *sentimental value*, researchers often attach to Bitcoin prices (in the absence of a dedicated asset pricing theory for cryptocurrency). By studying *cross-market* spillover in Bitcoin prices we have also complemented to a sparse body of literature (such as Cheah et al. (2018)) and have envisaged the importance of studying a systematic pattern of shocks' movement by capturing a 'system dynamics'. Because, as of now, price movements in Bitcoin market possess no (theoretical) policy bound for an effective control, a perhaps acceptable approach is to exploit 'system features' to provide a net predictive power.

Using the measure of volatility and well-established dynamic spillover methods, we have found that Bitcoin-USD holds high predictive power and Bitcoin-Euro acts as the net receiver. Moreover, higher uncertainty is found to accelerate spillover effects with larger impacts across markets. The results hold implications for cross-market dynamic inefficiency and predictive power of one market for tapping in the arbitrage conditions. Our results have implications for broad macroeconomic theory and investment decisions

as envisaged by islands with sticky price information: investors of a risky asset like Bitcoin need a well-defined information set which would determine - at least in part - their expected return value. In that sense, our research holds significant predictive value for cryptocurrency investors.

Table 2.6 Different Volatility measures across five selected exchange rates

(a) BTC/USD volatility

	Mean	St. Dev.	Max	Min	Skewness	Kurtosis
Parkinson (H-L)	0.709	1.008	20.68	0.0	9.086	139.2
GK (OC-HL)	0.773	1.140	24.33	0.010	9.389	150.5
GK-ABD	1.323	2.043	24.57	0.004	4.353	30.20
Rogers-Satchell	2.206	2.835	33.42	0.0	3.033	18.10
GK-YZ	1.011	1.294	24.61	0.02	8.209	116.5

(b) BTC/AUD volatility

	Mean	St. Dev.	Max	Min	Skewness	Kurtosis
Parkinson (H-L)	6.091	4.467	30.67	0.105	1.499	5.329
GK (OC-HL)	7.025	5.247	35.96	0.112	1.507	5.391
GK-ABD	5.664	3.371	21.20	0.114	1.150	4.352
Rogers-Satchell	8.023	6.541	44.12	0.0	1.607	5.747
GK-YZ	7.437	5.375	36.71	0.140	1.504	5.317

(c) BTC/CAD volatility

	Mean	St. Dev.	Max	Min	Skewness	Kurtosis
Parkinson (H-L)	7.248	4.681	30.01	0	1.054	4.330
GK (OC-HL)	8.176	5.449	35.18	0	1.058	4.346
GK-ABD	6.639	3.887	34.73	0	1.082	5.646
Rogers-Satchell	9.369	6.906	47.28	0	1.273	4.994
GK-YZ	9.097	5.792	40.88	0	1.149	4.838

(d) BTC/EUR volatility

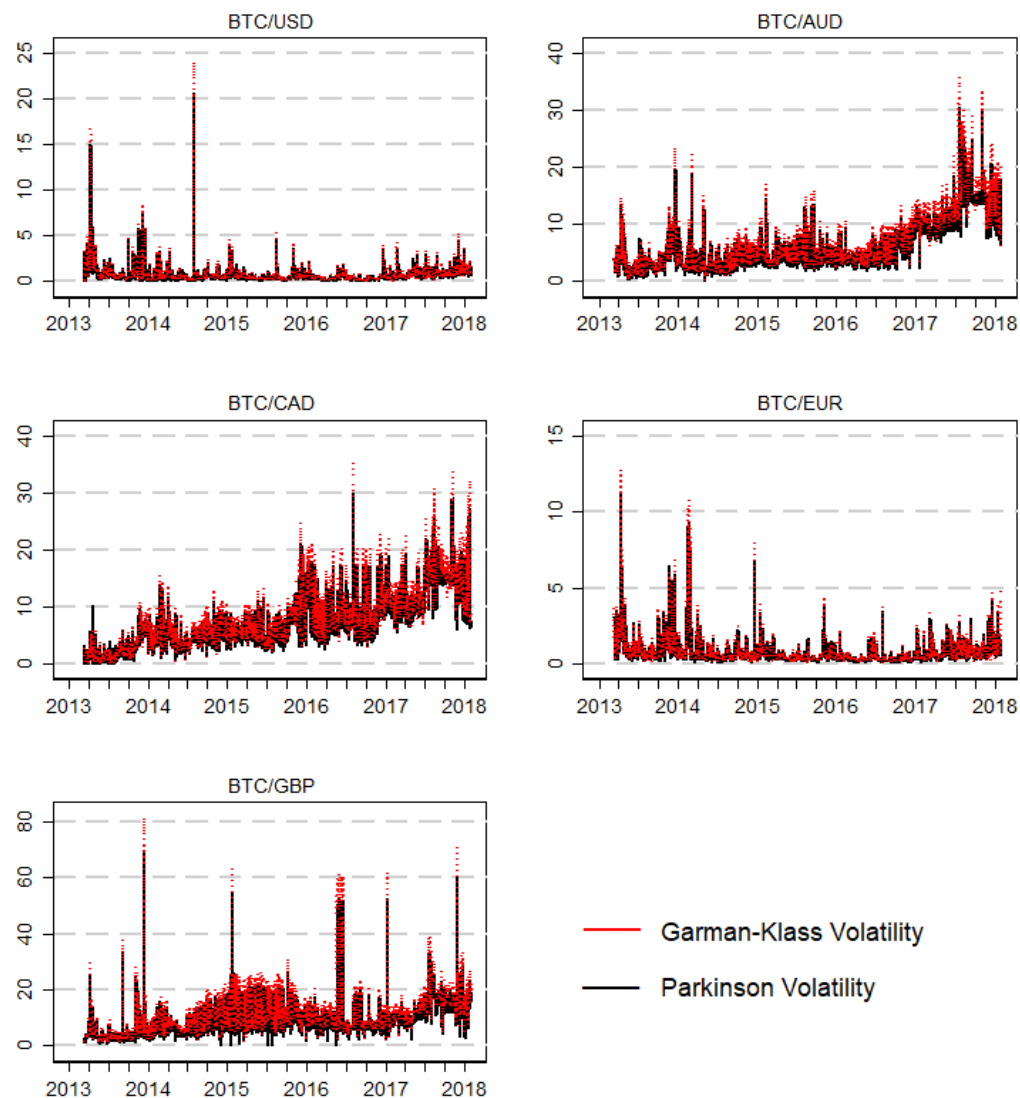
	Mean	St. Dev.	Max	Min	Skewness	Kurtosis
Parkinson (H-L)	0.740	0.899	11.29	0.069	4.899	39.67
GK (OC-HL)	0.794	1.043	12.72	0.007	5.001	40.09
GK-ABD	0.874	1.361	26.78	0.015	8.784	126.7
Rogers-Satchell	1.126	1.515	22.60	0.007	5.525	51.66
GK-YZ	1.052	1.266	14.27	0.104	4.561	32.73

(e) BTC/GBP volatility

	Mean	St. Dev.	Max	Min	Skewness	Kurtosis
Parkinson (H-L)	9.298	6.378	69.04	0	2.639	17.65
GK (OC-HL)	10.88	7.507	81.25	0.745	2.649	17.70
GK-ABD	10.85	7.569	80.01	0.753	2.657	17.66
Rogers-Satchell	14.92	10.73	109.1	0.0	2.506	16.32
GK-YZ	11.26	7.52	82.14	1.054	2.683	17.97

*Note:* GK: Garman-Klass (1980). GK-ABD: Garman-Klass extension, Alizadeh, Brandt and Diebold (2002). GK-YZ: Garman-Klass Yang-Zhang extinsion, Yang and Zhang, (2000). Rogers-Satchell (1991).

Figure 2.15 Comparison of GK and Parkinson Volatility Plots



*Note:* Exchange rate volatility series, daily. Dates on the x-axis indicate the start of the year, and ticks are quarterly.

Table 2.7 Volatility spillovers across five selected exchange rates: Garman-Klass measure

	BTC/USD	BTC/AUD	BTC/CAD	BTC/EUR	BTC/GBP	Directional FROM others
BTC/USD	81.25	3.99	0.39	13.62	0.75	18.75
BTC/AUD	3.41	85.94	3.50	6.43	0.72	14.06
BTC/CAD	0.25	5.19	91.61	1.53	1.42	8.39
BTC/EUR	17.25	4.07	0.67	76.48	1.51	23.5
BTC/GBP	0.58	1.56	1.33	0.97	95.55	4.44
Directional TO others	21.49	14.81	5.89	22.55	4.4	<i>TSI:</i> $69.14/500 =$
Net spillovers	2.74	0.75	-2.5	-0.95	-0.04	$13.83\%$

Note: Exchange rates volatility spillovers following Diebold and Yilmaz (2012). Numbers are percentages.  
“TSI” stands for Total Spillover Index.

Table 2.8 Volatility spillovers across five selected exchange rates - Frequency domain analysis: Garman-Klass Measure of Volatility

(a) Short horizon

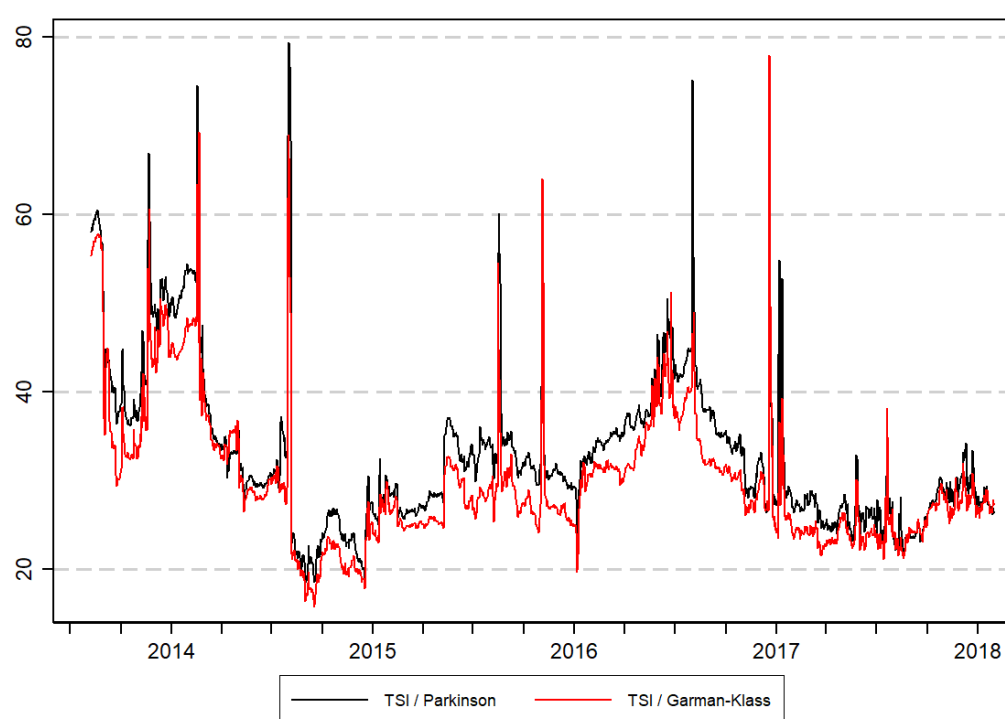
	BTC/USD	BTC/AUD	BTC/CAD	BTC/EUR	BTC/GBP	FROM others
BTC/USD	38.93	0.40	0.05	3.84	0.12	4.41
BTC/AUD	0.13	25.61	0.29	0.22	0.11	0.75
BTC/CAD	0.08	0.36	45.95	0.36	0.11	0.91
BTC/EUR	2.54	0.38	0.13	27.37	0.23	3.28
BTC/GBP	0.19	0.24	0.13	0.35	57.94	0.91
TO others	2.94	1.38	0.6	4.77	0.57	<i>TSI: 10.26/206 =</i> $4.99\%$

(b) Long horizon

	BTC/USD	BTC/AUD	BTC/CAD	BTC/EUR	BTC/GBP	FROM others
BTC/USD	42.32	3.59	0.34	9.77	0.62	14.32
BTC/AUD	3.28	60.34	3.22	6.21	0.61	13.32
BTC/CAD	0.17	4.83	45.66	1.17	1.31	7.48
BTC/EUR	14.71	3.69	0.54	49.11	1.29	20.23
BTC/GBP	0.39	1.32	1.20	0.62	37.61	3.53
TO others	18.55	13.43	5.3	17.77	3.83	<i>TSI: 58.88/293.92 =</i> $20.04\%$

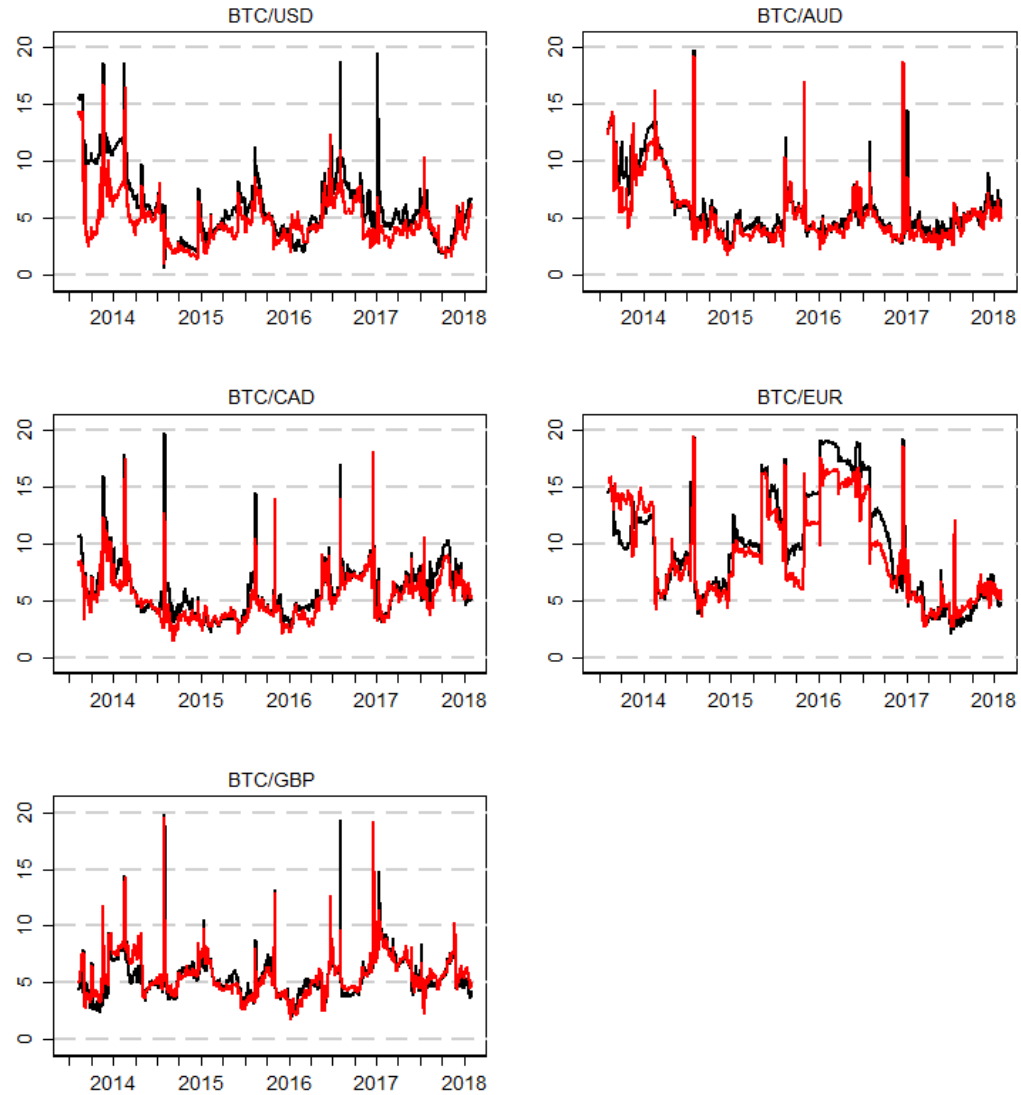
Note: Volatility spillovers, frequency domain analysis following Baruník and Křehlík (2018). Numbers are percentages. ‘Within’ refers to *within system* spillovers. *Short* and *Long* horizons refer to ‘4 days or less’ and ‘more than 4 days’, respectively.

Figure 2.16 Overall volatility spillovers (dynamic plot): Garman-Klass volatility measure



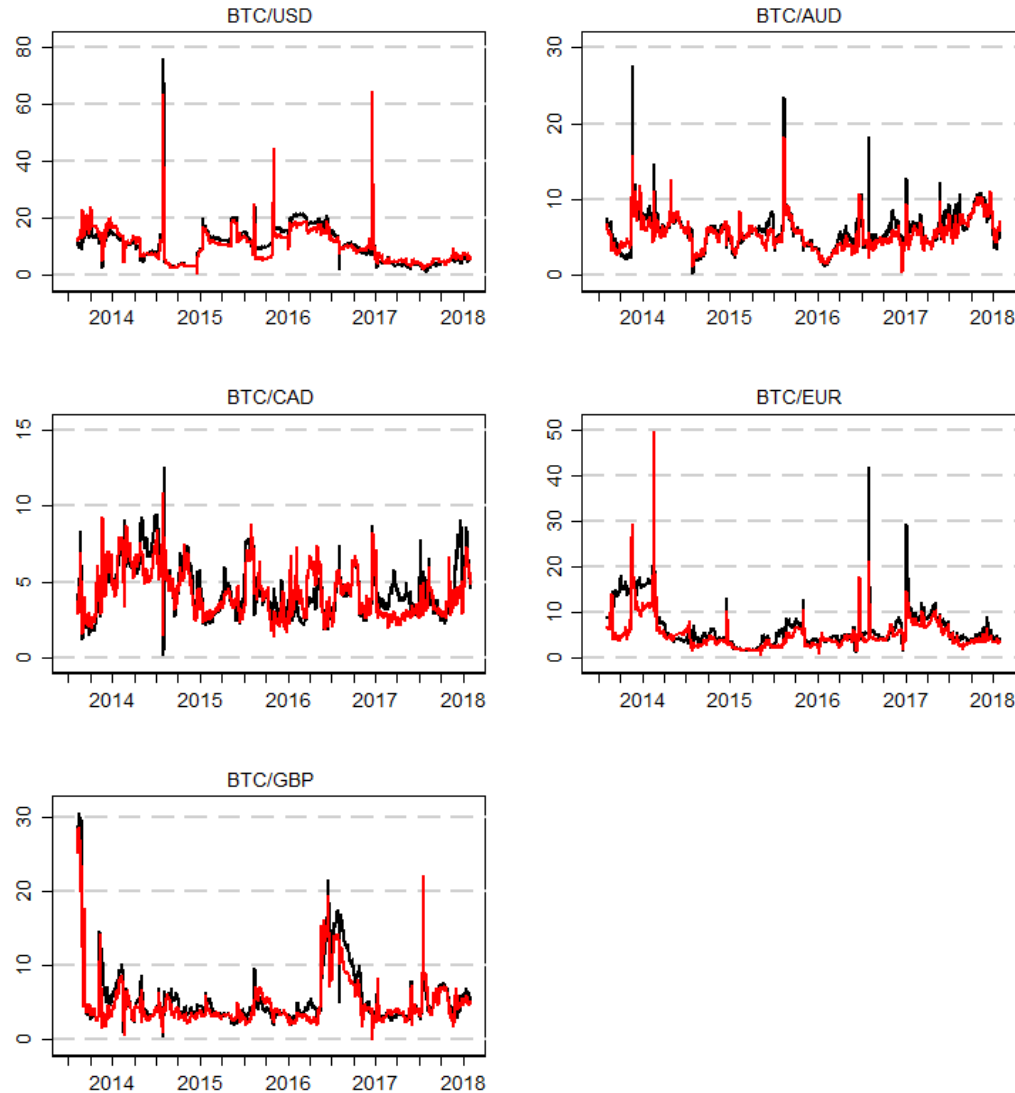
*Note:* The black line is the Dynamic overall based on Parkinson (1980) volatility, the red line is calculated based on GK-YZ (2002) volatility. Dynamic overall *volatility* spillovers computed following Diebold and Yilmaz (2012) with a 150-day rolling window, Y-axis in percentages. Dates on the x-axis indicate the start of the year, and ticks are quarterly.

Figure 2.17 Volatility spillovers from others, dynamic plot: Garman-Klass volatility measure



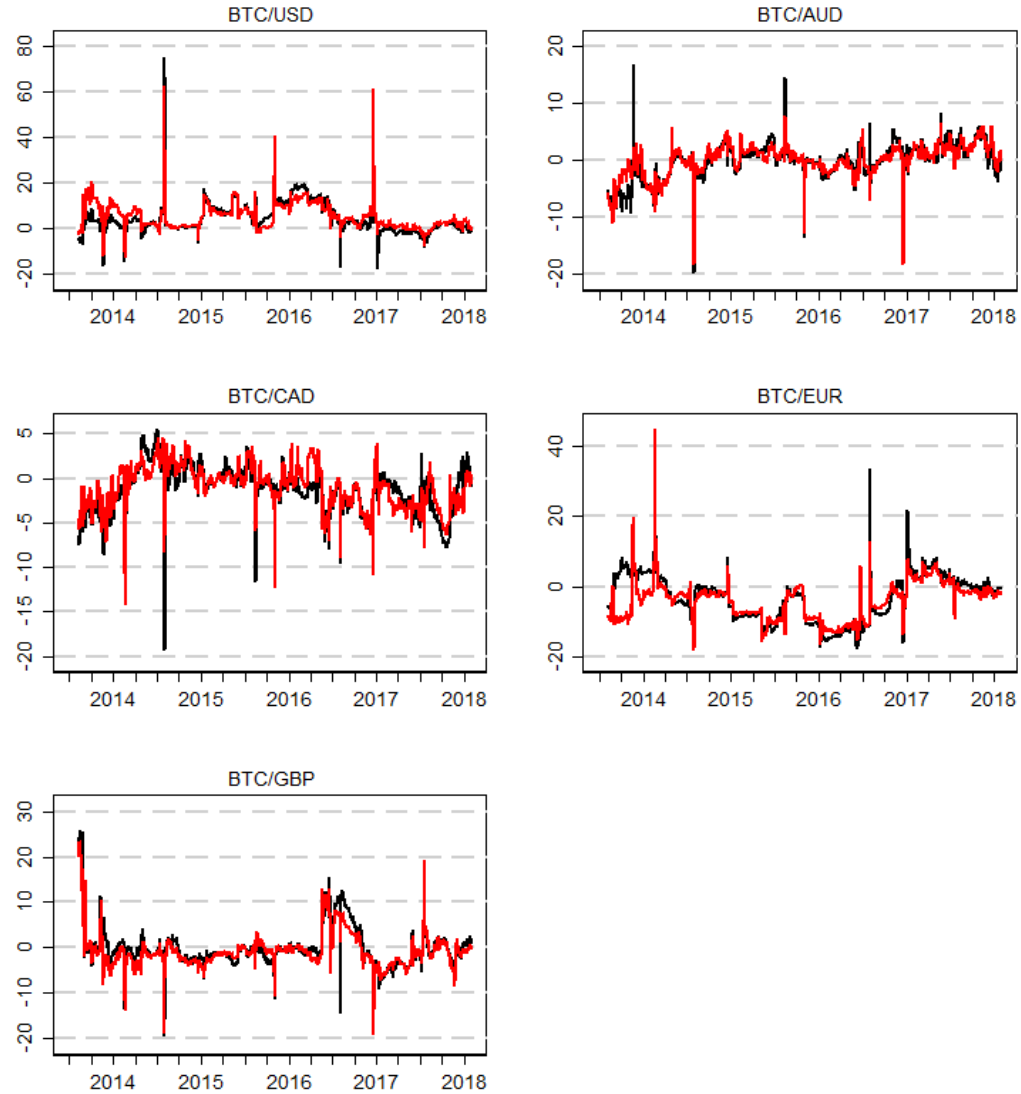
*Note:* Dynamic volatility spillovers *from* others computed following Diebold and Yilmaz (2012) with a 150-day rolling window. Y-scales in percentages. Dates on the x-axis indicate the start of the year, and ticks are quarterly.

Figure 2.18 Volatility spillovers to others, dynamic plot: Garman-Klass volatility measure



Note: Dynamic volatility spillovers *to* others computed following Diebold and Yilmaz (2012) with a 150-day rolling window. Y-scales in percentages. Dates on the x-axis indicate the start of the year, and ticks are quarterly.

Figure 2.19 Net volatility spillovers, dynamic plot



*Note:* Dynamic *net* volatility spillovers computed following Diebold and Yilmaz (2012) with a 150-day rolling window. Y-scales in percentages. Dates on the x-axis indicate the start of the year, and ticks are quarterly.

Table 2.9 Multivariate Qu and Perron Test for Structural Changes in VAR model

Tests		Test statistic	Critical Value
WD max test	m=2	454.41	17.57
	m=5	581.02	17.57
Seq test (m = 2)	(2   1)	583.4	18.38
Seq test (m = 5)	(2   1)	583.64	18.38
	(3   2)	107.98	19.26
	(4   3)	53.79	19.86
	(5   4)	0.045	20.33

*Note:* Exchange rates volatility are used to find the structural breaks. Trimming Percentage is 15% and the number of observations is 1787. The first test is the WD max test and the second one is the sequential test.

Table 2.10 ADF Test for the VAR Coefficients' Residuals

 (a) *Volatility*

Residuals	Test	Test stat	Critical Value 1%	Conclusion
BTC/USD	ADF	-29.88	-3.43	Reject
BTC/EUR	ADF	-42.16	-3.43	Reject
BTC/GBP	ADF	-42.14	-3.43	Reject
BTC/AUD	ADF	-42.33	-3.43	Reject
BTC/CAD	ADF	-42.20	-3.43	Reject

 (b) *Return*

Residuals	Test	Test stat	Critical Value 1%	Conclusion
BTC/USD	ADF	-41.93	-3.43	Reject
BTC/EUR	ADF	-42.08	-3.43	Reject
BTC/GBP	ADF	-42.07	-3.43	Reject
BTC/AUD	ADF	-42.14	-3.43	Reject
BTC/CAD	ADF	-42.10	-3.43	Reject



## Chapter 3

# The Relevance of Memory and Efficiency in Endogenously Switching Cross-market Bitcoin Prices

### Abstract

Bitcoin prices are fundamentally driven by the ‘feeling and the memory’ of investors at a point in time and their reaction could generate persistent endogenous responses. This chapter investigates the endogenous growth mechanisms and aligning designed empirical tests to show whether persistence is a product of such a model. The finding of persistence has relevance to the theory of learning: an agent that learns synchronously is an agent that will depict less persistence behaviour. However, characterising learning in the Bitcoin market is exceedingly complex as it is frequently affected by news and/or economic/financial dynamics. Sudden arrival of a shock (for instance, Brexit) can break the cycle of endogenous persistence generating mechanisms. We propose a variant of ARFIMA Markov Switching with endogenous switches governing the internal dynamics of the Bitcoin price or volatility system. We find that the Bitcoin markets depict true long memory over time which enables us to create a robust forecasting strategy. The model and empirical strategies are new and results hold promising information of true memory under episodes of structural breaks.

**Keywords:** Bitcoin; Cross-market volatility; Endogenous switch, MS-ARFIMA; structural breaks; Long memory ; Fractional integration; Persistence mechanism.

*“No memory is ever alone; it’s at the end of a trail of memories, a dozen trails that each have their own associations”***Louis L’Amour (An American Author)**

“The past beats inside me like a second heart.” John Banville, *The Sea*

### 3.1 Introduction

*Memory* is logically imperishable during the span of life of a boundedly rational agent. The only characteristic one might observe about the existence of memory is whether it is small or big, and the long or short ‘trail’ of associations it inherently defines over a period of time - just as Louis L’Amour (an American author) famously quoted. Following Granger (1980) and Hosking (1981), who independently defined and characterised the properties of ‘memory’ in a time series, its applications to real world data have exceeded its theoretical development (especially, identifying the source of its existence in economic and financial variables) in astronomic proportion. Economists and financial theorists have often come up with approximate theories identifying the possible source of long-memory in financial and economic data, see for instance (Farmer et al., 2006), (viz. Bouchaud et al., 2004, among others). However, in the majority of cases, extant research only focuses on the application of long-memory method for testing its existence in economic/financial data, without providing the theoretical source of its existence. In the case of cryptocurrency, a similar strand of research has begun to emerge (see for instance, (Bariviera, 2017)), barring some exceptions (viz. Cheah et al., 2018), where some directions of the source of long-memory are discussed.

This chapter contributes to the nascent literature on the source and implications of 'memory' in the cryptocurrency market, in particular in Bitcoin markets, in the following three significant ways. *First*, The chapter propose an identification strategy to demonstrate the source and implications of long-memory in Bitcoin markets. The chapter also, propose a demand-driven long-memory channel for Bitcoin, and show that there are waves of Buyer initiated transactions (given a fixed supply of Bitcoin), which follow a Beta distribution with memory, by following a linear algorithm of aggregation and power distribution. *Second*, we model the (non-)existence of long-memory to an endogenous market system mechanism which might give rise to a persistent shock with or without a mean reversion. We discuss this in the light of an endogenous switch in the memory and mean of the Bitcoin price process. *Third*, using daily Bitcoin data for five different markets, we study the nature of persistence in Bitcoin volatility, while considering an endogenous switch in volatility. From this, we shed light on the nature of the true long memory and quantify to what extent a true 'memory' governs the internal dynamics of the system.

The choice of Bitcoin for our empirical examination is led by the fact that it is the biggest and most active cryptocurrency with a market capitalisation over \$150<sup>1</sup> billion. To investigate the nature of such types of investment decisions and help governments design adequate regulations for limiting the cross-market movement of shocks, a remarkable growth of research has lately sprung up.

Volatility is more persistent when market interdependence is high, especially during financial crisis and episodes of economy-wide uncertainty (market inefficiency) (Cheah et al., 2018; Gillaizeau et al., 2019). Managing shocks *within* a system is relatively easy as one can exploit the *system dynamic* the features of shocks so as to monitor their movements and generate better predictive power for an asset (Gillaizeau et al., 2019). However, neglecting the long memory presence within the system can lead investors to spurious investment strategies. While former studies such as Bariviera (2017); Bouri et al. (2019) shed light on volatility persistence in the cryptocurrency market, Cheah et al. (2018) demonstrated the importance of cross-market dynamic interdependence of Bitcoin prices by estimating a system-wide long-memory. The focus on a cross-market rather than a single market cryptocurrency market in the latter study has significance within the chapter context: by modelling the ARFIMA process with Markov-switching, the fractional differencing parameter will create a stock of information for investors who decide on an arbitrage value of Bitcoin traded in various markets. Such a study is helpful in shaping the robust investment strategy of a single cryptocurrency traded in various markets.

The objective of this chapter is to study long-range dependence and potential breakpoints simultaneously and endogenously using the MS-ARFIMA model for Bitcoin cross-markets. The conclusion of structural break and fractional integration tests clearly show the presence of ten breaks in (BTC/USD, BTC/EUR and BTC/GBP), and eight breaks in (BTC/AUD and BTC/CAD), respectively, when Bai and Perron (1998, 2003) structural break test was used. In addition, the results show the presence of long memory across all the Bitcoin cross-markets. Therefore, a spurious long memory in volatility could be attributed to the presence of structural breaks if the standard ARFIMA model was applied to each of the Bitcoin cross-market respectively. Consequently, we applied the MS-ARFIMA model instead and find that the fractional integration displays constant long-memory for both states across all the MS-ARFIMA models. Therefore, having a constant long memory could confirm that even though the series in this analysis are subjected to different structural breaks over time, the accounted long-range dependence is true.

The finding in this chapter has two important implications for investors and policy makers. First, the presence of long memory could enable investors to capture speculative profits. This can be achieved through market timing. During a high-volatility regime, investors could buy and then subsequently sell when the market switches to a low-volatility regime

---

<sup>1</sup>coinmarketcap.com (June 2019)

in all Bitcoin cross-markets. Investors could also hedge during a high-volatility regime by purchasing Bitcoin futures from the Chicago Board Option Exchange (CBOE). Second, policy makers and regulators could introduce circuit breakers to stop trading in Bitcoin cross-markets when the market switches abruptly to a high-volatility regime, as the impact of a negative downturn would take a relatively long period of time to dissipate, given the nature of persistence in the price behaviour of Bitcoin in the cross-markets.

To investigate further, the rest of the chapter is planned as follows. Section 2 explores the literature on modelling long memory in Bitcoin markets. Section 3 discusses the empirical methodology in both MS-AR and MS-ARFIMA. Section 4 presents the data and summary statistics, illustrating with two stationarity tests. In Section 5, a discussion of the results is carried out under three subsections: structural breaks, fractional integration and MS-ARFIMA, respectively. Section 6 discusses some alternative measures to validate the robustness of the conducted analysis. Section 7 concludes and presents the main implications of our research. Finally, it is useful to view the Appendix B in appendices Section to check the robustness and validation of the empirical tests.

### 3.2 Literature review.

The literature on financial markets volatility has been investigated widely through different econometrics tools. These remarkable and stupendous studies have analysed and modelled financial market volatility to clarify the ambiguity of the dramatic fluctuation in financial assets prices. All this significant attention is due to the huge impact of volatilities on economies' components and global markets. Thus, a thorough and deep investigation should tackle this issue to increase the quality of decisions, plans and investments across financial markets. The following section highlights the main approaches to modelling volatilities, following which we recall the most relevant studies applied in financial market volatilities with respect to the structural breaks in financial time series and their importance in volatility modelling.

Prior to revising the literature, it would be helpful to provide an overview of the most relevant theories in financial markets volatility. Tracing the source of markets volatility could lead us to some well-known economic theories on efficient market hypothesis (EMH), speculative bubbles, overreaction and noise trading (Scott, 1991). These theories explain the mechanism of valuing or pricing financial assets within dynamic financial markets. Consequently, they should clarify and justify why and how prices are determined, and hence fluctuate over time (Scott, 1991). For instance, the concept of the seminal work of (Fama, 1976) explains that the current asset price should reflect all the available information in the market. However, newly arrived information (e.g. political news, monetary policies, fiscal policies) in financial markets will adjust prices randomly and unpredictably, and hence will generate some sort of different fluctuations over time (Bauwens et al., 2012)<sup>2</sup>. From an irrational perspective, speculative bubbles and noise theories have tried to examine the existence of deviation among the fundamental value of financial assets and their market prices (Scott, 1991). Based on the latter theories and the many financial theories, fluctuating prices play a core role in generating volatilities (systematic and idiosyncratic risk) in global financial assets and markets.

Recently, the augmentation of economic and political events alongside Bitcoin markets has created a state of uncertainty in the global financial markets. Generously, academics and practitioners have supported the literature of volatility by a bulk of contributions from different academic areas. Historical volatility (HV afterwards) is one of these areas that have been applied, especially by practitioners and traders from disciplines other than finance. HV is considered an important and principal financial tool for providing a good benchmark of volatility in a specific sector or market. By contrast, Parkinson claimed that traditional volatility measures give poor information and sensitive movements (high noise). Therefore, he endeavoured to provide a more professional technique based on geometric Brownian motion. The latter technique helps in eliminating undesirable drifts from the model, which basically solves the problem of jumps and drifts (close & open

---

<sup>2</sup>Further information see EMH hypotheses (Fama, 1970, 1976, 1991)

or weekend events) in the classic volatility equation (HV). Theoretically, Parkinson's High-Low historical volatility (HL-HV afterwards) is more efficient than the traditional volatility (HV) by 2 to 5 times (Bennett & Gil, 2012; Parkinson, 1980) . Many volatility modelling approaches (HV, HL-HV and others) have been applied in the literature (for more details see (Alizadeh et al., 2002; Bauwens et al., 2012; Beckers, 1983; Garman & Klass, 1980; Parkinson, 1980; Rogers & Satchell, 1991; Wiggins, 1992; Yang & Zhang, 2000). Further, exponentially weighted moving average process (EWMA) has been effectively employed for forecasting the volatility across financial markets, see (Chou, Chou, & Liu, 2010; Cox, 1961; Holt, 2004). For HV in Bitcoin Market, see (D. Baur & Dimpfl, 2017).

The performance of HV models was found to be poor in terms of capturing dynamic volatility (Engle, 1982; Hsieh, 1991; Parkinson, 1980). The latter problem has induced scholars to find different approaches that could improve the models to be more dynamic and flexible in capturing the behaviour of assets. Indeed, the development of more efficient and accurate models is necessary to face the complexity and non-linear behaviours of financial data (such as Leptokurtosis, volatility clustering, leverage effect, and many others) (Brooks, 2014). Further, it is well-known that the variance of the residual in financial time series models is unlikely to be constant (Brooks, 2014). Consequently, a new class of stochastic models, Auto-regressive conditional heteroscedasticity (ARCH afterwards) was introduced by (Engle, 1982) to cope with the aforementioned behaviours of financial data<sup>3</sup>. Despite the literature on analysing and forecasting volatility in financial markets having grown extensively after introducing the ARCH model, some weaknesses have been identified in the model<sup>4</sup>.

Therefore, introducing the generalised auto-regressive conditional heteroscedasticity (GARCH afterwards) model has helped in avoiding the latter weaknesses in the ARCH model (Bollerslev, 1986; Taylor, 1986). The new approach with its extensions has allowed scholars to trace the leverage effect and many characteristics which were not able to be captured in the ARCH model. Since then, a huge number of extensions to the GARCH model have been introduced, such as Exponential GARCH (EGARCH), GJR-GARCH, GARCH in mean (GARCH-M), and many others. For more details see the full survey (Andersen et al., 2009; Bauwens et al., 2006; Teräsvirta, 2009). Turning to cryptocurrencies markets, the GARCH family has been employed in this stream. For example, Chu et al. (2017) investigated the volatility of the most popular cryptocurrencies under twelve different extension of GARCH model. Their results suggest that most cryptocurrencies, including Bitcoin display extreme volatility, especially in enter-daily prices. The literature on cryptocurrencies under the GARCH family approaches has started to grow rapidly recently, see(Charles & Darné, 2018; Dyhrberg, 2016; Katsiampa, 2017).

---

<sup>3</sup>for a full survey and more theoretical details see (Bollerslev, Chou, & Kroner, 1992)

<sup>4</sup>(e.g. the model assumes that both negative and positive shocks have an equal effect on volatility, hence, the ARCH system is restrictive, especially if the ARCH order become higher)

However, Hsieh (1991, 1993, 1995) has introduced models through auto-regressive process, such as the Auto-regressive volatility model (AV afterwards), which is considered to be an efficient non-linear model compared with the HV and GARCH models. The non-linear models are able to capture the auto-correlation behaviour of variables and become more consistent with data fluctuating over time. For example, Hsieh (1995) and H. Li and Hong (2011) stated that AV approach, efficiently captures the mean-reversion and clustering volatility in financial data, while HV models are not able to capture these behaviours. Moreover, H. Li and Hong (2011) reported that estimating financial volatility data through the AV process gives more accurate and efficient forecasting than the GARCH model.

To draw a conclusion from all the above, financial market volatility has been studied intensively in the literature through different models, such as historical volatility, implied volatility or GARCH family. Many advantages and disadvantages are mentioned above, but one important issue has not received enough attention in forecasting volatility literature along with the other features of financial data. Researchers have claimed that neglecting the structural breaks (breakpoints) in exchange rates, cryptocurrencies and stock market volatility could lead to poor results and corrupted estimations (Bai, 1994; Hammoudeh & Li, 2008; Hansen, 2001).

Modelling structural breaks has been growing extensively in the literature via many streams. The focus will be divided into four streams: firstly, modelling the structural breaks in moving average process; secondly, modelling the breakpoints in auto-regressive models; thirdly, structural breaks with long memory process; fourthly, modelling ARMA and detecting the breakpoint simultaneously. Finally, modelling fractional integral process and structural breaks simultaneously.

### **3.2.1 Modelling the breakpoints in Moving average process**

Based on the Sunspot, Venus and credit cycle theories, a huge amount of literature has studied the modelling trends and cycles in economic history (Morgan, 1990). Therefore, in the mid-20th century, researchers started to pay attention to the cyclical and trends fluctuation during economic events. In order to reduce bias in modelling the fluctuations and jumps in cycles and trends, researchers resorted to dismantling the economic time series to fit the data accurately. For more details, see (Aldcroft & Fearon, 1972; Ford, 1981).

Since modelling and analysing the growth trend in business cycles by simple linear models (Frickey, 1947; Hoffman, 1955), many drawbacks have been found and documented in the literature. Consequently, scholars have been motivated to find a solution by isolating the trends in time series and examining them individually in the same system. Aldcroft and Fearon (1972) and Ford (1981) applied a moving average method to differentiate

between jumps in the system. They used this moving average model to treat the trend stochastically and ensure the system did not depend entirely on the cyclical component.

Ford (1969) investigated the impact of exports in the British economy during the years 1870 and 1914. According to him, the nature of data has a cyclical pattern with different trends. Consequently, in order to study these data, a deviation moving average technique was applied to extract some trends from the later cycles. By applying the later method, he answered the question, "What is the impact of export as a source of income and import as a leakage from the incomes and expenditure on the British economy?", explaining in precise detail the actual causes of fluctuation by virtue of separating the dynamic behaviours and distinguishing between them<sup>5</sup>.

Using moving average technique to study trend behaviour considers misleading, as providing the model with a small sample will result in losing the model's trend (Aldcroft & Fearon, 1972). Therefore, to solve the problem Leser (1961) & Hodrick and Prescott (1997) developed an unweighted moving average model, allowing the first part of the model to calculate the goodness of fit and the second part to measure the smoothness of parameters. Therefore, the later technique will save the sample size from any losses. Hodrick and Prescott (1997) rebuilt the latter model in a matrix form to obtain a filter weight (H-P filter) for calculating the trend repeatedly at each time in the series.

Ravn and Uhlig (2002) found that changing the observations frequency affects the results of the Hodrick-Prescott filter (HP filter). Hence they developed the latter method by using two different techniques: first, a time domain approach, focusing on calculating the smoothing parameter; second, a frequency domain approach, focusing on the transfer function of the HP filter. Thus, the two approaches are now able to adjust the smoothing parameter with respect to the change of frequency observation. Further, Maravall and del Río (2007); Ravn and Uhlig (2002) focused on monthly, quarterly and annual observations to analyse the HP filter from different angles. They studied both temporal aggregation and systematic sampling to increase the accuracy of HP filters. However, for more detail on moving average and structural breaks, see the excellent survey (Mills, 2016).

For recent research, Urquhart et al. (2015) applied a moving average model on the Japanese, UK and U.S. stock market data to determine how those markets adapted to the knowledge of the profitability of technical trading. However, *MA* model showed a clear structural break around the year 1987, and they found that the model's predictive power decreased remarkably after the breakpoint (1987). This suggests that applying the moving average model in time series could detect any changing point in the series. However, in the next subsection more advanced and flexible methods will be revised.

<sup>5</sup>For a full survey on modelling trend and cycle see (Mills, 2016).

### 3.2.2 Modelling the breakpoints in Auto-regressive model AR

Modelling the moving average and auto-regressive models to extract the trends and identify the breakpoint from economic time series has been successfully applied in the literature<sup>6</sup>. However, with the rapid development in financial markets and financial econometrics, more advanced approaches were needed to deal with the cons of modelling financial data (e.g. structural breaks). The seminal work of (Hamilton, 1989) provided an effective framework in forecasting and modelling the behaviour of macroeconomic and financial data<sup>7</sup>. Hamilton stated that involving multiple structure (models) or moving into an auto-regressive model, can explain the financial time series behaviour during different economic events (e.g. low and high interest rates). Thus, allowing the process to switch between these structures will help the system to capture more complex behaviours. The gold feature of Markov Switching Model (MSM, SM or MS afterwards) is that switching among the regimes is controlled by a latent variable with first-order Markov chain (Kuan, 2002)<sup>8</sup>.

Hamilton (1989) applied his new framework (MSM) to post-war U.S. data on real GNP between 1951 and 1984. This model attempted to study the U.S. business cycle by considering two states, a recessionary state and a growth state. So, allowing unobservable variables to switch between the two states, negative growth rate (recessions) and positive growth rate (normal time), respectively, will measure and analyse the behaviour of economic recession more accurately and efficiently. The model suggested that an economic depression is linked with a 3% permanent increase in the rate of GNP. Empirically speaking, Hamilton (1989) claimed that the model is flexible and more intuitive by allowing the value of current state to depend directly on its instant past value. Another extra feature is that the system permits the properties of the model to be determined by both the state variable and the innovation terms. The latter approach was provided to cover the shortcomings of (Quandt, 1972)'s model, which considered that switching between states is totally independent over time. Consequently, the realisation of the current state is independent from the past and future states, so the model could become "noisy" (switching back and forth between the states).

Hamilton's model regulates the auto-regressive model to include a unit root by assuming that the time series is the aggregate of a two-state Markovian process and a general auto-regressive model. This suggests that the series is trendless and not suitable for most macroeconomic series. The previous sharp criticism was admitted by (Lam, 1990), after explaining the importance of restricting the unit root in the model. He claimed that the impact of the error term on long-run forecasting of incomes depends on the existence of unit root. Therefore, based on the later criticism, he relaxed the auto-regressive model so as to be not restricted to the assumption of unity (generalising Hamilton's model).

---

<sup>6</sup>For full survey, see Mills (2016)

<sup>7</sup>For more information, see (Goldfeld & Quandt, 1973).

<sup>8</sup>For full survey, see (Andersen et al., 2009; Hamilton & Raj, 2013).

By applying the same data as Hamilton's paper (the log of real GNP of the USA), he proved that his model performed better than Hamilton's model in the long-run term. By contrast, he found that Hamilton's model outperformed his approach and the ARIMA model in the short-term horizon. From another dimension, Kim (1994) introduced a new technique to reduce the computation time and increase the filtering power in Hamilton's model. Also, Kim stated that relaxing his new approach on Lam's method was enabling the system to be more effective and powerful.

From another angle, F. X. Diebold et al. (1994) stated that although the Markov switching model is useful in capturing the dynamic behaviour of financial data, fixing the transition probabilities over time will let the switching probabilities from one regime to another would not depend on the behaviour of the econometric model. Thus, they proposed a modified Markov switching model in which the probabilities of transition are able to change with fundamentals. They supported their approach by providing a full simulation based on *EM* algorithm to prove that allowing the transition probabilities to vary with the dynamic model will increase the power of the model.

Since Hamilton (1989) focused on modelling the mean behaviour to allow the model to be involved in more complex dynamic behaviour (e.g. structural breaks), the literature started to grow extensively, particularly in financial markets. Garcia and Perron (1996) went a step further to find a special case in the behaviour of the U.S. real interest rate. They found three states could explain the behaviour of time series (1961-1973, 1973-1980 and 1980-1986), after employing Hamilton (1989)'s approach. The approach suggested that some structural events had occurred along the sample span, due to sudden changes in oil price, monetary policy and federal budget. They concluded that real interest rate is essentially random with different mean and variance in three segments of time. Moreover, Schaller and Norden (1997) investigated the behaviour of stock markets in both mean and variance through (Hamilton, 1989)'s method. They found very strong evidence for the structural breaks and switching behaviour. The power of their evidence came from applying different methods (e.g. switching in mean, switching in variance, and changing the transition probabilities over time). Lastly, they employed (Hansen, 1992b) and (Garcia, 1998) tests to prove that the switching regime was statistically significant.

In 1998, Kim and Nelson developed an approach based on (Shephard, 1994)'s methodology and processed it through Bayesian framework to enable the system to measure the regime probabilities at each point in time. Moreover, they answered the question, " Do the resulting estimates of regime switches show evidence of duration dependence?" by involving non-zero probabilities of duration dependence in the switching model. Their findings supported the literature on the switching model by suggesting that the recession state indicates a strong positive duration dependence, while the booms state suggests vice versa, within a uni-variate context (F. Diebold & Rudebusch, 1990; F. X. Diebold et al., 1993). Multivariate and Bayesian approaches were extended to measure the duration dependence, and to support the univariate context (F. Diebold & Rudebusch, 1990; Kim & Nelson,

1998). Since the later contributions and modification to the MS-AR model, extensive research has employed it with its application to study the dynamic behaviour across financial markets. Studying the behaviour of exchange markets is extremely important and useful to support investment decisions. Therefore, employing an advanced method to treat the complex behaviour of exchange markets and financial markets in general will help to improve the quality of financial decision making.

Hamilton (1989) introduced the MS-AR model, which has helped researchers and practitioners to trace the dynamic fluctuation with the existence of structural breaks in the system. (Abiad, 2003; Bazdresch & Werner, 2005; Chen & Lin, 2000; Fiess & Shankar, 2009; Jeanne & Masson, 2000; Kirikos, 2000; Li et al., 2010; Subagyo & Sugiarto, 2016; Xin, 2013) concluded similarly by supporting the stream of literature in financial markets, and particularly in exchange markets.

### 3.2.3 Modelling the long memory (Fractional integration)

Many aspects of real life could convert into time series data. Common examples might be: stock markets, astrophysics, macroeconomics, speech recognition and many others. Basically, to study these time series data, an analysis should be employed to extract all the useful characteristics and convert them into readable information that could add new knowledge and contribute to the literature. The key concept here, the analysis of time series, relies entirely on the interdependence among observations. In other words, the question, "how far do values in time series affect each other?" embodies the concept of studying the time series.

However, one of many characteristics of the time series is defined as a long memory process or long-range dependence. In the seminal work of Diebold and Inoue (2001), the long memory process was defined from two different perspectives: time and frequency domains. In the time domain, the process focused on the decay level of long-lag auto-correlations; while, in the frequency domain process, the focus was on the level of burst of low-frequency spectra. In other words, the long memory process means that the dependence between observations in the series is relatively strong. Detecting the origin of long memory could lead us to very significant literature, such as, (Cioczek-Georges & Mandelbrot, 1995; Granger, 1980). For more details see (Andersen et al., 2001; Diebold & Inoue, 2001).

In 1980, Granger tried to explain the long memory process by aggregating dynamic equations. He showed that cross-sectional aggregation could have a long-range dependence. Three possible suggestions were detected in the time series models: firstly, the time series has a spectrum of small frequencies  $d > 0$ . Secondly, the time series had infinite variance ( $d \geq 1/2$ ) or finite variance ( $d < 1/2$ ). Thirdly, a time series with  $d=1$  needs to be differenced to approach stationarity. Granger (1980) claimed that in practice, aggregating dynamic equations could generate a new class of models that have different properties

(e.g. long memory and integrated process). Consequently, the models should be diagnosed before analysis, otherwise the estimation will be inefficient or spurious (Granger, 1980). During the same period of time, Granger and Joyeux (1980) introduced the "fractional differencing" technique and suggested that the "d" order does not necessarily have to be an integer, as (Box & Jenkins, 1970)'s method. By allowing for a fractional "d" ( $1 > d > 0$ ) the model might provide a higher quality of forecasting in both the short-run and the long-run, especially in low-frequency modelling. As a result, Granger and Joyeux (1980) stated that proposing the fractional differencing process provides useful and fruitful long-dependence forecasting properties, particularly in low-frequency equations.

Long-range dependence models have been employed extensively in financial data (e.g. inflation rates, interest rates, forward premiums) (Baillie, 1996). Baillie (1996) claimed that long memory processes have gained significant success in examining the volatility in financial markets. Slightly wider, indeed the auto-regressive fractional integrated moving average (ARFIMA afterwards) model (Granger, 1980; Granger & Joyeux, 1980; Hosking, 1981) has several useful applications in financial markets literature, particularly in volatility forecasting. An example of the latter claim, F. X. Diebold et al. (1991) applied ARFIMA process to study the behaviour of 16 real exchange rates. Their conclusion was that applying *ARFIMA* models provided powerful long-run forecasts and effects of shocks. One more example to support ARFIMA process' literature, Crato and Rothman (1994) estimated the real exchange rate of nine currencies against the British pound between 1973 and 1990 to find the long-run purchasing power parity. They claimed that ARFIMA processes are more flexible and relatively more generalizable than other earlier studies. Others supported the accuracy and power of *ARFIMA* process. For more details in the literature, see (Coli et al., 2005; Comte & Renault, 1998; Granger & Ding, 1996; Martens et al., 2004). For full survies, see (Baillie, 1996; Liu, Chen, & Zhang, 2017).

The aforementioned literature claimed that *AR*, *MA*, *ARMA* and *ARIMA* processes can only capture short-run dependence (Liu et al., 2017). By contrast, the *ARFIMA* model provides a better fit and forecasting when dealing with long memory data (F. Diebold & Rudebusch, 1990; Liu et al., 2017). Although *ARFIMA* models perform better than previously, Hauser et al. (1999) criticised the processes and proved that *ARFIMA* is not suitable for the estimation of stability, because of the violation of behaviour in their spectral densities. For countering literature see, (Reschenhofer, 2000; Sitohang & Darmawan, 2017). Consequently, the development and building of more appropriate approaches to forecast macroeconomic and financial data under different circumstances is required (Gabriel & Martins, 2004; Haldrup & Nielsen, 2006). In the next section, a new set of approaches is developed within *ARFIMA* process to increase the accuracy and capabilities of forecasting.

### 3.2.4 Modelling structural breaks with ARFIMA process

Regime switching with long memory models has been employed and studied intensively in financial markets. However, distinguishing between terms is extremely important, as structural break and long-range dependence are very different fields for the same phenomenon (Diebold & Inoue, 2001; Haldrup & Nielsen, 2006). Thus, an active literature has been explored for these two phenomena to clear up the confusion between the aforementioned models and provide more understandable and distinct work in this area (Diebold & Inoue, 2001; Granger & Ding, 1996; Granger & Hyung, 2004; Hidalgo & Robinson, 1996; Lobato & Savin, 1998). Based on the aforementioned literature, it was agreed that a certain time series might show spurious long memory with respect to its fractional order, see (Baillie, 1996; Beran & Terrin, 1994; Diebold & Inoue, 2001).

Empirically, Haldrup and Nielsen (2006) developed a Markov regime switching model which allows us to divide the long memory into different regime states. They used hourly spot electricity prices for 4 Scandinavian countries between January 2000 and October 2003. The switching regime model permitted categorisation of the behaviour of electricity prices over time (long memory) into two states, the congestion and non-congestion market. Their analysis generated important and fruitful outputs regarding the behaviour of electricity prices. Analytically, the data (e.g. East Denmark and Sweden data pair) suggested that the two series were fractionally co-integrated, but applying a switching regime model reveals that the data were fractionally co-integrated in one state and not in the other state. Moreover, an important feature claimed by Haldrup and Nielsen is that the switching model system could have different levels of long memory from regime to regime in the system. Motivated by the previous advantage, Tsay (2008) applied the same methodology to discover the impact of oil prices on *U.S.* inflation between 1947 and 2007. Results suggested that oil price fluctuations play an important role in determining the paths of *U.S.* inflation.

On the same grounds, Haldrup et al. (2010) endeavoured to solve a disadvantage found in (Haldrup & Nielsen, 2006)'s framework by extending it from a univariate to a multivariate model. Econometrically, the latter limitation is that the model estimates the parameters separately, when actually the parameters are dominated by the same shock. Thus, proposing a model that allows for a long memory and regime dependent vector auto-regression (*VAR*) adds the advantage of permitting the variables to be incorporated in the same process, being dominated by the same shock. The proposed model has proved its effectiveness, particularly in forecasting, by providing a small mean absolute forecast error (MAFE) compared with the univariate estimation. On the contrary, the two proposed models above (Haldrup et al., 2010; Haldrup & Nielsen, 2006) consider the state variable in the regime switching model as an observable state, while the standard (Hamilton, 1989)'s model assumes the state variable as latent. Moreover, the latter two models do not satisfy the proposal of (Diebold & Inoue, 2001), who suggested that a

Markov switching model with latent variable can generate a long memory dependence process.

Turning from electricity markets to interest rate markets and the Nile river level, Tsay and Härdle (2009) proposed a general class of Markov-switching auto-regressive fractional integral moving average ( $MS - ARFIMA$  afterwards) processes, and used Durbin-Levinson-Viterbi algorithm to easily deal with the complexity of computation<sup>9</sup>. The distinguishing feature of the latter processes is that a hidden Markov model was employed. In other words, in contrast to (Haldrup & Nielsen, 2006)'s approach, Tsay and Härdle (2009) modelled  $MS - ARFIMA$  by assuming that the variable state is latent. By this method, the model became consistent with the Markov-switching  $AR$  model (Hamilton, 1989) and the puzzle proposed by (Diebold & Inoue, 2001) to build a latent Markov switching model that can generate long-range dependence. Tsay and Härdle (2009) applied their proposed model on  $US$  ex-post real interest rate and Nile river level data to prove the stability and consistency of the model. Both applications provided consistent results with the literature and were found to be useful in detecting structural breaks and fractional integration simultaneously and endogenously (Tsay & Härdle, 2009).

From South Africa, Balcilar et al. (2016) applied the latter model to study the duration of inflation persistence over time and across different monetary policy regimes. Thus, monthly  $CPI^{10}$  inflation between April, 1923 and April, 2014 was regressed to identify the structural breaks along the series. Three regimes were identified: 1 – a low inflation regime (1920 – 1960); 2 – a high inflation regime (1961 – 2003); 3 – a low inflation regime (2003 – 2014). Results suggest that inflation was persistent in all regimes, but was significantly more persistent in a high inflation regime. By contrast, considerably shorter persistence was found during the low inflation regime. Balcilar et al. claimed that applying  $MS-ARFIMA$  model could generate useful and effective results for monetary policies and macroeconomic applications.

Fofana et al. (2014) developed a regime switching univariate  $ARFIMA - GARCH$  model to examine the problem of confusion between long memory and non-stationarity in economics and financial time series. They analysed the daily volatility of two exchange rates between January, 1990 and March, 2014. Their results indicate that the model was capable of analysing the long-range dependence parameter and identifying non-stationarity. However, the proposed model could not be estimated by Maximum Likelihood approach because of the path dependence. Consequently, a Bayesian Markov chain Monte Carlo ( $MCMC$ ) method was used to embrace the problem. On the one hand, the authors claimed that  $RS - ARFIMA - GARCH$  model<sup>11</sup> was performing very well in modelling financial time series and structural changes; on the other hand, although the model considered the state variable to be latent (Tsay & Härdle, 2009), they assumed that

---

<sup>9</sup>More details are given in the methodology section

<sup>10</sup>Consumer price index

## <sup>11</sup>Regime switching-ARFIMA-GARCH

all regimes have the same probability of occurring (Fofana et al., 2014). Staying in financial markets volatility, Raggi and Bordignon (2012) proposed a framework in line with previous models, but the key difference in their framework is that the regime shifts were modelled via binary non-observable Markov process, which allows the states to stay dependent. They applied the latter approach to 5 minutes intra-daily data of *S&P 500* index from January, 2000 to February, 2005. The results suggest that implied volatility is important for forecasting realised volatility.

On the same grounds, Shi (2015) raised a question related to the above literature, "Can we distinguish regime switching from long memory?". On a theoretical base, he proved that smoothing probability causes long memory in regime switching. Thus, in this regard he modelled a Markov regime-switching and ARFIMA model to create a two-stage-ARFIMA (2S-ARFIMA) framework that could dominate the impact of the smoothing probability series. A simulation study was proposed to show that it can easily and efficiently separate the *ARFIMA* process from *MRS*<sup>12</sup> process. By applying the latter approach in a financial application, it could easily clear up the confusion between regime switching and long memory models. Similarly and on the same level, Shi and Ho (2015) proposed a *MRS – ARFIMA* model<sup>13</sup> to alleviate the confusion between long memory and regime switching. They applied their framework on German-Klass and realised volatility of the FTSE index between January, 2001 and December, 2012 to explain the usefulness and advantages of the proposed model. To support their results, a Monte Carlo simulation showed that the model could easily and effectively identify the pure *MRS* and the pure *ARFIMA* models<sup>14</sup>.

To sum up, volatility has been a controversial and important tool in financial markets for decades. Historical volatility was popular for studying the behaviour of financial instruments before the moving average *MA* and auto-regressive *AR* processes became more effective in forecasting the fluctuations of financial securities. Later on, auto-regressive conditional heteroscedasticity *ARCH* family and its extensions become more popular to deal with financial data behaviour, particularly leverage affect and clustering data. Although previous models perform very well in investigating volatilities across markets, a huge gap still exists in studying the dynamic behaviour of volatility. As a consequence, a strand of literature has started to investigate the dynamic behaviour of financial assets with regard to the structural breaks along the time series. Many studies have identified how break- points play an important role in determining the accuracy and robustness of stochastic models. Thus, researchers and scholars have tried to find the optimal model to cope with the complex behaviour of financial data. Unfortunately, the long memory process comes with structural breaks to cause confusion in identifying the latter terms. As a result, researchers such as (Tsay & Härdle, 2009) introduced a

---

<sup>12</sup>Markov-Regime Switching

<sup>13</sup>Markov regime switching-autoregressive fractional integrated moving average

<sup>14</sup>To explore more methodologies in investigating structural breaks and long memory see (Charfeddine & Guégan, 2012).

state-of-the-art endogenous model that can deal with all the limitations mentioned earlier in (Fofana et al., 2014; Haldrup et al., 2010; Haldrup & Nielsen, 2006). More empirical details will be discussed in the methodology section.

### **3.2.5   Review of the Cryptocurrency literature**

Cryptocurrency markets have recently received significant attention due to their important role in global financial markets. Thus, a significant growth of research has sprung up recently to help governments and policy makers to design adequate regulations on controlling cross-market movement shocks, and to discriminate and facilitate the best investment decisions for financial institutions, investors and portfolio managers.

An excellent systematic survey done recently (Corbet et al., 2019) reveals that the literature has focused mainly on three theoretical and empirical research areas: first, regulations and information system research; second, financial market and monetary theoretical formulation of cryptocurrency; and third, development of econometric and/or statistical mechanisms to understand price behaviour under different scenarios. Another systematic review done by (Kyriazis, 2019a) explores the cryptocurrency research under efficient market hypotheses and long-range dependence, in which the latter provides us with crucial inferences in determining the best investment strategies for gaining extraordinary returns. To maintain the flow, and minimise repetition and space of a succinct literature review, interested readers are encouraged to refer to the latter two surveys.

Investigating the regulations and information systems of cryptocurrencies allows authorities and legislators to derive suitable laws and regulations with boundaries to increase the efficiency and decrease frustration and manipulation of the market (Böhme et al., 2015; Dwyer, 2015; Gandal et al., 2018). A growing body of literature on economics and financial markets, simultaneously with the latter phase of research has helped individual investors, investment entities and risk managers to hedge and diversify their investment to maximise their profits with the lowest associated risk (Baur et al., 2018; Gillaizeau et al., 2019; Urquhart & Zhang, 2019). Despite the sparse amount of cryptocurrencies literature on finance and economics, much excellent research in different areas such as market efficiency, price and/or bubble dynamics, hedging and diversification strategies has attempted to examine the cryptocurrencies market and Bitcoin in particular.

A plethora of empirical research has systematically presented state-of-the-art estimation techniques to identify the efficiency of Bitcoin markets (Brauneis & Mestel, 2018; Khuntia & Pattanayak, 2018; Wei, 2018), adopting different methods to support it and concluding that the level of efficiency is associated with several factors, such as liquidity and size. On the contrary, many researchers support the fact that the Bitcoin market shows lack of efficiency, due to an imbalance between the true value of Bitcoin and its available

information in the market (Bouri et al., 2019; Urquhart, 2016; Vidal-Tomás & Ibañez, 2018). Investigating the connectedness/spillovers and market dynamics provides a clear indication of market inefficiency, together with useful information about the net receiver and net dispenser of Bitcoin volatility (viz. Corbet et al., 2018; Gillaizeau et al., 2019).

A wide range of empirical research also focuses on long-range persistence, cointegration and structural breaks to explain the complex behaviour and non-linear dynamics of Bitcoin prices (Alvarez-Ramirez et al., 2018; Caporale et al., 2018; Cheah et al., 2018). The existence of long-range dependence along the volatility series indicates informational inefficiency in the market; hence, speculation, forecasting and designing profitable investment strategies can be exploited to make abnormal profits, but ignoring the stability of the system during the analysis process could generate misleading information. Others have analysed the time varying behaviour of long range dependence through different tests such as Hurst exponent and detrended fluctuation analysis *DFA* and exact local whittle estimation with rolling windows (Alvarez-Ramirez et al., 2018; Bariviera, 2017; Bariviera et al., 2017; Caporale et al., 2018; Cheah et al., 2018). Statistical properties are subject to sudden change over time, especially in the Bitcoin market, which may leave some distortion shocks permanency; hence, structural breaks test are crucial to validate the long range stability process (Al-Yahyaee et al., 2018; Bouri et al., 2019; Charfeddine & Maouchi, 2019; Mensi et al., 2018, 2019). A long debate in the literature suggests that the presence of structural breaks in a time series could appear as high long-range persistence; thus, level shifts and long memory are easily confused as Diebold and Inoue (2001) suggested.

By contrast, former studies such as Chaim and Laurini (2018) shed light on stochastic volatility models with shifts in mean and variance for a ‘cryptocurrency market’ and ‘other asset markets’ (such as indices and gold), Cheah et al. (2018) demonstrating the importance of cross-market dynamic interdependence of Bitcoin prices by estimating a system-wide long-memory. The focus on a cross-market rather than a single market cryptocurrency market in the latter study has significance in our context: by employing *ARFIMA* Markov Switching with endogenous switch governing the internal dynamics of Bitcoin prices or volatility system, we will be able to distinguish between the true and spurious long memory with high accuracy.

### 3.3 Empirical Methodology

### 3.3.1 Markov Switching Auto-regressive Model MS-AR

Hamilton (1989) introduced a discrete shifts in regime process through an auto-regressive model to trace the dynamic behaviour of a time series. To illustrate that, we should consider that the mean (intercept) of an auto-regressive model is non-constant overtime. Thus, different auto-regressive models should be built after each break point to boost the efficiency of detecting the non-linearity in a time series. Models (3.1) and (3.2)<sup>15</sup>, below, illustrate how considering two different intercept could help in solving the turning point problems in time series.

$$x_t = \alpha_1 + \beta x_{t-1} + \epsilon_t, \quad (3.1)$$

$$x_t = \alpha_2 + \beta x_{t-1} + \epsilon_t, \quad (3.2)$$

Where,  $\alpha_{1\&2}$  the constant terms and  $\epsilon_t \sim i.i.dN(0, \sigma^2)$ . The concept of the latter models is plausible, but not effective to be processed individually. Econometrically, changing the behaviour of series in the past and in the future (e.g. changing the intercept) should be considered in the same model to provide a reliable forecasting. In this regard, the above models could be compressed in a one framework and then allow the process to switch among intercepts by an unobserved variable  $S_t$ , which  $S_t$  called regime or state variable (e.g.  $S_t = 1, 2, 3, \dots$ ) <sup>16</sup>. Consequently, equations (3.1) and (3.2) can be rewritten as:

$$x_t = \alpha_{S_t} + \beta x_{t-1} + \epsilon_t, \quad (3.3)$$

Where  $S_t = 1$  when the process is in state 1 ( $\alpha_1$ ), in contrast,  $S_t = 2$  when the process is in state 2 ( $\alpha_2$ ). Equation (3.3) follows a normal distribution with different means and variances. Hamilton considered latter regimes to be an unobserved random variable or in other words discrete-valued stochastic variable. Mathematically, Markov chain process is the simplest and proper model to deal with the travelling processes among regimes within a system. Before start explaining Markov chain, let us firstly set  $S_t$  to be an integer number as  $(1, 2, 3, \dots, N)$ . Secondly, Assume that  $S_t$  equals a specific amount of  $j$  and the probability of obtaining  $j$  depends totally on the most recent past value  $S_{t-1}$ . Latter

<sup>15</sup>Some researchers considering these models as zero mean, see (Cochrane, 2005; Hamilton, 1994)

$$x_t - \alpha_1 = \beta(x_{t-1} - \alpha_1) + \epsilon_t.$$

<sup>16</sup>Notice here, if  $S_t, t = 1, 2, \dots$  is defined as observable variable (known in advance), then the process is simply a dummy variable auto-regressive.

specification can be written mathematically as:

$$p = \{S_t = j | S_{t-1} = i, S_{t-2} = m, \dots\} = p\{S_t = j | S_{t-1} = i\} = p_{ij}^{17} \quad (3.4)$$

Where  $p_{ij}, i, j = 1, 2, 3, \dots, N$ . Which  $p_{ij}$  is the transition probability,  $i$  is the state in time  $\{t-1\}$  and  $j$  is the state in time  $\{t\}$ . By probability law the sum of all  $p_{ij}$  must be equal to 1.

$$p_{i1} + p_{i2} + p_{i3} + \dots + p_{iN} = 1, \quad (3.5)$$

Transition probabilities could be compressed into  $(N \times N)$  matrix, called the transition probability matrix or  $P$ :

$$P = \begin{pmatrix} p_{11} & p_{21} & \dots & p_{N1} \\ p_{12} & p_{22} & \dots & p_{N2} \\ \vdots & \vdots & \dots & \vdots \\ p_{1N} & p_{2N} & \dots & p_{NN} \end{pmatrix} \quad (3.6)$$

In this transition probabilities matrix the column indicates to  $i^{th}$  and the row indicates to the  $j^{th}$  of  $p_{ij}$  in equation (3.5). For instance, the column 2, row 1 parameter indicates to the probability that state 2 will be followed by state 1. In other words, transition probabilities should give some inference for choosing the current state among the states in the system:

$$\begin{aligned} P\{S_t = 2 | S_{t-1} = 2\} &= p \\ P\{S_t = 1 | S_{t-1} = 1\} &= q \end{aligned} \quad (3.7)$$

In case the system has two states, four transition probabilities will be generated: staying in the same state ( $p$  or  $q$ ) or switching from state to state ( $1 - p$  or  $1 - q$ ). In general, after forecasting the Markov chain a Maximum Likelihood Estimation *MLE* method can be employed to analyse the mixture model<sup>18,19</sup>. Estimating the model can be executed by the expectation maximisation (ME) algorithm<sup>20</sup>.

<sup>17</sup>Notice here, Hamilton assumed that the state is just depends on the most recent past value  $\{S_{t-1}\}$  and ignore all others  $\{S_{t-2}, S_{t-3}, S_{t-4}, \dots\}$ .

<sup>18</sup>Markov chain can be represent through vector auto-regression frame to calculate all the possible number of ahead forecasts of the process. Notice here, the matrix  $P$  must be irreducible ( $p_{11} < 1$  and  $p_{22} < 1$ ) otherwise the state will be an absorbing state (the process will stay in this process forever), to review the full process see (Hamilton, 1989, 1994).

<sup>19</sup>After forecasting the probabilities, an inference on the regimes can be build through Bayesian theorem, by combining the information of current and past data, transition probabilities and distributions. The latter combination can generate inference for each date  $t$  in the sample data, this process called the smoother recursion, see (Kim, 1994) for more details.

<sup>20</sup>The first equation displays the normal distribution function:

$$f(X_t | S_t = j; \theta) = \frac{1}{\sqrt{2\pi\sigma^2}} \cdot \exp\left(\frac{-(x_t - \alpha_j)^2}{2\sigma_j^2}\right) \times P(S_t = j | x_{t-1})$$

where,  $X_t$  is the data set,  $S_t$  is the number of states,  $\theta$  is a vector of population parameter  $\theta = (\alpha_1, \alpha_2, \sigma_1, \sigma_2, p_{11}, p_{22})$ . For more information about analysing *MS-AR* see Kim (1994). See also (Kim & Nelson, 1999) to explore different calculation methods of Markov switching model. Moreover, the second equation represents log *MLE*:

$$\log L(\theta) = \sum_{t=1}^T \log \{ \sum_{S_t=0}^1 f(x_t | S_t, x_{t-1}; \theta) P(S_t | x_{t-1}) \}.$$

### 3.3.2 Markov Switching Auto-regressive moving Average MS-ARMA

The latter subsection introduced a general class of  $MS - AR$  process (Hamilton, 1989). In this subsection an  $MS - ARMA$  model will be introduced to build an initial idea about  $MS - ARFIMA$  model. Chen and Tsay (2011) investigated the problem of " $N^t$  possible routs" when the system contains  $MA$  parameters by building a new algorithm based on (Gray, 1996; Hamilton, 1989) ideas and call it the extended Hamilton-gray  $EHG$  algorithm. However,  $N - state$  in  $MS - ARMA(p, q)$  model can be written as follows with respect to the equations between (3.4) and (3.7):

$$x_t = \alpha_{st} + \sum_{i=1}^p \beta_i (x_{t-i} - \alpha_{st-i}) + \epsilon_t + \sum_{i=1}^q \delta_i \epsilon_{t-i}, \quad \epsilon_t \sim i.i.d.N(0, \sigma_{st}^2) \quad (3.8)$$

The model above is identical with equation (3.3) plus the MA term ( $\delta_i \epsilon_{t-i}$ ). Some restrictions as invertibility and stationarity on *AR* & *MA* polynomials among each state should be identified:

$$\Upsilon_{st}(L) = 1 - \alpha_{1,st}L - \cdots - \alpha_{p,st}L^p, \quad \Xi_{st}(L) = 1 + \delta_{1,st}L + \cdots + \delta_{q,st}L^q. \quad (3.9)$$

Where,  $\Upsilon_{st}(L)$  &  $\Xi_{st}(L)$  are the roots of polynomial and by assumption they should be all outside the unit root circle. Moreover, both polynomials of  $AR$  &  $MA$  do not share any common roots<sup>21</sup>. However, when  $q = 0$ ,  $EM$  algorithm cannot be employed, basically, because the possible routes of regimes that running from  $t_1$  to  $t_i$  is going to expand exponentially " $N^T$ "<sup>22</sup>. Consequently, their algorithm is able to trace the past history of  $x_t$  up to a particular lag to extract the error terms from  $x_t$  instead of tracing the entire past history of  $x_t$ . Hence, the approach is recursively analysing the conditional expectation of lagged  $\epsilon_{t-N}$  the  $MLE$  can be estimated efficiently. For more approaches to resolve the same problem see (Billio & Monfort, 1998; Billio, Monfort, & Robert, 1999; Kim, 1994).

After calculating the population parameters of the switching-regime model based on *EHG* algorithm<sup>23</sup> a smooth and efficient process can easily analyse the mixture model in equation (3.8).

---

<sup>21</sup>See, (Chen & Tsay, 2011), Assumption 1

<sup>22</sup>Notice here, this problem arise when the system is going to filter out all the sequence of error terms  $(\epsilon_1, \dots, \epsilon_t)$  to proceed the *MLE*

<sup>23</sup>see, (Chen & Tsay, 2011) for the full process.

### 3.3.3 Markov-Switching Auto-regressive Fractional Integral Moving Average MS-ARFIMA

A conquer method developed by (Tsay & Härdle, 2009) will be adopted to investigate the persistence of Bitcoin volatility across different markets. In this subsections *ARFIMA* process and Markov switching model will be demonstrated in details.

*AR*, *ARMA* or *ARIMA* are formally a special case of the most generalised model *ARFIMA* process. The former models functionally are capturing only the short-range dependence *SRD*, per contra the latter process was modified to be able to trace the short-range and long-range *LRD* dependence. However, combining Markov-switching model with long memory enable us to study the fractional order of integrations with the presence of structural breaks simultaneously and endogenously through a unified framework. This process is known to be more efficient and robust for capturing the complex behaviour of exchange rates across financial markets, otherwise, neglecting the both latter phenomenon could generate very deceptive inferences (Diebold & Inoue, 2001; Haldrup & Nielsen, 2006; Tsay & Härdle, 2009).

Previous subsections explore how an *AR* and *ARMA* models with Markov-switching process can be employed to trace the complex dynamic behaviour of a time series. Tsay and Härdle (2009) introduced fractional integration to the above model *MS – ARMA*, thus three main parameters are able to switch within *MS – ARFIMA*( $p, d, q$ ) processes. A fractional integral process ( $\eta$ ), is defined as follows:

$$(1 - L)^d x_t = \epsilon_t \quad (3.10)$$

Where "L" is the back shift operator,  $\epsilon_t$  is identically independently distributed and  $0 < d < 1$ . Long memory process is stationary when  $d > 0$  and non-stationary when  $d \geq 0.5$ . Fractional integration process "d" features by the slow hyperbolic decaying of the auto-correlation function:

$$\rho(\eta) = \frac{\Gamma(\eta + d)\Gamma(1 - d)}{\Gamma(\eta - d + 1)\Gamma(d)}, \quad \text{where } \rho(\eta) \sim \frac{\Gamma(1 - d)}{\Gamma(d)}\eta^{2d-1} \quad (3.11)$$

Where  $\rho(\eta)$  is the auto-correlation function of  $x_t$  at lag  $\eta$ ,  $\Gamma(\cdot)$  is gamma function,  $(x_t)$  in equation 3.10 represents *ARFIMA*(0,  $d$ , 0),  $\eta$  is the lag of  $x_t$ .

After introducing *MS – AR* between the equations 3.3 and 3.7 the long memory process in the latter equations can be combine with Markov chain approach to produce *MS-ARFIMA*( $p, d, q$ ) as follows:

$$x_t = \alpha_{st} \cdot I(t \geq 1) + (1 - L)^{-d_{st}} \cdot \sigma_{st} \cdot \psi_t \cdot I(t \geq 1) = \alpha_{st} I(t \geq 1) + y_t \quad (3.12)$$

Where,  $x_t$  is the observed time series,  $I(\cdot)$  is the indicator function,  $\psi_t$  is a stationary zero mean process with spectral density  $F_\psi(\lambda) \sim G_0$  as  $\lambda \rightarrow 0$  at each state. The ARMA process is stationary and invertible and  $y$  is simple *ARFIMA* (0,  $d$ , 0) process.

The fractional differencing ( $d_{st}$ ) in the latter process is permitted to be a Markov chain, but with considering one condition that  $s_t$  is independent of  $\psi_\tau$  for all  $t$  and  $\tau$ . However, it is well known that (Hamilton, 1989)'s algorithm cannot be employed to estimate the latter process and the reason is consist with the problem of estimating *MS – ARMA* in the previous subsection<sup>24</sup>. Thus, the possible routs of regimes that running from  $t_1$  to  $t_i$  are expanding exponentially " $N^T$ "<sup>25</sup>. Moreover, because of the fractional differencing parameter, *MS – ARFIMA* process cannot be build in a state-space form. As a consequence, Tsay and Härdle (2009) derived a new algorithm called Durbin-Levinson-Viterbi (*DLV*) to cop with the limitation above. Their new algorithm was built based on a combination of two separate and well known algorithms in the literature; Durbin-Levinson algorithm and the Viterbi algorithm. *DLV* algorithm is now solving two major problems: *ARFIMA* model with hidden Markov process can be estimated efficiently and the puzzle proposed by (Diebold & Inoue, 2001) is solved now. *DLV* algorithm now can capture the long memory of a time series with the existence of potential structural breaks.

To perform the *DLV* algorithm mathematically let us consider equation (3.12) in its simplest case which the long memory parameters are constant among the states ( $d_0$ ).  $\epsilon_t$  is a zero mean and independently and identically distributed. Technically, We can employ Durbin-Levinson algorithm to execute the latter specification ( $d_0$ ) and the likelihood function of the process can be written as:

$$L(S_T, X_T; \zeta) = \prod_{t=1}^T (2\pi)^{-0.5} \cdot u_{t-1}^{-0.5} \cdot \exp\left(-\frac{(y_t - \hat{y}_t)^2}{2u_{t-1}}\right) \cdot P(s_t | s_{t-1}), \quad (3.13)$$

Where  $T$  is the total sample,  $X_T = (x_1, \dots, x_T)^\perp$  is the column vector for the whole observation from time 1 to  $t$ ,  $S_t = (s_1, \dots, s_t)^\perp$  is the corresponding regimes and  $\zeta$ <sup>26</sup> is column vector of both the transition probabilities  $p_{ij}$  and the vector parameter  $\nu$ , which  $\nu = (\alpha_1, \dots, \alpha_N; \sigma_1, \dots, \sigma_N; \Upsilon_{11}, \dots, \Upsilon_{1p}; \Upsilon_{21}, \dots, \Upsilon_{Np}; d_1, \dots, d_N; \Xi_{11}, \dots, \Xi_{Nq})^\perp$ .  $\hat{y}_t$  is a one-step ahead predictor of  $y_t$ ,  $u_t$  is the corresponding one-step ahead forecasting variance.

Equation (3.13) is appropriate to implement the Viterbi algorithm. Therefore, by combining the latter algorithm to Durbin-Levinson algorithm,  $d_0$  can shifts among two states  $d_{s_t}$ , which *DLV* now can detect the long memory parameter of a time series with the presence of a Markov-switching in mean.

<sup>24</sup>Notice here, if  $d_{st}=0$ , then the process is still *MS – AR* model (Hamilton, 1989).

<sup>25</sup>This problem arise when the process is going to filter out all the sequence of error terms  $(\epsilon_1, \dots, \epsilon_t)$  to proceed the MLE

<sup>26</sup>Notice here, this parameter is representing the conditional density function *CDF* of  $X_t$

As we mentioned earlier that model (3.12) is no longer can be written in a state space form because of the long memory parameter and identifying the possible states paths expand exponentially as follows<sup>27</sup>:

$$(S_{t-1}(s_t = j), s_t = j) = (s_1(s_t = j), s_2(s_t = j), \dots, s_{t-1}(s_t = j), s_t = j), \quad (3.14)$$

Where  $(S_{t-1}(s_t = j), s_t = j)$  called the survivor and associated with node  $(s_t = j)$ .

## 3.4 Data and estimation results

### 3.4.1 Data

The collected data were daily high and low ( $H - L$ ) exchange rates of Bitcoin against five major currencies across the globe – namely the *U.S.* dollar (*USD*), the Australian dollar (*AUD*), the Canadian dollar (*CAD*), the Euro (*EUR*) and the British Pound (*GBP*). The sample span ran from Jan 1<sup>st</sup>, 2015 to March, 13<sup>th</sup>, 2019. All the Bitcoin prices were obtained from (Bitcoinity.org)<sup>28</sup>, and to check the accuracy of prices we compared our sample spans with Quandle and bitcoicharts. As mentioned above, a plethora of literature has claimed that the Bitcoin market is isolated from other conventional markets. Consequently, we are interested in investigating the cross-market Bitcoin prices. To choose the ideal Bitcoin prices against each currency, we took into consideration the trading volume across all the platforms of each currency (e.g. *USD*, *CAD*, *GBP*, *AUD* and *EUR*) in Bitcoin markets. We found that the trading volume of *USD* in Bitfinex platform has exceeded 185 Billion over the last five years, which makes the market share of the latter platform at around 40.98%, overtaking almost half the market in trading Bitcoin in *USD*. Kraken platform has executed transactions of *BTC/EUR* by around 32 Billion over the last five years, and the market share of trading *Bitcoin/Eur* via this platform was around 34%<sup>29</sup>. *GBP*, *CAD* and *AUD* were traded intensively on Bit-x, Quadrigacx and Btcmarkets platforms respectively. The market share of trading Bitcoin in the latter three currencies is 52%, 75% and 85% respectively.

We computed Parkinson's High-Low historical volatility ( $HL - HV$ ) model to overcome the weaknesses in the conventional volatility model. Close-to-close volatility model neglects the sensitivity of trading hours; hence, lots of valuable information will be excluded (Bennett & Gil, 2012). Parkinson's model produces more significant signals and improves the efficiency of the volatility estimate (Parkinson, 1980). Bennett and Gil (2012); Parkinson (1980) claim that Parkinson's volatility measure is more efficient and productive than conventional close-to-close volatility estimates.

<sup>27</sup>For the full process of Viterbi algorithm see(Tsay & Härdle, 2009)

<sup>28</sup><http://data.bitcoinity.org/markets/volume/30d?c=e&t=b>

<sup>29</sup>from Jan 1, 2015 to March 13, 2019

Formally,  $V$  for each of our five Bitcoin to currency exchange rates is calculated as follows.

$$V = \frac{1}{4 \ln(2)} \cdot \ln \frac{h}{l}^2 \quad (3.15)$$

where  $h$  and  $l$  are the highest and lowest exchange rates on a given trading day, respectively. The estimator above computes the daily variance, hence, the corresponding estimate of the annualised daily percent standard deviation (volatility) is computed as follows:

### 3.4.2 Summary statistics

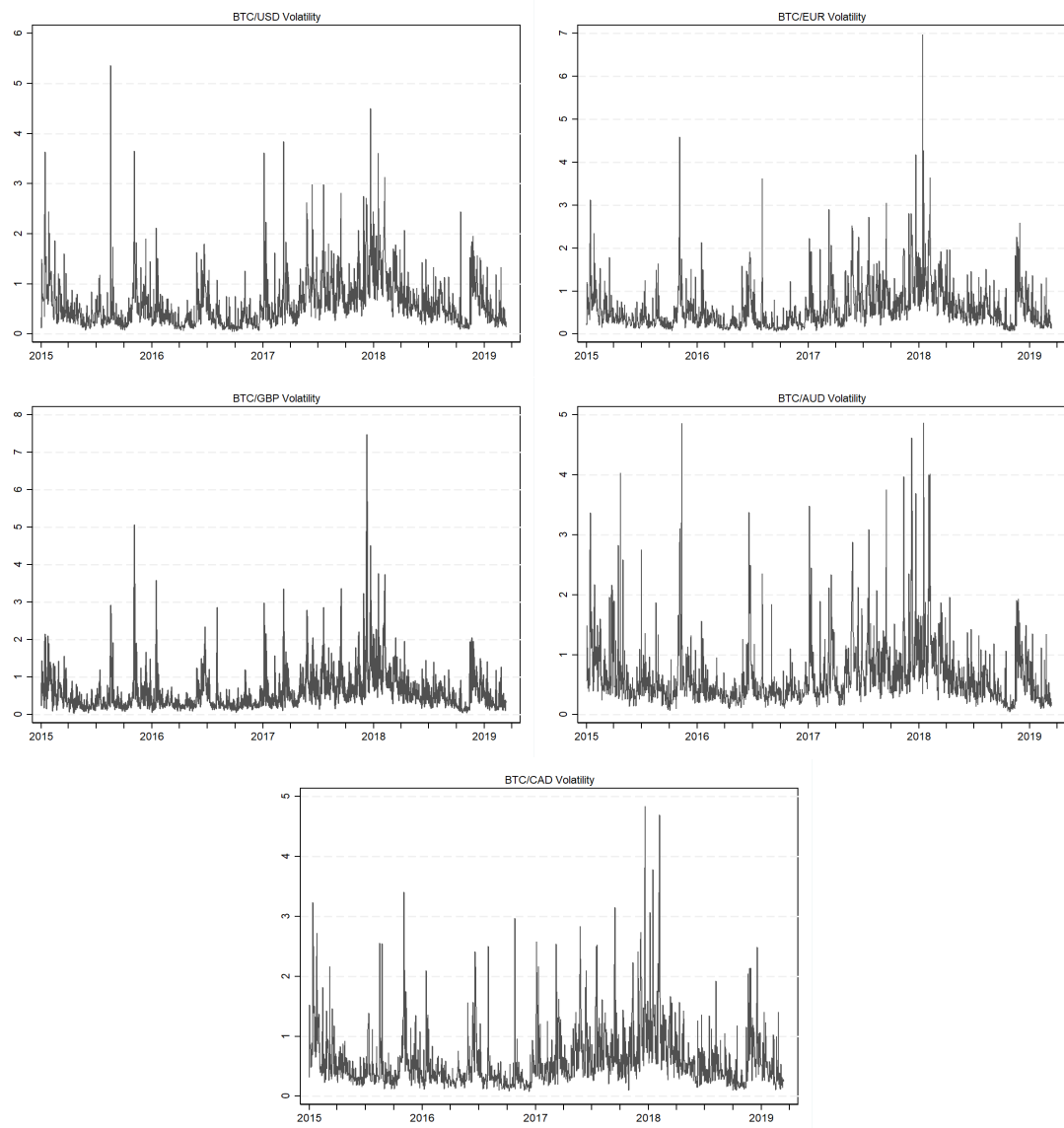
Table 3.1 displays the descriptive statistics of Bitcoin volatility for the five major currencies. The number of observations are 1533 for each market<sup>30</sup>. The average volatility across all variables is swinging around 0.6. The highest and lowest mean across the sample are AUD (0.661) and GBP (0.602) respectively. Observing the second moment, we can notice that the S.D. across the five variables is fluctuating between CAD (0.515) and AUD (0.565). Thus, the average of S.D. is approximately 0.5. The five exchange rates display large positive skewness, suggesting a large concentration of observations to the left of their central tendency; hence, volatility series are asymmetrically distributed. Bitcoin prices are sensitive to the major economic and political events, and all extreme shocks can be explained through the four moments. All series show unequivocally leptokurtic behaviours, of which Kurtosis is different across individual series, ranging from around 14 on average (BTC/USD, BTC/CAD and BTC/AUD) to about 25 (BTC/EUR and BTC/GBP).

Figure 3.1 displays the volatility of five Bitcoin markets over time. BTC/EUR and BTC/GBP show the highest shock across the whole system, recording only around 7 in both markets. Visually, we can confirm that BTC/USD and BTC/EUR are the most stable markets, of which both series are fluctuating below 2 most of the time, except for the period around 2018. Also, extensive fluctuations across the entire system appear mainly around 2018 and partially between 2015 and 2016, hinting that certain events such as Brexit and platform breaches lead Bitcoin prices to be remarkably sensitive.

In the next subsection, the series proprieties are diagnosed, including stationarity, long memory and structural breaks.

<sup>30</sup>We find the optimal Bitcoin data can be obtained from [bitcoiniity.org](http://bitcoiniity.org) and [coincharts.com](http://coincharts.com)

Figure 3.1 Bitcoin daily volatility of five markets



*Note:* Top left corner BTC/USD, top right BTC/EUR, middle left BTC/GBP, middle right BTC/AUD and bottom BTC/CAD. Exchange rate volatility, daily. Dates on the x-axis indicate the start of the year and ticks are quarterly.

Table 3.1 Summary statistics, exchange rate volatility

Exchange rate	Mean	S.D.	Min	Max	Skewness	Kurtosis
BTC/USD	0.631	0.543	0.051	5.364	2.560	13.79
BTC/EUR	0.609	0.554	0.062	6.975	3.082	21.11
BTC/GBP	0.602	0.556	0.045	7.468	3.507	26.63
BTC/AUD	0.661	0.565	0.050	4.866	2.941	15.47
BTC/CAD	0.617	0.515	0.079	4.838	2.731	14.23
Obs.	1533					

### 3.4.3 Stationarity and the presence of long memory

Diagnosing the stationarity of exchange rates series through Augmented Dicky Fuller (ADF) and the Kwiatkowski–Phillips–Schmidt–Shin (KPSS) unit root tests is required (Dickey & Fuller, 1979; Kwiatkowski, Phillips, Schmidt, & Shin, 1992). The latter tests give an initial evidence on the presence of long memory. If the conclusion of both tests is different, this means a long memory process may exist in every individual series. Table 3.2 shows both the latter tests, of which ADF and KPSS tests rejected the null hypothesis at 1% significance level. On the one hand, ADF test admits the stationarity of the five exchange rates series. On the other hand, KPSS test confirms the rejection of all the null hypothesis, which indicates that all the series are unity. Consequently, the joined rejection of both tests hints that both tests provided insufficient representation, either  $I(0)$  or  $I(1)$ , and a fractional process should be adopted. Thus, to explore the long memory process, we should employ more advanced techniques to study the long range dependence in depth, such as "Local, Exact local, Feasible Exact Local and 2-step Exact local whittle" estimation of fractional integration (Shimotsu, 2010; Shimotsu & Phillips, 2005). However, before moving directly to the fractional integration, we should stop a while to investigate the potential breakpoints in Bitcoin markets, since the long memory and turning points phenomenon are easily confused (Diebold & Inoue, 2001).

Although ADF and KPSS tests are efficient in detecting the stationarity of time series, accounting for multiple structural breaks along with the unit root in a unified framework is very important for detecting the original source of persistence across the different markets. Narayan and Popp (2010) developed a test that can diagnose unity and multiple structural breaks simultaneously. Table 3.3 shows the t-statistics and potential break dates in each market. Based on the analysis, we reject the null hypothesis of unity across the five markets. In Table 3.2 the joint rejection of both tests (ADF and KPSS) suggested that both tests provided insufficient representation, and that a long memory test should be carried out to clarify and identify the source of persistence. On the contrary, (Narayan & Popp, 2010)'s test confirms the stationarity of all the series and detects two turning points in each market. The conflict between the latter two tests raises the following question: Which phenomena (e.g. structural breaks or stationarity) feed the volatility persistence?

To answer this question, the next section illustrates the structural breaks separately; we then combine the latter phenomenon in one framework (MS-ARFIMA) to easily distinguish between them.

Table 3.2 ADF and KPSS unit root tests, exchange rate volatility

Exchange rate	Model with constant				Model without constant		
	Test	Test stat	Critical value 1%	Conclusion	Test stat	Critical value 1%	Conclusion
BTC/USD	ADF	-7.682	-3.43	Rejected	-4.191	-2.58	Rejected
	KPSS	0.952	0.739		-	-	-
BTC/EUR	ADF	-9.254	-3.43	Rejected	-4.122	-2.58	Rejected
	KPSS	1.044	0.739		-	-	-
BTC/GBP	ADF	-8.714	-3.43	Rejected	-2.932	-2.58	Rejected
	KPSS	0.991	0.739		-	-	-
BTC/AUD	ADF	-9.237	-3.43	Rejected	-4.0917	-2.58	Rejected
	KPSS	0.412	0.347		-	-	-
BTC/CAD	ADF	-9.291	-3.43	Rejected	-3.680	-2.58	Rejected
	KPSS	0.625	0.463		-	-	-
Model with trend							
Exchange rate	Test	Test stat	Critical value 1%	Conclusion	Test stat	Critical value 1%	Conclusion
	ADF	-7.832	-3.96	Rejected	-7.683	-2.328	Rejected
BTC/USD	KPSS	0.402	0.216		-	-	-
	ADF	-9.472	-3.96	Rejected	-8.489	-2.328	Rejected
BTC/EUR	KPSS	0.368	0.216		-	-	-
	ADF	-8.888	-3.96	Rejected	-8.715	-2.328	Rejected
BTC/GBP	KPSS	0.405	0.216		-	-	-
	ADF	-9.236	-3.96	Rejected	-9.238	-2.328	Rejected
BTC/AUD	KPSS	0.385	0.216		-	-	-
	ADF	-9.359	-3.96	Rejected	-9.292	-2.328	Rejected
BTC/CAD	KPSS	0.354	0.216		-	-	-

Table 3.3 Narayan and Popp (2010) Unit Root Test with Multiple Break Points for The Five Bitcoin Markets

Exchange rate	Test	Test- stat	Conclusion	Br1	Br2
BTC/USD	ADF	-9.768	Reject	29/04/2017	11/04/2018
BTC/EUR	ADF	-9.66	Reject	21/11/2017	05/02/2018
BTC/GBP	ADF	-8.22	Reject	27/11/2017	05/02/2018
BTC/AUD	ADF	-10.91	Reject	04/12/2017	05/02/2018
BTC/CAD	ADF	-11.31	Reject	03/12/2017	04/02/2018

Note: The analysis above represent model A (Break in level) proposed by (Narayan & Popp, 2010). Br1 and Br2 are the break dates across the five markets. The critical value at 1% significance level is -4.672. The sample span is from 01/01/2015 to 13/03/2019. If t-stat is greater than the critical value we reject the null of constant parameter. All critical values are obtained from (Hansen, 1990), Table 1.

### 3.5 Discussion of results

In this section, various methods to analyse fractional integration and switching models are introduced to shed light on the dynamics of Bitcoin prices. The results of the multiple breakpoint test (Bai & Perron, 1998) and fractional integration test (Shimotsu, 2010) are initially discussed to allow us explain how *MS – ARFIMA* process aggregates

the latter two phenomena and clear up the confusion between turning points and long memory in a time series<sup>31</sup>. Indeed, investigating the dynamics of Bitcoin markets under *MS-ARFIMA* will allow us to study simultaneously and endogenously the persistence of fractional integration and the potential breakpoints.

We comment on the results in three distinct sub-sections. In the first sub-section, the potential break-points that have been detected through multiple breakpoint test will be under scrutiny. In the second sub-section, Local Whittle, Exact Local Whittle, Feasible Exact Local Whittle and Two-step Exact Local Whittle test will be illustrated in detail. The last sub-section will demonstrate the endogenous shifts of long memory, mean and variance parameters to clear the confusion between long memory and breakpoints. Then, a brief illustration of the transition probability among the states will be displayed statically and dynamically. Finally, we will provide a comparison between the fitted values of *ARFIMA* and *MS – ARFIMA* processes to show the accuracy of the latter process.

### 3.5.1 Structural Breaks

Detecting potential breaks in a time series is a crucial matter to validate the performance of an econometric model and control potential bias. Bai and Perron (1998, 2003)'s test is applied to detect if there are potential turning points over time. The previous section has confirmed the stationarity across the five series. Basically, by holding the stationarity assumption, we confirm that the joint statistical probability of the five series does not change over time (e.g. constant mean, constant variance, and trendless series). The normal stationary tests such as *ADF* and *KPSS* are not powerful enough to detect the joint statistical distribution among observations and specify the breakpoints. Multiple breakpoint test is adopted to find if any of the five stationary exchange rate series has any breaks in the joint probability over the time. Figure 3.2 reveals interesting information which claims, contrary to stationarity assumption, that mean and variance are constant along the sample span.

In Figure 3.2 the blue line illustrates the possible turning point in the mean over the sample span across the five exchange rates. We use global information criterion method to specify the breaks across the five markets. Ten breaks in (BTC/USD, BTC/EUR, BTC/GBP) and eight breaks in (BTC/AUD and BTC/CAD) are selected by Bayesian Information Criteria (BIC). Bai and Perron recommended using the highest trimming percentage (15%) if the sample span is small. On the contrary, the used sample span is 1533 observations, and choosing a lower trimming percentage as (5%) to detect the turning points should be acceptable. By allowing for shifts in the constant, we can see clearly from Figure 3.2 that the coefficient value during the first break in all series is swinging between 0.7 and 0.94. Upward shifts appear in all series ranging around 1.5 from the second quarter of 2017 to approximately the second quarter of 2018, then start to

<sup>31</sup>see (Diebold & Inoue, 2001)

shift down again back to the normal shifts. Different upward and downward shifts across the five exchange rates are recorded, but all conclude that the period from 2017 to the middle of 2018 experienced waves of turmoil that distorted the distributional propriety during that time.

Table 3.4 illustrates the number and date of breaks in each Bitcoin market. Three markets (e.g. BTC/USD, BTC/EUR and BTC/GBP) showed ten breaks, while the rest (e.g. BTC/AUD and BTC/CAD) had eight turning points over time. To minimise space and avoid repetition of a similar discussion, interested readers are encouraged to see Table 4.4 and read the discussion in Section (4.5.3), Chapter Four. We mention here two significant events that caused structural changes to market properties. The flash crash of Bitfinex platform in August 2016 triggered thousands of investors' wallets and hackers stole around \$ 72 million. Also, in February 2018, a significant attack disturbed the Bitcoin network and caused a loss of \$ 5 million.

It is worth pointing out that Bai and Perron provide the structural breaks in the mean, but do we have breaks in the variance and AR terms? To answer this question, we run (Hansen, 1992b) test to diagnose the parameters stability. Based on Table 3.5, we cannot reject the consistency of  $\mu$  across the five markets. Also, we fail to reject the null hypothesis of  $\phi$  parameters across the markets, except for BTC/USD. Finally, BTC/USD and BTC/AUD markets have constant  $\sigma^2$  over time, while the rest of the markets showed the variance drifting along the sample span.

**Table 3.4 Estimated breaks in the volatility of Bitcoin exchange markets, (Bai and Perron) test**

Breaks Order	BTC/USD	BTC/EUR	BTC/GBP	BTC/AUD	BTC/CAD
1	20 Mar 2015	27 Mar 2015	26 Mar 2015	02 May 2015	21 Mar 2015
2	29 Oct 2015	29 Oct 2015	30 Oct 2015	29 Oct 2015	11 Aug 2016
3	26 Jan 2016	25 Jan 2016	23 Jan 2016	23 Jan 2016	20 Dec 2016
4	27 May 2016	27 May 2016	27 May 2016	04 Jan 2017	07 May 2017
5	11 Aug 2016	11 Aug 2016	11 Aug 2016	22 May 2017	28 Nov 2017
6	21 Dec 2016	22 Dec 2016	21 Dec 2016	29 Nov 2017	12 Feb 2018
7	22 May 2017	02 May 2017	04 May 2017	13 Feb 2018	29 Apr 2018
8	29 Nov 2017	29 Nov 2017	29 Nov 2017	30 Apr 2018	13 Nov 2018
9	13 Feb 2018	13 Feb 2018	13 Feb 2018	-	-
10	30 Apr 2018	30 Apr 2018	30 Apr 2018	-	-

*Note:* The above dates corresponded to Bai and Perron test in figure 3.2

Based on the above, some structural break models postulate that the shifting mechanism is deterministic, and the switching is determined exogenously. Alternatively, (Bai & Perron, 2003) developed a model to detect structural breaks endogenously; hence there is no need to determine the timing of breaks beforehand. However, the trimming percentage, and allowing for serial correlation and heterogeneity restrict the model efficiency. Detecting

Table 3.5 Hansen 1992's Test for Stability of Bitcoin Markets

Exchange rate	Parameters	Estimated	Test stat	Critical value 5%	Conclusion
BTC/USD	$\mu$	0.000	0.002		Fail
	$\phi$	-0.326	0.575	0.47	Reject
	$\sigma^2$	0.213	0.155		Fail
BTC/EUR	$\mu$	0.000	0.001		Fail
	$\phi$	-0.322	0.071	0.47	Fail
	$\sigma^2$	0.216	0.839		Reject
BTC/GBP	$\mu$	0.000	0.001		Fail
	$\phi$	-0.347	0.018	0.47	Fail
	$\sigma^2$	0.229	0.566		Reject
BTC/AUD	$\mu$	0.000	0.001		Fail
	$\phi$	-0.304	0.031	0.47	Fail
	$\sigma^2$	0.248	0.461		Fail
BTC/CAD	$\mu$	0.000	0.002		Fail
	$\phi$	-0.344	0.130	0.47	Fail
	$\sigma^2$	0.201	1.088		Reject

*Note:* If t-stat is greater than the critical value we reject the null of constant parameter. All critical values are obtained from (Hansen, 1990), Table 1.

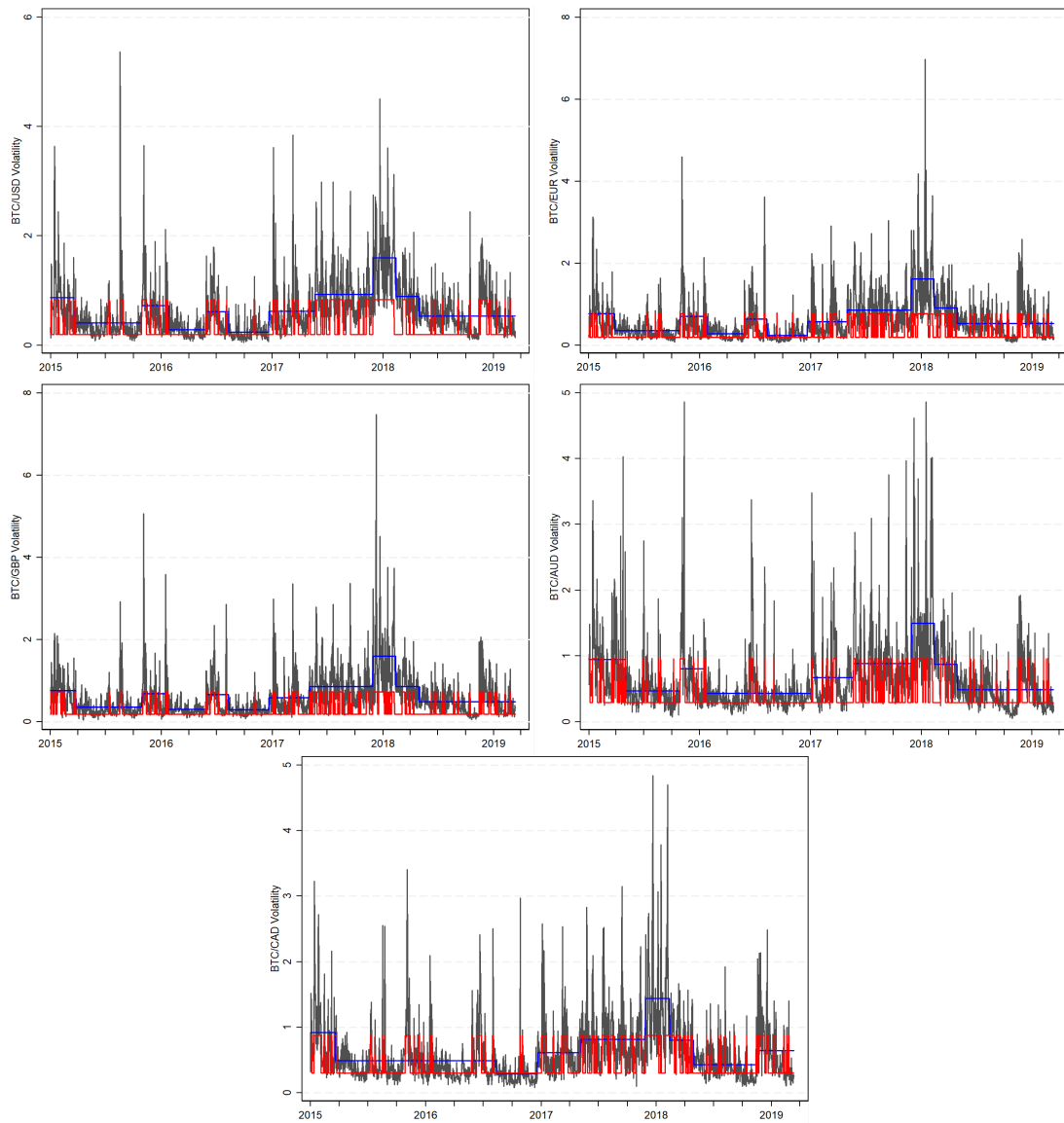
the structural breaks and identifying the changing points (e.g. mean, variance, AR and long memory) across a series is very helpful, especially if the series is displaying a long memory. Why is this important? Because, as we mentioned above, the slow decaying of auto-correlation function could be accounted from both short memory series with potential breakpoints (structural breakpoints phenomenon) or strong dependence among observations within the series (long memory phenomena) Diebold and Inoue (2001). An important question arises here, to clear up the confusion between the latter two very similar phenomena: "Should we test both long memory and structural breaks simultaneously in a unified framework?" or "Should we account for the last two problems separately?"

### 3.5.2 Fractional Integration

In the previous section we ran convectional unitroot tests to diagnose the stability of the statistical properties of Bitcoin volatility series over time, an indication arising that proper long memory tests should be adopted to discover if the series fell within the co-variance stationary zone or not.

Thus, the Local Whittle and its extended versions (e.g. ELW, TSELW) with and without de-trending and de-meaning were employed to detect the long memory across the five markets. The analysis was implemented in different bandwidths (e.g.  $m = T^{0.5}$ ,  $m = T^{0.6}$ ,  $m = T^{0.7}$ ,  $m = T^{0.8}$ ,  $m = T^{0.9}$ ,) to insure that the long memory was not sensitive to the choice of one particular bandwidth. Moreover, rolling windows of the estimated  $d$  were applied to diagnose the stability of the estimated  $d$  parameters over time.

Figure 3.2 Estimated breaks in the volatility of Bitcoin exchange markets (Bai and Perron)



Note: Top left corner BTC/USD, top right BTC/EUR, middle left BTC/GBP, middle right BTC/AUD and bottom BTC/CAD. Blue line represents Bai and Perron multiple structural test, red line is the MS-ARFIMA process. Dates on the X-axis indicate the start of the year, and ticks are quarterly.

Tables 3.6, 3.7, 3.8 and 3.9 illustrate the degree of fractional integration based on Local Whittle (LW), Exact Local Whittle (ELW), Feasible Exact Local Whittle (FELW) and Two-step Exact Local Whittle (TSELW) estimations of the volatility under different band width respectively. All tests provide 4 bandwidths (e.g.  $m = T^{0.5}$  to  $m = T^{0.8}$ ) to detect the sensitivity of  $d$  under different specific bandwidths. Results among the latter tables show that each exchange rate series has a significant long memory. All the outcomes display a value higher than zero  $d > 0$ , which means the series are strongly persistent along the sample span. The values of  $d$  are bounded in the  $(0, 0.5)$  interval for the five markets across almost all the bandwidths, which indicate that all series are

co-variance stationary except  $m = T^{0.5}$  across the BTC/USD and BTC/EUR markets. Generally, we can confirm that the major of  $d$  values are co-variance stationary and mean-reverting, which implies that the shock effects will die out in the long run. A close look at the series individually shows that the value of  $d$  across different bandwidths for all markets are swinging between "0.35 and 0.54". All tests provide approximately identical results, hinting at stable estimations, which implies that the series contains long memory and this may have useful implication within this context.

For each  $d$  value, the asymptotic standard error can be estimated as  $[4m]^{-0.5}$ . The total number of observations in each series is 1533, and the bandwidths are ranging from 0.5 to 0.8. For example, in Table 3.8,  $m = T^{0.5}$  the approximate  $SE$  is 0.0799. Similarly, the approximate  $S.E$  of  $m = T^{0.6}$  to  $m = T^{0.8}$  bandwidths are 0.055, 0.0383, and 0.026 respectively.

We extended the work in this chapter and took a further step to roll the estimated  $d$  by setting a suitable window of the (TSELW) estimation in Table 3.9. A window of 360 days with five days increments was used to detect the sensitivity of  $d$  within  $m = T^{0.6}$  bandwidth across all the markets. Figure 3.3 displays the stability of long memory parameter across the five markets. We can see that the long memory in *BTC/USD* market was stable ( $d \approx 0.4$ ) during the first half of 2015 and from the second half of 2016 to the end of the sample span. The period between the middle of 2015 and 2016 shows upward and downwards fluctuations, hinting that investors might overreact to their investment decisions in the *BTC/USD* market. The *BTC/GBP* market shows stable persistence over the first half of the sample span, with stable downwards over the second half of the period before coming back again to its normal value over the last few days of the rolled  $d$  parameters. The rest of the markets (e.g. *BTC/EUR*, *BTC/AUD* and *BTC/CAD*) display more upward and downward fluctuations over the sample span. All markets show high persistence through the first year, the persistence starting to decline gradually before it increases again.

Finally, we obtain the time series of the estimated "d" in each market, then identify a suitable window for this series and roll it again to find the speed of decaying in the rolling windows of estimated "d". Figures B.1 to B.5 represent the rolling windows of parameter  $d$  against the rolling windows of the rolled "d" parameter<sup>32</sup>. All the figures show upward trend over time, hinting at a slow decay along the sample span. Moreover, the speed of decaying is in-stable across the five series which indicates that the dependence among observations is changing over time.

<sup>32</sup>See appendix B

Table 3.6 Estimates of Local Whittle (LW) for the volatility of the five BTC markets

	$\hat{d}_{LW}$			
	$m = T^{0.5}$	$m = T^{0.6}$	$m = T^{0.7}$	$m = T^{0.8}$
BTC/USD	0.514	0.445	0.410	0.360
BTC/EUR	0.521	0.370	0.389	0.378
BTC/GBP	0.471	0.408	0.340	0.352
BTC/AUD	0.436	0.350	0.362	0.346
BTC/CAD	0.417	0.400	0.334	0.347

Table 3.7 Estimates of Exact Local Whittle (ELW) for the volatility of the five BTC markets

	$\hat{d}_{ELW}$			
	$m = T^{0.5}$	$m = T^{0.6}$	$m = T^{0.7}$	$m = T^{0.8}$
BTC/USD	0.541	0.463	0.428	0.390
BTC/EUR	0.539	0.368	0.400	0.408
BTC/GBP	0.469	0.410	0.345	0.379
BTC/AUD	0.492	0.376	0.388	0.384
BTC/CAD	0.430	0.423	0.352	0.382

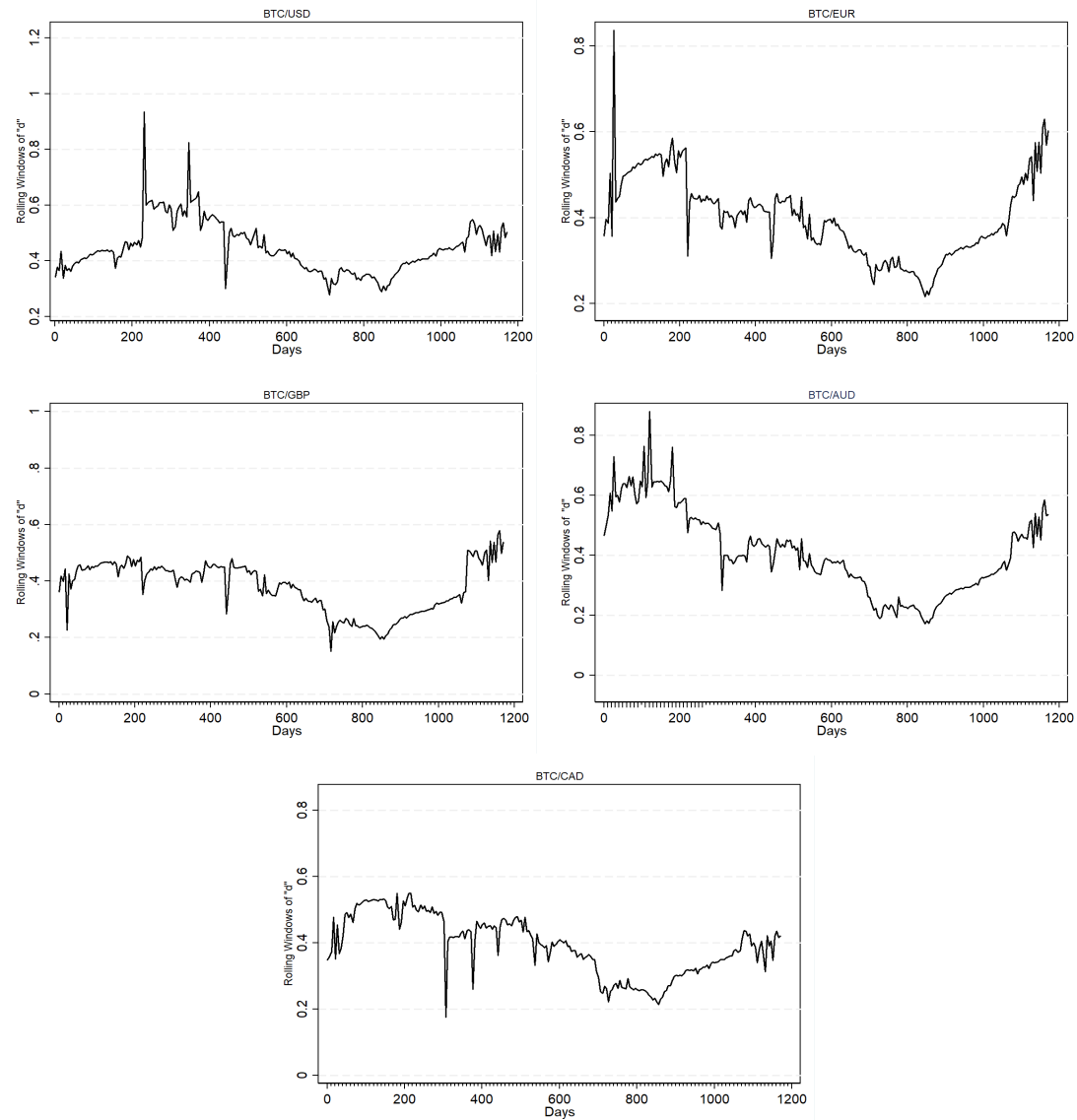
Table 3.8 Estimates of Feasible Exact Local Whittle (FELW) for the volatility of the five BTC markets

	$\hat{d}_{FELW}$			
	$m = T^{0.5}$	$m = T^{0.6}$	$m = T^{0.7}$	$m = T^{0.8}$
BTC/USD	0.520	0.451	0.417	0.380
BTC/EUR	0.524	0.374	0.396	0.400
BTC/GBP	0.479	0.413	0.346	0.374
BTC/AUD	0.454	0.354	0.368	0.367
BTC/CAD	0.439	0.408	0.341	0.368

Table 3.9 Estimates of Two-step Exact Local Whittle (TSELW) for the volatility of the five BTC markets)

	$\hat{d}_{TSELW}$			
	$m = T^{0.5}$	$m = T^{0.6}$	$m = T^{0.7}$	$m = T^{0.8}$
BTC/USD	0.532	0.451	0.417	0.380
BTC/EUR	0.537	0.374	0.396	0.400
BTC/GBP	0.479	0.413	0.346	0.374
BTC/AUD	0.454	0.354	0.368	0.367
BTC/CAD	0.439	0.408	0.341	0.368

Figure 3.3 The rolling windows of estimated "d" in Bitcoin markets.



*Note:* top left corner BTC/USD, top right BTC/EUR, middle left BTC/GBP, middle right BTC/AUD and bottom BTC/CAD. Rolling windows, daily. Dates on the x-axis indicate the start date by 1 and ticks are 10 days each.

### 3.5.3 MS-ARFIMA model

Berkes et al. (2006); Diebold and Inoue (2001); Granger and Hyung (2004); Kunsch (1987), and others<sup>33</sup> claimed that long range dependence and structural breaks are easily confused. In the above sections, long memory tests and multiple structural break tests were carried out to prove that each BTC exchange rate series has long range dependence and turning points over time. Much research has studied the properties of Bitcoin markets by detecting the fractional integration and structural changes of different approaches as we have done in the first two subsections above (Bariviera, 2017; Bariviera et al., 2017; Bouri et al., 2019; Charfeddine & Maouchi, 2019; Jiang et al., 2018; Mensi et al., 2018, 2019).

However, Diebold and Inoue (2001) claimed that a spurious long memory could be generated due to the presence of structural breaks (persistence along the hyperbolic decaying). Indeed, ignoring the structural breaks in a long memory time series could generate unstable results, hence underestimating the long range dependence parameter. To overcome the puzzle proposed by Diebold and Inoue, many authors have tried to build a model that aggregates both structural breaks with long memory (Haldrup & Nielsen, 2006; Ray & Tsay, 2002). Many gaps in the latter approaches were solved in *MS – ARFIMA* (Tsay & Härdle, 2009). This model computes the degree of fractional integration and structural breaks simultaneously and endogenously by shifting the *ARFIMA* parameters via Markov switching process into different regimes.

Table 3.11 presents the static results of *MS – ARFIMA* process across the five different Bitcoin markets. Although the results across different specifications are stable<sup>34</sup>, Table 3.11 shows the best fit of *MS – ARFIMA* in which each estimation has been selected according to the highest log likelihood for each series under different *MS – ARFIMA* orders. The best order of each exchange rate is as follows: *BTC/USD*  $\sim$  *MS – ARFIMA* (1,  $d$ , 1), *BTC/EUR*  $\sim$  *MS – ARFIMA* (1,  $d$ , 0), *BTC/GBP*  $\sim$  *MS – ARFIMA* (1,  $d$ , 1), *BTC/AUD*  $\sim$  *MS – ARFIMA* (1,  $d$ , 1), *BTC/CAD*  $\sim$  *MS – ARFIMA* (0,  $d$ , 1).

To investigate the volatility persistence in Bitcoin markets, we should first distinguish between low and high volatility waves. Hence, we set up our *MS – ARFIMA* model to switch between two states: State 1 (high volatility regime) and State 2 (low volatility regime). To confirm the choice of a two-regime switching model, we perform (Hansen, 1992a, 1996)'s test across the five volatility series. Table 3.10 shows the LR statistics and critical values for each market. The null hypothesis of no regime switching (autoregression) across the five markets can be rejected at 1% and 5% significance level, results confirming that all series reveal two state Markov switching model.

<sup>33</sup>For excellent survey on structural breaks and long memory, see (Baillie, 1996)

<sup>34</sup>See appendix B to explore the different specifications of *MS – ARFIMA* process across the five Bitcoin markets.

Observing Table 3.11 the first column shows the *MS – ARFIMA* parameters, from the top left corner ( $d_1$  and  $d_2$ ) represents the long memory parameters in state 1 and state 2 respectively. The mean and standard deviation of BTC exchange rate for each market are ( $\mu_1$  and  $\mu_2$ ) and ( $\sigma_1$  and  $\sigma_2$ ) parameters respectively. The ( $p_{11}$  and  $p_{22}$ ) are the probability parameters,  $p_{11}$  illustrates the probability that the process will stay in state 1 and  $(1 - p_{11})$  is the probability that the process will move from state 1 to state 2.  $p_{22}$  infers the probability of the process staying in state 2 and  $(1 - p_{22})$  is the probability of moving from state 2 to state 1.  $\phi$  and  $\theta$  are the auto-regressive and moving average parameters. *BTC/USD* in Table 3.11 show that the estimated standard deviation in regime 1 is higher than the standard deviation in regime 2, ( $\sigma_1 = 0.71$ ) and ( $\sigma_2 = 0.18$ ), which indicates that state 1 ( $S_1$ ) is a high-volatility regime and state 2 ( $S_2$ ) is a low-volatility regime. Relatively, if the variation around the mean shows a particular behaviour, then the associated mean  $\mu_1 > \mu_2$  are displaying the same conclusion with the volatility, which is  $\mu_1 = 0.83$  "state 1" and  $\mu_2 = 0.19$  "state 2".

Table 3.10 Hansen Linearity Test

Breaks Order	BTC/USD	BTC/EUR	BTC/GBP	BTC/AUD	BTC/CAD
LR stat	11.32	10.57	11.82	12.45	11.22
Critical Value	0.000	0.000	0.000	0.000	0.000

*Note:* The null hypothesis represents a one-state model against the alternative of two-state mode. 3.2

The memory properties explain the persistence in the *BTC/USD* market, if  $d > 0$  means that past shocks affect BTC price behaviour in the future. We can see that ( $d_1$  and  $d_2$ ) are greater than zero, which  $d_1 = 0.422$  ( $S_1$ ) and  $d_2 = 0.425$  ( $S_2$ ). The value of fractional integration in both regimes is bounding within  $0 < d < 0.5$  interval, which means the process is stationary with strong persistence over time. Transition probability of  $S_1$  is  $p_{11} = 0.83$  and for  $S_2$  is  $p_{22} = 0.95$ , which implies the probability of staying in regime 2 is higher than staying in regime 1 by approximately 12%. Discussing the static data of *BTC/USD* markets is useful, but visualising the switching parameters is very helpful to explore the structural breaks in fractional integration and the first two statistical moments ( $\mu$  and  $\sigma$ ). Figure 3.4 illustrates the switching in mean of all Bitcoin markets over time. In the top left corner *BTC/USD*, we can observe that a cluster of switches appears during some episodes of high shocks. These episodes can be related to political or economic events that might have happened in Bitcoin market over time. Switches within the system are treated endogenously, which means the model is synchronised with growth-theoretic mechanisms that allow the process to generate shifts based on the internal dynamics of BTC prices.

Moving to the second column in Table 3.11 (*BTC/EUR* market), the analysis displays almost the same behaviour as the *BTC/USD* market. The mean/volatility parameters switch from 0.9/0.7 in  $S_1$  to 0.2/0.16 in  $S_2$ . Based on the transition probabilities, the

Table 3.11 Estimates of MS-ARFIMA model of volatility across the five Bitcoin markets

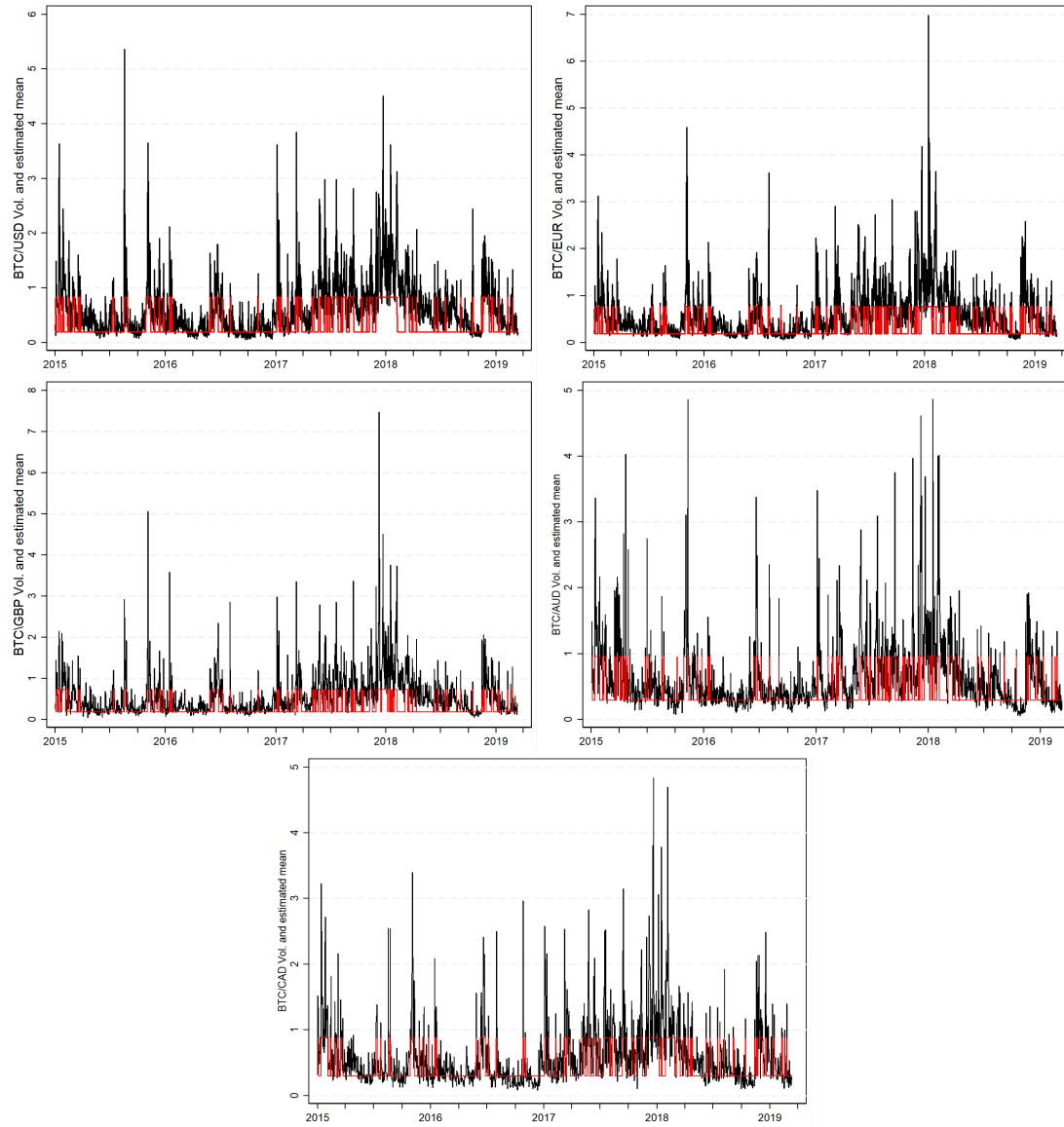
	BTC/USD		BTC/EUR		BTC/GBP		BTC/AUD		BTC/CAD	
	MS-ARFIMA (1, d, 1)		MS-ARFIMA (1, d, 0)		MS-ARFIMA (1, d, 1)		MS-ARFIMA (1, d, 1)		MS-ARFIMA (0, d, 1)	
	Estimate	S.E.								
$d_1$	0.4224	0.0520	0.3472	0.0314	0.3570	0.0355	0.3427	0.0355	0.2914	0.0445
$d_2$	0.4249	0.0329	0.3488	0.0199	0.3253	0.0240	0.3100	0.0177	0.2899	0.0221
$\mu_1$	0.8314	0.1095	0.9056	0.0873	0.7206	0.1188	0.9596	0.1249	0.8757	0.0828
$\mu_2$	0.1936	0.0691	0.2350	0.0523	0.1786	0.0541	0.2938	0.0552	0.2997	0.0427
$\sigma_1$	0.7098	0.0291	0.7165	0.0296	0.7981	0.0359	0.7956	0.0358	0.6611	0.0249
$\sigma_2$	0.1856	0.0038	0.1682	0.0034	0.1762	0.0035	0.1847	0.0037	0.1617	0.0034
$p_{11}$	0.8339	0.0212	0.7662	0.0244	0.7323	0.0273	0.7303	0.0275	0.8410	0.0191
$p_{22}$	0.9585	0.0057	0.9433	0.0066	0.9450	0.0064	0.9443	0.0064	0.9496	0.0064
$\phi$	0.3018	0.1022	-0.0328	0.0326	0.4184	0.3289	-0.4565	0.2795	-	-
$\theta$	-0.4734	0.1025	-	-	-0.4446	0.3265	0.4948	0.2696	0.0526	0.0362
$L$	<b>-358.38933</b>		<b>-310.734501</b>		<b>-333.830679</b>		<b>-392.023359</b>		<b>-292.341567</b>	

Note:  $d$ : long memory,  $\mu$ : mean,  $\sigma$ : standard deviation,  $P$ : transition probability,  $\phi$ : Autoregressive parameter,  $\theta$ : Moving average parameter,  $L$ : Log-likelihood of switching model,  $S.E$ : standard error

probability to stay in  $S_2$  within the system is greater than the probability to stay in  $S_1$  by 18%, which indicates that the process is most likely to generate its infer when the mean/volatility of data is swinging between 1.67/1.44 respectively. As previously mentioned, the conduct of statistical properties in  $S_1$  implies that the  $BTC/EUR$  market has a series of high shocks over time. Regarding fractional integration, the memory parameters in both regimes indicate that the persistence is strong over the sample span, and past events will engage in depicting the future price of  $BTC/EUR$ . We can observe from Table 3.11 that the "d" parameter of ( $BTC/EUR$ ) is greater than zero and less than 0.5 which indicates that the  $BTC/EUR$  series is stationary and mean reverting. In addition,  $d_1$  and  $d_2$  almost carry the same persistence value among the regimes, which indicates that the persistence is running continuously along the whole period from *Jan, 2015 to March, 2019*. Dynamically, the top right corner of Figure 3.4 demonstrates the switching mean of  $BTC/EUR$  volatility and identifies any intervening point that happened because of abnormal events which may have occurred over time. On the contrary, the  $BTC/USD$  market (left top corner),  $BTC/EUR$  market (top right corner) shows a significant switch after 2017 over the same period. Consequently, it is likely these fast switches happen due to the high speed of unusual events occurring in cryptocurrency markets.

On the same pattern, in Table 3.11 the  $BTC/GBP$ ,  $BTC/AUD$  and  $BTC/CAD$  markets display interesting results within the two-regime Markov switching system. If Bitcoin markets possess episodes of high uncertainty, the markets will react randomly with high volatilities as in  $S_1$  across the latter markets. On the other hand, low volatility state is identified in  $S_2$  within the latter three markets. The mean of  $BTC/GBP$ ,  $BTC/AUD$

Figure 3.4 Bitcoin exchange rates and the path of estimated switching in the mean of volatility



Note: Top left corner BTC/USD, top right BTC/EUR, middle left BTC/GBP, middle right BTC/AUD and bottom BTC/CAD. Red line represents estimated  $\mu_{st}$  from MS-ARFIMA model. Dates on the X-axis indicate the start of the year, and ticks are quarterly.

and  $BTC/CAD$  series in  $S_1$  and  $S_2$  are 0.72/0.17, 0.95/0.29 and 0.87/0.29 respectively, whereas the volatility in both regimes is 0.79/0.17, 0.79/0.18 and 0.66/0.16 respectively. The most important parameter across the tables is the fractional integration,  $BTC/GBP$  market, displaying a high persistence stationary behaviour with 0.35 in  $S_1$  and 0.32 in  $S_2$ , which refers to stable persistence through time. In the  $BTC/AUD$  market the fractional differencing parameter in  $S_1$  shows a persistence by 0.34, while in  $S_2$  it reveals 0.31. Long memory parameters  $d_1$  and  $d_2$  show almost steady persistence in  $BTC/CAD$  markets during the chosen period. Further, the transition probability parameters for  $BTC/GBP$ ,

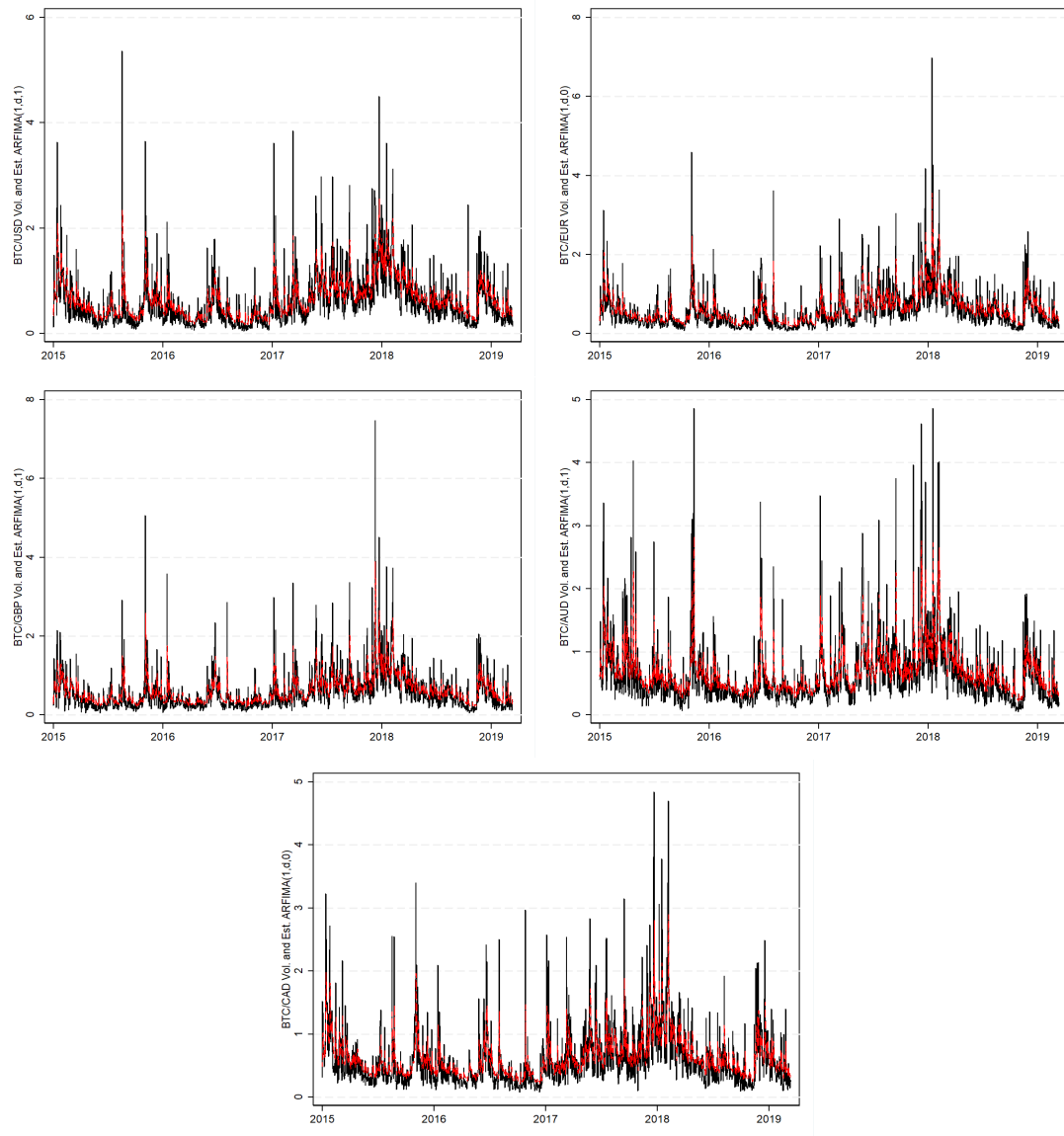
$BTC/AUD$  and  $BTC/CAD$   $p_{22}$  are greater than  $p_{11}$  and the process stays in regime two much longer.

The transition probability parameters explain the dynamics of Bitcoin prices. We can see in 3.11 that the transition probability  $p_{11}$  is always lower than  $p_{22}$  across the five markets. As discussed in the previous section, some events (e.g. cyber attacks) could induce the system to be extremely volatile and break the cycle of persistence in the process. Therefore, transition probability  $p_{11}$  is always lower than  $p_{22}$  as the calculation process consumes less time to analyse the peaks and shocks within the high volatility regime. Further, as the value of both transition probabilities is relatively high, this gives an indication that the process has spent most of the time calculating the parameter in States 1 and 2 instead of switching between the two regimes.

In Figure 3.4, the middle row left and right illustrates the  $BTC/GBP$ ,  $BTC/AUD$  markets respectively and the  $BTC/CAD$  market at the bottom. Among the five markets we can observe that the  $BTC/AUD$  market (middle row right) has the highest transitions number in mean,  $S.D$  and long memory parameters, albeit that along the year 2016 there were no significant structural breaks, but the rest of the anterior and posterior years have remarkable turning points. In all the markets except  $BTC/AUD$  we can aver that the period from 2015 to 2017 experienced a lower number of structural breaks than the period 2017 to 2019. Indeed, after 2017 each market shows different breakpoints over the time, depicting almost the same behaviour across the switching parameters.

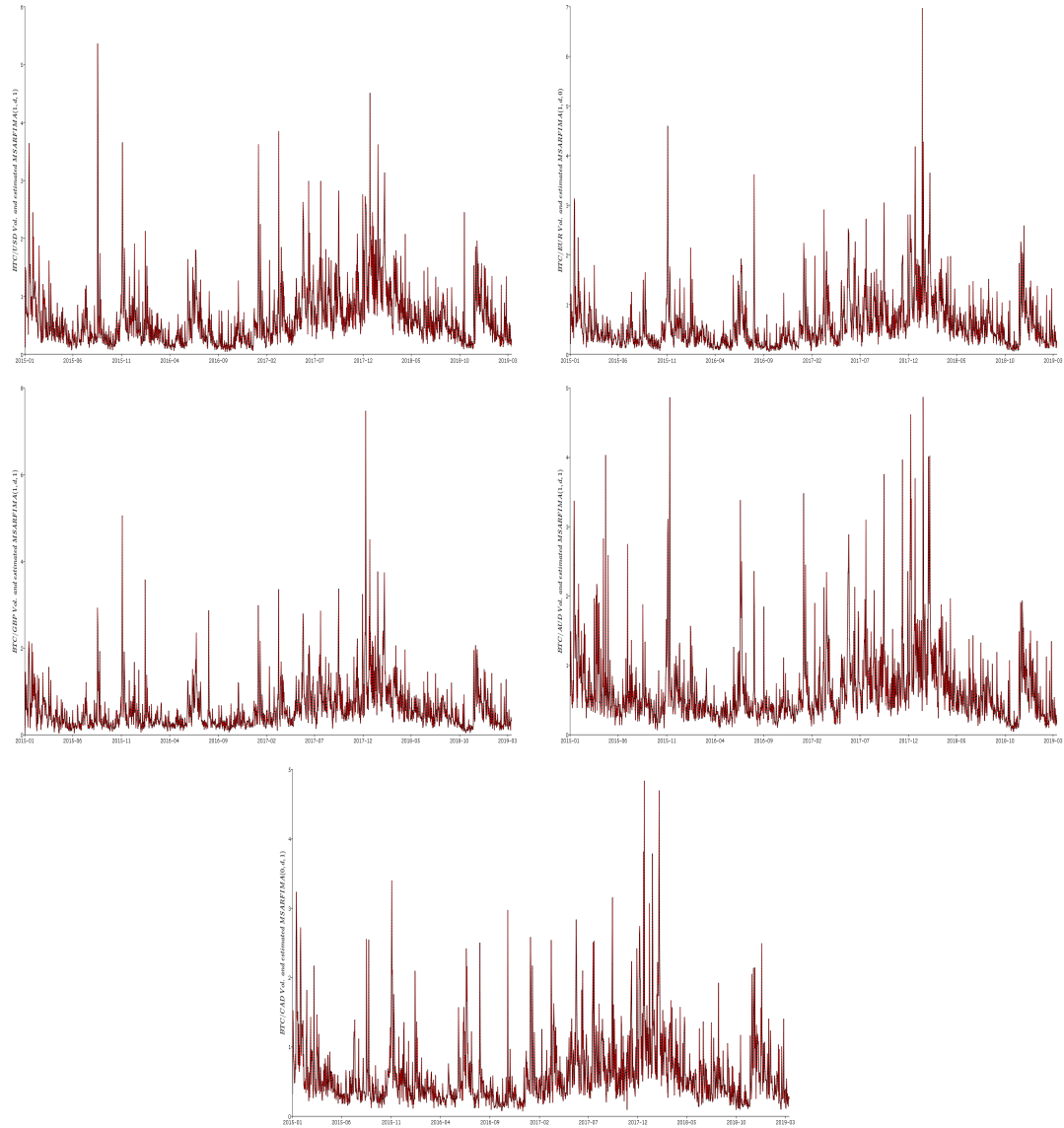
Finally, Figure 3.5 shows the  $BTC$  volatility for each market with its fitted  $ARFIMA$  values. For each market we can observe how the estimated value of  $ARFIMA$  process (dotted red line) fitted the original volatility series (black line) for each market.  $ARFIMA$  process performed all the series perfectly in different specifications. It appears that in Figure 3.5 the process detects the behaviour of each series, but it indicates that most of the values far from the mean are not detected. By contrast, if we examine the fitted  $MS - ARFIMA$  plots in Figure 3.6, we will notice the difference between the estimated values of  $ARFIMA$  and the estimated value of  $MS - ARFIMA$ . The fitted values (dotted red line) in the latter figures fit the original series exactly and detect the behaviour of markets perfectly and accurately.

Figure 3.5 Bitcoin Exchange rates volatility and the estimated value of ARFIMA process



Note: Top left corner BTC/USD, top right BTC/EUR, middle left BTC/GBP, middle right BTC/AUD and bottom BTC/CAD. Black solid line represents the Bitcoin exchange rate volatility, red dotted line represents the fitted value from ARFIMA model.

Figure 3.6 Bitcoin Exchange rates volatility and the estimated values of MS-ARFIMA model



*Note:* Top left corner BTC/USD, top right BTC/EUR, middle left BTC/GBP, middle right BTC/AUD and bottom BTC/CAD. Black solid line represents the Bitcoin exchange rate volatility, red dotted line represents the fitted value from MS-ARFIMA model.

### 3.5.4 Robustness

How sensitive are the results to the choice of alternative volatility measure and long memory bandwidth?

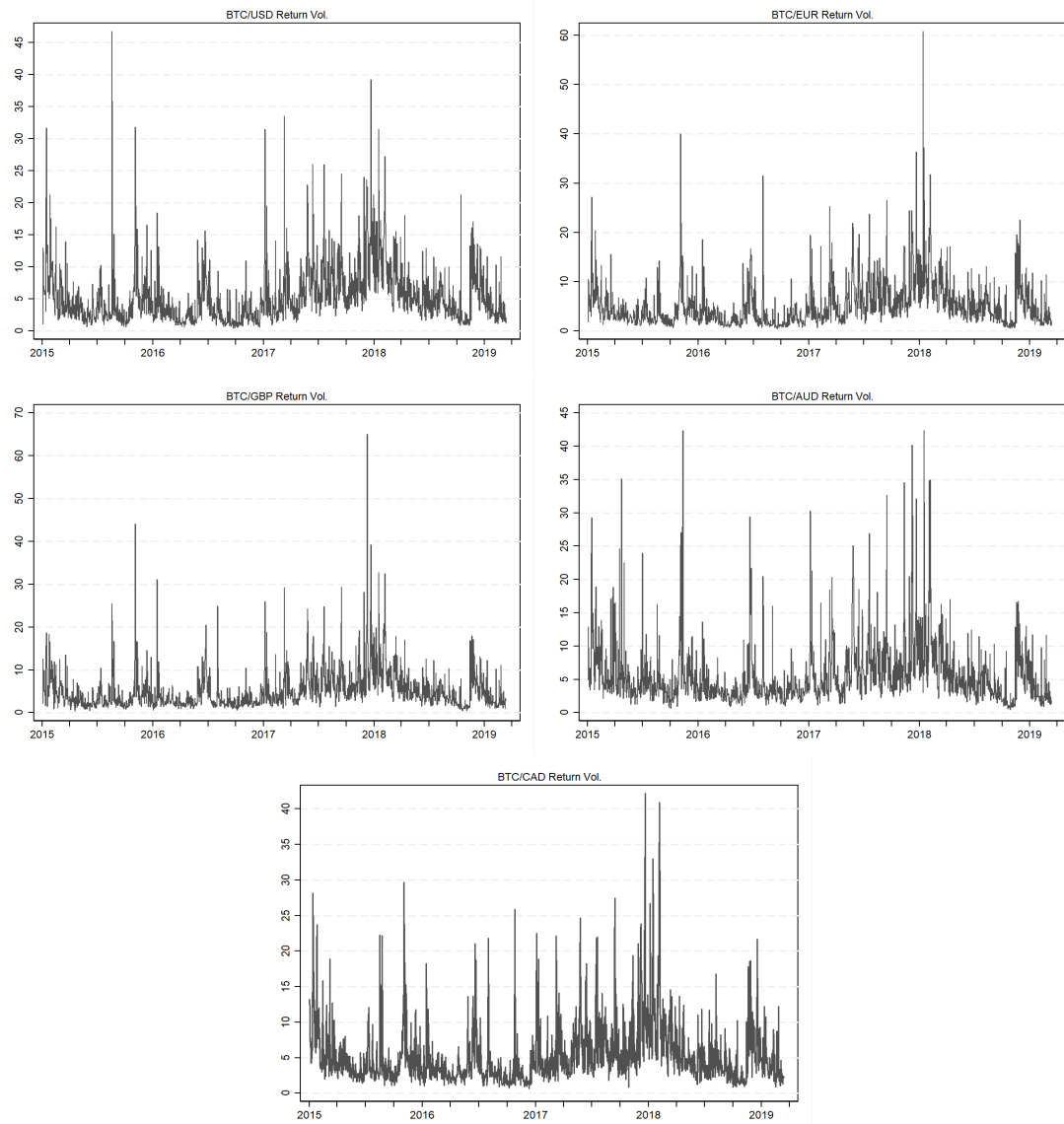
We check the robustness of the full sample analysis results based on the volatility measure and the bandwidth of the long memory parameter. Recall that the empirical analysis is based on (Parkinson, 1980)'s High-Low historical volatility measure. This measure provides more useful information regarding future volatility than a close-to-close estimator, but following the literature, we can calculate the volatility as the logarithmic difference between high and low Bitcoin prices  $Return\ volatility = \ln P_{high} - \ln P_{low}$  (Bariviera, 2017).

As robustness checks, we use the latter estimator to re-estimate the structural breaks, long memory and MS-ARFIMA model to obtain both static and dynamic data. Comparing Parkinson's measure with return volatility measure, we find no significant differences among the switches especially during the high fluctuation periods. The conclusion for both measures is the same, as all Bitcoin exchange rates volatility show high persistence over time (Table 3.14) with significant structural breaks, particularly after 2017 (Figures 3.8 & 3.9). Further, (Shimotsu, 2010)'s long memory measures were applied in different bandwidths to assess the stability of the analysis. Feasible local Whittle (Table 3.12) and Two-step Exact local Whittle (Table 3.13) with different bandwidths (0.5 to 0.8) were employed to assess the value of  $d$ . Both Parkinson's and return volatility measures show stable and consistent results across the five Bitcoin markets.

Appendix B shows the static estimations of  $MS - ARFIMA$  process of the return volatility across all the markets and under different specifications (tables B.6 to B.10), all the results co-moves and have a similar conclusion to the estimations of  $MS - ARFIMA$  of Parkinson's volatility in section (3.5). Fitted values against the original return volatility series are displayed in appendix B also, to support the latter claim and show that the  $MS - ARFIMA$  process is mimicking the complex behaviour of return volatility across the five Bitcoin markets (figures B.11 to B.15)<sup>35</sup>.

<sup>35</sup> Figures (B.6 to B.10) in appendix B show the fitted value of *ARFIMA* process against the five return volatility markets. Clearly we can identify that *MS-ARFIMA* process (figures B.11 to B.15) is detecting the complex behaviour more efficiently and accurately.

Figure 3.7 The Bitcoin daily return-volatility of the five markets

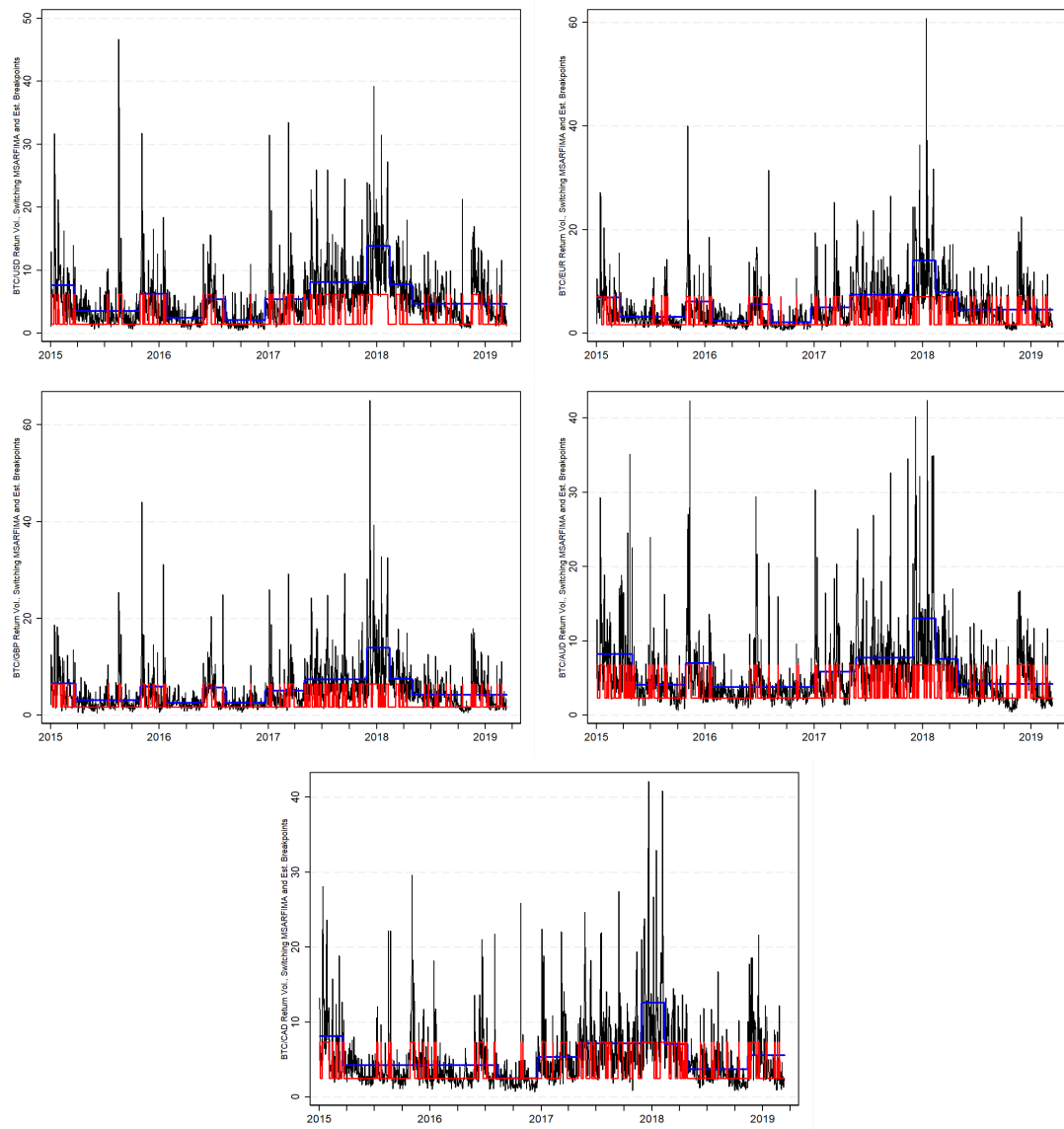


Note: Top left corner BTC/USD, top right BTC/EUR, middle left BTC/GBP, middle right BTC/AUD and bottom BTC/CAD. Exchange rate volatility, daily. Dates on the x-axis indicate the start of the year and ticks are quarterly.

Table 3.12 Estimates of Feasible Exact Local Whittle (FELW) for the return volatility of the five BTC markets

	$\hat{d}_{FELW}$			
	$m = T^{0.5}$	$m = T^{0.6}$	$m = T^{0.7}$	$m = T^{0.8}$
BTC/USD	0.516	0.451	0.418	0.381
BTC/EUR	0.524	0.375	0.396	0.401
BTC/GBP	0.479	0.412	0.346	0.374
BTC/AUD	0.454	0.354	0.368	0.368
BTC/CAD	0.440	0.407	0.341	0.369

Figure 3.8 Estimated breaks in the daily return volatility of Bitcoin exchange markets (Bai and Perron)

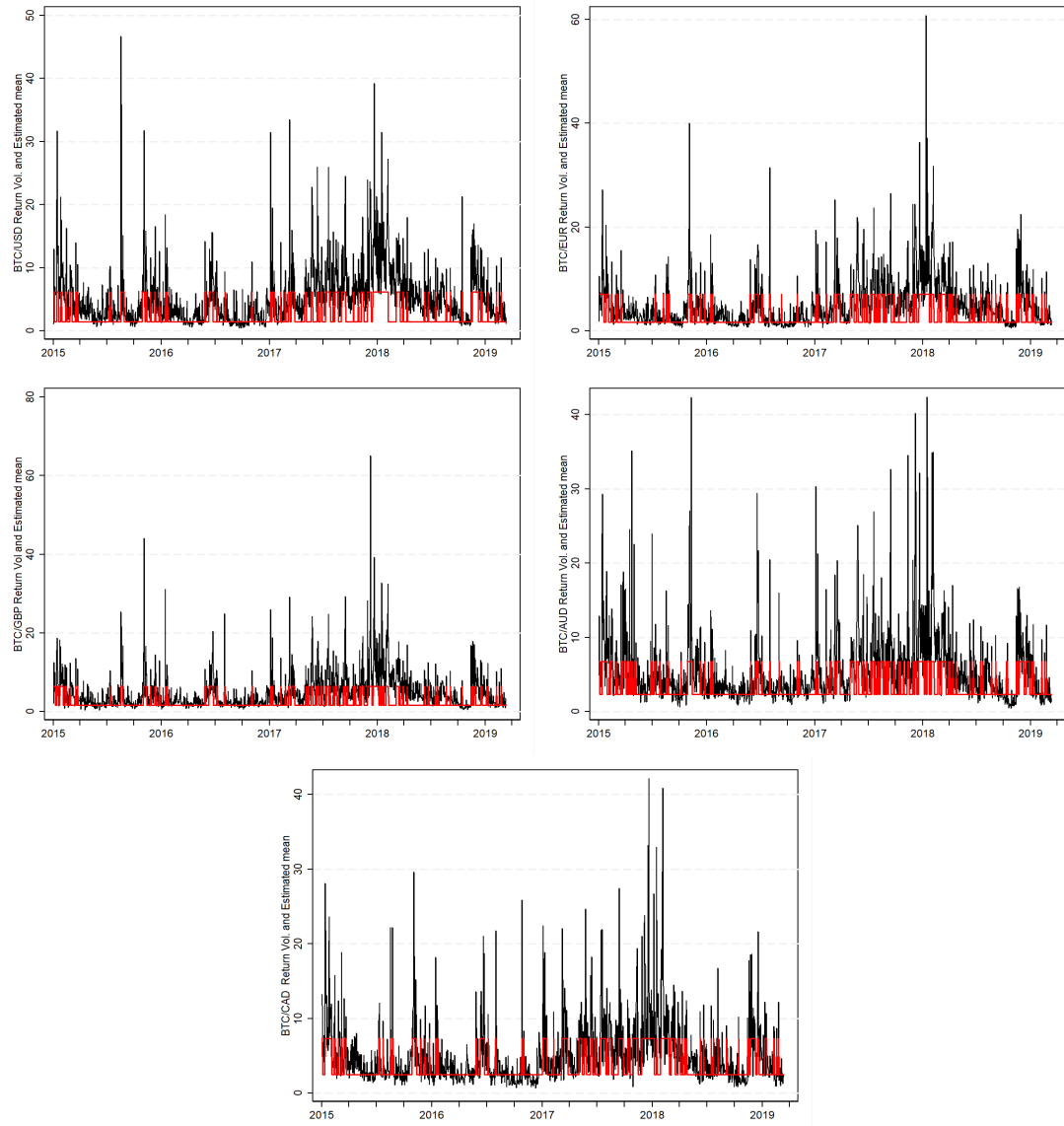


Note: Top left corner BTC/USD, top right BTC/EUR, middle left BTC/GBP, middle right BTC/AUD and bottom BTC/CAD. Blue line represents Bai and Perron multiple structural test, red line is the MS-ARFIMA process. Dates on the X-axis indicate the start of the year, and ticks are quarterly.

Table 3.13 Estimates of Two-step Exact Local Whittle (TSELW) for the return volatility of the five BTC markets

	$\hat{d}_{TSELW}$			
	$m = T^{0.5}$	$m = T^{0.6}$	$m = T^{0.7}$	$m = T^{0.8}$
BTC/USD	0.533	0.451	0.418	0.381
BTC/EUR	0.538	0.375	0.396	0.401
BTC/GBP	0.479	0.412	0.346	0.374
BTC/AUD	0.454	0.354	0.368	0.368
BTC/CAD	0.440	0.407	0.341	0.369

Figure 3.9 Bitcoin exchange rates and the path of estimated switching in the mean of return volatility



*Note:* Top left corner BTC/USD, top right BTC/EUR, middle left BTC/GBP, middle right BTC/AUD and bottom BTC/CAD. Red line represents estimated  $\mu_{st}$  from MS-ARFIMA model. Dates on the X-axis indicate the start of the year, and ticks are quarterly.

Table 3.14 Estimates of MS-ARFIMA model of volatility return across the five Bitcoin markets

	BTC/USD		BTC/EUR		BTC/GBP		BTC/AUD		BTC/CAD	
	MS-ARFIMA (1, d, 1)		MS-ARFIMA (0, d, 1)		MS-ARFIMA (1, d, 0)		MS-ARFIMA (0, d, 1)		MS-ARFIMA (1, d, 1)	
	Estimate	S.E.								
$d_1$	0.4772	0.0486	0.3563	0.0322	0.3407	0.029	0.3561	0.0316	0.2756	0.0837
$d_2$	0.4423	0.0336	0.3485	0.0209	0.3117	0.0174	0.2982	0.0194	0.2663	0.0526
$\mu_1$	6.2306	1.3547	7.1305	0.9302	6.4464	1.0258	6.7589	1.1148	6.2231	0.9982
$\mu_2$	1.482	0.767	1.6703	0.5471	1.7022	0.461	2.3365	0.4484	2.1388	0.4621
$\sigma_1$	6.1884	0.2546	6.1937	0.2491	6.9928	0.3163	6.4412	0.255	5.4306	0.1790
$\sigma_2$	1.6003	0.0324	1.4403	0.0232	1.5378	0.0307	1.4006	0.0289	1.2759	0.0283
$p_{11}$	0.8224	0.0218	0.7818	0.0232	0.7341	0.0274	0.7406	0.0239	0.8961	0.0138
$p_{22}$	0.9553	0.0059	0.9425	0.0067	0.9451	0.0064	0.9265	0.0075	0.9516	0.0066
$\phi$	0.2769	0.0896	-	-	-0.0015	0.0194	-	-	-0.0902	0.0919
$\theta$	-0.474	0.0898	-0.0436	0.036	-	-	0.0549	0.0356	0.1382	0.0838
$L$	<b>-3672.7555</b>		<b>-3628.32752</b>		<b>-3647.5388</b>		<b>-3708.4664</b>		<b>-3612.41</b>	

Note:  $d$ : long memory,  $\mu$ : mean,  $\sigma$ : standard deviation,  $P$ : transition probability,  $\phi$ : Auto-regressive parameter,  $\theta$ : Moving average parameter,  $L$ : Log-likelihood of switching model,  $S.E.$ : standard error

### 3.6 Conclusions

The presence of structural breaks could create the impression of long memory in the volatility of Bitcoin cross-markets. However, one of the benefits of using a Markov-switching approach to the *ARFIMA* model is to overcome the possibility of spurious long memory due to the presence of structural breaks. The objective of this chapter is to investigate the persistence of fractional integration and potential break-points simultaneously and endogenously using the *MS – ARFIMA* model for Bitcoin cross-markets.

When structural break and fractional integration were tested separately, results show clearly the presence of ten breaks in (*BTC/USD*, *BTC/EUR* and *BTC/GBP*) and eight breaks in (*BTC/AUD* and *BTC/CAD*), respectively, when Bai and Perron (1998) test was used. In addition, the results show the presence of long memory across all the Bitcoin cross-markets. Therefore, a spurious long memory in volatility could be attributed to the presence of structural breaks if the standard *ARFIMA* model was applied to each of the Bitcoin cross-markets respectively. Consequently, we applied the *MS – ARFIMA* model instead. We find that the fractional integration displayed long-memory for all the *MS – ARFIMA* models.

The finding in this chapter has two important implications for investors and policy makers. First, the presence of long memory could enable investors to capture speculative profits. This can be achieved through market timing. During a high-volatility regime, investors can buy and then subsequently sell when the market switches to low-volatility regime in all Bitcoin cross-markets. Investors could also hedge during high-volatility regime by purchasing Bitcoin futures from the Chicago Board Option Exchange (*CBOE*). Second, policy makers and regulators could introduce circuit breakers to stop trading in Bitcoin cross-markets when the market switches abruptly to high-volatility regime, as the impact of a negative downturn would take a relatively long period of time to dissipate, given the nature of persistence in the price behaviour of Bitcoin in the cross-markets.

Apart from purchasing Bitcoin futures from the *CBOE*, the ability of portfolio investment managers can be further enhanced if speculative and hedging activities between Bitcoin cross-markets can be carried out as well. Therefore, we would extend the investigation by employing the same approach to study the Bitcoin market and other financial assets. Indeed, by examining a wide range of financial assets, including cryptocurrencies, we will be able to develop a dynamic hedge ratio to enable both users and investors in Bitcoin to formulate the appropriate hedging strategies between these cross-financial markets to protect their respective portfolios from abrupt structural changes.



## Chapter 4

# Dynamic Co-movements and Cyberattacks in Cross-market Bitcoin Prices: Spillover and Variance Decomposition of Network Topology

## Abstract

We investigate and detect the flow of volatility across the major Bitcoin markets under episodes of cyber attacks and discuss several diversification strategies in this context. Adopting both variance decomposition and weighted, directed networks analysis, allows us to estimate the magnitude and direction of spillover effects among the six markets. Security breaches have a significant impact on the Bitcoin prices and weaknesses in the infrastructure of the Bitcoin network. We found that cyber attacks over the years create a high degree of spillover because investors' reaction to negative information depreciates the price and creates a turmoil status across the markets. Our results show a strong volatility spillover between the markets with upward spillover trending over time. Network analysis helps us to zoom in on the propriety of spillover index to examine the direction and magnitude of spillover effects over time. We studied 19 major cyber attacks between 2015 and 2019, scrutinising the connectedness among the six major Bitcoin markets. We find that cyber attacks leave some distortion in the network depending on the size and connectedness. On average BTC/USD and BTC/EUR and BTC/JPY possess stronger predictive power, and transmit the volatility to the rest of the markets. A robustness exercise generally supports our claim. Different hedging and investment strategies are provided to help investors and policy makers.

**Keywords:** Keywords: Variance Decomposition, volatility spillover, Network analysis, Cyberattacks, Cross-market Bitcoin prices.

## 4.1 Introduction

The popularity and interest in Bitcoin markets is growing rapidly. Indeed, Bitcoin is the most active cryptocurrency with market capitalisation exceeding \$ 145 billion<sup>1</sup>, which can be traded or exchanged, anonymously and instantaneously around the world. Bitcoin is an application (digital currency) that can be transacted through anonymous, public and open disrupted ledger without any central authority. To build the latter system, Nakamoto (2008) rely on the block chain method<sup>2</sup> to build a safe, secure distributed ledger needed to complete a state-of-the-art mathematical puzzle called proof of work (PoW), to firstly verify transactions and secondly, build new blocks and add them to the chain. These Bitcoins can be stored in secure software called a ‘wallet’, for which a private key is provided to be able to access the Bitcoin addresses and all related information. Bitcoin investors and others interested in the cryptocurrency market are seriously cautious and alert to network safety and security, as a cyber attack or any other security breach is going to affect and threaten the Bitcoin price substantially, and hence, their investment. As Bitcoin prices are fundamentally driven by the feeling and memory of investors, cyber crime events in Bitcoin markets should be controlled and the network security increased to provide a safe environment for investors. To investigate the nature of such types of investment decisions, and to help governments design adequate regulations for limiting cross-market movement of shocks, a remarkable growth of research has lately sprung up.

Literature has focused on two main aspects of cryptocurrency price movements. First, conceptual designs aiming to depict potential weaknesses of this market and show how the latter can subject investors to insurmountable unsystematic risks (see for instance, Cheah & Fry, 2015; Cheah et al., 2018). Second, a plethora of empirical research has systematically presented state-of-the-art estimation techniques to identify, among others, informational inefficiency (viz. Urquhart, 2016), long-range persistence behaviour and cointegration (viz. Alvarez-Ramirez et al., 2018; Caporale et al., 2018; Cheah et al., 2018), volatility spillovers and dynamic interactions with other financial assets (viz. Gillaizeau et al., 2019), cyber criminality and market regulation (viz. Caporale et al., 2019; Corbet et al., 2020; Gandal et al., 2018). Thus far, the extant research has largely focused on a cross-section of cryptocurrencies and sparsely on the cross-market dynamics of a single cryptocurrency. The current chapter aims to contribute to the nascent literature by studying the issue of cyber crimes and identifying their affects across Bitcoin markets exchanged in various currencies based on the network topology of variance decomposition.

The issue of networks has been studied everywhere in modern life, such as social sciences, physics, biology and many others. Regarding the finance literature, F. Diebold and Yilmaz (2014) designed a network connectedness framework in conjunction with variance decomposition to understand and analyse the interdependence between network

---

<sup>1</sup>Coinmarketcap(Jan, 2020)

<sup>2</sup>Remember that the block chain is a one type of distributed ledger, so a block chain can be a distributed ledger but not the reverse

components. Indeed, the latter framework simplifies and demonstrates volatility spillover through the distance of diameters and degree of nodes in the network. Monitoring and characterising the evolution of interdependence, especially during financial crisis and episodes of economy-wide uncertainty help us to understand the flow and direction of information within markets. Further, detecting shocks within a network is relatively easy as one can exploit the different network features to monitor the movements and generate better predictive power for an asset. Although the Bitcoin market is regulated to some extent, it is still less safe than other conventional regulated markets around the globe and cross-economies, which may increase the risk generated by investor sentiment concerning the security of the network infrastructure. While former studies, such as Corbet et al. (2020) shed light on the financial market effects of recent cyber criminality in cryptocurrency markets, Caporale et al. (2019) investigated the effects of a wide range of cyber attacks on cryptocurrency returns. The focus on a single market, rather than a cross market cryptocurrency market in the latter study holds significance in our context: designing a weighted directed network can create a stock of information for investors seeking arbitrage value of Bitcoin traded in various markets. Further, regulators could introduce circuit breakers to stop trading in Bitcoin cross-markets when the market receives a severe shock that might impact negative down. This study provides a helpful and robust investment strategy for a single cryptocurrency traded in various markets.

The main aim of the current chapter is to improve our limited understanding of the serious damage and risk that could be generated from cyber attacks. Corbet et al. (2020) find that the degree of risk within cryptocurrency markets is heavily dependent on the stability and security of the market with the co-movement of extreme events. Thus, a thorough understanding of network variance decomposition across Bitcoin markets is important to gauge the level and magnitude of threat received by a security breach or cyber attack. Therefore, this chapter contributes to the literature in two significant ways. First, we study *the network topology of Bitcoin prices volatilities* by designing several weighted directed networks during nineteen major cyber attacks. Although economic and political events could generate volatilities within financial markets, but cyber attacks could leave more significant impacts on cryptocurrencies market, hence, the markets are fully electronic and vulnerable to cyberattacks. Each cryptocurrency has unique and distinct infrastructure (network), thus, focusing on Bitcoin market rather than cryptocurrencies markets allows us investigating the network more thoroughly and efficiently. Second, we examine the impact of a series of cyber attacks across Bitcoin markets through variance decomposition method. To the best of our knowledge there is no available financial theoretical model to justify conditioning the predictive power of an asset market on volatility in a cryptocurrency market. In this sense, a major contribution of the current chapter is to measure and identify the network connectedness between Bitcoin markets under several cyber attacks. By doing so, we aim to shed light on six Bitcoin markets under different security breaches to identify their magnitudes and directions, statically,

dynamically and graphically. Eventually, such tendencies could help investors and policy makers to design useful strategies to systematically hedge and save the market.

To investigate further, the rest of the chapter is planned as follows: Section 2 revises the cryptocurrency literature; Section 3 discusses data and summary statistics; Section 4 discusses estimation methods; Section 5 presents empirical results and robustness analyses; Section 6 concludes and presents the main implications of our research.

## 4.2 Literature review

Although the Bitcoin system is based on the proof-of-work method to securely and confidentially record users' details on the distributed ledger, because of the decentralisation and undetectable characteristics of the system, attackers and hackers exploit the opportunity to commit fraudulent transactions, control the network and access sensitive details. Attackers mainly target the users (investors), merchants (platform owners), Bitcoin system (the network) and miners (builders of the chain) to hijack private keys, sensitive details and control the network to gain more rewards (Conti et al., 2018). For example, *DDoS attacks* can target a platform website or network and disturb the normal traffic by flooding the target with loads of internet traffic, *Wallet theft* which mainly targets users and individuals or businesses, and *Double spending attacks* which target both platforms and sellers<sup>3</sup>. Some excellent surveys have been performed recently (Conti et al., 2018; Ghimire & Selvaraj, 2018; Shalini & Santhi, 2019) in the computer science and network security field to characterise, facilitate and clarify all the technical aspects of the network, protocols (e.g. payment system), blocks and blockchain, proof-of-work and mining processes in cryptocurrencies/Bitcoin.

A wide range of attacks on the Bitcoin system (e.g. Sybil attack, Eclipse attack, Block withholding attack and many others) are revised in the literature and addressed to identify the most hidden, vulnerable points in Bitcoin, and several solutions have been found to improve the level of security(Conti et al., 2018). Pachal and Ruj (2019) introduced a new mining approach that boosts the computational power to maximise the individual miner's gain against Selfish mining, Stubborn mining and others. A novel approach called ByzCoin was proposed to leverage the security of Bitcoin and protect the mining and consensus system (Kogias et al., 2016). Almukaynizi et al. (2018) proposed an approach that can detect and identify cyber breaches and illegal activities in the Dark Web targeting cryptocurrency platforms and traders. Another famous way of attacking Bitcoin is via the internet routing infrastructure (IP hijacking), in which hackers manipulate the Bitcoin traffic to hijack BGP prefixes<sup>4</sup> to slow down the network and partially occupy the processing power to generate more rewards. Almukaynizi et al. (2018) proposed

---

<sup>3</sup>This could happen via a 51% attack; when one hacker or miner manages to occupy more than 51% of a network, the double spending method will be possible to apply

<sup>4</sup>Border Gateway Protocol

comprehensive short and long-term measures to limit attackers' ability to redirect miners' IP addresses to their servers. To explore more of the technological and technical literature see (Ahamad et al., 2013; Chyžmar et al., 2019; Mukhopadhyay et al., 2016).

All the above technology and security challenges are associated with the significant risk generated by the hijackers or attackers. However, the Bitcoin market is significantly integrated with the global economy; thus, the associated risk could leak to economies, social networks and many financial entities, and result in a remarkable distortion to the system, users, markets and even the global economy. To identify and understand this in cryptocurrency and the Bitcoin market, a systematic survey undertaken recently (Corbet et al., 2019) reveals that the theoretical and empirical research in the cryptomarket investigates mainly the regulations and information system, the financial market, the monetary theoretical formulation of cryptocurrency, and finally the development of empirical methods and mechanisms to study the complex interaction of prices under different scenarios.

Other systematic surveys (Kyriazis, 2019a, 2019b) explore the empirical literature to clarify and investigate market efficiency, connectedness and spillovers across the cryptocurrency markets. The latter empirical results allow us to make decisive inferences and draw on efficient and accurate investment strategies with lowest associated risk. Several pieces of research have systematically proposed and investigated a plethora of techniques to measure the level of efficiency in Bitcoin markets. Brauneis and Mestel (2018); Khuntia and Pattanayak (2018); Wei (2018) applied several approaches and found that the Bitcoin market is mostly efficient, and the level of market efficiency relatively impacted by liquidity and size. By contrast, a plethora of research has supported the inefficiency of Bitcoin markets, due to the imbalance between the true value of Bitcoin and its available information in the market (Bouri et al., 2019; Urquhart, 2016). Empirical studies on spillover volatility and price dynamics could be a good measurement for identifying the level of efficiency in Bitcoin market and providing rich information about the net receiver and net dispenser of Bitcoin volatility (Corbet et al., 2018; Gillaizeau et al., 2019; Koutmos, 2018; Symitsi & Chalvatzis, 2018; Zięba et al., 2019, viz.). A stream of literature has investigated structural breaks, co-integration and fractional integration to detect and investigate the complex behaviour of cryptocurrency prices. Indeed, studying the long memory in Bitcoin prices could determine the level of inefficiency in the market and help investors to speculate and design several investment strategies that can generate abnormal returns (Alvarez-Ramirez et al., 2018; Al-Yahyaee et al., 2018; Bouri et al., 2019; Caporale et al., 2018; Charfeddine & Maouchi, 2019; Cheah et al., 2018; Mensi et al., 2019). However, ignoring the stability of the system during the analysis process could generate misleading information and bias investment strategies.

The third main strand of the literature focuses on the regulations, information systems and cyber criminality of cryptocurrency markets that allow legislators and decision makers to design appropriate regulations and create an efficient environment with flexible boundaries

to restrict the frustration and manipulation across the cryptocurrency market (Böhme et al., 2015; Dwyer, 2015; Gandal et al., 2018). Abhishta et al. (2019) investigated one of the most important DDoS attacks mentioned earlier and its economic impact on Bitcoin. They showed that DDoS attacks have a direct negative impact on the daily volume of Bitcoin, most generating a one day shock, followed by recovery, although some react after two to five days before recovering again. Marella et al. (2017) classified the cyber attacks on Bitcoin (e.g. DDoS, code bugs or user errors) and the common response from users (e.g. code revision, computer security measures or temporary suspension). They conclude that cyber attacks can diminish the value of Bitcoin and leave a serious impact for its users, exchange and different aspects. Caporale et al. (2019) investigated the impact of cyber attacks on the return of four cryptocurrencies (e.g. Bitcoin, Stellar, Litecoin and Ethernam) through Markov switching analysis and cumulative measures. Their results suggest that cyber attacks induce the system to be highly volatile, and when the number of cyber attacks increases dramatically, the probability of volatility to stay mostly stable is low. Another interesting piece of research studied the influence of cyber criminal events on price volatility and cross-cryptocurrency correlation. Significant results suggest that during cyber attacks, there are very high episodes of volatility and broad co-movement in cryptocurrency markets. They also found that there is a chance of abnormal returns (which vary depending on the cyber attack event) just before the cyber attack occurs, and zero returns during the time and announcement of the cyber attack (Corbet et al., 2020) .

It is evident in the literature that Bitcoin prices are typically volatile during cyber attacks and can be seriously manipulated in some markets (Gandal et al., 2018). In the meantime, exchange rate differentials across markets offer investors the opportunity to enhance their portfolio returns. Under these scenarios, it is expected that price volatility on one particular Bitcoin-to-currency exchange market (e.g. Bitcoin-USD) can flow to other markets, and can also be acquired from others. Any quantitative information on the centrality or relative isolation of some Bitcoin-to-currency markets can actually help investors to better anticipate their complex dynamic behaviour and exploit the potential for forecastable gains. These premises are rigorously tested in the current chapter by using daily price data on six major Bitcoin-to-currency exchange rates. In the next section, we design the net predictive power and the net receiver of volatility during different cyber attacks.

### 4.3 Data and summary statistics

Table 4.1 Summary statistics, exchange rate volatility

	Mean	St. Dev.	Median	Max	Min	Skewness	Kurtosis
BTC/USD	0.033	0.028	0.025	0.281	0.003	2.559	13.820
BTC/EUR	0.032	0.029	0.023	0.365	0.003	3.058	20.907
BTC/GBP	0.031	0.029	0.022	0.391	0.002	3.478	26.439
BTC/JPY	0.031	0.032	0.021	0.345	0.003	3.539	22.559
BTC/AUD	0.041	0.118	0.025	2.419	0.003	16.646	310.221
BTC/CAD	0.035	0.081	0.024	2.864	0.004	28.622	962.340

As mentioned above, a plethora of literature has claimed that the Bitcoin market is isolated from other conventional markets. Consequently, we were interested in investigating the cross-market Bitcoin prices system, as studying the dynamics of Bitcoin will provide rich information about the factors affecting price developments and help us to devise efficient investment strategies.

Bitcoin is traded across different countries in diverse exchanges. This chapter considers daily high and low (H-L) exchange rates data against Bitcoin for six major currencies across the world, namely the U.S. dollar (USD), Australian dollar (AUD), Canadian dollar (CAD), Euro (EUR), British pound (GBP) and Japanese yen (JPY). The data span from Jan 1<sup>st</sup>, 2015 to May, 31<sup>st</sup>, 2019.

Bitcoin prices are publicly available and provided by several electronic platforms (Alexander & Dakos, 2020). However, selecting the ideal Bitcoin prices against each currency is crucial and depends on the selected platform. Thus, we take into consideration the traded prices, ranking and trading volume for each market (e.g. BTC/USD, BTC/AUD, BTC/CAD, BTC/EUR, BTC/GBP, and BTC/JPY) to cover the optimal Bitcoin prices across the markets. We found that the highest rank of the market and trading volume of USD in Bitfinex platform exceeded 211 Billion over the last five years, which makes the market share of the latter platform around 37.35%, overtaking more than a third of the market trading in Bitcoin/USD. Kraken platform has executed transactions of BTC/EUR of around 43 Billion Eur over the last five years, the market share of BTC/Eur via this platform being around 36.5%. The highest trading volume of JAP yen against BTC is on Bitflyer platform with 9.61 Trillion JPY volume and 99.72% market share. GBP, CAD and AUD were traded intensively on Bit-x, Quadrigacx and Btcmarkets platforms with trading volumes approaching 11.7 Billion GBP, 2.65 Billion CAD and 3.95 Billion AUD respectively. The market share of trading Bitcoin on the latter three currencies is 67.4%, 77.32% and 91.11% respectively. We obtained our data directly from these platforms to reflect the actual traded behaviour for each fiat currency, and neglect all the platforms

showing suspicious trading activities<sup>5</sup> or low rank and trading volumes. To borrow more comparisons, we compared all the Bitcoin prices with Bitcoinity.org and Bitcoincharts<sup>6,7</sup>.

We study the daily volatilities of exchange rate returns of bitcoins. The daily variance is computed using daily high and low prices and the high-Low volatility (HL-HV) measure by Parkinson (1980):<sup>8</sup>

$$V = \sqrt{\frac{1}{4 \ln(2)} \ln \frac{h}{l}^2} \quad (4.1)$$

where  $V$  denotes the volatility of price,  $h$  and  $l$  are the highest and lowest exchange rates on a given trading day, respectively. All volatility series are checked for stationarity with the help of Augmented Dicky Fuller (ADF) unit root tests (Dickey & Fuller, 1979). Both tests suggest to systematically reject the null of the presence of a unit root with 95% confidence for every daily volatility series, suggesting the latter are co-variance stationary.

The dynamics of Bitcoin price volatility are illustrated in Figure 4.1, while Table 4.1 summarises the descriptive statistics. The number of observations is 1612 across all variables. The average volatility across markets is bouncing around 0.032. The highest and lowest mean across the sample are AUD (0.035) and GBP (0.031) respectively, while the standard deviation across the 6 markets is fluctuating between CAD (0.027) and JPY (0.032). Thus, the average of S.D. is approximately 0.029. The six exchange rates display large positive skewness, suggesting a large concentration of observations to the left of their central tendency, hence, volatility series are asymmetrically distributed. Bitcoin prices are sensitive to major economic and political events, and all extreme shocks can be explained through the four moments. All series show unequivocally leptokurtic behaviours, of which Kurtosis is different across individual series, ranging from around 14.6 on average (BTC/USD, BTC/AUD and BTC/CAD) to about 23.3 (BTC/JPY, BTC/GBP and BTC/EUR).

Figure 4.1 displays the volatility of six Bitcoin markets over time. BTC/GBP and BTC/EUR show the highest shock across the whole system, recording only around 0.37 in both markets. Visually, we can confirm that BTC/USD and BTC/EUR are the most stable markets with both series fluctuating below 0.1 most of the time, except for the period around 2018. Also, extensive fluctuations across the entire system appear mainly around 2018, and partially between 2015 and 2016, hinting that events such as platform breaches lead Bitcoin prices to be remarkably sensitive.

---

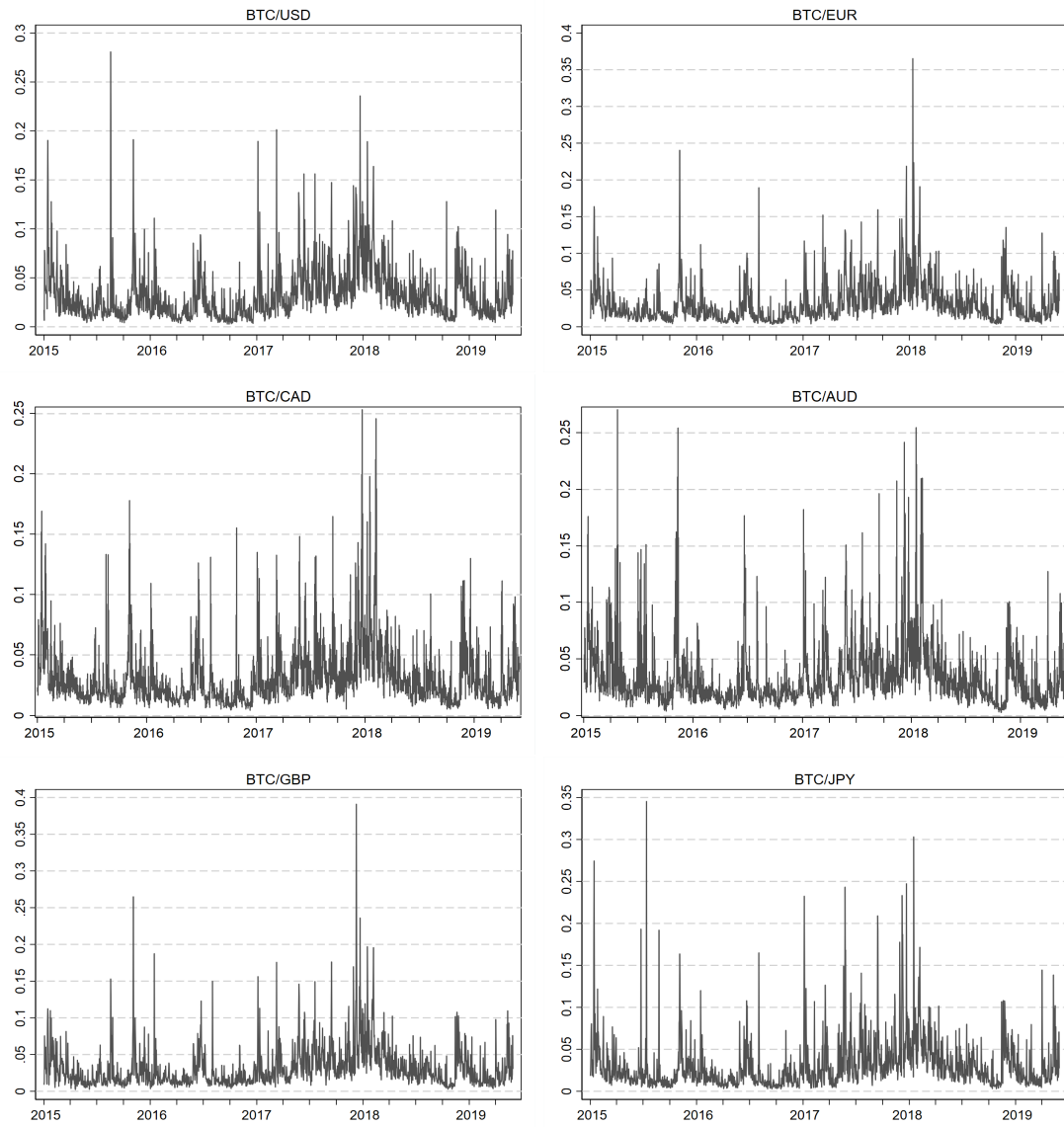
<sup>5</sup> All the trading volumes and Ranking information obtained from Bitcoinity.org

<sup>6</sup> Bitcoinity.

<sup>7</sup> Bitcoincharts API.

<sup>8</sup> Bennett and Gil (2012) argue that Parkinson's volatility model is more efficient than other conventional measure of volatility, such as that of close-to-close.

Figure 4.1 Volatility Exchange Rates



*Note:* Exchange rate volatility series, daily. Dates on the x-axis indicate the start of the year, and ticks are quarterly.

## 4.4 Methodology

Let us consider the following  $N$ -dimensional covariance-stationary data generating process with orthogonal shocks (see F. Diebold & Yilmaz, 2014):

$$y_t = \Theta(L)u_t \quad (4.2)$$

where  $\Theta(L) = \Theta_0 + \Theta_1 L + \Theta_2 L^2 + \dots$ , with  $E(u_t u_t') = I$ , and  $y_t$  contains the series of Bitcoin exchange rate returns volatility under investigation in our analysis. In particular,  $\Theta_0$  summarises the contemporaneous aspects of connectedness and  $\{\Theta_1, \Theta_2, \dots\}$  the dynamic aspects. The understanding of the connectedness through the matrices of coefficients  $\{\Theta_0, \Theta_1, \Theta_2, \dots\}$  can be problematic if many parameters are to be estimated. Therefore, one can transform  $\{\Theta_0, \Theta_1, \Theta_2, \dots\}$  by using variance decomposition technique to resolve the issue (F. Diebold & Yilmaz, 2014).

In order to understand the measures of connectedness, F. Diebold and Yilmaz (2014) provide the so-called *connectedness table*, which is illustrated in Table 4.2. The  $N \times N$  upper-left block matrix contains the variance decompositions, which are denoted by  $DH = [d_{ij}^H]$  and indicate the fraction of variable  $i$ 's  $H$ -step forecast error variance due to shocks in variable  $j$ . This matrix is called “variance decomposition matrix”.

Table 4.2 Connectedness table

	$y_{1t}$	$y_{2t}$	$\dots$	$y_{Nt}$	From others
$y_{1t}$	$d_{11}^H$	$d_{12}^H$	$\dots$	$d_{1N}^H$	$\sum_{j=1}^N d_{1j}^H, j = 1$
$y_{2t}$	$d_{21}^H$	$d_{22}^H$	$\dots$	$d_{2N}^H$	$\sum_{j=1}^N d_{2j}^H, j = 2$
$\vdots$	$\vdots$	$\vdots$	$\ddots$	$\vdots$	$\vdots$
$y_{Nt}$	$d_{N1}^H$	$d_{N2}^H$	$\dots$	$d_{NN}^H$	$\sum_{j=1}^N d_{Nj}^H, j = N$
To others	$\sum_{i=1}^N d_{i1}^H$ $i = 1$	$\sum_{i=1}^N d_{i2}^H$ $i = 2$	$\dots$	$\sum_{i=1}^N d_{iN}^H$ $i = N$	$\frac{1}{N} \sum_{i=1}^N \sum_{j=1}^N d_{ij}^H$ $i = j$

Notes:  $\tilde{\theta}_{ij}(H)$  represents the contribution of variable  $j$  to variable  $i$ 's  $H$ -step-ahead generalized forecast error variance. FO (From Others) and TO (To Others) denote the magnitude of the contribution from others and to the rest of the system, respectively. The bottom-right element of the table is the total connectedness and represents a system-wide measure of interdependence.  $H$  is the forecasting horizon.  $N$  is the total number of variables.

The connectedness table augments  $DH$  with a rightmost column (From others) containing row sums, a bottom row containing column sums (To others), and a bottom-right element containing the grand average, in all cases for  $i = j$ . The off-diagonal elements of  $D^H$  measure the pairwise directional connectedness from  $j$  to  $i$ , which is defined as

$$C_{i \leftarrow j}^H = d_{ij}^H. \quad (4.3)$$

In general,  $C_{i \leftarrow j}^H = C_{j \leftarrow i}^H$ . In addition to the *gross pairwise directional connectedness* is possible to define the *net pairwise directional connectedness* which is given by  $C_{ij}^H =$

$C_{j \leftarrow i}^H - C_{i \leftarrow j}^H$ . When considering the off-diagonal row or column sums of  $D^H$ , we have the *total directional connectedness from others to i*:

$$C_{i \leftarrow \bullet}^H = \sum_{\substack{j=1 \\ j=i}}^N d_{ij}^H. \quad (4.4)$$

and the *total directional connectedness to others from j*:

$$C_{\bullet \leftarrow j}^H = \sum_{\substack{i=1 \\ i=j}}^N d_{ij}^H. \quad (4.5)$$

Likewise the net pairwise directional connectedness, one can define the net total directional connectedness as  $C_i^H = C_{\bullet \leftarrow i}^H - C_{i \leftarrow \bullet}^H$ . Lastly, grand total of the off-diagonal entries in  $D^H$  defines the total connectedness:

$$C^H = \frac{1}{N} \sum_{\substack{i,j=1 \\ i=j}}^N d_{ij}^H. \quad (4.6)$$

In order to obtain the variance decomposition, the general variance decomposition (GVD) framework is used (see Koop et al., 1996; Pesaran & Shin, 1998). The H-step-ahead generalized variance decomposition matrix  $D^{gH} = [d_{ij}^{gH}]$  is as follows:

$$d_{ij}^{gH} = \frac{\sigma_{jj}^{-1} \sum_{h=0}^{H-1} (e_i \Theta_h \Sigma e_j)^2}{\sum_{h=0}^{H-1} (e_i \Theta_h \Sigma \Theta_h e_j)} \quad (4.7)$$

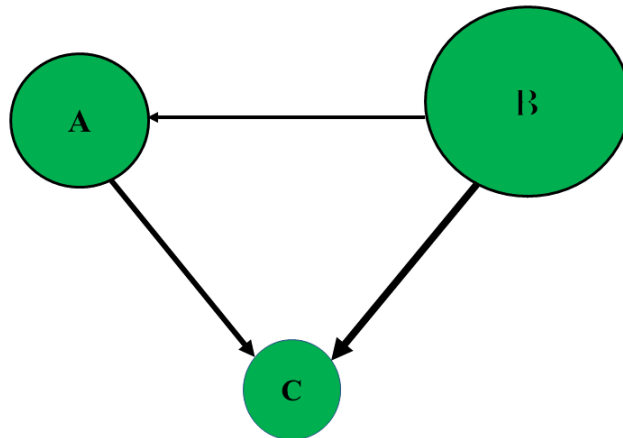
where  $e_i$  is the selection vector with its  $i^{th}$  element equal to one and zeros otherwise  $\Theta_h$  is the coefficient matrix times the h-lagged shock vector in the moving-average representation of the non-orthogonalized VAR,  $\Sigma$  is the covariance matrix of the shock vector in the non-orthogonalized VAR, and  $\sigma_{jj}$  is the  $i^{th}$  diagonal element of  $\Sigma$  (see F. Diebold & Yilmaz, 2014). Since the shocks in the GVD framework are not necessarily equal to one, F. Diebold and Yilmaz (2014) base their generalized connectedness indexes on  $\tilde{D}^g = [\tilde{d}_{ij}^g]$ , with  $\tilde{d}_{ij}^g = \frac{d_{ij}^{gH}}{\sum_{j=1}^N d_{ij}^{gH}}$  ( $\sum_{j=1}^N \tilde{d}_{ij}^g = 1$  and  $\sum_{i,j=1}^N \tilde{d}_{ij}^g = N$ ).

The connectedness measures examined so far are linked to the network connectedness: the variance decompositions are networks (F. Diebold & Yilmaz, 2014). A network  $\mathcal{N}$  consists of  $N$  nodes and  $L$  links between the nodes, and the distance between two nodes  $i$  and  $j$ , denoted by  $S_{ij}$ , is the smallest number of links that must be crossed to move from  $i$  to  $j$ .  $\mathcal{N}$  is connected if  $S_{ij} \leq N - 1$ ,  $\forall i, j$ . Put another way, a network is a  $N \times N$  adjacency matrix  $A$  of zeros and ones,  $A = [A_{ij}]$ , where  $A_{ij} = 1$  if nodes  $i$  and  $j$  are

connected, and  $A_{ij} = 0$  elsewhere. The variance decomposition matrix  $D$  is a network adjacency matrix  $A$  (F. Diebold & Yilmaz, 2014).

Figure 4.2 illustrates the mechanism of the network with an example. The network involves a set of nodes (bitcoins markets) and edges which represent connectedness among nodes. The largest node is B, which implies that this node gives the highest contribution (the highest contribution is from B to C). C is the smallest node, and its contribution to the other nodes is the smallest. B is a net contributor to A and C, while C is a net receiver from A to B (the direction of the arrow among two nodes reveals the net receiver). Lastly, node A is a net receiver from B and a net contributor to C.

Figure 4.2 Net pairwise directional networks.



*Note:* The Nodes are the bitcoin markets and the link between two nodes (edge) is given by net pairwise directional connectedness. The edge size shows the magnitude of the net contribution of bitcoin markets in terms of net pairwise directional connectedness.

The full-sample connectedness releases “average” information on aspects of each of the connectedness measures, but by construction it does not relate to connectedness dynamics (F. Diebold & Yilmaz, 2014). A dynamic analysis of connectedness can be accomplished by rolling estimation. To this end, the total (global) connectedness (TC) (see the bottom-right element of Table 4.2) can be evaluated dynamically using a rolling scheme based on the following formula

$$TC(s) = \frac{1}{N} \sum_{i=1}^N \sum_{j=1}^N d_{ij,s}^H, \quad i = j, \quad (4.8)$$

where  $s$  is the sequence of the rolling estimates of TC in equation (4.8). With a total sample size of  $T$  observations and a rolling window size of  $R$  observations, the sequence of estimates of TC is always generated from a sample of size  $R$ : the first estimates of  $TC(s)$

is obtained with a sample running from 1 to R, the next one with a sample running from 2 to R+1, and the final one with a sample running from T-R+1 to T.

## 4.5 Results

In this section, we examine the exchange rate return volatilities of Bitcoin for six currencies, namely the U.S. dollar (USD), Australian dollar (AUD), Canadian dollar (CAD), Euro (EUR), British pound (GBP) and Japanese yen (JPY). The analysis proceeds in three steps. First, a static analysis of connectedness is carried out using the connectedness table and the network framework. Second, a rolling estimation scheme is applied for the connectedness dynamics. In particular, this step involves an examination of total connectedness, along with total directional spillover effects. Third, the network framework is used to ascertain whether, and to what extent cyber attacks impacted on Bitcoins during the period under investigation. Lastly, a robustness exercise is carried out to validate the spillover index analysis.

### 4.5.1 Static connectedness

Table 4.3 reports the full-sample total connectedness results. The horizon is H=30 days. The following main findings emerge: first, the total connectedness is a very high 77% (see the bottom-right element in boldface). Second, the elements on the main diagonal of the table (own connectedness) display the highest values. Third, looking at the off-diagonal elements of the upper  $6 \times 6$  submatrix, the largest value of pairwise directional connectedness is recorded from GBP to USD, 17.14%, while for the lower  $6 \times 6$  submatrix the highest value is from USD to GBP, almost 18%. Fourth, the total connectedness from others to each Bitcoin market (see last column **FROM**) ranges from 75.49% to 77.66%, while the total connectedness to others (see the second last row **TO**) varies from 65.50% to 82.12%.

BTC/JPY and BTC/AUD markets inject almost symmetric shocks across the system (see columns BTC/JPY and BTC/ AUD) and absorb the shocks in different magnitudes. The BTC/AUD market transmits just below 14% to each market, which makes this the most vulnerable market in the system. Looking into the power of influence within the system, we can categorise the table into three sections: first, the Giver group (e.g. the markets which generate the risk), which consists of BTC/USD and BTC/EUR markets. Secondly, the Receiver group, which can be easily identified from the table as BTC/AUD and BTC/JPY. However, the Alleviate group (e.g. the mitigator group) indicates that both markets BTC/GBP and BTC/CAD could act as intermediary, allowing volatility to circulate between the main components of the system.

In sum, among the six markets, BTC/USD and BTC/EUR are “strongly” connected, while BTC/AUD appears to be the most isolated market. The pairs BTC/USD - BTC/EUR, BTC/GBP - BTC/CAD and BTC/JPY - BTC/AUD are the most closely interlinked markets. However, static information is inefficient for explaining economic and financial events; hence, to study market behaviour during episodes of financial shocks, we should study the dynamic spillover across the selected markets.

#### 4.5.2 Dynamic connectedness

Globalisation and technology have a huge impact on the high level of connectedness we see between financial markets nowadays. In particular, the cryptocurrencies market is a fully electronic platform in which trading through the Internet is essential; hence, the market plays a tremendous role in connecting and transmitting risk all over the world. Thus, to investigate the continuous interdependence between the six Bitcoin markets, we should take a closer look and trace the important financial events that could be related to the cryptocurrencies market. Corbet et al. (2018); Damianov and Elsayed (2020); Wang, Zhao, and Li (2019) and many others claim that the cryptocurrencies market is more or less isolated from the conventional financial markets, which makes it reasonable to trace financial events that might affect or connect to the cryptocurrencies market. Regarding Bitcoin markets, the Bitcoin was created to be an independent currency that remains unaffected by economic situations (e.g. inflation or recession), as Satoshi Nakamoto included in his first Bitcoin transaction, "The Times 03-Jan-2009 Chancellor on brink of second bailout for banks". Hence, it is unreliable to claim that economic events might affect Bitcoin price, but rather that such prices are fundamentally driven by the ‘feeling and the memory’ of investors at a point in time (Cheah et al., 2018) .

The full-sample connectedness in Table 4.3 gives ‘average’ results on connectedness (F. Diebold & Yilmaz, 2014). Figure 4.3 illustrates the dynamic of total volatility connectedness over 120-day rolling-sample windows in which the volatility spillover between the six markets (Table 4.3) is compressed in a one dynamic series, as shown in Figure 4.3. From the Figure, the overall behaviour of connectedness is clearly increasing dramatically over time. Observing the first half of the sample span, we can clearly identify wide and deep fluctuations along 2015 and 2016, while on the contrary, the second half shows relatively smooth and upward shifting with high interdependence along 2017 to 2019. The latter upward shifting can be linked to the increasing popularity of Bitcoin, when the price started to rocket and hit a peak, recording almost 20000\$ around December 2017. Since then, investors, regulators and hijackers have started to pay more attention to this digital currency which has been creating this magnitude of connectedness since 2017. The dynamic connectedness among the six markets reveals important information about several key events that occurred between 2015 and 2019, and shows how those events have induced the system to generate such behaviour.

The major events that might affect Bitcoin prices can be categorised as cyber criminality, halvings, exchange or hijacking events. The first and worst crash in the Bitcoin Market was when Mt.Gox in 2014 claimed that around 100,000 BTC had been stolen, affecting around 750,000 customers<sup>9</sup>. Later, in August 2015, the Japanese police arrested the CEO of Mt.Gox platform, Mark Karpeles, claiming that he manipulated the platform system and its financial reports<sup>10</sup>. Moreover, Bitfinx platform had a ‘flash crash’ on 19 August in the same year, in which the Bitcoin price in this exchange declined by 29%<sup>11</sup>. Thus, the latter two events generated enough uncertainty to negatively depreciate the Bitcoin price during the last third of 2015, and created a volatility spillover spike among the second and third quarter of 2015, to record above 70% and 82% shocks, respectively, as shown in Figure 4.3.

In late 2015 and during the first half of 2016, volatility spillover increased dramatically to record two significant shocks (in Nov 2015 and Aug 2016) that might have been generated from several important events, including the announcement of hacking in the Bitfinx platform and stolen Bitcoins worth around 72\$ million, and the announcement of the Bitcoin Investment Trust (GBTC) that the Bitcoin price was going to appreciate dramatically during 2016<sup>12 13</sup>.

The total connectedness has become more constant and intensive since the beginning of 2017, the high linkage being explained by the dramatic increase in Bitcoin price, exceeding 1000\$. Indeed, the high price has encouraged lots of new users and investors to participate and invest in Bitcoin, as well as several projects being established to support the market. As a result, the network has started to grow rapidly, the infrastructure of Bitcoin becoming stronger and more consistent, with Bitcoin wallets, Bitcoin applications, Bitcoin miners and many others.

In this chapter, we focus on cyber attacks to investigate the distortion left in the network infrastructure because of the various different fraudulent transactions and attempts to hijack users’ accounts. In the next section, we will zoom in and scrutinise the total connectedness under episodes of cyber attack, and identify the net dispensers and net givers among the markets.

---

<sup>9</sup> Mtgox.com

<sup>10</sup> Japanese police arrest Mark Karpeles

<sup>11</sup> Coindesk.com

<sup>12</sup> Reuters.com

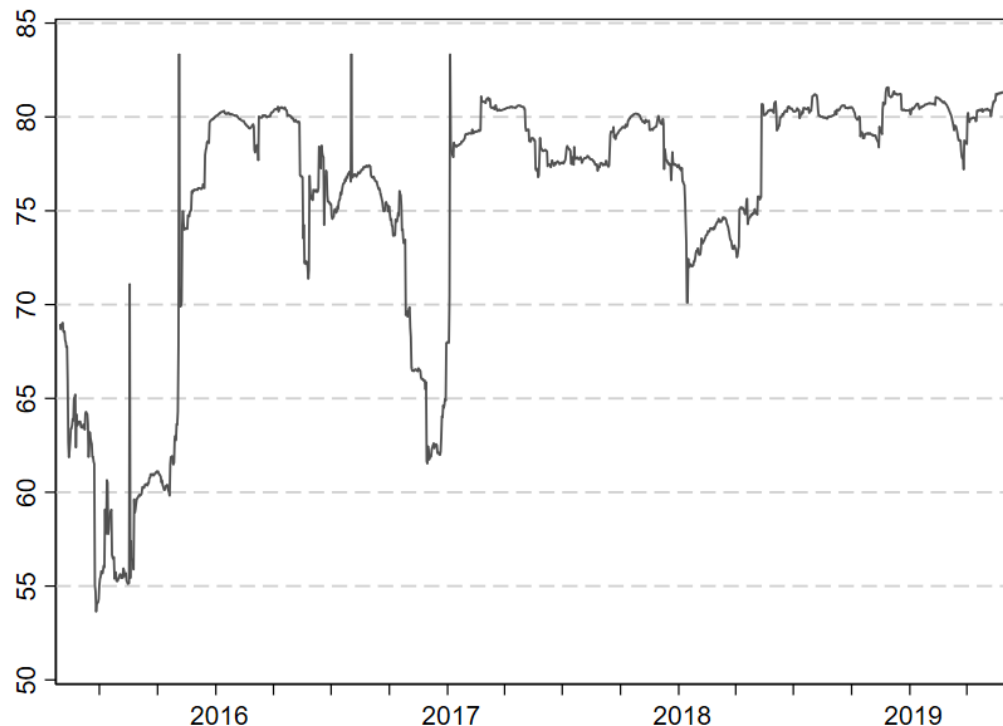
<sup>13</sup> Coindesk.com

Table 4.3 **Volatility spillovers across six selected exchange rates in time domain – 30-day ahead forecast**

	BTC/USD	BTC/EUR	BTC/GBP	BTC/JPY	BTC/AUD	BTC/CAD	Directional FROM others
BTC/USD	22.34	16.81	17.14	14.57	12.88	16.27	77.66
BTC/EUR	16.82	23.25	16.19	14.73	12.86	16.15	76.75
BTC/GBP	17.69	16.49	22.28	14.71	12.82	16.01	77.72
BTC/JPY	15.88	16.35	15.44	23.08	13.64	15.61	76.92
BTC/AUD	15.10	15.62	14.80	14.96	24.51	15.00	75.49
BTC/CAD	16.63	16.48	15.83	14.90	13.30	22.86	77.14
Directional TO others	82.12	81.75	79.41	73.88	65.50	79.03	<b><i>TSI: 76.95%</i></b>

*Note:* Data cover the period from January 1, 2015 to May 31, 2019. The rightmost (**FROM**) column gives total directional connectedness (from). The bottom (**TO**) row gives total directional connectedness (to). Numbers are in percentage. The bottom-right element (in boldface) is total connectedness (see also F. Diebold & Yilmaz, 2014).

Figure 4.3 **Overall volatility spillovers (dynamic plot)**



*Note:* Dynamic overall *volatility* spillovers computed following Diebold and Yilmaz (2014) with a 30-120-day rolling window, y-axis scale is in percentages. Dates on the x-axis indicate the start of the year, and ticks are quarterly.

#### 4.5.3 Network Analysis of variance decomposition

Figure 4.3 provides us with the total connectedness of the six markets over time, in which is difficult to distinguish between the dominant and non-dominant markets, or the direction of spillover among the dynamic connectedness. In this regard, we diffuse the rolling window estimation in the previous section and extract the spillover index at every point in time from 2015 to 2019, in order to study the impact of cyber attacks on the Bitcoin network infrastructure. Table 4.4 shows the most important cyber attacks taking place during the sample span.

Table 4.4 shows 25 cyber attacks that targeted several Bitcoin platforms in this section. We identify the most important attacks that took place during the five years, and present the rest of the network figures in Appendix C, from Figure C.12 to Figure C.25. In the second half of 2016, the Bitcoin infrastructure received the second biggest security breach after the Mt.Gox collapse, in which hijackers stole around 120 000 BTC units from the Hong Kong-based Bitfinex platform. On the other hand, a small amount of units, amounting to 8 BTC were stolen in Jan 2019 by hackers from LocalBitcoin platform. The question here is "Does the amount of stolen Bitcoin determine the magnitude of such a shock?" Or are there different factors that may induce the system to generate more risk, such as 'the feeling and memory' of investors? Indeed, a small amount of stolen BTC, with good media coverage, might generate more risk than an unknown large attack (e.g. a cyber attack in South Africa) within the network.

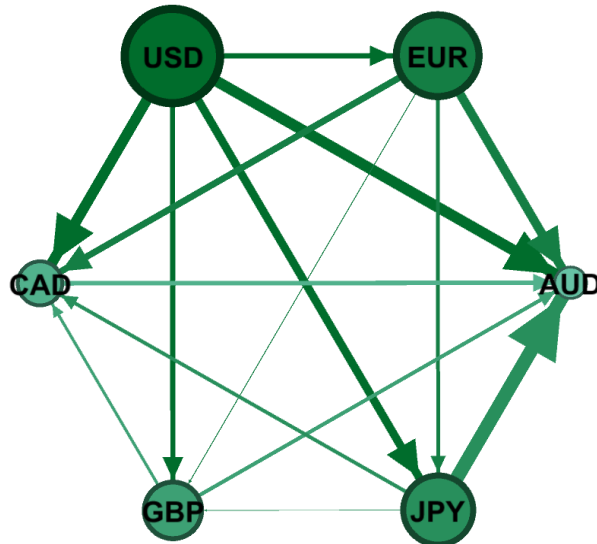
The network graphs of the cyber attacks in Table 4.4 will be presented in the Appendix C, and we will discuss the most important cyber security breaches in each year. In June 2015 a cloud mining service, Scrypt, announced a security breach in one of their hot wallets. Hijackers had managed to steal around 3500 BTC units from the Scrypt account and other registered users' accounts. As discussed earlier, while Figure 4.1 does not provide detailed information about the individual markets in the system, we can clearly see the total spillover index during the cyber attack, which was high as 61%. However, variance decomposition network analysis in Figure 4.4 reveals significant information about the individual Bitcoin markets when a cyber attack took a place during June, 2015. We can identify the direction and the dominant markets here. BTC/USD appears to be the net giver here, followed by BTC/EUR, then BTC/JPY. On the contrary, the Australian market absorbed all the shocks generated within the system, as all the arrows go into BTC/AUD with no sign of any arrow going out of the Australian market. The second vulnerable Bitcoin market is the Canadian market, which has received systematic shocks in different magnitudes including BTC/USD, BTC/EUR, BTC/JPY and BTC/GBP. Overall, investors and policy makers can take advantage of being able to identify the most dominant market - here USD Bitcoin market - to base their investment decisions on, taking into consideration the flow and direction of risk in each market within the system.

Table 4.4 Cyberattacks in Bitcoin Markets

Attack Date	Amount \$	Type	Target	Dominant Market
22/05/2015	329000	BTC	Bitfinex	USD
22/06/2015	864500	BTC	Scrypt.cc	USD
15/02/2016	103000	BTC	brain wallets	EUR
02/08/2016	72000000	BTC	Bitfinex	EUR
13/10/2016	1500000	BTC	Bitcurex	EUR
26/04/2017	7600000	BTC	Yapizon	AUD
17/05/2017	2900000	BTC	eBitz	EUR
06/12/2017	68000000	BTC	NiceHash	EUR
18/12/2017	37000000	BTC	Youbit's	EUR
26/12/2017	1000000	BTC	Exmo	EUR
07/01/2018	23000000	BTC	Michael Terpin	EUR
15/02/2018	50000000	BTC	Network attack	JPY
04/03/2018	50000000	BTC	BTC Global check	JPY
12/04/2018	3000000	BTC	CoinSecure	GBP
20/09/2018	60000000	BTC	Zaif	AUD
21/12/2018	890000	BTC	Electrum Bitcoin wallets	AUD
27/12/2018	800000	BTC	Electroneum Wallet	AUD
26/01/2019	28000	BTC	LocalBitcoin	AUD
07/05/2019	41000000	BTC	Binance	JPY

*Note:* The table contain a list of nineteen of the largest Bitcoin hacking events between 2015 and 2019. All hacking events obtained mainly from the aggregation website [hackmageddon.com](http://hackmageddon.com) and Reuters

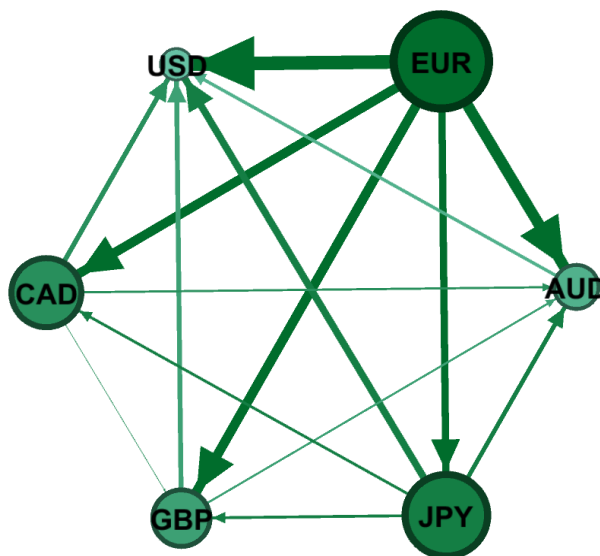
Figure 4.4 Directional-volatility connectedness network, 22/06/2015



*Note:* The Nodes are the bitcoin markets and the link between two nodes (edge) is given by net pairwise directional connectedness. The edge size shows the magnitude of the net contribution of bitcoin markets in terms of net pairwise directional connectedness.

Bitfinex platform lost around 120 000 BTC in a security breach on Aug 2, 2016, considered to be one of the largest hacks in Bitcoin history. The platform published a statement that a security breach had been detected and investigation begun to identify the problem and causes. In Figure 4.1 we can see a clear and high spike on the same date of a breach recording a very high total spillover of around 83%. Looking at the network Figure 4.5 on the same date provides us with the net dispenser and net receiver within the network. Interestingly, the BTC/EUR is contributing in each market with remarkable spillover from BTC/EUR to other markets, of which the thickest/largest arrow hits BTC/USD, and the thinnest/smallest arrow is received by BTC/JPY. While the BTC/USD is the net receiver, the network does not show any contribution from BTC/USD, but receives a modest contribution from BTC/CAD and BTC/JPY.

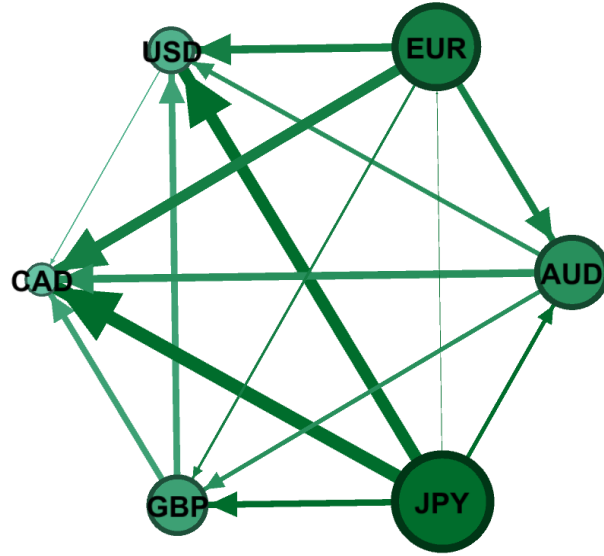
Figure 4.5 Directional-volatility connectedness network, 02/08/2016



*Note:* The Nodes are the bitcoin markets and the link between two nodes (edge) is given by net pairwise directional connectedness. The edge size shows the magnitude of the net contribution of bitcoin markets in terms of net pairwise directional connectedness.

On Dec 06, 2017 NiceHash platform woke up to a cyber attack which led to a loss of around 4700 BTC and caused a massive reduction to the BTC price in the following weeks. Figure 4.1 shows that in Dec, 2017 the total spillover index was around 61%; then the indicator started to accelerate upward very rapidly, to hit 83% after just a few days. From Figure 4.6 the dominant markets tend to be BTC/JPY, BTC/EUR and BTC/AUD respectively, which indicates that the three markets are transmitting volatility to the other markets in different magnitudes. By contrast, BTC/CAD market is the net receiver, in which the inflow volatility to the market is very different among the five channels, BTC/JPY being the largest, and BTC/USD the smallest. Both BTC/GBP and BTC/AUD act as a moderator by receiving and transmitting volatility between the other markets. Exploiting the opportunity to invest here is probable by taking advantage of being able to identify the direction of the volatility wave.

Figure 4.6 Directional-volatility connectedness network, 06/12/2017

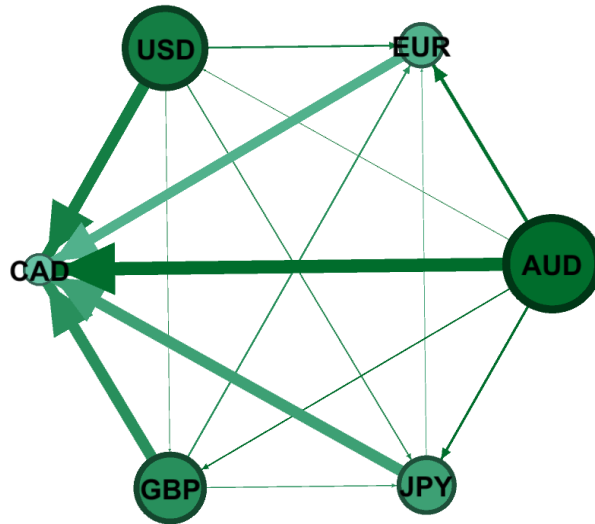


*Note:* The Nodes are the bitcoin markets and the link between two nodes (edge) is given by net pairwise directional connectedness. The edge size shows the magnitude of the net contribution of bitcoin markets in terms of net pairwise directional connectedness.

Around Sep 2018, Zaif platform noticed a large amount of outflow funds on the platform, and after a deep investigation they suspended the platform service until further notice, later announcing that some hijackers with unauthorised access had stolen 5966 BTC and other cryptocurrencies worth around \$60 million. Over the years, the Bitcoin network has become more profound and the total spillover index shown more persistence, of which the total spillover is as high as 80% most of the time. Luckily, the network analysis looked into the latter percentage to understand and identify the different markets and directions. Figure 4.7 shows that BTC/AUD and BTC/USD markets, respectively, are dominating the other markets. We can see from the Figure that all markets except BTC/CAD are transmitting risk to each other in small magnitude *thinarrow*. By contrast, BTC/CAD is the most vulnerable market within the system and interestingly receives a large amount of volatility from each market *thickarrow*.

The largest cyber security breach in 2019 hit Binance platform, one of the largest cryptocurrency exchanges, from which hackers managed to withdraw around 7000 BTC units in a single transaction. The platform admitted that on May 7, 2019, hijackers used various techniques such as phishing and viruses to access the secured private data in the platform's servers. The total spillover was floating around 80%, the BTC/JPY market being net dispenser. In Figure 4.8 the same behaviourin appears, where BTC/CAD market again received systematic large shocks from all the other markets compared with the others. On the contrary, BTC/JPY disrupted the volatility of the other markets in different magnitudes. However, BTC/USD and BTC/EUR received and transmitted the

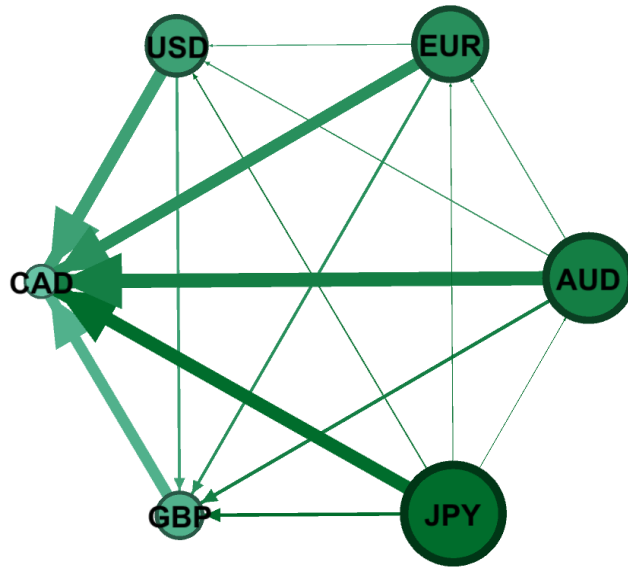
Figure 4.7 Directional-volatility connectedness network, 20/09/2018



*Note:* The Nodes are the bitcoin markets and the link between two nodes (edge) is given by net pairwise directional connectedness. The edge size shows the magnitude of the net contribution of bitcoin markets in terms of net pairwise directional connectedness.

risk interchangeably, and mostly in similar inward and outward channels, which enabled them to act as a bridge between the net dispenser and net receiver.

Figure 4.8 Directional-volatility connectedness network, 07/05/2019



*Note:* The Nodes are the bitcoin markets and the link between two nodes (edge) is given by net pairwise directional connectedness. The edge size shows the magnitude of the net contribution of bitcoin markets in terms of net pairwise directional connectedness.

#### 4.5.4 Robustness

How sensitive are our results to the choice of forecast horizon, window size and alternative measure of volatility? In this section, we undertake a robustness exercise in each aspect mentioned above.

We check the robustness of our full sample analysis results to the choice of the forecast horizon and the tuning of frequency bands that identify short- and long-run components of the forecast error GVD. Recall that our results are based on 30-days-ahead forecasts. We performed similar estimations with 60-, 90-, and 120-days-ahead forecasts. The ensuing results (reported in the Appendix C) corresponding to Tables C.1, C.2, and C.3 presented above produced very similar values for the estimated spillovers, and yielded qualitatively identical conclusions.

Next, Figures C.1 to C.8 plot dynamic overall volatility spillovers using 15, 30 and 60 days forecast horizon with 120-, 150- 180-rolling windows , respectively. We observe that the latter graphs are strongly consistent with Figure 4.3, not only in the estimated values of the total spillover index, but also in the shape of the evolution that records the same extreme events in every case.

##### 4.5.4.1 VAR model Stability

We carried out the same procedure as in the first chapter to clarify the extreme shocks and potential breaks in the VAR system. (Qu & Perron, 2007) break test could achieve our goals by detecting the structural breaks in the VAR process, hence identifying the sudden changes in the spillover index within the six markets.

Table 4.5 presents the results of (Qu & Perron, 2007)'s test. The VAR dataset consists of the six Bitcoin markets from January 2015 to May 2019. The trimming percentage is 15% of the sample span and the maximum breaks allowed individually for two and five respectively. The test statistics for both WD max and sequential tests exceed the critical values except for the fifth break (Seq test ( $m = 5$ )  $\sim (5 \mid 4)$ ). Thus, the null hypothesis of no structural breaks is rejected for the WD max and indicates four breaks (out of five breaks) based on the sequential test. The four break dates suggested by the test are as follows: 1- 30/08/2015. 2- 30/07/2016. 3- 27/05/2017. 4- 31/01/2018. The latter dates can be linked to significant events that impact the cryptocurrency market stability. As we discussed in the results section, several hacking events could break the cycle of persistency, and change time series' properties over time. These structural breaks could impact the VAR system and induce dynamic spillover analysis to generate significant spikes over time, see Figure 4.3.

To check the VAR stability, we extract the coefficients' residuals and test their stationarity to ensure the consistency of the mean and variance of residuals over time. Table 4.6

shows that the test rejects the null of unit root for all exchange rates. Further, Figures C.26 show the inverse roots of AR characteristic polynomial for volatility lie inside the unit circle, which indicates that the VAR process is stable.

## 4.6 Conclusions

The presence of cyber attacks could limit and create the volatility in Bitcoin cross-markets. However, variance decompositions as weighted, directed networks form a superior and effective approach to detect a shock within a system and identify the future direction of the volatility flow between markets. The objective of this chapter is to study the reaction of the major Bitcoin markets under a series of cyber attacks using the weighted, directed networks approach.

After performing the static and dynamic results, we built a number of networks from the latter analysis to show the impact of security breaches in Bitcoin cross-markets. Six major Bitcoin markets were considered, including BTC/USD, BTC/EUR, BTC/GBP, BTC/JPY, BTC/AUD and BTC/CAD. We focused on five major cyber attacks in each year from 2015 to 2019, the results showing that in June 2015, BTC/USD was the leading market, transmitting risk to other markets in different magnitudes. In 2016 and 2017, BTC/EUR and BTC/JPY were the dominant markets, and those most connected to the system. However, in the following year, BTC/AUD and BTC/USD made a significant contribution to affect the Canadian market. Further, in 2019 the BTC/CAD market became the absorber within the system, to receive major shock from the other five markets.

This chapter offers many important implications for investors and policy makers. First, dynamic and static volatility spillover could provide a clear perception on the most affected market in the context of cyber attacks. Thus investors may be able to capture speculative profits or draw a systematic investment strategy to beat the market. Indeed, market timing is very important to build such a strategy, and network analysis is a useful tool to determine the best next move. Second, policy regulators could introduce some controlling strategy such as circuit breakers to prevent some speculators taking advantage when the market suddenly crashes or jumps, which may leave a long impact on the market.

Hedging activities can also be managed and identified between Bitcoin cross-markets. For future research, we would extend our investigation by employing dynamic network analysis to study the Bitcoin market in depth.

**Table 4.5 Multivariate Qu and Perron Test for Structural Changes in VAR model**

Tests		Test statistic	Critical Value
WD max test	m=2	874.7	23.748
	m=5	892.3	25.81
Seq test (m = 2)	(2   1)	692.9	24.63
Seq test (m = 5)	(2   1)	692.9	24.63
	(3   2)	335.4	25.59
	(4   3)	609.1	26.23
	(5   4)	0.121	26.75

*Note:* Exchange rates volatility are used to find the structural breaks. Trimming Percentage is 15% and the number of observations is 1612. The first test is the WD max test and the second one is the sequential test. All the critical values represent the 5% significance level.

**Table 4.6 ADF Test for the VAR Coefficients' Residuals**

Residuals	Test	Test stat	Critical Value 1%	Conclusion
BTC/USD	ADF	-29.88	-3.43	Reject
BTC/EUR	ADF	-12.13	-3.43	Reject
BTC/GBP	ADF	-12.71	-3.43	Reject
BTC/JPY	ADF	-9.056	-3.43	Reject
BTC/AUD	ADF	-42.02	-3.43	Reject
BTC/CAD	ADF	-43.16	-3.43	Reject



## Chapter 5

# Conclusions

## 5.1 Conclusion and Policy Implications

In conclusion, to insure a successful and coherent investment strategy we should insure its sustainability, security and validity in global markets based on three important cornerstones in Bitcoin (internal, external and security factors). The thesis studies in depth the exogenous determinants (Chapter 1), endogenous determinants (chapter 2), cyber security determinants (chapter 3) and their impact on the volatility of Bitcoin prices. The main and core objective of this thesis is to understand the dynamic linkage between Bitcoin markets and see how the above different factors can majorly contribute to the price fluctuations over the time . A major outcome that trading on Bitcoin markets depends largely on investor sentiment, and a lack of confidence eventually heightens volatility on these markets which become more intensely interlinked as investors diversify to mitigate risks pertaining to a particular market.

chapter two examine the return and volatility spillover effects across Bitcoin markets and under episodes of external shocks. Also, We have investigated how spillover effects are governed by uncertainty episodes. The chapter discuss important insights on the dynamic interdependence of spillover effects during high/low uncertainty episodes and capturing the *sentimental value* of Bitcoin prices. The chapter also complemented to a sparse body of literature and have envisaged the importance of studying a systematic pattern of shocks' movement by capturing a 'system dynamics'. Using the latter measure of volatility and well-established dynamic spillover methods, we have found that Bitcoin-USD holds high predictive power and Bitcoin-Euro acts as the net receiver. Also, higher uncertainty is found to accelerate spillover effects with larger impacts across markets.

Chapter three investigate the persistence of fractional integration and potential break points simultaneously and endogenously using MS-ARFIMA model for Bitcoin cross-markets. We found that financial and economic events are generated by agents who handle them, which could generate persistent endogenous responses. Therefore, a spurious long memory in volatility could be attributed to the presence of structural breaks rather than true long memory. We found the presence of both long memory and structural breaks along the different Bitcoin markets. The key issue here is to distinguish between the long memory and structural breaks as both phenomenon share the same properties and investors could confuse between them very easily. Consequently, we applied the Markov switching ARFIMA model to move between the different regimes endogenously. We find that the fractional integration display true long-memory for all the MS-ARFIMA models.

Chapter four study the reaction of the major Bitcoin markets under series of cyberattacks using the weighted, directed networks approach. We found that cyberattacks have a major impact on the Bitcoin network infrastructure, and the sustainability of the market. After performing the static and dynamic results, we build a number of networks from the latter analysis and show the impact of security breaches in Bitcoin cross-markets as asymmetric network. We identify the directions of volatility spillover effects across

Bitcoin markets and show the reaction of a dynamic system with respect to the graphing theory.

Thus, very valuable and fruitful policy implications are provided to decision makers, investors and speculators. we have created a first-hand information set for cryptocurrency investors to predict the next best investment strategy. The investors will be able to exploit information on the predictive power of each market, such as the net receiver and net giver of volatility. Studying the long memory could enable investors to capture speculative profits by controlling market timing. Policy makers and regulators could introduce circuit breakers to stop trading in Bitcoin cross-markets when the market switches abruptly to high-volatility regime as the impact of a negative down turn would take a relatively long period of time to dissipate given the nature of persistence in the price behaviour of Bitcoin in the cross-markets. Training to the security of network, investors can decide how to diversify and tap on arbitrage during cyber security attacks. Decision makers can synchronise the cyber threats with volatility spillover to detect the flow of risk within the markets.

## 5.2 Future Research Directions

The thesis has studied and investigated the cross-market dynamic of Bitcoin prices through different empirical tests. The latter measurements and investigations could be extended further to provide more in-depth understanding of Bitcoin markets and volatility behaviours.

First, instead of measuring the volatility spillover index for five Bitcoin markets, future research could investigate the spillover effects among sets of variables in each market within a unified framework, such as Panel VAR (Koop & Korobilis, 2016). The latter model allows us to investigate the spillover of a particular shock across different Bitcoin markets, as well as the interactive relationship among several variables under each market. Further, the number of markets could be extended, especially in the Pacific-Asian area to provide a comprehensive study across the major markets in the world.

Second, the third chapter assesses and identifies the long memory and structural breaks simultaneously and endogenously using MS-ARFIMA model. Forecasting the volatility persistence through the aforementioned model in each market could help us to identify true long-range dependence in the future in order to build coherent investment strategies. Moreover, investigating the memory within fractional co-integration VAR system (Johansen & Nielsen, 2012) rather than uni-variate model provides fruitful information about the co-integrating relationship between Bitcoin markets, and could find the long-run equilibrium in the system.

Thirdly, the fourth chapter attempts to design weighted, directed networks to study the volatility of Bitcoin markets under episodes of cyber attack. However, extending this research by designing dynamic networks (DNA) allows us to investigate further the networks' behaviour and social interactions. Moreover, analysing dynamic networks could help us to assess the stability of a network.

Finally, as Bitcoin prices are fundamentally driven by the feeling and memory of investors, finding a complex method such as Machine Learning or Artificial Intelligence is required to understand the human cognitive and complex behavioural interactions across Bitcoin markets.

## Appendix A

# Supplement to Chapter 2

### (A) Stationarity tests

Table A.1 ADF and Phillips-Perron unit root tests, exchange rate returns

Exchange rate	Model without constant				Model with constant		
	Test	Test stat	Critical value 1%	Conclusion	Test stat	Critical value 1%	Conclusion
BTC/USD	<i>ADF</i>	-36.866	-2.58	Rejected	-37	-3.43	Rejected
	<i>pperron</i>	-36.97			-37.05		
BTC/AUD	<i>ADF</i>	-70.413	-2.58	Rejected	-70.42	-3.43	Rejected
	<i>pperron</i>	-96.582			-97.128		
BTC/CAD	<i>ADF</i>	-67.489	-2.58	Rejected	-67.487	-3.43	Rejected
	<i>pperron</i>	-95.544			-95.856		
BTC/EUR	<i>ADF</i>	-40.037	-2.58	Rejected	-40.153	-3.43	Rejected
	<i>pperron</i>	-40.106			-40.197		
BTC/GBP	<i>ADF</i>	-62.83	-2.58	Rejected	-62.833	-3.43	Rejected
	<i>pperron</i>	-83.162			-83.449		
Model with trend							
Exchange rate	Test	Test stat	Critical value 1%	Conclusion			
BTC/USD	<i>ADF</i>	-36.992	-3.96	Rejected			
	<i>pperron</i>	-37.048					
BTC/AUD	<i>ADF</i>	-70.405	-3.96	Rejected			
	<i>pperron</i>	-97.103					
BTC/CAD	<i>ADF</i>	-67.468	-3.96	Rejected			
	<i>pperron</i>	-95.822					
BTC/EUR	<i>ADF</i>	-40.143	-3.96	Rejected			
	<i>pperron</i>	-40.187					
BTC/GBP	<i>ADF</i>	-62.816	-3.96	Rejected			
	<i>pperron</i>	-83.424					

Table A.2 ADF and Phillips-Perron unit root tests, exchange rate volatility

Exchange rate	Model without constant				Model with constant		
	Test	Test stat	Critical value 1%	Conclusion	Test stat	Critical value 1%	Conclusion
BTC/USD	<i>ADF</i>	-18.461			-23.646		
	<i>pperron</i>	-19.199	-2.58	Rejected	-25.209	-3.43	Rejected
BTC/AUD	<i>ADF</i>	-7.695			-13.456		
	<i>pperron</i>	-5.083	-2.58	Rejected	-12.341	-3.43	Rejected
BTC/CAD	<i>ADF</i>	-8.332			-16.105		
	<i>pperron</i>	-5.78	-2.58	Rejected	-16.155	-3.43	Rejected
BTC/EUR	<i>ADF</i>	-14.42			-19.368		
	<i>pperron</i>	-13.88	-2.58	Rejected	-20.316	-3.43	Rejected
BTC/GBP	<i>ADF</i>	-14.192			-28.885		
	<i>pperron</i>	-13.42	-2.58	Rejected	-32.279	-3.43	Rejected
Model with trend							
Exchange rate	Test	Test stat	Critical value 1%	Conclusion	Test stat	Critical value 1%	Conclusion
BTC/USD	<i>ADF</i>	-23.737			-23.646		
	<i>pperron</i>	-25.302	-3.96	Rejected	-	-2.328	Rejected
BTC/AUD	<i>ADF</i>	-19.534			-13.456		
	<i>pperron</i>	-21.096	-3.96	Rejected	-	-2.328	Rejected
BTC/CAD	<i>ADF</i>	-26.65			-16.105		
	<i>pperron</i>	-29.721	-3.96	Rejected	-	-2.328	Rejected
BTC/EUR	<i>ADF</i>	-19.676			-19.368		
	<i>pperron</i>	-20.692	-3.96	Rejected	-	-2.328	Rejected
BTC/GBP	<i>ADF</i>	-33.257			-28.885		
	<i>pperron</i>	-35.645	-3.96	Rejected	-	-2.328	Rejected

## (B) Robustness check

### Returns spillover tables with various forecast horizons

Table A.3 Returns spillovers across five selected exchange rates – 7-day ahead forecast

	BTC/USD	BTC/AUD	BTC/CAD	BTC/EUR	BTC/GBP	Directional FROM others
BTC/USD	86.08	1.69	0.63	9.41	2.19	13.92
BTC/AUD	1.80	87.67	1.39	5.51	3.63	12.33
BTC/CAD	1.12	1.25	94.67	1.83	1.13	5.33
BTC/EUR	10.08	6.59	2.57	73.15	7.62	26.85
BTC/GBP	2.14	3.02	1.42	6.60	86.82	13.18
Directional TO others	15.13	12.56	6.00	23.35	14.57	<i>TSI:</i> $71.61/500 =$
Net spillovers	1.21	0.23	0.67	-3.50	1.39	$14.32\%$

Note: Exchange rates returns spillovers following Diebold and Yilmaz (2012) using a 7-day ahead forecast horizon. Numbers are percentages. “TSI” stands for Total Spillover Index.

Table A.4 Returns spillovers across five selected exchange rates – 10-day ahead forecast

	BTC/USD	BTC/AUD	BTC/CAD	BTC/EUR	BTC/GBP	Directional FROM others
BTC/USD	84.85	1.95	1.33	9.44	2.43	15.15
BTC/AUD	1.80	87.16	1.79	5.50	3.75	12.84
BTC/CAD	1.21	1.37	94.22	1.87	1.33	5.78
BTC/EUR	10.45	6.57	2.65	72.60	7.72	27.40
BTC/GBP	2.22	3.25	1.48	6.61	86.43	13.57
Directional TO others	15.67	13.14	7.26	23.42	15.23	<i>TSI:</i> $74.73/500 =$
Net spillovers	0.52	0.30	1.48	-3.97	1.67	$14.95\%$

Note: Exchange rates returns spillovers following Diebold and Yilmaz (2012) using a 10-day ahead forecast horizon. Numbers are percentages. “TSI” stands for Total Spillover Index.

**Table A.5 Returns spillovers across five selected exchange rates – 60-day ahead forecast**

	BTC/USD	BTC/AUD	BTC/CAD	BTC/EUR	BTC/GBP	Directional FROM others
BTC/USD	83.56	2.37	1.70	9.60	2.78	16.44
BTC/AUD	3.19	83.91	2.83	5.73	4.34	16.09
BTC/CAD	1.82	1.88	92.51	2.15	1.64	7.49
BTC/EUR	14.29	6.51	2.90	68.84	7.46	31.16
BTC/GBP	3.75	3.51	2.12	6.72	83.90	16.10
Directional TO others	23.05	14.26	9.55	24.20	16.22	<i>TSI:</i> $87.28/500 =$
Net spillovers	6.61	-1.83	2.06	-6.96	0.12	$17.46\%$

*Note:* Exchange rates returns spillovers following Diebold and Yilmaz (2012) using a 60-day ahead forecast horizon. Numbers are percentages. “TSI” stands for Total Spillover Index.

### Volatility spillover tables with various forecast horizons

Table A.6 Volatility spillovers across five selected exchange rates – 7-day ahead forecast

	BTC/USD	BTC/AUD	BTC/CAD	BTC/EUR	BTC/GBP	Directional FROM others
BTC/USD	82.99	1.81	0.21	14.49	0.49	17.01
BTC/AUD	2.92	89.54	2.37	4.90	0.27	10.46
BTC/CAD	0.16	3.77	94.09	1.42	0.55	5.91
BTC/EUR	19.22	2.43	0.32	77.48	0.56	22.52
BTC/GBP	0.55	0.55	0.70	0.95	97.25	2.75
Directional TO others	22.86	8.56	3.60	21.76	1.87	<i>TSI:</i> $58.65/500 =$
Net spillovers	5.85	-1.89	-2.31	-0.76	-0.89	<i>11.73%</i>

Note: Exchange rates volatility spillovers following Diebold and Yilmaz (2012) using a 7-day ahead forecast horizon. Numbers are percentages. “TSI” stands for Total Spillover Index.

Table A.7 Volatility spillovers across five selected exchange rates – 10-day ahead forecast

	BTC/USD	BTC/AUD	BTC/CAD	BTC/EUR	BTC/GBP	Directional FROM others
BTC/USD	81.69	2.36	0.27	15.01	0.67	18.31
BTC/AUD	3.31	88.11	2.74	5.47	0.37	11.89
BTC/CAD	0.17	4.57	92.99	1.54	0.74	7.01
BTC/EUR	20.00	2.86	0.42	75.85	0.87	24.15
BTC/GBP	0.57	0.66	0.92	0.94	96.90	3.10
Directional TO others	24.04	10.44	4.36	22.96	2.65	<i>TSI:</i> $64.45/500 =$
Net spillovers	5.73	-1.44	-2.65	-1.18	-0.45	<i>12.89%</i>

Note: Exchange rates volatility spillovers following Diebold and Yilmaz (2012) using a 10-day ahead forecast horizon. Numbers are percentages. “TSI” stands for Total Spillover Index.

Table A.8 Volatility spillovers across five selected exchange rates – 60-day ahead forecast

	BTC/USD	BTC/AUD	BTC/CAD	BTC/EUR	BTC/GBP	Directional FROM others
BTC/USD	78.23	4.97	0.57	15.27	0.96	21.77
BTC/AUD	4.52	83.09	4.43	6.98	0.98	16.91
BTC/CAD	0.37	7.56	88.81	1.93	1.33	11.19
BTC/EUR	20.55	5.69	1.07	71.17	1.52	28.83
BTC/GBP	0.65	1.68	1.72	1.01	94.94	5.06
Directional TO others	26.10	19.91	7.79	25.18	4.78	<i>TSI:</i> $83.76/500 =$
Net spillovers	4.33	3.00	-3.40	-3.65	-0.28	$16.75\%$

*Note:* Exchange rates volatility spillovers following Diebold and Yilmaz (2012) using a 60-day ahead forecast horizon. Numbers are percentages. “TSI” stands for Total Spillover Index.

**Returns spillover tables – Frequency domain analysis with various forecast horizons and frequency bands**

**Table A.9 Returns spillovers across five selected exchange rates – Frequency domain analysis with 4-day frequency band and 7-day ahead forecast**

(a) *Short horizon*

	BTC/USD	BTC/AUD	BTC/CAD	BTC/EUR	BTC/GBP	FROM others
BTC/USD	74.66	1.20	0.62	6.91	1.72	10.46
BTC/AUD	0.75	87.03	1.34	4.50	2.86	9.45
BTC/CAD	0.85	1.07	94.48	1.52	0.98	4.42
BTC/EUR	6.51	5.58	2.39	64.54	6.11	20.59
BTC/GBP	1.23	2.61	1.25	5.18	85.64	10.27
TO others	9.34	10.46	5.60	18.10	11.67	<i>TSI: 55.18/461.53 = 11.96%</i>

(b) *Long horizon*

	BTC/USD	BTC/AUD	BTC/CAD	BTC/EUR	BTC/GBP	FROM others
BTC/USD	11.42	0.49	0.01	2.51	0.46	3.46
BTC/AUD	1.05	0.64	0.05	1.01	0.78	2.88
BTC/CAD	0.27	0.18	0.19	0.32	0.15	0.91
BTC/EUR	3.57	1.01	0.18	8.60	1.50	6.26
BTC/GBP	0.90	0.42	0.17	1.42	1.18	2.91
TO others	5.79	2.09	0.40	5.25	2.89	<i>TSI: 16.42/38.47 = 42.69%</i>

*Note:* Returns spillovers, frequency domain analysis following Baruník and Křehlík (2018) using 7-day ahead forecast horizon. Numbers are percentages. ‘Within’ refers to *within system* spillovers. *Short* and *Long* horizons refer to ‘4 days or less’ and ‘more than 4 days’, respectively.

**Table A.10 Returns spillovers across five selected exchange rates – Frequency domain analysis with 16-day frequency band and 7-day ahead forecast**

(a) *Short horizon*

	BTC/USD	BTC/AUD	BTC/CAD	BTC/EUR	BTC/GBP	FROM others
BTC/USD	74.66	1.20	0.62	6.91	1.72	10.46
BTC/AUD	0.75	87.03	1.34	4.50	2.86	9.45
BTC/CAD	0.85	1.07	94.48	1.52	0.98	4.42
BTC/EUR	6.51	5.58	2.39	64.54	6.11	20.59
BTC/GBP	1.23	2.61	1.25	5.18	85.64	10.27
TO others	9.34	10.46	5.60	18.10	11.67	<i>TSI: 55.18/461.53 = 11.96%</i>

(b) *Long horizon*

	BTC/USD	BTC/AUD	BTC/CAD	BTC/EUR	BTC/GBP	FROM others
BTC/USD	11.42	0.49	0.01	2.51	0.46	3.46
BTC/AUD	1.05	0.64	0.05	1.01	0.78	2.88
BTC/CAD	0.27	0.18	0.19	0.32	0.15	0.91
BTC/EUR	3.57	1.01	0.18	8.60	1.50	6.26
BTC/GBP	0.90	0.42	0.17	1.42	1.18	2.91
TO others	5.79	2.09	0.40	5.25	2.89	<i>TSI: 16.42/38.47 = 42.69%</i>

*Note:* Returns spillovers, frequency domain analysis following Baruník and Křehlík (2018) using 7-day ahead forecast horizon. Numbers are percentages. ‘Within’ refers to *within system* spillovers. *Short* and *Long* horizons refer to ‘16 days or less’ and ‘more than 16 days’, respectively.

**Table A.11 Returns spillovers across five selected exchange rates – Frequency domain analysis with 30-day frequency band and 7-day ahead forecast**

(a) *Short horizon*

	BTC/USD	BTC/AUD	BTC/CAD	BTC/EUR	BTC/GBP	FROM others
BTC/USD	74.66	1.20	0.62	6.91	1.72	10.46
BTC/AUD	0.75	87.03	1.34	4.50	2.86	9.45
BTC/CAD	0.85	1.07	94.48	1.52	0.98	4.42
BTC/EUR	6.51	5.58	2.39	64.54	6.11	20.59
BTC/GBP	1.23	2.61	1.25	5.18	85.64	10.27
TO others	9.34	10.46	5.60	18.10	11.67	<i>TSI: 55.18/461.53 = 11.96%</i>

(b) *Long horizon*

	BTC/USD	BTC/AUD	BTC/CAD	BTC/EUR	BTC/GBP	FROM others
BTC/USD	11.42	0.49	0.01	2.51	0.46	3.46
BTC/AUD	1.05	0.64	0.05	1.01	0.78	2.88
BTC/CAD	0.27	0.18	0.19	0.32	0.15	0.91
BTC/EUR	3.57	1.01	0.18	8.60	1.50	6.26
BTC/GBP	0.90	0.42	0.17	1.42	1.18	2.91
TO others	5.79	2.09	0.40	5.25	2.89	<i>TSI: 16.42/38.47 = 42.69%</i>

*Note:* Returns spillovers, frequency domain analysis following Baruník and Křehlík (2018) using 7-day ahead forecast horizon. Numbers are percentages. ‘Within’ refers to *within system* spillovers. *Short* and *Long* horizons refer to ‘30 days or less’ and ‘more than 30 days’, respectively.

**Table A.12 Returns spillovers across five selected exchange rates – Frequency domain analysis with 4-day frequency band and 10-day ahead forecast**

(a) *Short horizon*

	BTC/USD	BTC/AUD	BTC/CAD	BTC/EUR	BTC/GBP	FROM others
BTC/USD	62.05	1.36	0.63	5.36	1.09	8.43
BTC/AUD	0.69	82.38	1.43	3.65	3.10	8.88
BTC/CAD	0.95	0.97	91.18	1.29	1.10	4.31
BTC/EUR	4.43	4.82	2.25	55.17	5.38	16.88
BTC/GBP	0.59	2.14	1.03	4.22	82.50	7.98
TO others	6.66	9.29	5.34	14.51	10.67	<i>TSI: 46.48/419.75 = 11.07%</i>

(b) *Long horizon*

	BTC/USD	BTC/AUD	BTC/CAD	BTC/EUR	BTC/GBP	FROM others
BTC/USD	22.81	0.60	0.70	4.08	1.33	6.72
BTC/AUD	1.11	4.78	0.36	1.85	0.65	3.96
BTC/CAD	0.25	0.40	3.04	0.58	0.23	1.46
BTC/EUR	6.01	1.75	0.40	17.43	2.35	10.51
BTC/GBP	1.63	1.11	0.45	2.40	3.94	5.59
TO others	9.01	3.85	1.92	8.91	4.56	<i>TSI: 28.25/80.25 = 35.20%</i>

*Note:* Returns spillovers, frequency domain analysis following Baruník and Křehlík (2018) using 10-day ahead forecast horizon. Numbers are percentages. ‘Within’ refers to *within system* spillovers. *Short* and *Long* horizons refer to ‘4 days or less’ and ‘more than 4 days’, respectively.

**Table A.13 Returns spillovers across five selected exchange rates – Frequency domain analysis with 16-day frequency band and 10-day ahead forecast**

(a) *Short horizon*

	BTC/USD	BTC/AUD	BTC/CAD	BTC/EUR	BTC/GBP	FROM others
BTC/USD	76.35	1.83	1.26	7.98	1.90	12.97
BTC/AUD	1.14	86.30	1.65	4.55	3.39	10.73
BTC/CAD	1.02	1.19	94.08	1.65	1.26	5.13
BTC/EUR	7.78	5.82	2.52	66.43	6.38	22.50
BTC/GBP	1.41	2.86	1.39	5.55	85.60	11.21
TO others	11.35	11.71	6.83	19.74	12.92	<i>TSI: 62.55/471.31 = 13.27%</i>

(b) *Long horizon*

	BTC/USD	BTC/AUD	BTC/CAD	BTC/EUR	BTC/GBP	FROM others
BTC/USD	8.50	0.13	0.06	1.46	0.52	2.18
BTC/AUD	0.67	0.86	0.14	0.94	0.36	2.11
BTC/CAD	0.19	0.17	0.14	0.22	0.07	0.65
BTC/EUR	2.66	0.75	0.13	6.17	1.35	4.89
BTC/GBP	0.81	0.39	0.09	1.06	0.84	2.35
TO others	4.32	1.43	0.43	3.68	2.31	<i>TSI: 12.18/28.69 = 42.44%</i>

*Note:* Returns spillovers, frequency domain analysis following Baruník and Křehlík (2018) using 10-day ahead forecast horizon. Numbers are percentages. ‘Within’ refers to *within system* spillovers. *Short* and *Long* horizons refer to ‘16 days or less’ and ‘more than 16 days’, respectively.

Table A.14 Returns spillovers across five selected exchange rates – Frequency domain analysis with 30-day frequency band and 10-day ahead forecast

(a) *Short horizon*

	BTC/USD	BTC/AUD	BTC/CAD	BTC/EUR	BTC/GBP	FROM others
BTC/USD	76.35	1.83	1.26	7.98	1.90	12.97
BTC/AUD	1.14	86.30	1.65	4.55	3.39	10.73
BTC/CAD	1.02	1.19	94.08	1.65	1.26	5.13
BTC/EUR	7.78	5.82	2.52	66.43	6.38	22.50
BTC/GBP	1.41	2.86	1.39	5.55	85.60	11.21
TO others	11.35	11.71	6.83	19.74	12.92	<i>TSI: 62.55/471.31 = 13.27%</i>

(b) *Long horizon*

	BTC/USD	BTC/AUD	BTC/CAD	BTC/EUR	BTC/GBP	FROM others
BTC/USD	8.50	0.13	0.06	1.46	0.52	2.18
BTC/AUD	0.67	0.86	0.14	0.94	0.36	2.11
BTC/CAD	0.19	0.17	0.14	0.22	0.07	0.65
BTC/EUR	2.66	0.75	0.13	6.17	1.35	4.89
BTC/GBP	0.81	0.39	0.09	1.06	0.84	2.35
TO others	4.32	1.43	0.43	3.68	2.31	<i>TSI: 12.18/28.69 = 42.44%</i>

*Note:* Returns spillovers, frequency domain analysis following Baruník and Křehlík (2018) using 10-day ahead forecast horizon. Numbers are percentages. ‘Within’ refers to *within system* spillovers. *Short* and *Long* horizons refer to ‘30 days or less’ and ‘more than 30 days’, respectively.

**Table A.15 Returns spillovers across five selected exchange rates – Frequency domain analysis with 4-day frequency band and 30-day ahead forecast (baseline estimates)**

(a) *Short horizon*

	BTC/USD	BTC/AUD	BTC/CAD	BTC/EUR	BTC/GBP	FROM others
BTC/USD	64.96	1.52	1.35	5.78	1.89	10.54
BTC/AUD	2.07	81.66	2.66	4.29	3.64	12.66
BTC/CAD	1.50	1.59	90.51	1.50	1.39	5.98
BTC/EUR	9.15	4.96	2.51	53.60	5.73	22.35
BTC/GBP	2.40	2.77	1.75	4.68	81.17	11.59
TO others	15.12	10.83	8.26	16.25	12.65	<i>TSI: 63.11/435.01 = 14.51%</i>

(b) *Long horizon*

	BTC/USD	BTC/AUD	BTC/CAD	BTC/EUR	BTC/GBP	FROM others
BTC/USD	18.62	0.84	0.34	3.82	0.88	5.89
BTC/AUD	1.10	2.31	0.16	1.43	0.68	3.38
BTC/CAD	0.32	0.28	2.03	0.65	0.24	1.48
BTC/EUR	5.11	1.53	0.38	15.32	1.71	8.73
BTC/GBP	1.33	0.74	0.35	2.04	2.78	4.46
TO others	7.86	3.39	1.24	7.94	3.51	<i>TSI: 23.94/64.99 = 36.83%</i>

*Note:* Returns spillovers, frequency domain analysis following Baruník and Křehlík (2018) using 30-day ahead forecast horizon. Numbers are percentages. ‘Within’ refers to *within system* spillovers. *Short* and *Long* horizons refer to ‘4 days or less’ and ‘more than 4 days’, respectively.

Table A.16 Returns spillovers across five selected exchange rates – Frequency domain analysis with 16-day frequency band and 30-day ahead forecast

(a) *Short horizon*

	BTC/USD	BTC/AUD	BTC/CAD	BTC/EUR	BTC/GBP	FROM others
BTC/USD	79.62	2.28	1.67	8.78	2.50	15.24
BTC/AUD	2.72	83.78	2.79	5.38	4.14	15.03
BTC/CAD	1.67	1.83	92.47	2.03	1.58	7.11
BTC/EUR	12.44	6.27	2.83	66.69	6.94	28.49
BTC/GBP	3.20	3.40	2.06	6.27	83.61	14.93
TO others	20.04	13.78	9.36	22.46	15.17	<i>TSI: 80.81/486.98 = 16.59%</i>

(b) *Long horizon*

	BTC/USD	BTC/AUD	BTC/CAD	BTC/EUR	BTC/GBP	FROM others
BTC/USD	3.96	0.08	0.02	0.82	0.27	1.19
BTC/AUD	0.45	0.19	0.03	0.35	0.18	1.00
BTC/CAD	0.15	0.04	0.07	0.12	0.05	0.35
BTC/EUR	1.82	0.22	0.06	2.22	0.50	2.60
BTC/GBP	0.53	0.10	0.03	0.44	0.35	1.11
TO others	2.94	0.44	0.13	1.73	1.00	<i>TSI: 6.24/13.02 = 47.93%</i>

*Note:* Returns spillovers, frequency domain analysis following Baruník and Křehlík (2018) using 30-day ahead forecast horizon. Numbers are percentages. ‘Within’ refers to *within system* spillovers. *Short* and *Long* horizons refer to ‘16 days or less’ and ‘more than 16 days’, respectively.

**Table A.17 Returns spillovers across five selected exchange rates – Frequency domain analysis with 30-day frequency band and 30-day ahead forecast**

(a) *Short horizon*

	BTC/USD	BTC/AUD	BTC/CAD	BTC/EUR	BTC/GBP	FROM others
BTC/USD	79.62	2.28	1.67	8.78	2.50	15.24
BTC/AUD	2.72	83.78	2.79	5.38	4.14	15.03
BTC/CAD	1.67	1.83	92.47	2.03	1.58	7.11
BTC/EUR	12.44	6.27	2.83	66.69	6.94	28.49
BTC/GBP	3.20	3.40	2.06	6.27	83.61	14.93
TO others	20.04	13.78	9.36	22.46	15.17	<i>TSI: 80.81/486.98 = 16.59%</i>

(b) *Long horizon*

	BTC/USD	BTC/AUD	BTC/CAD	BTC/EUR	BTC/GBP	FROM others
BTC/USD	3.96	0.08	0.02	0.82	0.27	1.19
BTC/AUD	0.45	0.19	0.03	0.35	0.18	1.00
BTC/CAD	0.15	0.04	0.07	0.12	0.05	0.35
BTC/EUR	1.82	0.22	0.06	2.22	0.50	2.60
BTC/GBP	0.53	0.10	0.03	0.44	0.35	1.11
TO others	2.94	0.44	0.13	1.73	1.00	<i>TSI: 6.24/13.02 = 47.93%</i>

*Note:* Returns spillovers, frequency domain analysis following Baruník and Křehlík (2018) using 30-day ahead forecast horizon. Numbers are percentages. ‘Within’ refers to *within system* spillovers. *Short* and *Long* horizons refer to ‘30 days or less’ and ‘more than 30 days’, respectively.

Table A.18 Returns spillovers across five selected exchange rates – Frequency domain analysis with 4-day frequency band and 60-day ahead forecast

(a) *Short horizon*

	BTC/USD	BTC/AUD	BTC/CAD	BTC/EUR	BTC/GBP	FROM others
BTC/USD	63.65	1.50	1.32	5.64	1.83	10.30
BTC/AUD	1.99	81.09	2.66	4.21	3.64	12.50
BTC/CAD	1.42	1.56	90.08	1.48	1.39	5.85
BTC/EUR	8.50	4.88	2.52	53.09	5.67	21.57
BTC/GBP	2.28	2.63	1.74	4.62	80.67	11.26
TO others	14.18	10.57	8.24	15.95	12.53	<i>TSI: 61.48/430.06 = 14.30%</i>

(b) *Long horizon*

	BTC/USD	BTC/AUD	BTC/CAD	BTC/EUR	BTC/GBP	FROM others
BTC/USD	19.91	0.87	0.37	3.96	0.94	6.14
BTC/AUD	1.20	2.82	0.18	1.52	0.70	3.59
BTC/CAD	0.41	0.32	2.43	0.67	0.25	1.64
BTC/EUR	5.79	1.62	0.38	15.76	1.79	9.58
BTC/GBP	1.47	0.88	0.38	2.10	3.23	4.83
TO others	8.87	3.69	1.31	8.24	3.68	<i>TSI: 25.79/69.94 = 36.88%</i>

*Note:* Returns spillovers, frequency domain analysis following Baruník and Křehlík (2018) using 60-day ahead forecast horizon. Numbers are percentages. ‘Within’ refers to *within system* spillovers. *Short* and *Long* horizons refer to ‘4 days or less’ and ‘more than 4 days’, respectively.

**Table A.19 Returns spillovers across five selected exchange rates – Frequency domain analysis with 16-day frequency band and 60-day ahead forecast**

(a) *Short horizon*

	BTC/USD	BTC/AUD	BTC/CAD	BTC/EUR	BTC/GBP	FROM others
BTC/USD	78.77	2.26	1.68	8.63	2.48	15.06
BTC/AUD	2.69	83.62	2.80	5.29	4.11	14.89
BTC/CAD	1.67	1.82	92.42	2.01	1.58	7.09
BTC/EUR	12.28	6.14	2.84	65.91	6.84	28.10
BTC/GBP	3.19	3.34	2.07	6.17	83.45	14.77
TO others	19.84	13.57	9.39	22.10	15.02	<i>TSI: 79.91/484.08 = 16.51%</i>

(b) *Long horizon*

	BTC/USD	BTC/AUD	BTC/CAD	BTC/EUR	BTC/GBP	FROM others
BTC/USD	4.79	0.11	0.02	0.97	0.30	1.39
BTC/AUD	0.50	0.29	0.03	0.44	0.22	1.20
BTC/CAD	0.15	0.05	0.10	0.14	0.06	0.40
BTC/EUR	2.00	0.36	0.06	2.93	0.63	3.06
BTC/GBP	0.56	0.17	0.05	0.55	0.45	1.33
TO others	3.21	0.69	0.16	2.10	1.20	<i>TSI: 7.37/15.92 = 46.28%</i>

*Note:* Returns spillovers, frequency domain analysis following Baruník and Křehlík (2018) using 60-day ahead forecast horizon. Numbers are percentages. ‘Within’ refers to *within system* spillovers. *Short* and *Long* horizons refer to ‘16 days or less’ and ‘more than 16 days’, respectively.

Table A.20 Returns spillovers across five selected exchange rates – Frequency domain analysis with 30-day frequency band and 60-day ahead forecast

(a) *Short horizon*

	BTC/USD	BTC/AUD	BTC/CAD	BTC/EUR	BTC/GBP	FROM others
BTC/USD	81.43	2.32	1.69	9.16	2.64	15.80
BTC/AUD	2.94	83.81	2.82	5.54	4.24	15.54
BTC/CAD	1.75	1.86	92.48	2.09	1.61	7.31
BTC/EUR	13.27	6.37	2.87	67.70	7.20	29.72
BTC/GBP	3.46	3.45	2.10	6.49	83.72	15.50
TO others	21.42	14.00	9.49	23.27	15.69	<i>TSI: 83.88/493.01 = 17.01%</i>

(b) *Long horizon*

	BTC/USD	BTC/AUD	BTC/CAD	BTC/EUR	BTC/GBP	FROM others
BTC/USD	2.13	0.05	0.01	0.44	0.14	0.64
BTC/AUD	0.25	0.10	0.01	0.19	0.09	0.55
BTC/CAD	0.08	0.02	0.03	0.06	0.03	0.18
BTC/EUR	1.01	0.13	0.03	1.14	0.27	1.44
BTC/GBP	0.28	0.06	0.02	0.23	0.18	0.59
TO others	1.63	0.26	0.07	0.92	0.53	<i>TSI: 3.40/ 6.99 = 48.62%</i>

*Note:* Returns spillovers, frequency domain analysis following Baruník and Křehlík (2018) using 60-day ahead forecast horizon. Numbers are percentages. ‘Within’ refers to *within system* spillovers. *Short* and *Long* horizons refer to ‘30 days or less’ and ‘more than 30 days’, respectively.

**Volatility spillover tables – Frequency domain analysis with various forecast horizons and frequency bands**

Table A.21 Volatility spillovers across five selected exchange rates – Frequency domain analysis with 4-day frequency band and 7-day ahead forecast

(a) *Short horizon*

	BTC/USD	BTC/AUD	BTC/CAD	BTC/EUR	BTC/GBP	FROM others
BTC/USD	39.53	0.44	0.11	4.68	0.15	5.38
BTC/AUD	0.29	34.80	0.39	0.61	0.13	1.41
BTC/CAD	0.07	0.55	47.33	0.46	0.16	1.23
BTC/EUR	2.71	0.58	0.12	26.89	0.14	3.56
BTC/GBP	0.22	0.23	0.16	0.24	62.30	0.85
TO others	3.29	1.80	0.78	5.98	0.58	<i>TSI: 12.43/223.28 = 5.57%</i>

(b) *Long horizon*

	BTC/USD	BTC/AUD	BTC/CAD	BTC/EUR	BTC/GBP	FROM others
BTC/USD	43.46	1.37	0.10	9.82	0.34	11.63
BTC/AUD	2.63	54.74	1.98	4.29	0.14	9.04
BTC/CAD	0.10	3.22	46.77	0.96	0.39	4.68
BTC/EUR	16.50	1.85	0.19	50.59	0.42	18.97
BTC/GBP	0.33	0.33	0.54	0.71	34.95	1.90
TO others	19.56	6.77	2.82	15.78	1.29	<i>TSI: 46.21/276.72 = 16.70%</i>

*Note:* Volatility spillovers, frequency domain analysis following Baruník and Křehlík (2018) using 7-day ahead forecast horizon. Numbers are percentages. ‘Within’ refers to *within system* spillovers. *Short* and *Long* horizons refer to ‘4 days or less’ and ‘more than 4 days’, respectively.

Table A.22 Volatility spillovers across five selected exchange rates – Frequency domain analysis with 16-day frequency band and 7-day ahead forecast

(a) *Short horizon*

	BTC/USD	BTC/AUD	BTC/CAD	BTC/EUR	BTC/GBP	FROM others
BTC/USD	39.53	0.44	0.11	4.68	0.15	5.38
BTC/AUD	0.29	34.80	0.39	0.61	0.13	1.41
BTC/CAD	0.07	0.55	47.33	0.46	0.16	1.23
BTC/EUR	2.71	0.58	0.12	26.89	0.14	3.56
BTC/GBP	0.22	0.23	0.16	0.24	62.30	0.85
TO others	3.29	1.80	0.78	5.98	0.58	<i>TSI: 12.43/223.28 = 5.57%</i>

(b) *Long horizon*

	BTC/USD	BTC/AUD	BTC/CAD	BTC/EUR	BTC/GBP	FROM others
BTC/USD	43.46	1.37	0.10	9.82	0.34	11.63
BTC/AUD	2.63	54.74	1.98	4.29	0.14	9.04
BTC/CAD	0.10	3.22	46.77	0.96	0.39	4.68
BTC/EUR	16.50	1.85	0.19	50.59	0.42	18.97
BTC/GBP	0.33	0.33	0.54	0.71	34.95	1.90
TO others	19.56	6.77	2.82	15.78	1.29	<i>TSI: 46.21/276.72 = 16.70%</i>

*Note:* Volatility spillovers, frequency domain analysis following Baruník and Křehlík (2018) using 7-day ahead forecast horizon. Numbers are percentages. ‘Within’ refers to *within system* spillovers. *Short* and *Long* horizons refer to ‘16 days or less’ and ‘more than 16 days’, respectively.

**Table A.23 Volatility spillovers across five selected exchange rates – Frequency domain analysis with 30-day frequency band and 7-day ahead forecast**

(a) *Short horizon*

	BTC/USD	BTC/AUD	BTC/CAD	BTC/EUR	BTC/GBP	FROM others
BTC/USD	39.53	0.44	0.11	4.68	0.15	5.38
BTC/AUD	0.29	34.80	0.39	0.61	0.13	1.41
BTC/CAD	0.07	0.55	47.33	0.46	0.16	1.23
BTC/EUR	2.71	0.58	0.12	26.89	0.14	3.56
BTC/GBP	0.22	0.23	0.16	0.24	62.30	0.85
TO others	3.29	1.80	0.78	5.98	0.58	<i>TSI: 12.43/223.28 = 5.57%</i>

(b) *Long horizon*

	BTC/USD	BTC/AUD	BTC/CAD	BTC/EUR	BTC/GBP	FROM others
BTC/USD	43.46	1.37	0.10	9.82	0.34	11.63
BTC/AUD	2.63	54.74	1.98	4.29	0.14	9.04
BTC/CAD	0.10	3.22	46.77	0.96	0.39	4.68
BTC/EUR	16.50	1.85	0.19	50.59	0.42	18.97
BTC/GBP	0.33	0.33	0.54	0.71	34.95	1.90
TO others	19.56	6.77	2.82	15.78	1.29	<i>TSI: 46.21/276.72 = 16.70%</i>

*Note:* Volatility spillovers, frequency domain analysis following Baruník and Křehlík (2018) using 7-day ahead forecast horizon. Numbers are percentages. ‘Within’ refers to *within system* spillovers. *Short* and *Long* horizons refer to ‘30 days or less’ and ‘more than 30 days’, respectively.

Table A.24 Volatility spillovers across five selected exchange rates – Frequency domain analysis with 4-day frequency band and 10-day ahead forecast

(a) *Short horizon*

	BTC/USD	BTC/AUD	BTC/CAD	BTC/EUR	BTC/GBP	FROM others
BTC/USD	29.75	0.23	0.04	2.38	0.14	2.78
BTC/AUD	0.16	27.30	0.16	0.26	0.10	0.68
BTC/CAD	0.07	0.21	39.70	0.27	0.11	0.67
BTC/EUR	1.47	0.21	0.07	18.22	0.08	1.84
BTC/GBP	0.12	0.21	0.14	0.22	53.46	0.70
TO others	1.82	0.86	0.42	3.13	0.43	<i>TSI: 6.66/175.10 = 3.81%</i>

(b) *Long horizon*

	BTC/USD	BTC/AUD	BTC/CAD	BTC/EUR	BTC/GBP	FROM others
BTC/USD	51.94	2.13	0.23	12.63	0.53	15.52
BTC/AUD	3.15	60.81	2.58	5.21	0.27	11.20
BTC/CAD	0.10	4.35	53.29	1.27	0.63	6.35
BTC/EUR	18.53	2.65	0.35	57.63	0.78	22.31
BTC/GBP	0.45	0.45	0.78	0.72	43.44	2.40
TO others	22.22	9.58	3.94	19.83	2.21	<i>TSI: 57.78/324.90 = 17.79%</i>

*Note:* Volatility spillovers, frequency domain analysis following Baruník and Křehlík (2018) using 10-day ahead forecast horizon. Numbers are percentages. ‘Within’ refers to *within system* spillovers. *Short* and *Long* horizons refer to ‘4 days or less’ and ‘more than 4 days’, respectively.

**Table A.25 Volatility spillovers across five selected exchange rates – Frequency domain analysis with 16-day frequency band and 10-day ahead forecast**

(a) *Short horizon*

	BTC/USD	BTC/AUD	BTC/CAD	BTC/EUR	BTC/GBP	FROM others
BTC/USD	42.60	0.43	0.11	5.04	0.15	5.73
BTC/AUD	0.27	33.23	0.36	0.59	0.13	1.35
BTC/CAD	0.07	0.53	48.83	0.46	0.16	1.21
BTC/EUR	3.31	0.55	0.12	29.67	0.16	4.15
BTC/GBP	0.26	0.23	0.16	0.39	67.11	1.04
TO others	3.91	1.75	0.75	6.48	0.60	<i>TSI: 13.48/234.93 = 5.74%</i>

(b) *Long horizon*

	BTC/USD	BTC/AUD	BTC/CAD	BTC/EUR	BTC/GBP	FROM others
BTC/USD	39.09	1.93	0.16	9.97	0.52	12.57
BTC/AUD	3.03	54.89	2.39	4.88	0.24	10.54
BTC/CAD	0.10	4.03	44.15	1.09	0.58	5.80
BTC/EUR	16.69	2.30	0.30	46.18	0.70	20.00
BTC/GBP	0.31	0.43	0.76	0.55	29.79	2.06
TO others	20.13	8.70	3.61	16.49	2.04	<i>TSI: 50.96/265.07 = 19.23%</i>

*Note:* Volatility spillovers, frequency domain analysis following Baruník and Křehlík (2018) using 10-day ahead forecast horizon. Numbers are percentages. ‘Within’ refers to *within system* spillovers. *Short* and *Long* horizons refer to ‘16 days or less’ and ‘more than 16 days’, respectively.

Table A.26 Volatility spillovers across five selected exchange rates – Frequency domain analysis with 30-day frequency band and 10-day ahead forecast

(a) *Short horizon*

	BTC/USD	BTC/AUD	BTC/CAD	BTC/EUR	BTC/GBP	FROM others
BTC/USD	42.60	0.43	0.11	5.04	0.15	5.73
BTC/AUD	0.27	33.23	0.36	0.59	0.13	1.35
BTC/CAD	0.07	0.53	48.83	0.46	0.16	1.21
BTC/EUR	3.31	0.55	0.12	29.67	0.16	4.15
BTC/GBP	0.26	0.23	0.16	0.39	67.11	1.04
TO others	3.91	1.75	0.75	6.48	0.60	<i>TSI: 13.48/234.93 = 5.74%</i>

(b) *Long horizon*

	BTC/USD	BTC/AUD	BTC/CAD	BTC/EUR	BTC/GBP	FROM others
BTC/USD	39.09	1.93	0.16	9.97	0.52	12.57
BTC/AUD	3.03	54.89	2.39	4.88	0.24	10.54
BTC/CAD	0.10	4.03	44.15	1.09	0.58	5.80
BTC/EUR	16.69	2.30	0.30	46.18	0.70	20.00
BTC/GBP	0.31	0.43	0.76	0.55	29.79	2.06
TO others	20.13	8.70	3.61	16.49	2.04	<i>TSI: 50.96/265.07 = 19.23%</i>

*Note:* Volatility spillovers, frequency domain analysis following Baruník and Křehlík (2018) using 10-day ahead forecast horizon. Numbers are percentages. ‘Within’ refers to *within system* spillovers. *Short* and *Long* horizons refer to ‘30 days or less’ and ‘more than 30 days’, respectively.

**Table A.27 Volatility spillovers across five selected exchange rates – Frequency domain analysis with 4-day frequency band and 30-day ahead forecast (baseline estimates)**

(a) *Short horizon*

	BTC/USD	BTC/AUD	BTC/CAD	BTC/EUR	BTC/GBP	FROM others
BTC/USD	35.09	0.38	0.08	3.91	0.16	4.52
BTC/AUD	0.19	23.94	0.23	0.39	0.08	0.88
BTC/CAD	0.07	0.43	42.71	0.35	0.12	0.96
BTC/EUR	2.64	0.39	0.09	22.93	0.11	3.24
BTC/GBP	0.15	0.22	0.14	0.22	58.48	0.74
TO others	3.05	1.42	0.54	4.87	0.47	<i>TSI: 10.34/193.49 = 5.34%</i>

(b) *Long horizon*

	BTC/USD	BTC/AUD	BTC/CAD	BTC/EUR	BTC/GBP	FROM others
BTC/USD	44.07	3.77	0.37	11.41	0.77	16.32
BTC/AUD	4.08	60.46	3.64	6.28	0.71	14.71
BTC/CAD	0.23	6.20	47.28	1.47	1.14	9.05
BTC/EUR	18.09	4.36	0.79	49.25	1.35	24.59
BTC/GBP	0.48	1.17	1.48	0.75	36.89	3.89
TO others	22.88	15.50	6.27	19.92	3.98	<i>TSI: 68.55/306.51 = 22.37%</i>

*Note:* Volatility spillovers, frequency domain analysis following Baruník and Křehlík (2018) using 30-day ahead forecast horizon. Numbers are percentages. ‘Within’ refers to *within system* spillovers. *Short* and *Long* horizons refer to ‘4 days or less’ and ‘more than 4 days’, respectively.

Table A.28 Volatility spillovers across five selected exchange rates – Frequency domain analysis with 16-day frequency band and 30-day ahead forecast

(a) *Short horizon*

	BTC/USD	BTC/AUD	BTC/CAD	BTC/EUR	BTC/GBP	FROM others
BTC/USD	57.41	0.50	0.11	8.34	0.23	9.19
BTC/AUD	0.39	30.95	0.34	0.80	0.11	1.64
BTC/CAD	0.07	0.88	58.79	0.60	0.20	1.76
BTC/EUR	8.72	0.62	0.12	46.50	0.25	9.71
BTC/GBP	0.35	0.24	0.26	0.60	81.50	1.45
TO others	9.53	2.24	0.82	10.35	0.79	<i>TSI: 23.74/298.89 = 7.94%</i>

(b) *Long horizon*

	BTC/USD	BTC/AUD	BTC/CAD	BTC/EUR	BTC/GBP	FROM others
BTC/USD	21.76	3.65	0.34	6.98	0.69	11.65
BTC/AUD	3.87	53.46	3.53	5.87	0.69	13.95
BTC/CAD	0.23	5.75	31.20	1.22	1.06	8.25
BTC/EUR	12.01	4.13	0.76	25.68	1.21	18.12
BTC/GBP	0.29	1.15	1.36	0.37	13.87	3.17
TO others	16.40	14.67	5.99	14.43	3.65	<i>TSI: 55.15/201.11 = 27.42%</i>

*Note:* Volatility spillovers, frequency domain analysis following Baruník and Křehlík (2018) using 30-day ahead forecast horizon. Numbers are percentages. ‘Within’ refers to *within system* spillovers. *Short* and *Long* horizons refer to ‘16 days or less’ and ‘more than 16 days’, respectively.

Table A.29 Volatility spillovers across five selected exchange rates – Frequency domain analysis with 30-day frequency band and 30-day ahead forecast

(a) *Short horizon*

	BTC/USD	BTC/AUD	BTC/CAD	BTC/EUR	BTC/GBP	FROM others
BTC/USD	57.41	0.50	0.11	8.34	0.23	9.19
BTC/AUD	0.39	30.95	0.34	0.80	0.11	1.64
BTC/CAD	0.07	0.88	58.79	0.60	0.20	1.76
BTC/EUR	8.72	0.62	0.12	46.50	0.25	9.71
BTC/GBP	0.35	0.24	0.26	0.60	81.50	1.45
TO others	9.53	2.24	0.82	10.35	0.79	<i>TSI: 23.74/298.89 = 7.94%</i>

(b) *Long horizon*

	BTC/USD	BTC/AUD	BTC/CAD	BTC/EUR	BTC/GBP	FROM others
BTC/USD	21.76	3.65	0.34	6.98	0.69	11.65
BTC/AUD	3.87	53.46	3.53	5.87	0.69	13.95
BTC/CAD	0.23	5.75	31.20	1.22	1.06	8.25
BTC/EUR	12.01	4.13	0.76	25.68	1.21	18.12
BTC/GBP	0.29	1.15	1.36	0.37	13.87	3.17
TO others	16.40	14.67	5.99	14.43	3.65	<i>TSI: 55.15/201.11 = 27.42%</i>

*Note:* Volatility spillovers, frequency domain analysis following Baruník and Křehlík (2018) using 30-day ahead forecast horizon. Numbers are percentages. ‘Within’ refers to *within system* spillovers. *Short* and *Long* horizons refer to ‘30 days or less’ and ‘more than 30 days’, respectively.

Table A.30 Volatility spillovers across five selected exchange rates – Frequency domain analysis with 4-day frequency band and 60-day ahead forecast

(a) *Short horizon*

	BTC/USD	BTC/AUD	BTC/CAD	BTC/EUR	BTC/GBP	FROM others
BTC/USD	33.46	0.39	0.07	3.63	0.15	4.24
BTC/AUD	0.19	22.89	0.24	0.40	0.07	0.91
BTC/CAD	0.07	0.45	41.82	0.33	0.13	0.98
BTC/EUR	2.51	0.43	0.10	21.75	0.12	3.16
BTC/GBP	0.13	0.22	0.15	0.22	56.80	0.73
TO others	2.91	1.49	0.57	4.58	0.47	<i>TSI: 10.02/186.74 = 5.37%</i>

(b) *Long horizon*

	BTC/USD	BTC/AUD	BTC/CAD	BTC/EUR	BTC/GBP	FROM others
BTC/USD	44.77	4.58	0.50	11.64	0.81	17.53
BTC/AUD	4.33	60.20	4.19	6.58	0.90	15.99
BTC/CAD	0.30	7.10	46.99	1.60	1.21	10.21
BTC/EUR	18.04	5.26	0.98	49.42	1.40	25.68
BTC/GBP	0.52	1.46	1.57	0.78	38.14	4.33
TO others	23.19	18.41	7.23	20.60	4.32	<i>TSI: 73.74/313.26 = 23.54%</i>

*Note:* Volatility spillovers, frequency domain analysis following Baruník and Křehlík (2018) using 60-day ahead forecast horizon. Numbers are percentages. ‘Within’ refers to *within system* spillovers. *Short* and *Long* horizons refer to ‘4 days or less’ and ‘more than 4 days’, respectively.

**Table A.31 Volatility spillovers across five selected exchange rates – Frequency domain analysis with 16-day frequency band and 60-day ahead forecast**

(a) *Short horizon*

	BTC/USD	BTC/AUD	BTC/CAD	BTC/EUR	BTC/GBP	FROM others
BTC/USD	54.06	0.65	0.12	7.94	0.23	8.95
BTC/AUD	0.51	30.67	0.45	0.98	0.09	2.02
BTC/CAD	0.07	1.13	57.30	0.64	0.20	2.04
BTC/EUR	7.91	0.82	0.13	42.71	0.22	9.09
BTC/GBP	0.32	0.26	0.26	0.57	77.88	1.41
TO others	8.82	2.86	0.97	10.13	0.74	<i>TSI: 23.51/286.13 = 8.22%</i>

(b) *Long horizon*

	BTC/USD	BTC/AUD	BTC/CAD	BTC/EUR	BTC/GBP	FROM others
BTC/USD	24.17	4.32	0.45	7.32	0.73	12.82
BTC/AUD	4.01	52.42	3.98	6.00	0.89	14.88
BTC/CAD	0.30	6.43	31.50	1.29	1.14	9.15
BTC/EUR	12.64	4.87	0.94	28.45	1.29	19.75
BTC/GBP	0.33	1.43	1.46	0.44	17.06	3.65
TO others	17.28	17.05	6.83	15.05	4.05	<i>TSI: 60.26/213.87 = 28.17%</i>

*Note:* Volatility spillovers, frequency domain analysis following Baruník and Křehlík (2018) using 60-day ahead forecast horizon. Numbers are percentages. ‘Within’ refers to *within system* spillovers. *Short* and *Long* horizons refer to ‘16 days or less’ and ‘more than 16 days’, respectively.

Table A.32 Volatility spillovers across five selected exchange rates – Frequency domain analysis with 30-day frequency band and 60-day ahead forecast

(a) *Short horizon*

	BTC/USD	BTC/AUD	BTC/CAD	BTC/EUR	BTC/GBP	FROM others
BTC/USD	65.69	1.01	0.14	10.72	0.42	12.29
BTC/AUD	0.97	38.14	0.69	1.69	0.15	3.50
BTC/CAD	0.09	1.83	69.26	0.85	0.47	3.24
BTC/EUR	13.18	1.17	0.21	56.14	0.60	15.16
BTC/GBP	0.42	0.40	0.63	0.69	87.41	2.14
TO others	14.66	4.41	1.68	13.95	1.64	<i>TSI: 36.33/352.98 = 10.29%</i>

(b) *Long horizon*

	BTC/USD	BTC/AUD	BTC/CAD	BTC/EUR	BTC/GBP	FROM others
BTC/USD	12.54	3.96	0.43	4.55	0.54	9.48
BTC/AUD	3.55	44.95	3.74	5.29	0.82	13.41
BTC/CAD	0.29	5.73	19.55	1.07	0.86	7.95
BTC/EUR	7.37	4.53	0.86	15.03	0.92	13.67
BTC/GBP	0.23	1.28	1.09	0.32	7.52	2.92
TO others	11.44	15.50	6.12	11.23	3.15	<i>TSI: 47.43/147.02 = 32.26%</i>

*Note:* Volatility spillovers, frequency domain analysis following Baruník and Křehlík (2018) using 60-day ahead forecast horizon. Numbers are percentages. ‘Within’ refers to *within system* spillovers. *Short* and *Long* horizons refer to ‘30 days or less’ and ‘more than 30 days’, respectively.

Figure A.1

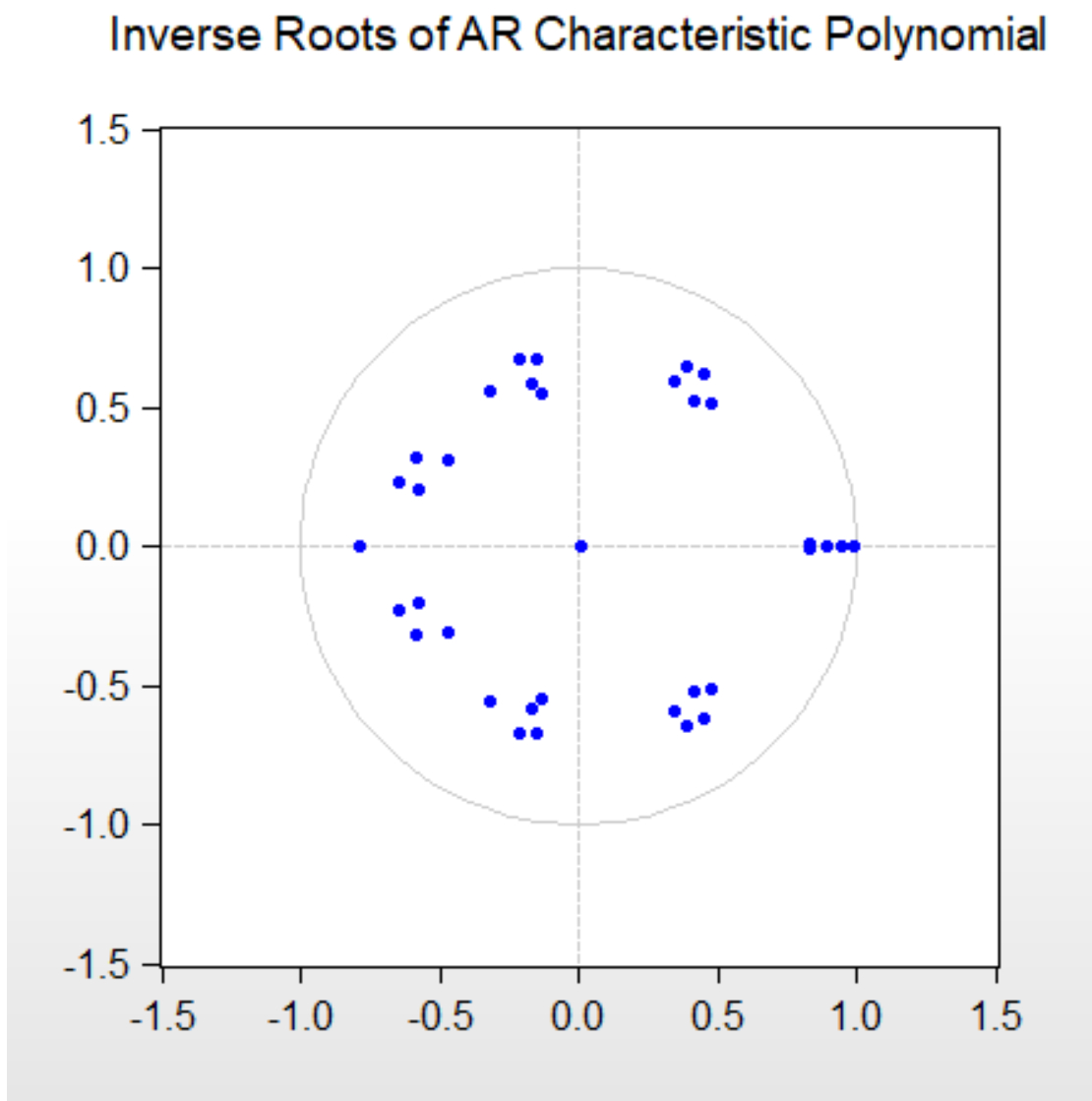
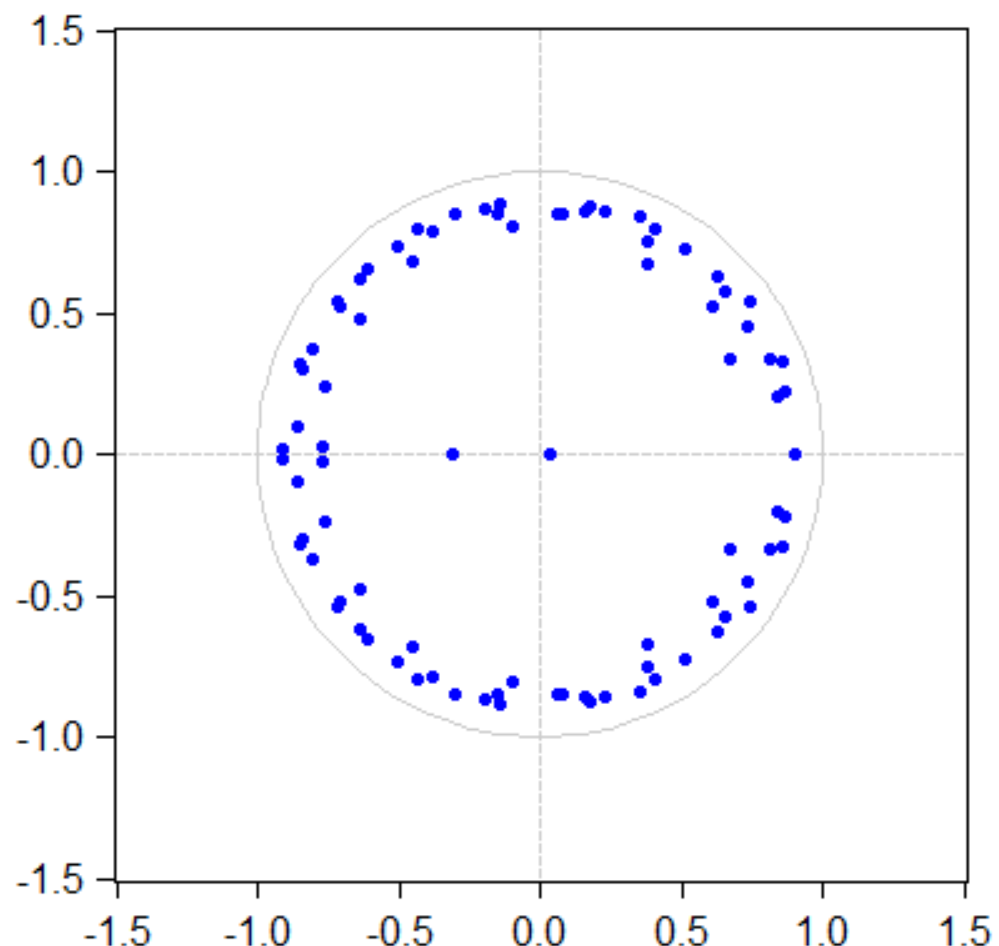


Figure A.2

### Inverse Roots of AR Characteristic Polynomial

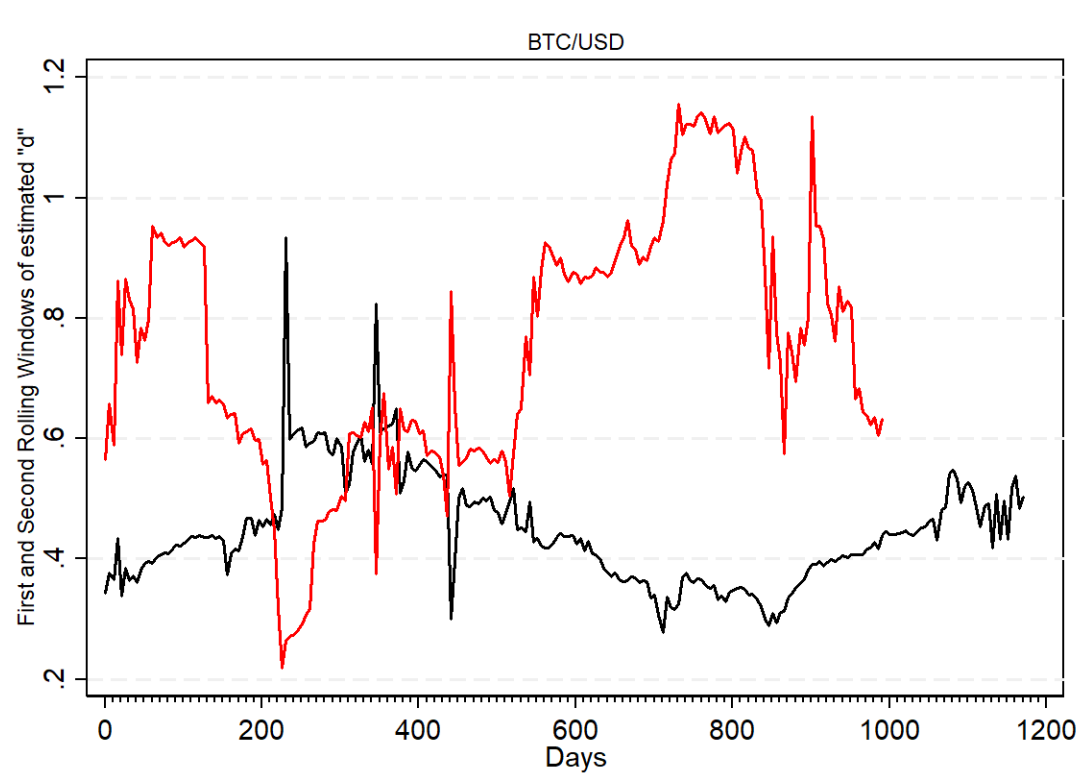


## Appendix B

# Supplement to Chapter 3

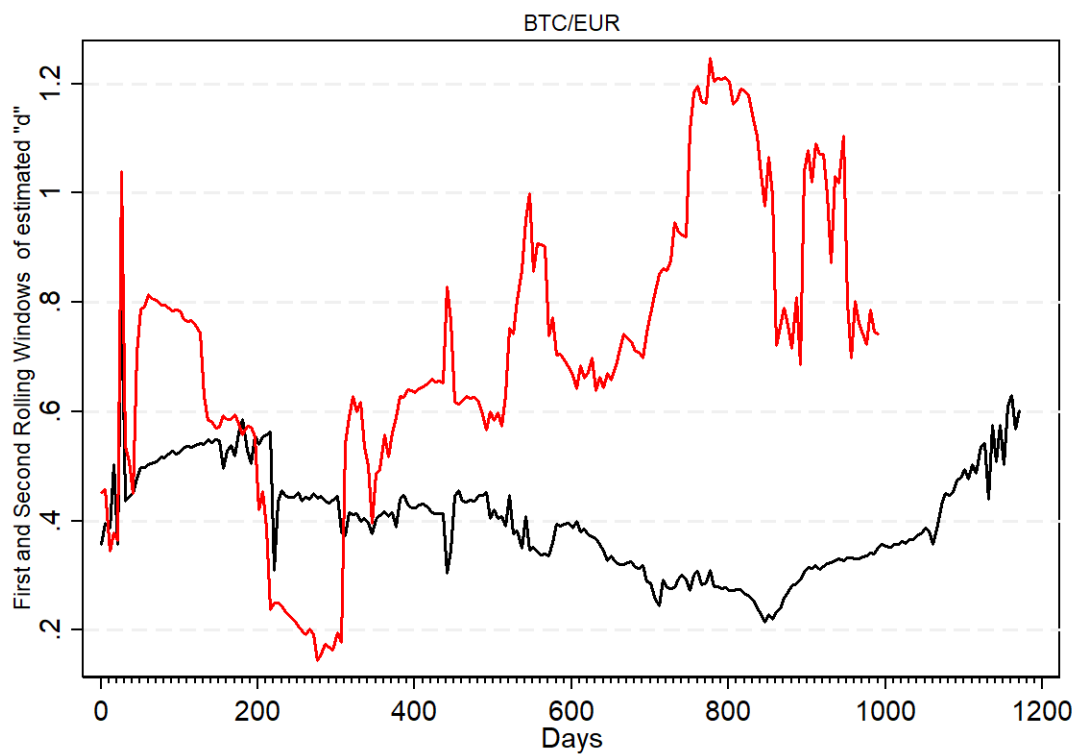
### A, Rolling windows of the rolling windows series for each market

Figure B.1 The Rolling Windows of the estimated "d" parameter and the rolling windows of "rolled d" in BTC/USD market



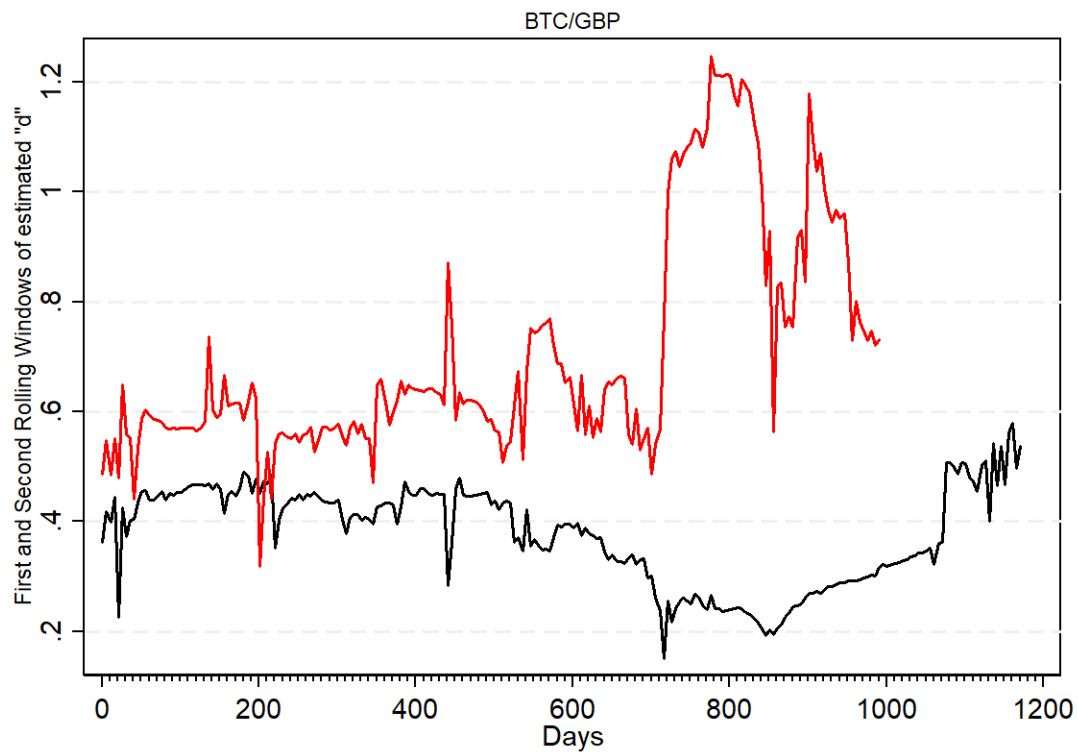
Note: Black line is the rolling windows of the estimated "d". Red line is the rolling windows of the latter rolling windows. X-axis indicate daily data which the first day is 1 and ticks are 10 days each.

Figure B.2 The Rolling Windows of the estimated "d" parameter and the rolling windows of "rolled d " in BTC/EUR market



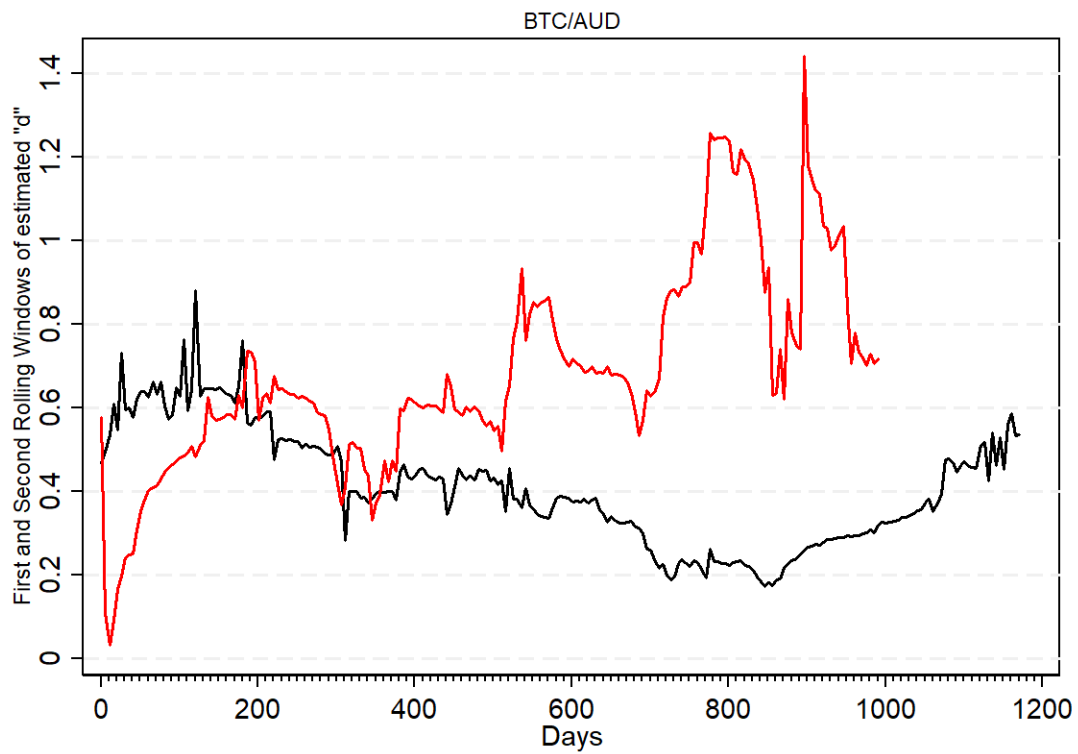
Note: Black line is the rolling windows of the estimated "d". Red line is the rolling windows of the latter rolling windows. X-axis indicate daily data which the first day is 1 and ticks are 10 days each.

Figure B.3 The Rolling Windows of the estimated "d" parameter and the rolling windows of "rolled d " in BTC/GBP market



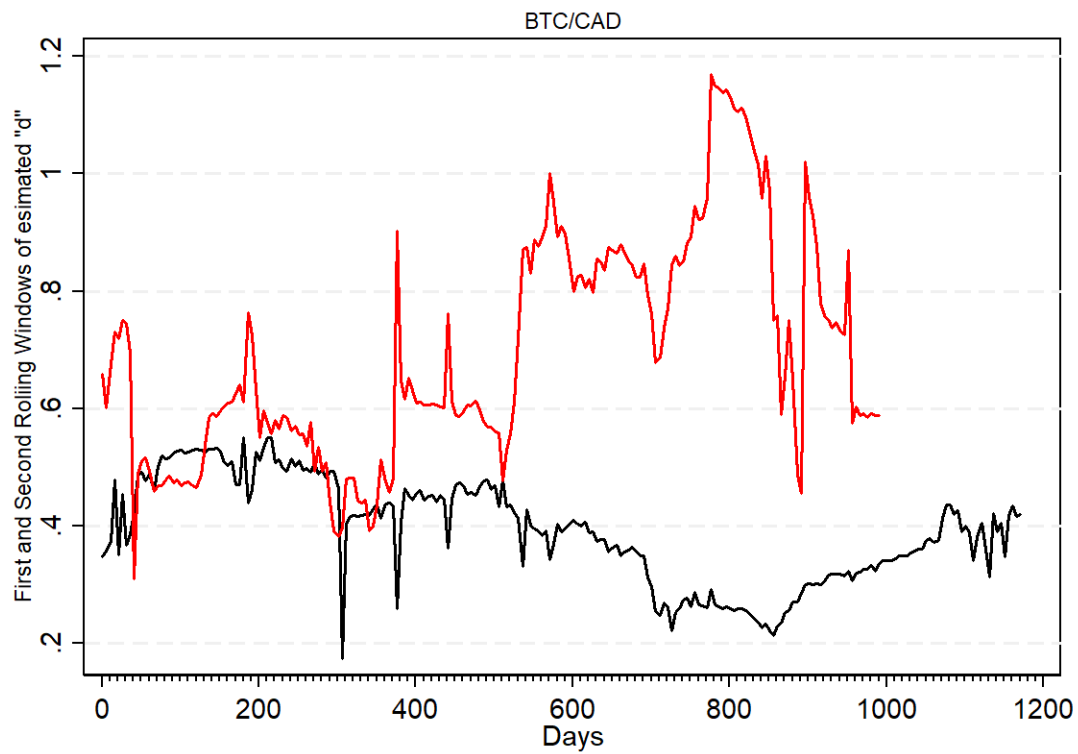
Note: Black line is the rolling windows of the estimated "d". Red line is the rolling windows of the latter rolling windows. X-axis indicate daily data which the first day is 1 and ticks are 10 days each.

Figure B.4 The Rolling Windows of the estimated "d" parameter and the rolling windows of "rolled d " in BTC/AUD market



Note: Black line is the rolling windows of the estimated "d". Red line is the rolling windows of the latter rolling windows. X-axis indicate daily data which the first day is 1 and ticks are 10 days each.

Figure B.5 The Rolling Windows of the estimated "d" parameter and the rolling windows of "rolled d " in BTC/CAD market



Note: Black line is the rolling windows of the estimated "d". Red line is the rolling windows of the latter rolling windows. X-axis indicate daily data which the first day is 1 and ticks are 10 days each.

## B, Different specification for the estimated MS-ARFIMA process

Table B.1 Estimates of BTC/USD market volatility under different specifications of MS-ARFIMA process

MS-ARFIMA (0, d, 0)		MS-ARFIMA (0, d, 1)		MS-ARFIMA (1, d, 0)		MS-ARFIMA (1, d, 1)		
Estimate	S.E.	Estimate	S.E.	Estimate	S.E.	Estimate	S.E.	
$d_1$	0.2615	0.0332	0.3838	0.0447	0.3313	0.0391	0.4224	0.0520
$d_2$	0.3202	0.0156	0.3880	0.0272	0.3630	0.0219	0.4249	0.0329
$\mu_1$	0.9745	0.0697	0.7869	0.1035	0.8872	0.0870	0.8314	0.1095
$\mu_2$	0.2576	0.0490	0.2008	0.0644	0.2184	0.0584	0.1936	0.0691
$\sigma_1$	0.7046	0.0296	0.7193	0.0287	0.7148	0.0295	0.7098	0.0291
$\sigma_2$	0.1870	0.0038	0.1851	0.0038	0.1857	0.0038	0.1856	0.0038
$p_{11}$	0.8189	0.0222	0.8544	0.0196	0.8295	0.0215	0.8339	0.0212
$p_{22}$	0.9564	0.0058	0.9613	0.0055	0.9577	0.0057	0.9585	0.0057
$\phi$	-	-	-	-	-0.0914	0.0331	0.3018	0.1022
$\theta$	-	-	-0.1418	0.0435	-	-	-0.4734	0.1025
$L$	<b>-365.67568</b>		<b>-363.261213</b>		<b>-362.471718</b>		<b>-358.38933</b>	

Note:  $d$ : long memory,  $\mu$ : mean,  $\sigma$ : standard deviation,  $P$ : transition probability,  $\phi$ : Autoregressive parameter,  $\theta$ : Moving average parameter,  $L$ : Log-likelihood of switching model,  $S.E$ : standard error

Table B.2 Estimates of BTC/EUR market volatility under different specifications of MS-ARFIMA process

MS-ARFIMA (0, d, 0)		MS-ARFIMA (0, d, 1)		MS-ARFIMA (1, d, 0)		MS-ARFIMA (1, d, 1)		
Estimate	S.E.	Estimate	S.E.	Estimate	S.E.	Estimate	S.E.	
$d_1$	0.3306	0.0263	0.3529	0.0321	0.3472	0.0314	0.2874	0.0284
$d_2$	0.3382	0.0155	0.3474	0.0211	0.3488	0.0199	0.3171	0.0177
$\mu_1$	0.9113	0.0820	0.8362	0.0956	0.9056	0.0873	0.7674	0.0676
$\mu_2$	0.2376	0.0498	0.2004	0.0556	0.2350	0.0523	0.1905	0.0466
$\sigma_1$	0.7132	0.0293	0.7090	0.0034	0.7165	0.0296	0.6562	0.0217
$\sigma_2$	0.1665	0.0034	0.1653	0.0285	0.1682	0.0034	0.1513	0.0033
$p_{11}$	0.7627	0.0244	0.7787	0.0233	0.7662	0.0244	0.8919	0.0144
$p_{22}$	0.9415	0.0067	0.9425	0.0067	0.9433	0.0066	0.9534	0.0064
$\phi$	-	-	-	-	-0.0328	0.0326	-0.5040	0.2178
$\theta$	-	-	-0.0413	0.0376	-	-	0.5469	0.2077
$L$	<b>-311.252655</b>		<b>-313.96913</b>		<b>-310.734501</b>		<b>-324.6173</b>	

Note:  $d$ : long memory,  $\mu$ : mean,  $\sigma$ : standard deviation,  $P$ : transition probability,  $\phi$ : Autoregressive parameter,  $\theta$ : Moving average parameter,  $L$ : Log-likelihood of switching model,  $S.E$ : standard error

Table B.3 Estimates of BTC/GBP market volatility under different specifications of MS-ARFIMA process

	MS-ARFIMA (0, d, 0)		MS-ARFIMA (0, d, 1)		MS-ARFIMA (1, d, 0)		MS-ARFIMA (1, d, 1)	
	Estimate	S.E.	Estimate	S.E.	Estimate	S.E.	Estimate	S.E.
$d_1$	0.3391	0.0272	0.3267	0.0359	0.3250	0.0303	0.3570	0.0355
$d_2$	0.3121	0.0159	0.3086	0.0213	0.3027	0.0182	0.3253	0.0240
$\mu_1$	0.7375	0.1130	0.7479	0.1107	0.7535	0.1099	0.7206	0.1188
$\mu_2$	0.1885	0.0501	0.1925	0.0510	0.1948	0.0485	0.1786	0.0541
$\sigma_1$	0.8013	0.0363	0.7840	0.0339	0.8017	0.0365	0.7981	0.0359
$\sigma_2$	0.1765	0.0035	0.1739	0.0035	0.1769	0.0035	0.1762	0.0035
$p_{11}$	0.7303	0.0275	0.7628	0.0253	0.7293	0.0276	0.7323	0.0273
$p_{22}$	0.9451	0.0064	0.9465	0.0064	0.9451	0.0064	0.9450	0.0064
$\phi$	-	-	-	-	0.0106	0.0288	0.4184	0.3289
$\theta$	-	-	0.0197	0.0359	-	-	-0.4446	0.3265
$L$	<b>-333.95178</b>		<b>-336.939603</b>		<b>-334.518996</b>		<b>-333.830679</b>	

Note:  $d$ : long memory,  $\mu$ : mean,  $\sigma$ : standard deviation,  $P$ : transition probability,  $\phi$ : Autoregressive parameter,  $\theta$ : Moving average parameter,  $L$ : Log-likelihood of switching model,  $S.E$ : standard error

Table B.4 Estimates of BTC/AUD market volatility under different specifications of MS-ARFIMA process

	MS-ARFIMA (0, d, 0)		MS-ARFIMA (0, d, 1)		MS-ARFIMA (1, d, 0)		MS-ARFIMA (1, d, 1)	
	Estimate	S.E.	Estimate	S.E.	Estimate	S.E.	Estimate	S.E.
$d_1$	0.3670	0.0322	0.2820	0.0316	0.3446	0.0385	0.3427	0.0355
$d_2$	0.3235	0.0159	0.2627	0.0174	0.3098	0.0200	0.3100	0.0177
$\mu_1$	0.9242	0.1343	0.8686	0.0898	0.9503	0.1290	0.9596	0.1249
$\mu_2$	0.2865	0.0587	0.2841	0.0419	0.2919	0.0561	0.2938	0.0552
$\sigma_1$	0.8008	0.0360	0.7210	0.0273	0.7978	0.0360	0.7956	0.0358
$\sigma_2$	0.1855	0.0037	0.1631	0.0034	0.1855	0.0037	0.1847	0.0037
$p_{11}$	0.7331	0.0275	0.8006	0.0208	0.7331	0.0275	0.7303	0.0275
$p_{22}$	0.9451	0.0064	0.9367	0.0071	0.9451	0.0064	0.9443	0.0064
$\phi$	-	-	-	-	0.0283	0.0336	-0.4565	0.2795
$\theta$	-	-	0.1119	0.0328	-	-	0.4948	0.2696
$L$	<b>-393.729588</b>		<b>-400.962282</b>		<b>-393.212967</b>		<b>-392.023359</b>	

Note:  $d$ : long memory,  $\mu$ : mean,  $\sigma$ : standard deviation,  $P$ : transition probability,  $\phi$ : Autoregressive parameter,  $\theta$ : Moving average parameter,  $L$ : Log-likelihood of switching model,  $S.E$ : standard error

Table B.5 Estimates of BTC/CAD market volatility under different specifications of MS-ARFIMA process

	MS-ARFIMA (0, d, 0)		MS-ARFIMA (1, d, 0)		MS-ARFIMA (0, d, 1)		MS-ARFIMA (1, d, 1)	
	Estimate	S.E.	Estimate	S.E.	Estimate	S.E.	Estimate	S.E.
$d_1$	0.3192	0.0292	0.2757	0.0381	0.2914	0.0445	0.2692	0.0429
$d_2$	0.2961	0.0001	0.2684	0.0225	0.2899	0.0221	0.2761	0.0234
$\mu_1$	0.6522	0.0848	0.7072	0.0783	0.8757	0.0828	0.8865	0.0765
$\mu_2$	0.2183	0.0416	0.2434	0.0409	0.2997	0.0427	0.3057	0.0394
$\sigma_1$	0.6235	0.0201	0.6209	0.0201	0.6611	0.0249	0.6560	0.0244
$\sigma_2$	0.1459	0.0032	0.1461	0.1461	0.1617	0.0034	0.1602	0.0034
$p_{11}$	0.9012	0.0135	0.9024	0.0133	0.8410	0.0191	0.8452	0.0186
$p_{22}$	0.9522	0.0067	0.9530	0.0066	0.9496	0.0064	0.9492	0.0065
$\phi$	-	-	-	-	0.0526	0.0362	-0.0591	0.2372
$\theta$	-	-	0.0476	0.0355	-	-	0.1216	0.2297
$L$	<b>-300.4434</b>		<b>-299.755155</b>		<b>-292.341567</b>		<b>-293.877633</b>	

Note:  $d$ : long memory,  $\mu$ : mean,  $\sigma$ : standard deviation,  $P$ : transition probability,  $\phi$ : Autoregressive parameter,  $\theta$ : Moving average parameter,  $L$ : Log-likelihood of switching model,  $S.E$ : standard error

### Robustness check for MS-ARFIMA

Table B.6 Estimates of BTC/USD market return volatility under different specifications of MS-ARFIMA process

	MS-ARFIMA (0, d, 0)		MS-ARFIMA (0, d, 1)		MS-ARFIMA (1, d, 0)		MS-ARFIMA (1, d, 1)	
	Estimate	S.E.	Estimate	S.E.	Estimate	S.E.	Estimate	S.E.
$d_1$	0.289	0.0373	0.4052	0.0434	0.3414	0.0404	0.4772	0.0486
$d_2$	0.3312	0.0165	0.3948	0.0277	0.3645	0.0224	0.4423	0.0336
$\mu_1$	8.0361	0.7577	7.0224	1.0794	7.6371	0.851	6.2306	1.3547
$\mu_2$	2.2246	0.4887	1.6597	0.6382	1.9668	0.5559	1.482	0.767
$\sigma_1$	6.2061	0.0296	6.2362	0.2624	6.2388	0.257	6.1884	0.2546
$\sigma_2$	1.6228	0.033	1.6014	0.0323	1.6103	0.0327	1.6003	0.0324
$p_{11}$	0.8378	0.0208	0.8015	0.0233	0.8301	0.0214	0.8224	0.0218
$p_{22}$	0.9586	0.0056	0.9525	0.0060	0.9569	0.0058	0.9553	0.0059
$\phi$	-	-	-	-	-0.0901	0.0336	0.2769	0.0896
$\theta$	-	-	-0.1534	0.0427	-	-	-0.474	0.0898
$L$	<b>-3680.41552</b>		<b>-3675.6816</b>		<b>-3676.6468</b>		<b>-3672.7555</b>	

Note:  $d$ : long memory,  $\mu$ : mean,  $\sigma$ : standard deviation,  $P$ : transition probability,  $\phi$ : Autoregressive parameter,  $\theta$ : Moving average parameter,  $L$ : Log-likelihood of switching model,  $S.E$ : standard error

Table B.7 Estimates of BTC/EUR market return volatility under different specifications of MS-ARFIMA process

	MS-ARFIMA (0, d, 0)		MS-ARFIMA (0, d, 1)		MS-ARFIMA (1, d, 0)		MS-ARFIMA (1, d, 1)	
	Estimate	S.E.	Estimate	S.E.	Estimate	S.E.	Estimate	S.E.
$d_1$	0.3313	0.0242	0.3563	0.0322	0.3252	0.0263	0.3982	0.0349
$d_2$	0.3275	0.0151	0.3485	0.0209	0.3252	0.0162	0.3767	0.0249
$\mu_1$	6.117	0.8061	7.1305	0.9302	6.6828	0.7578	6.6038	1.1054
$\mu_2$	1.299	0.4677	1.6703	0.5471	1.5626	0.4358	1.4191	0.6199
$\sigma_1$	5.9374	0.2136	6.1937	0.2491	6.0102	0.2239	6.2007	0.2505
$\sigma_2$	1.3257	0.028	1.4403	0.0293	1.3436	0.028	1.4453	0.0294
$p_{11}$	0.8303	0.0188	0.7818	0.0232	0.8043	0.0206	0.7924	0.0224
$p_{22}$	0.9403	0.007	0.9425	0.0067	0.9374	0.0071	0.9391	0.007
$\phi$	-	-	-	-	0.0048	0.0175	0.4308	0.1468
$\theta$	-	-	-0.0436	0.036	-	-	-0.5108	0.1393
$L$	<b>-3636.3705</b>		<b>-3628.32752</b>		<b>-3633.4137</b>		<b>-3629.0322</b>	

Note:  $d$ : long memory,  $\mu$ : mean,  $\sigma$ : standard deviation,  $P$ : transition probability,  $\phi$ : Autoregressive parameter,  $\theta$ : Moving average parameter,  $L$ : Log-likelihood of switching model,  $S.E$ : standard error

Table B.8 Estimates of BTC/GBP market return volatility under different specifications of MS-ARFIMA process

	MS-ARFIMA (0, d, 0)		MS-ARFIMA (0, d, 1)		MS-ARFIMA (1, d, 0)		MS-ARFIMA (1, d, 1)	
	Estimate	S.E.	Estimate	S.E.	Estimate	S.E.	Estimate	S.E.
$d_1$	0.3368	0.0283	0.3243	0.0294	0.3407	0.029	0.3586	0.035
$d_2$	0.31	0.0163	0.301	0.0174	0.3117	0.0174	0.319	0.0239
$\mu_1$	6.2948	0.975	6.6595	0.9924	6.4464	1.0258	5.9658	1.0984
$\mu_2$	1.6881	0.4473	1.7871	0.4468	1.7022	0.461	1.5756	0.4916
$\sigma_1$	6.7525	0.2869	1.9465	0.0456	6.9928	0.3163	6.8499	0.301
$\sigma_2$	1.496	0.0303	0.4362	0.02	1.5378	0.0307	1.5117	0.0304
$p_{11}$	0.7708	0.0245	1.025	0.1413	0.7341	0.0274	0.745	0.0263
$p_{22}$	0.9452	0.0065	2.8618	0.1238	0.9451	0.0064	0.9436	0.0065
$\phi$	-	-	-	-	-0.0015	0.0194	0.448	0.3721
$\theta$	-	-	0.0131	0.0276	-	-	-0.4745	0.3681
$L$	<b>-3652.7169</b>		<b>-3648.0290</b>		<b>-3647.5388</b>		<b>-3650.6794</b>	

Note:  $d$ : long memory,  $\mu$ : mean,  $\sigma$ : standard deviation,  $P$ : transition probability,  $\phi$ : Autoregressive parameter,  $\theta$ : Moving average parameter,  $L$ : Log-likelihood of switching model,  $S.E$ : standard error

Table B.9 Estimates of BTC/AUD market return volatility under different specifications of MS-ARFIMA process

	MS-ARFIMA (0, d, 0)		MS-ARFIMA (0, d, 1)		MS-ARFIMA (1, d, 0)		MS-ARFIMA (1, d, 1)	
	Estimate	S.E.	Estimate	S.E.	Estimate	S.E.	Estimate	S.E.
$d_1$	0.3943	0.0261	0.3561	0.0316	0.2679	0.0405	0.3616	0.0297
$d_2$	0.3273	0.0153	0.2982	0.0194	0.1984	0.017	0.3056	0.018
$\mu_1$	6.1178	1.2219	6.7589	1.1148	7.7231	0.8654	6.7486	1.1279
$\mu_2$	2.0657	0.4971	2.3365	0.4484	2.9966	0.2636	2.2934	0.4553
$\sigma_1$	6.6483	0.2719	6.4412	0.255	6.0819	0.2282	6.6111	0.2699
$\sigma_2$	1.4496	0.0296	1.4006	0.0289	1.4277	0.0301	1.4451	0.0295
$p_{11}$	0.732	0.025	0.7406	0.0239	0.8121	0.02	0.7337	0.0248
$p_{22}$	0.9303	0.0073	0.9265	0.0075	0.9377	0.0071	0.9302	0.0073
$\phi$	-	-	-	-	0.1833	0.0346	-0.3809	0.2002
$\theta$	-	-	0.0549	0.0356	-	-	0.4433	0.1905
$L$	<b>-3710.7950</b>		<b>-3708.4664</b>		<b>-3720.1556</b>		<b>-3708.7575</b>	

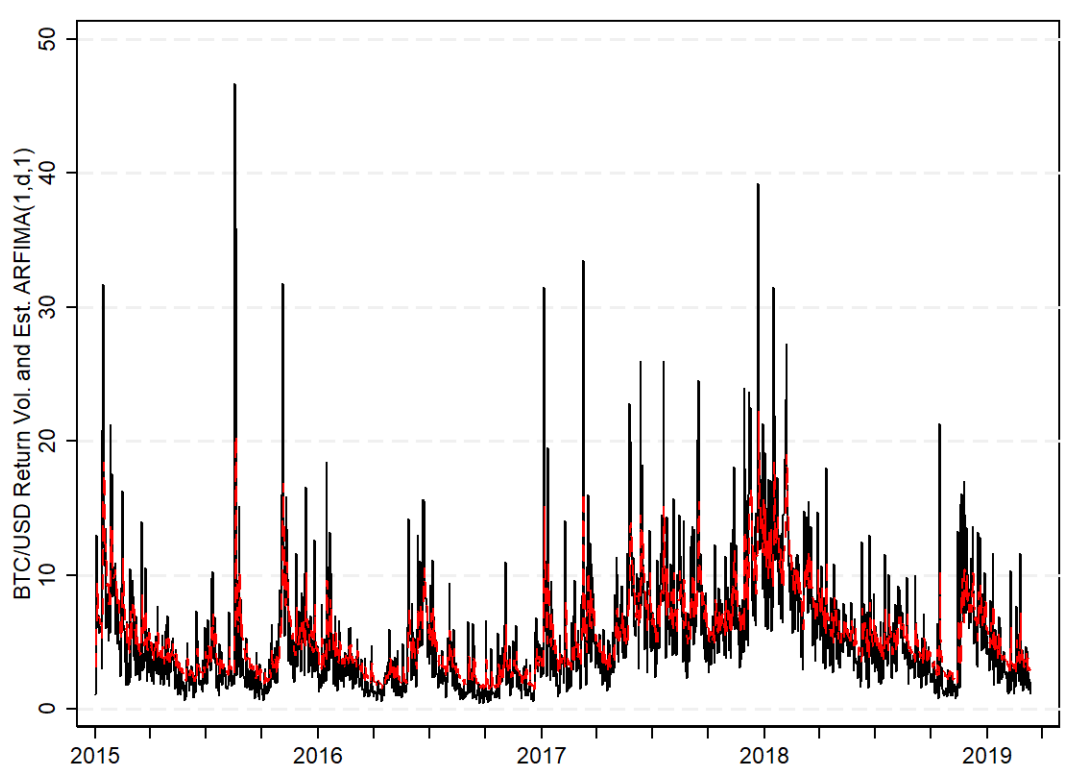
Note:  $d$ : long memory,  $\mu$ : mean,  $\sigma$ : standard deviation,  $P$ : transition probability,  $\phi$ : Autoregressive parameter,  $\theta$ : Moving average parameter,  $L$ : Log-likelihood of switching model,  $S.E$ : standard error

Table B.10 Estimates of BTC/CAD market return volatility under different specifications of MS-ARFIMA process

	MS-ARFIMA (0, d, 0)		MS-ARFIMA (0, d, 1)		MS-ARFIMA (1, d, 0)		MS-ARFIMA (1, d, 1)	
	Estimate	S.E.	Estimate	S.E.	Estimate	S.E.	Estimate	S.E.
$d_1$	0.3332	0.0351	0.2734	0.0365	0.2729	0.0391	0.2756	0.0837
$d_2$	0.3194	0.0174	0.2646	0.0225	0.2642	0.0246	0.2663	0.0526
$\mu_1$	7.3241	0.7584	6.2463	0.6632	6.2514	0.6875	6.2231	0.9982
$\mu_2$	2.5028	0.4152	2.1525	0.3469	2.1559	0.3604	2.1388	0.4621
$\sigma_1$	5.7882	0.2169	5.4286	0.1778	5.4282	0.1782	5.4306	0.179
$\sigma_2$	1.407	0.0293	1.2761	0.0281	1.2762	0.0282	1.2759	0.0283
$p_{11}$	0.8446	0.0189	0.8961	0.0138	0.8961	0.0138	0.8961	0.0138
$p_{22}$	0.9503	0.0064	0.9516	0.0066	0.9516	0.0066	0.9516	0.0066
$\phi$	-	-	-	-	0.0499	0.0417	-0.0902	1.9193
$\theta$	-	-	0.0502	0.0359	-	-	0.1382	1.8389
$L$	<b>-3605.945</b>		<b>-3612.4253</b>		<b>-3612.456</b>		<b>3612.4100</b>	

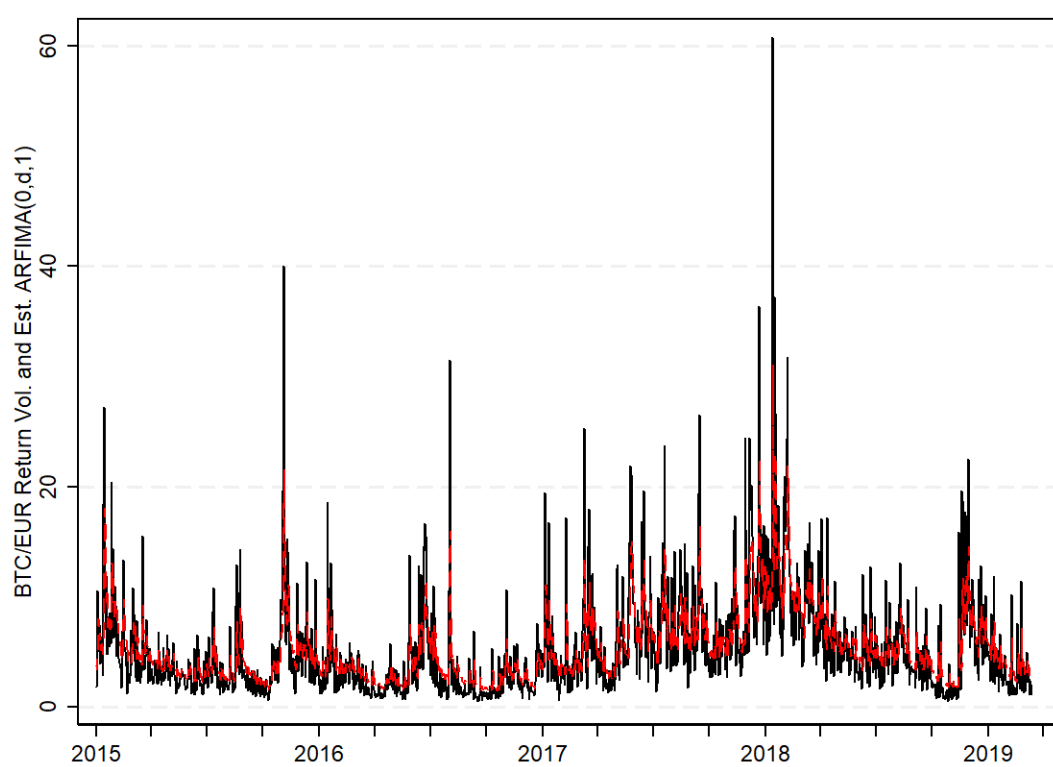
Note:  $d$ : long memory,  $\mu$ : mean,  $\sigma$ : standard deviation,  $P$ : transition probability,  $\phi$ : Auto-regressive parameter,  $\theta$ : Moving average parameter,  $L$ : Log-likelihood of switching model,  $S.E$ : standard error

Figure B.6 BTC/USD Exchange rates return volatility and the estimated values of ARFIMA model



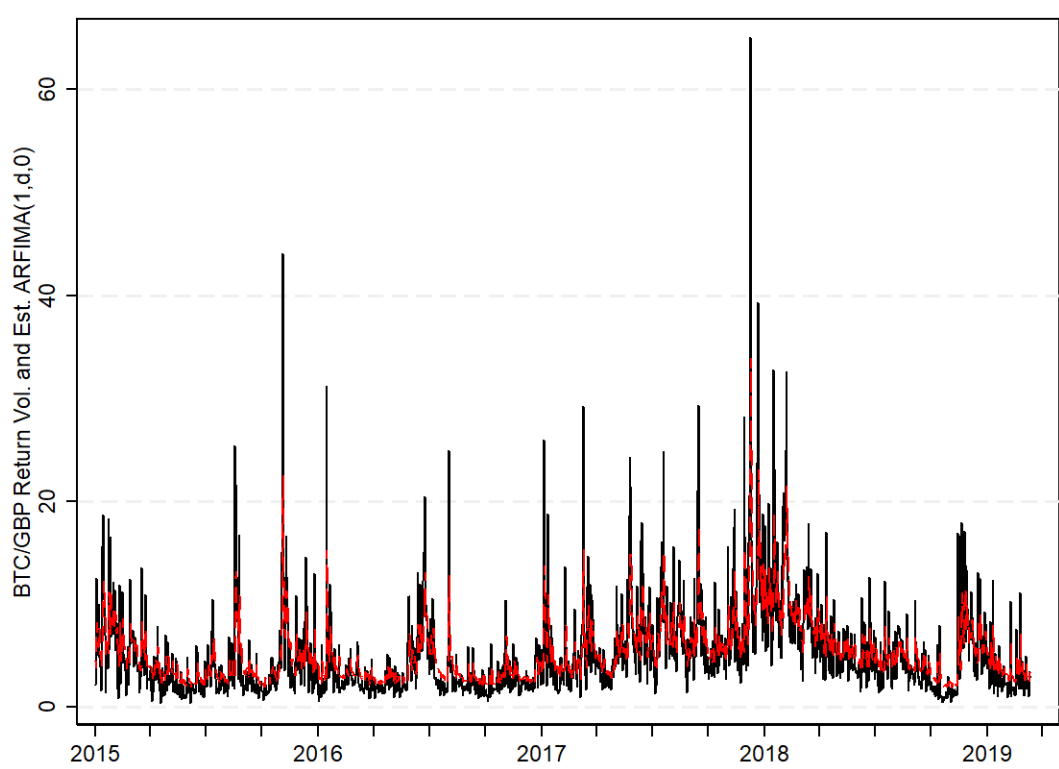
*Note:* Black solid line represents the Bitcoin exchange rate volatility, red dotted line represents the fitted value from ARFIMA model. X-axis represents a daily data from 2015 to 2019, ticks are quarterly.

Figure B.7 BTC/EUR Exchange rates return volatility and the estimated values of ARFIMA model



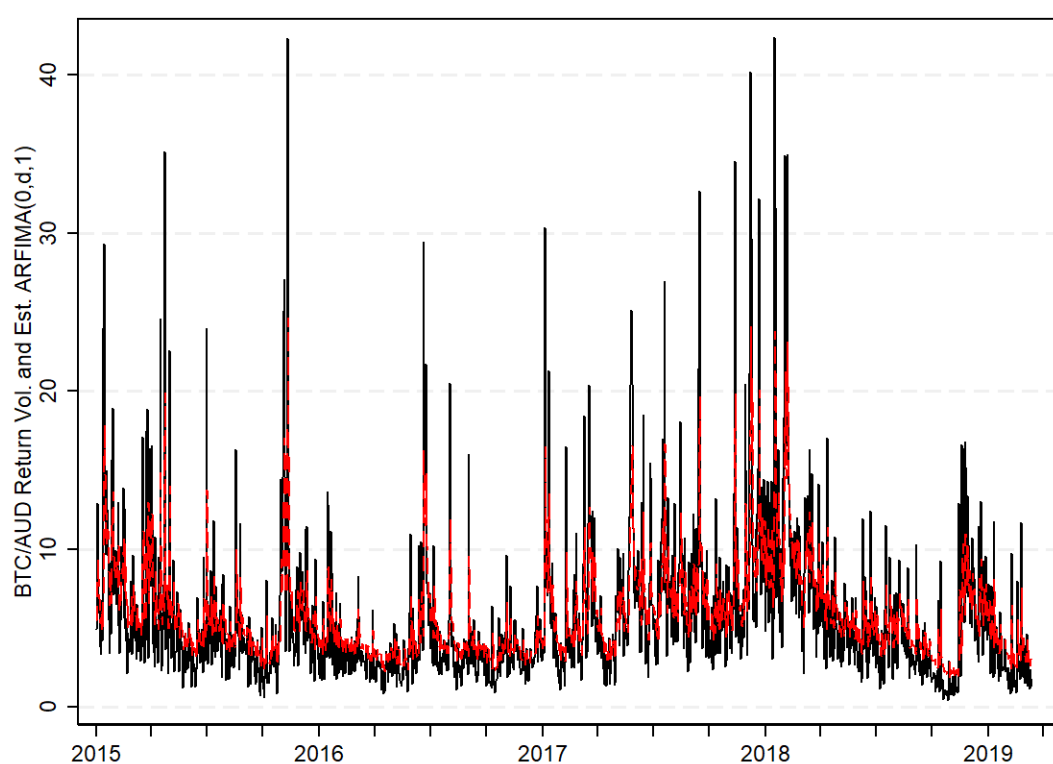
Note: Black solid line represents the Bitcoin exchange rate volatility, red dotted line represents the fitted value from ARFIMA model. X-axis represents a daily data from 2015 to 2019, ticks are quarterly.

Figure B.8 BTC/GBP Exchange rates return volatility and the estimated values of ARFIMA model



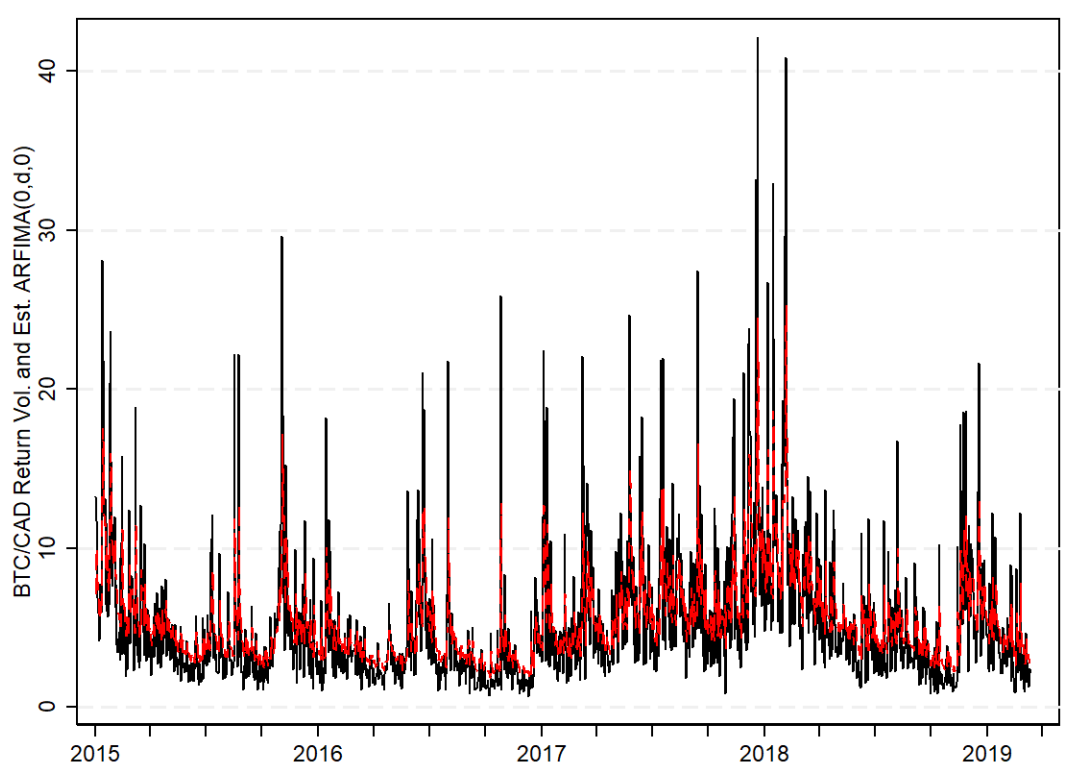
*Note:* Black solid line represents the Bitcoin exchange rate volatility, red dotted line represents the fitted value from ARFIMA model. X-axis represents a daily data from 2015 to 2019, ticks are quarterly.

Figure B.9 BTC/AUD Exchange rates return volatility and the estimated values of ARFIMA model



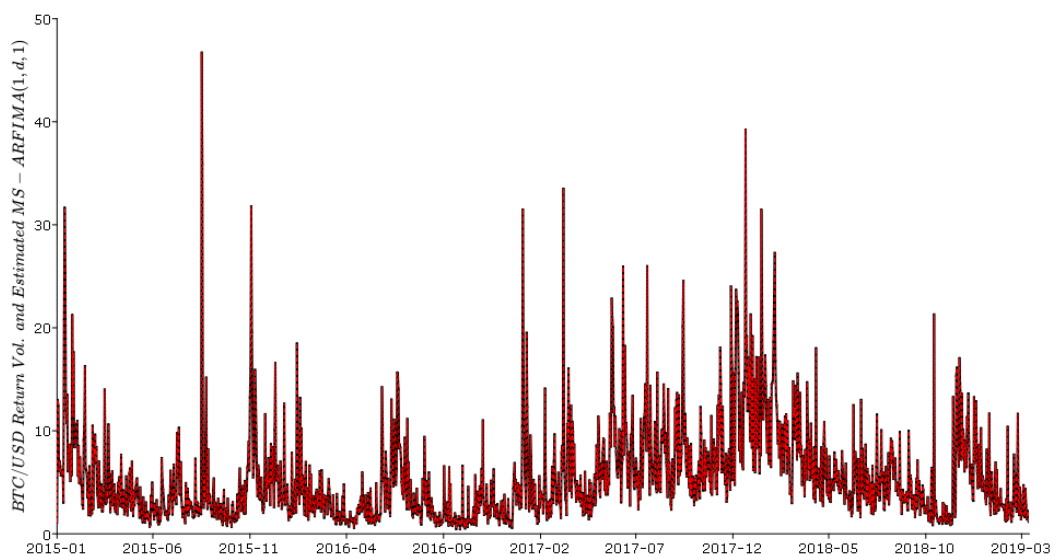
Note: Black solid line represents the Bitcoin exchange rate volatility, red dotted line represents the fitted value from ARFIMA model. X-axis represents a daily data from 2015 to 2019, ticks are quarterly.

Figure B.10 BTC/CAD Exchange rates return volatility and the estimated values of ARFIMA model



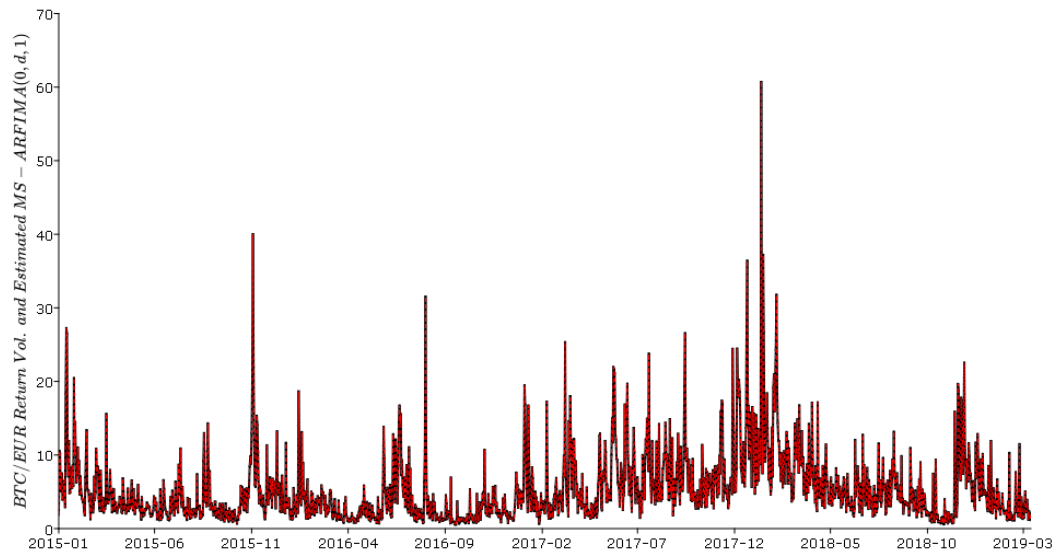
*Note:* Black solid line represents the Bitcoin exchange rate volatility, red dotted line represents the fitted value from ARFIMA model. X-axis represents a daily data from 2015 to 2019, ticks are quarterly.

Figure B.11 BTC/USD Exchange rates return volatility and the estimated values of MS-ARFIMA model



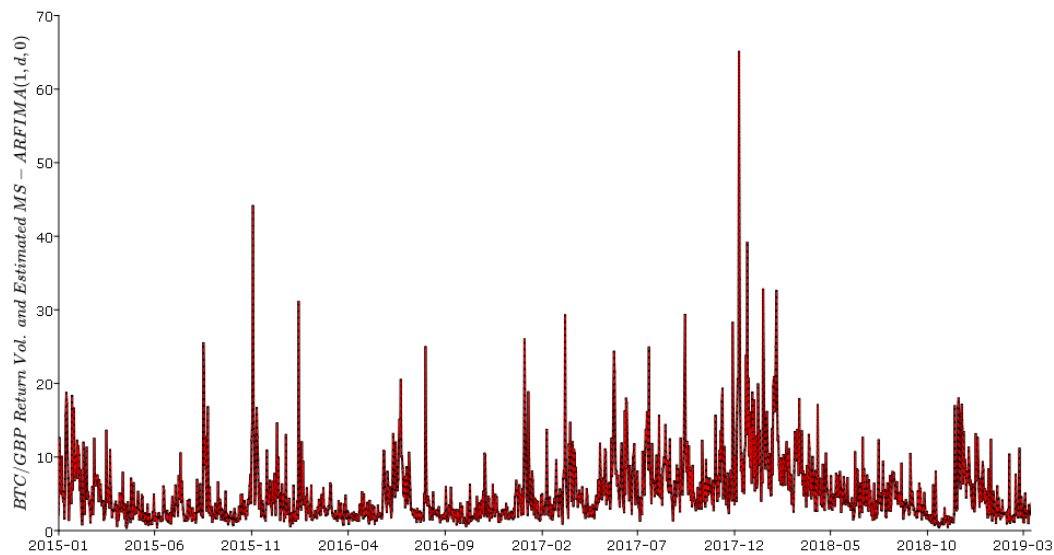
*Note:* Black solid line represents the Bitcoin exchange rate volatility, red dotted line represents the fitted value from MS-ARFIMA model. X-axis represents a daily data from 2015 to 2019, ticks are quarterly.

Figure B.12 BTC/EUR Exchange rates return volatility and the estimated values of MS-ARFIMA model



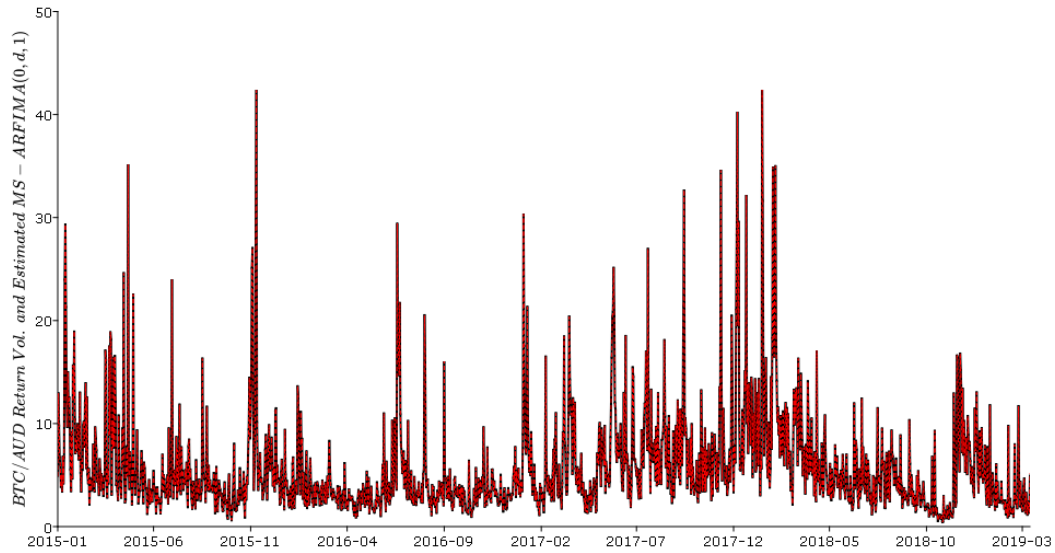
Note: Black solid line represents the Bitcoin exchange rate volatility, red dotted line represents the fitted value from MS-ARFIMA model. X-axis represents a daily data from 2015 to 2019, ticks are quarterly.

Figure B.13 BTC/GBP Exchange rates return volatility and the estimated values of MS-ARFIMA model



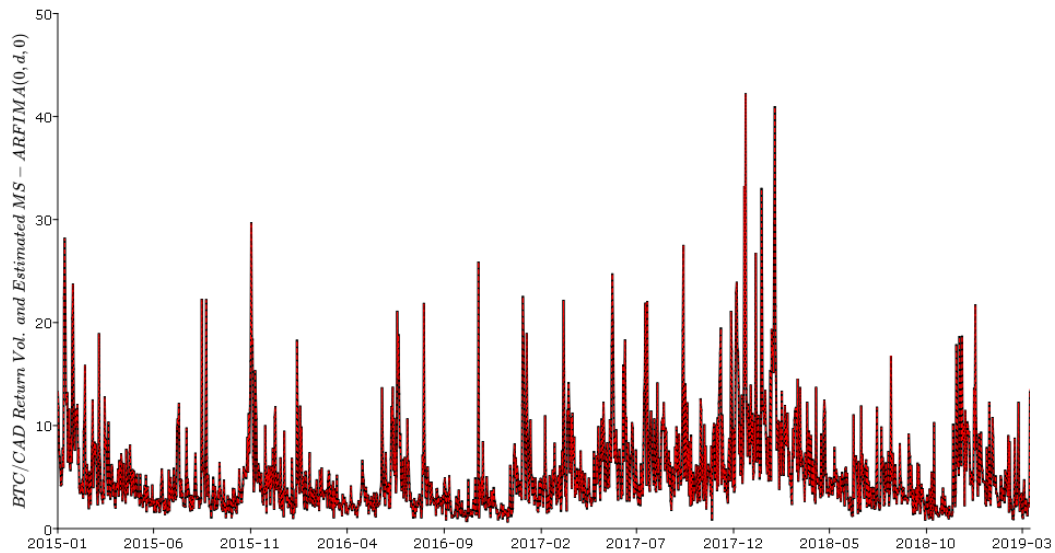
Note: Black solid line represents the Bitcoin exchange rate volatility, red dotted line represents the fitted value from MS-ARFIMA model. X-axis represents a daily data from 2015 to 2019, ticks are quarterly.

Figure B.14 BTC/AUD Exchange rates return volatility and the estimated values of MS-ARFIMA model



Note: Black solid line represents the Bitcoin exchange rate volatility, red dotted line represents the fitted value from MS-ARFIMA model. X-axis represents a daily data from 2015 to 2019, ticks are quarterly.

Figure B.15 BTC/CAD Exchange rates return volatility and the estimated values of MS-ARFIMA model



Note: Black solid line represents the Bitcoin exchange rate volatility, red dotted line represents the fitted value from MS-ARFIMA model. X-axis represents a daily data from 2015 to 2019, ticks are quarterly.

## Appendix C

# Supplement to Chapter 4

Table C.1 Volatility spillovers across six selected exchange rates in time domain – 60-day ahead forecast

	BTC/USD	BTC/EUR	BTC/GBP	BTC/JPY	BTC/AUD	BTC/CAD	Directional FROM others
BTC/USD	22.34	16.81	17.14	14.57	12.88	16.27	77.66
BTC/EUR	16.82	23.25	16.19	14.73	12.86	16.15	76.75
BTC/GBP	17.69	16.49	22.28	14.71	12.82	16.01	77.72
BTC/JPY	15.88	16.35	15.44	23.08	13.64	15.61	76.92
BTC/AUD	15.10	15.62	14.80	14.96	24.51	15.00	75.49
BTC/CAD	16.63	16.48	15.83	14.90	13.30	22.86	77.14
Directional TO others	82.12	81.75	79.41	73.88	65.50	79.03	<b><i>TSI: 76.95%</i></b>

*Note:* Data cover the period from January 1, 2015 to May 31, 2019. The rightmost (**FROM**) column gives total directional connectedness (from). The bottom (**TO**) row gives total directional connectedness (to). Numbers are in percentage. The bottom-right element (in boldface) is total connectedness (see also F. Diebold & Yilmaz, 2014).

Table C.2 Volatility spillovers across six selected exchange rates in time domain – 90-day ahead forecast

	BTC/USD	BTC/EUR	BTC/GBP	BTC/JPY	BTC/AUD	BTC/CAD	Directional FROM others
BTC/USD	22.34	16.81	17.14	14.57	12.88	16.27	77.66
BTC/EUR	16.82	23.25	16.19	14.73	12.86	16.15	76.75
BTC/GBP	17.69	16.49	22.28	14.71	12.82	16.01	77.72
BTC/JPY	15.88	16.35	15.44	23.08	13.64	15.61	76.92
BTC/AUD	15.10	15.62	14.80	14.96	24.51	15.00	75.49
BTC/CAD	16.63	16.48	15.83	14.90	13.30	22.86	77.14
Directional TO others	82.12	81.75	79.41	73.88	65.50	79.03	<i>TSI: 76.95%</i>

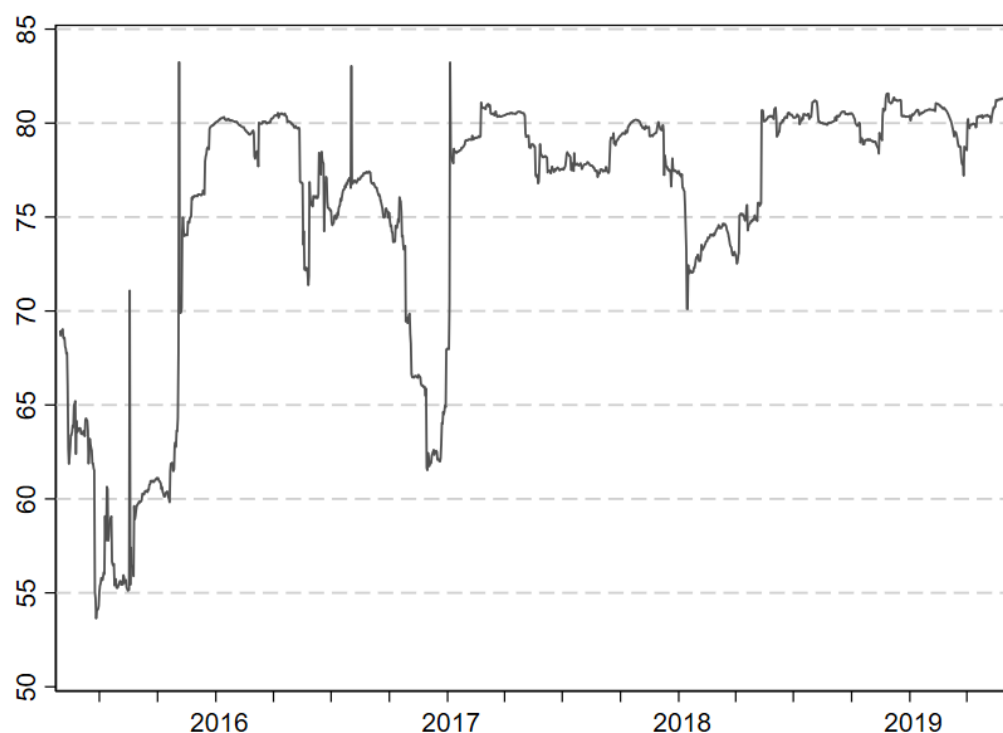
*Note:* Data cover the period from January 1, 2015 to May 31, 2019. The rightmost (**FROM**) column gives total directional connectedness (from). The bottom (**TO**) row gives total directional connectedness (to). Numbers are in percentage. The bottom-right element (in boldface) is total connectedness (see also F. Diebold & Yilmaz, 2014).

Table C.3 Volatility spillovers across six selected exchange rates in time domain – 120-day ahead forecast

	BTC/USD	BTC/EUR	BTC/GBP	BTC/JPY	BTC/AUD	BTC/CAD	Directional FROM others
BTC/USD	22.34	16.81	17.14	14.57	12.88	16.27	77.66
BTC/EUR	16.82	23.25	16.19	14.73	12.86	16.15	76.75
BTC/GBP	17.69	16.49	22.28	14.71	12.82	16.01	77.72
BTC/JPY	15.88	16.35	15.44	23.08	13.64	15.61	76.92
BTC/AUD	15.10	15.62	14.80	14.96	24.51	15.00	75.49
BTC/CAD	16.63	16.48	15.83	14.90	13.30	22.86	77.14
Directional TO others	82.12	81.75	79.41	73.88	65.50	79.03	<i>TSI: 76.95%</i>

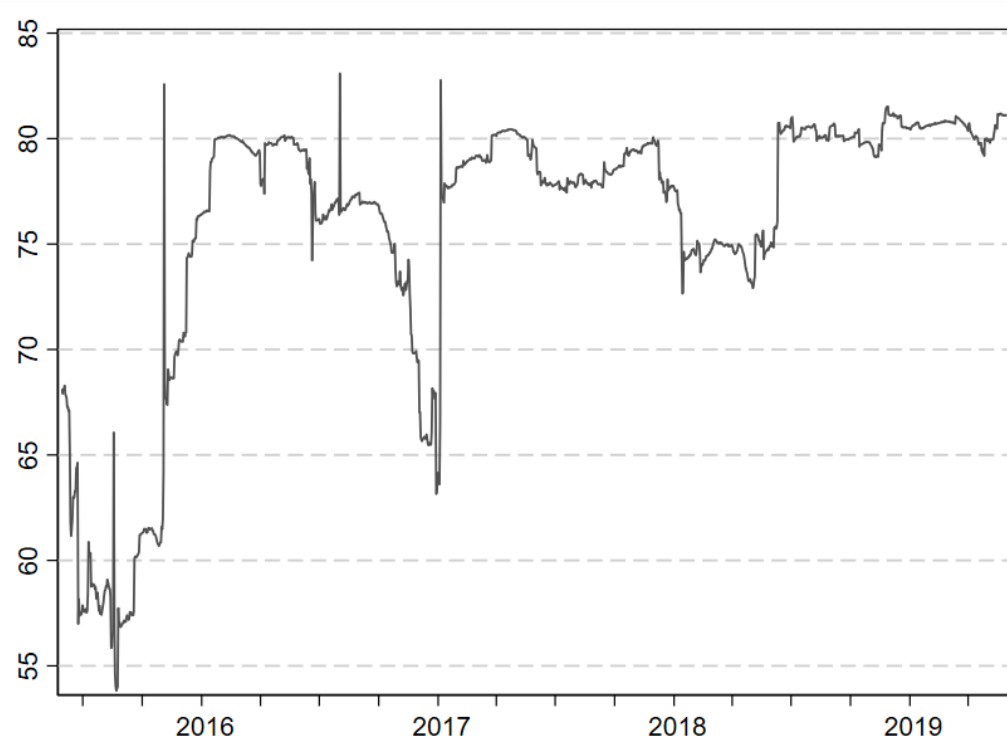
*Note:* Data cover the period from January 1, 2015 to May 31, 2019. The rightmost (**FROM**) column gives total directional connectedness (from). The bottom (**TO**) row gives total directional connectedness (to). Numbers are in percentage. The bottom-right element (in boldface) is total connectedness (see also F. Diebold & Yilmaz, 2014).

Figure C.1 Overall volatility spillovers (dynamic plot), 15-120-Day Rolling Window



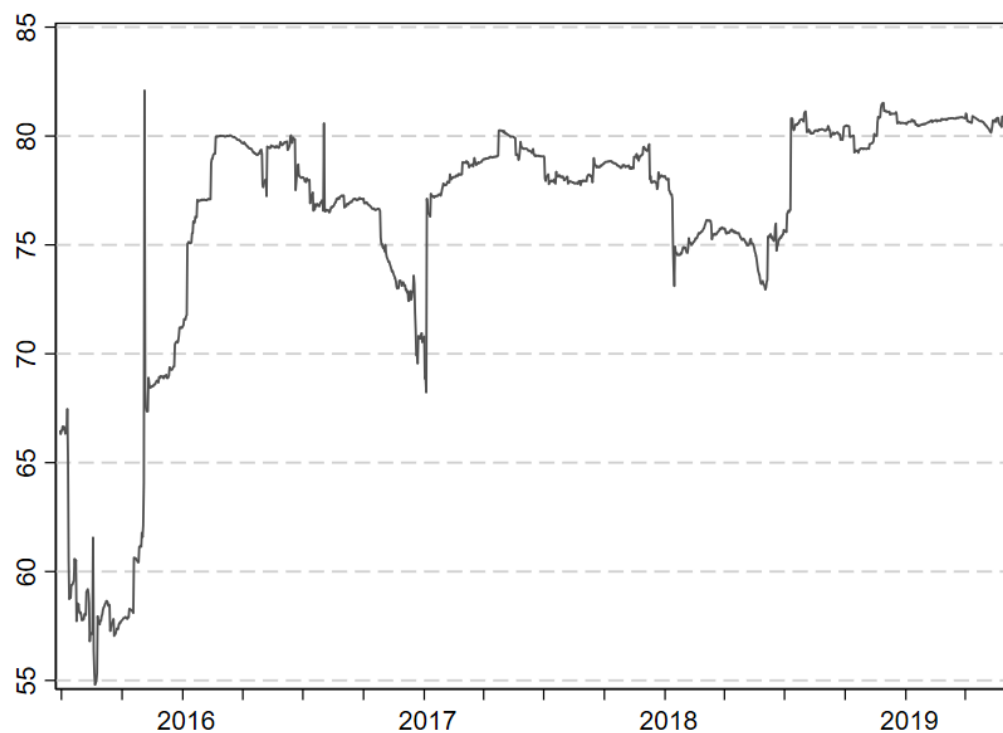
*Note:* Dynamic overall *volatility* spillovers computed following Diebold and Yilmaz (2014) with a 15-120-day rolling window, y-axis scale is in percentages. Dates on the x-axis indicate the start of the year, and ticks are quarterly.

Figure C.2 Overall volatility spillovers (dynamic plot), 15-150-Day Rolling Window



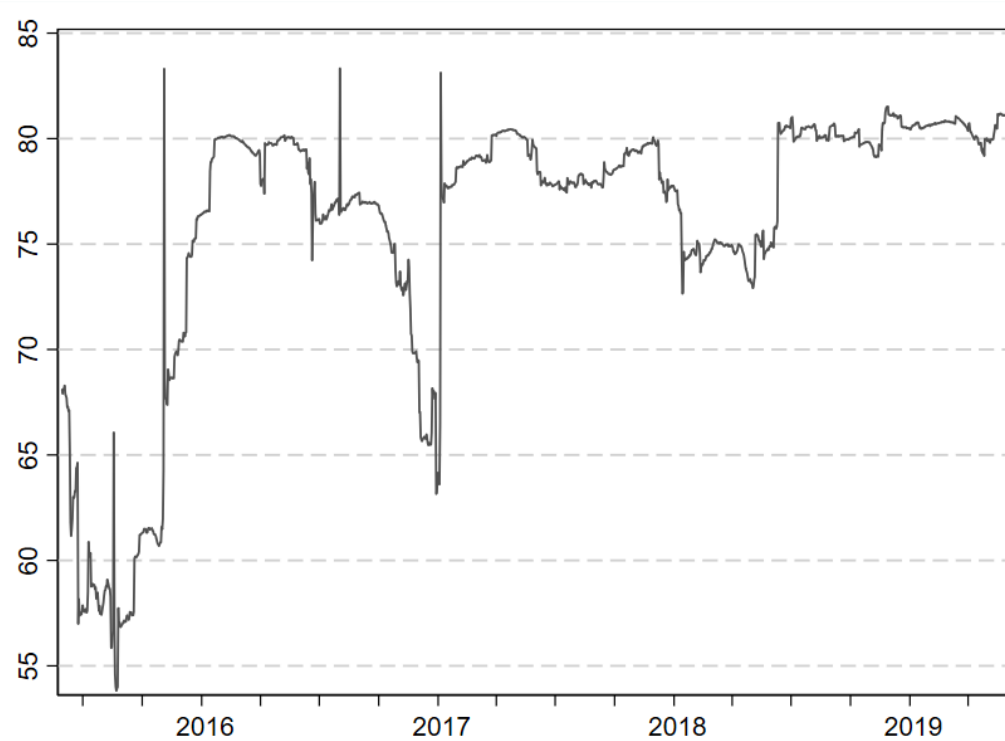
*Note:* Dynamic overall *volatility* spillovers computed following Diebold and Yilmaz (2014) with a 15-150-day rolling window, y-axis scale is in percentages. Dates on the x-axis indicate the start of the year, and ticks are quarterly.

Figure C.3 Overall volatility spillovers (dynamic plot), 15-180-Day Rolling Window



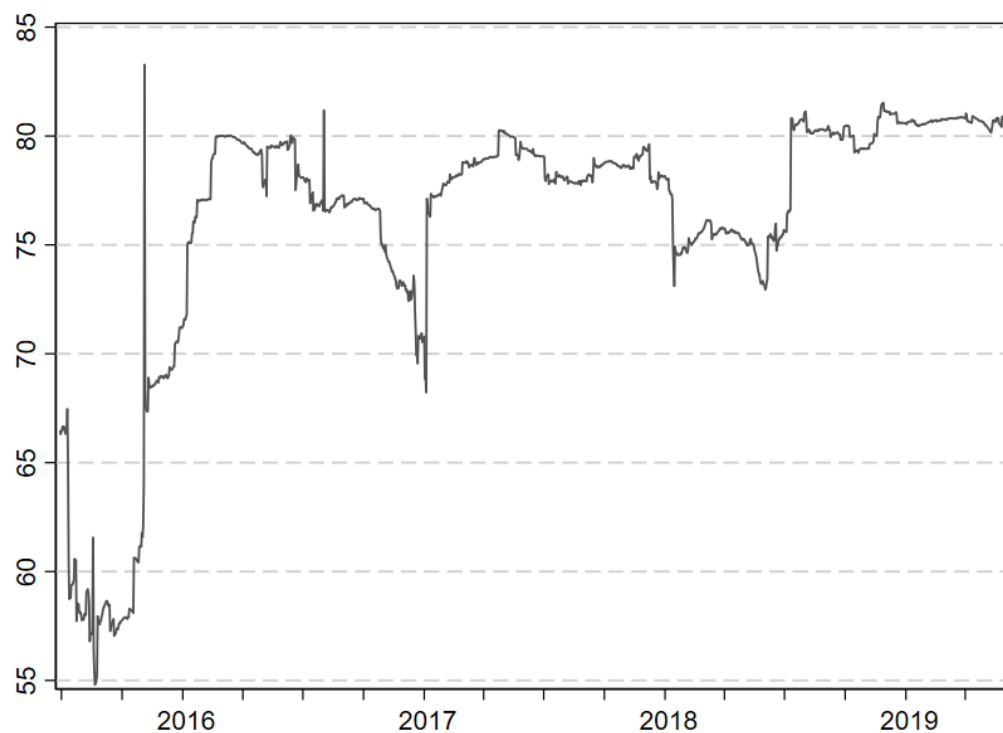
Note: Dynamic overall *volatility* spillovers computed following Diebold and Yilmaz (2014) with a 15-180-day rolling window, y-axis scale is in percentages. Dates on the x-axis indicate the start of the year, and ticks are quarterly.

Figure C.4 Overall volatility spillovers (dynamic plot), 30-150-Day Rolling Window



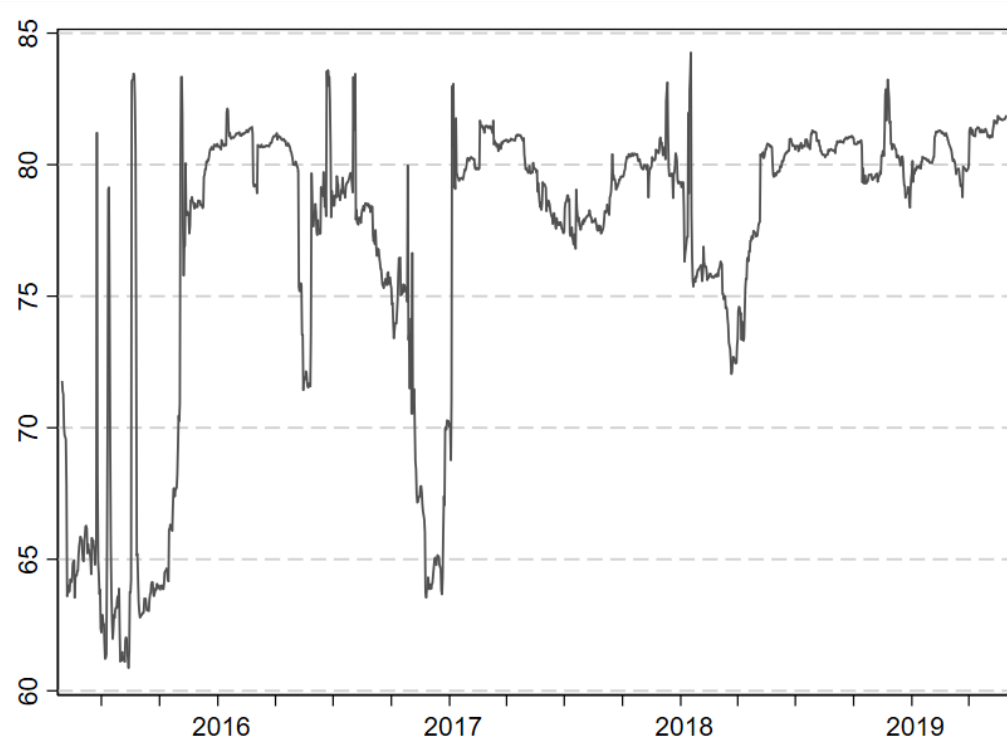
*Note:* Dynamic overall *volatility* spillovers computed following Diebold and Yilmaz (2014) with a 30-150-day rolling window, y-axis scale is in percentages. Dates on the x-axis indicate the start of the year, and ticks are quarterly.

Figure C.5 Overall volatility spillovers (dynamic plot), 30-180-Day Rolling Window



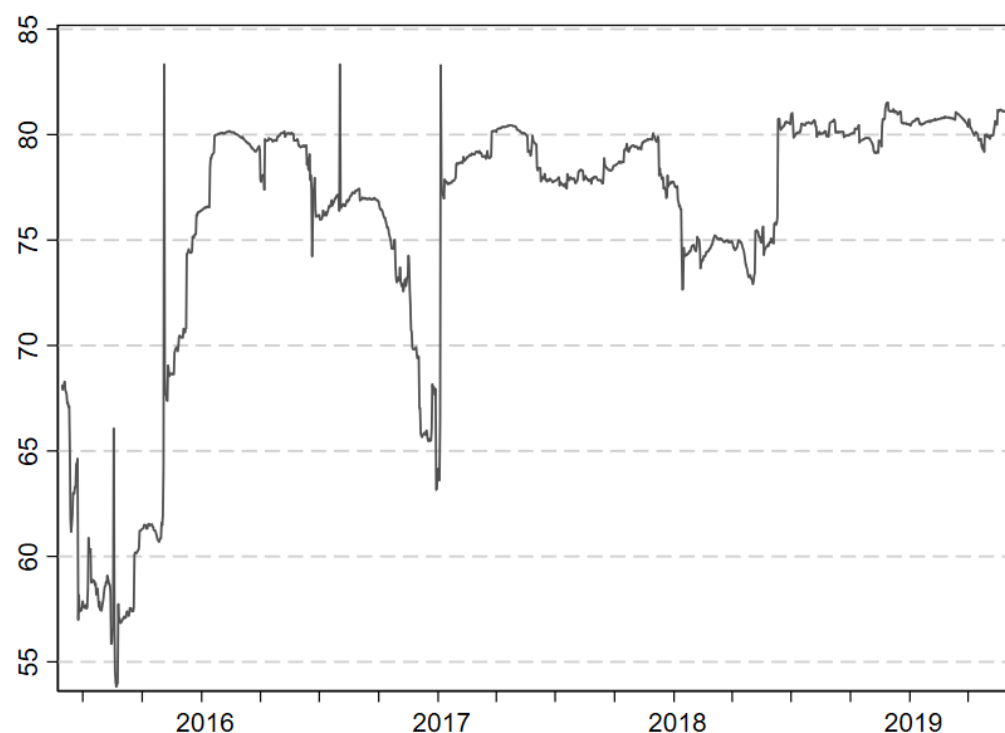
*Note:* Dynamic overall *volatility* spillovers computed following Diebold and Yilmaz (2014) with a 30-180-day rolling window, y-axis scale is in percentages. Dates on the x-axis indicate the start of the year, and ticks are quarterly.

Figure C.6 Overall volatility spillovers (dynamic plot), 60-120-Day Rolling Window



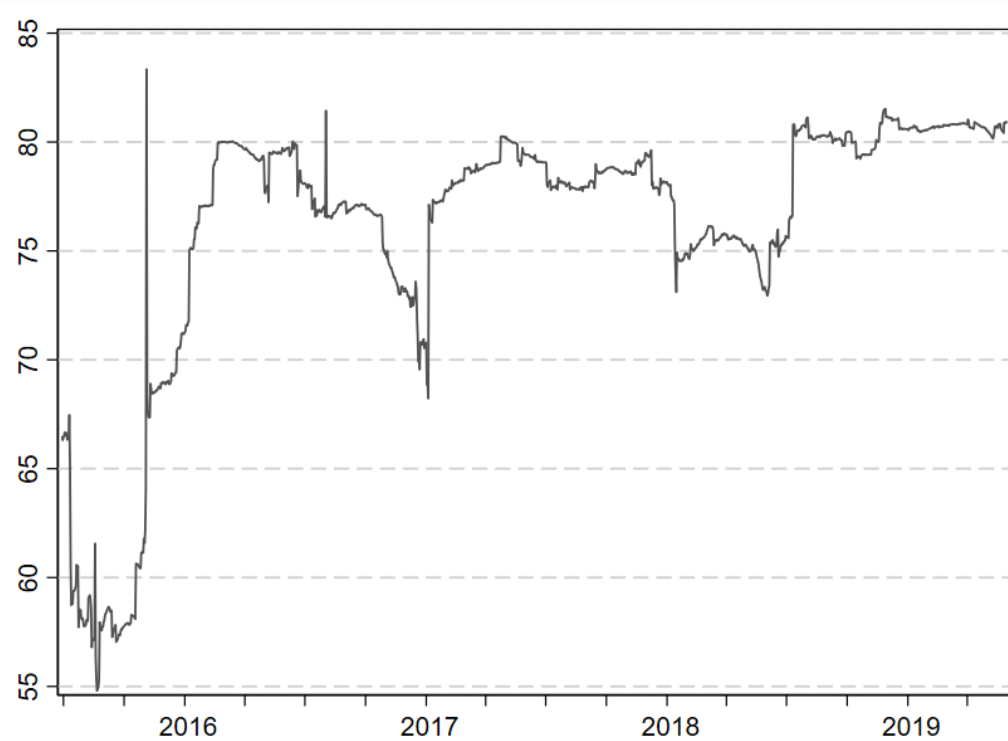
*Note:* Dynamic overall *volatility* spillovers computed following Diebold and Yilmaz (2014) with a 60-120-day rolling window, y-axis scale is in percentages. Dates on the x-axis indicate the start of the year, and ticks are quarterly.

Figure C.7 Overall volatility spillovers (dynamic plot), 60-150-Day Rolling Window



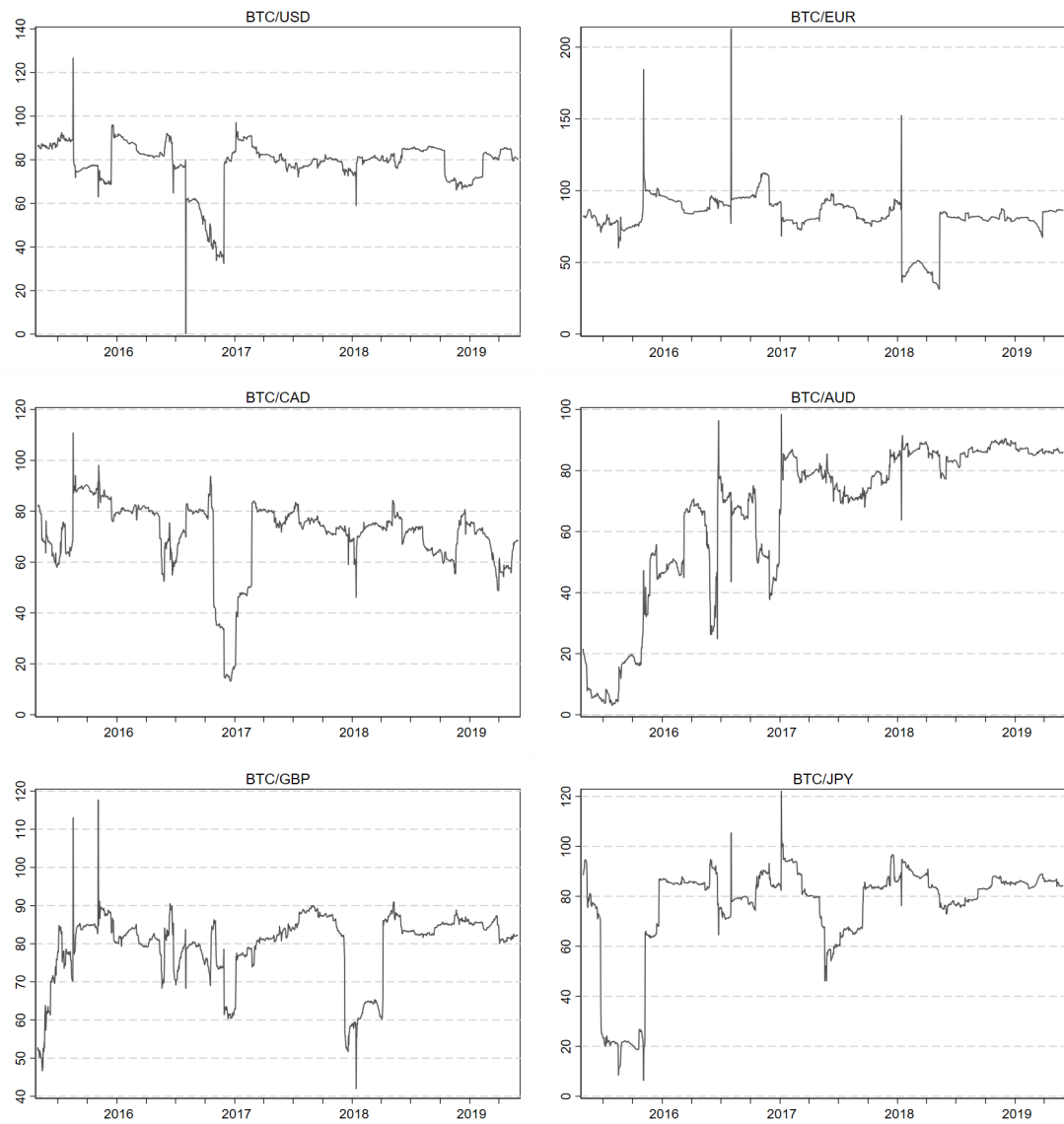
*Note:* Dynamic overall *volatility* spillovers computed following Diebold and Yilmaz (2014) with a 60-150-day rolling window, y-axis scale is in percentages. Dates on the x-axis indicate the start of the year, and ticks are quarterly.

Figure C.8 Overall volatility spillovers (dynamic plot), 60-180-Day Rolling Window



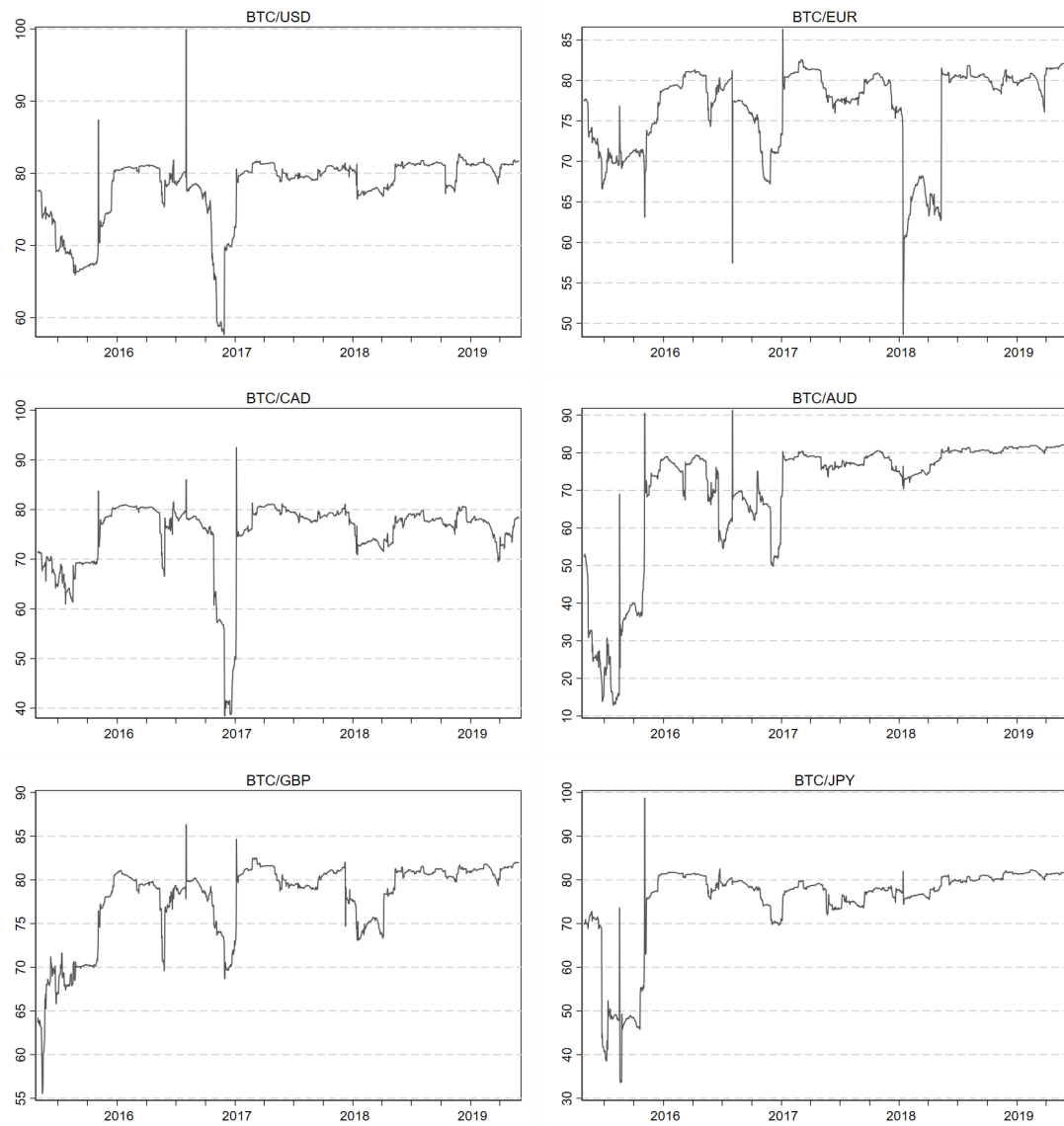
*Note:* Dynamic overall *volatility* spillovers computed following Diebold and Yilmaz (2014) with a 60-180-day rolling window, y-axis scale is in percentages. Dates on the x-axis indicate the start of the year, and ticks are quarterly.

Figure C.9 Volatility spillovers to others, dynamic plot



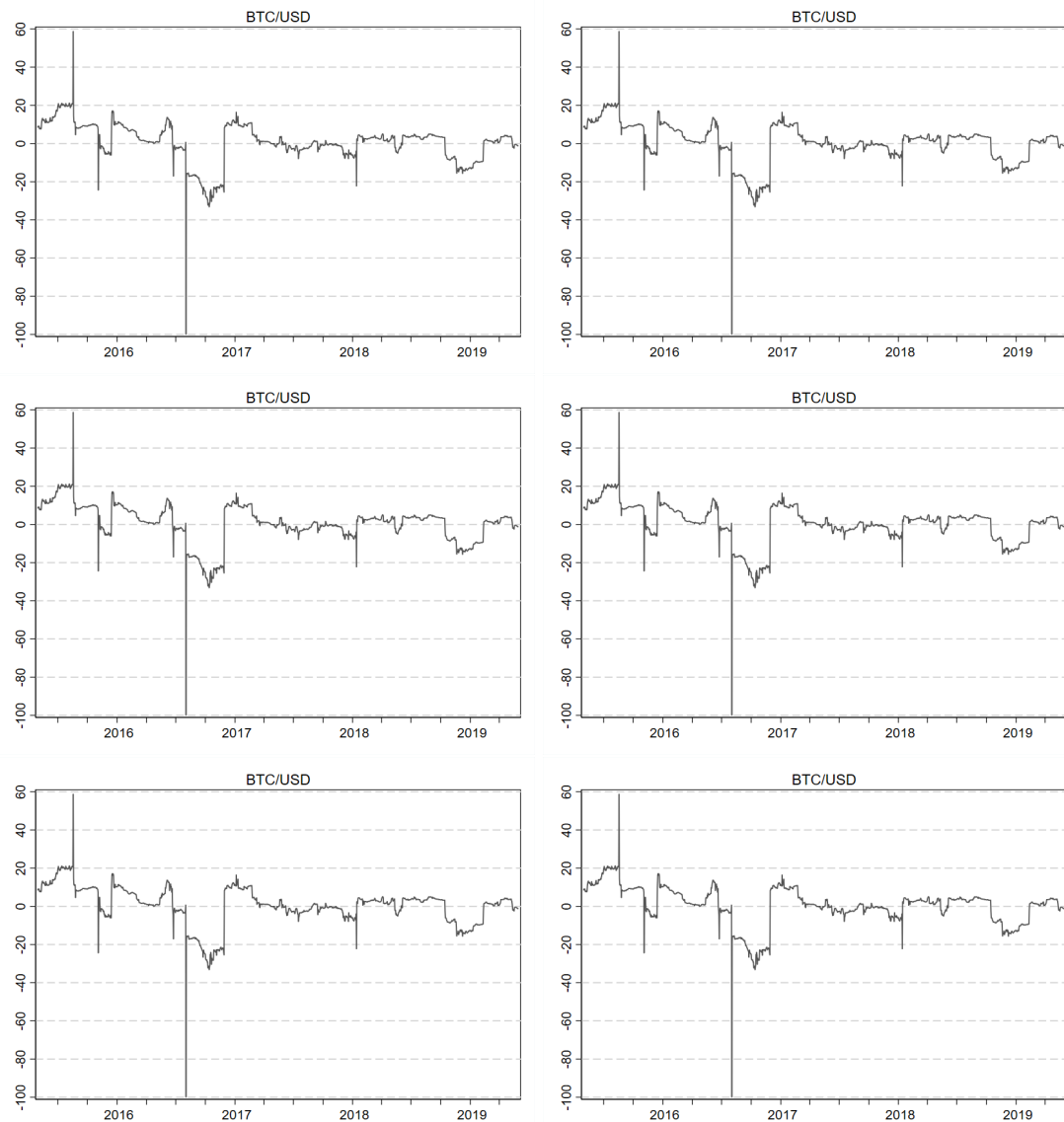
*Note:* series, daily. Dates on the x-axis indicate the start of the year, and ticks are quarterly.

Figure C.10 Volatility spillovers from others, dynamic plot



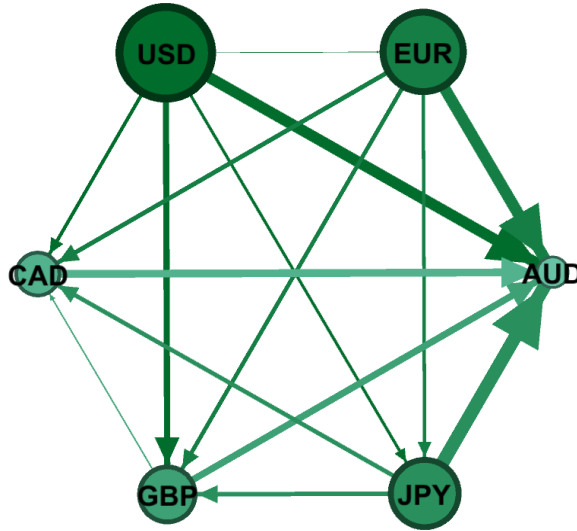
*Note:* series, daily. Dates on the x-axis indicate the start of the year, and ticks are quarterly.

Figure C.11 Net Volatility spillovers, dynamic plot



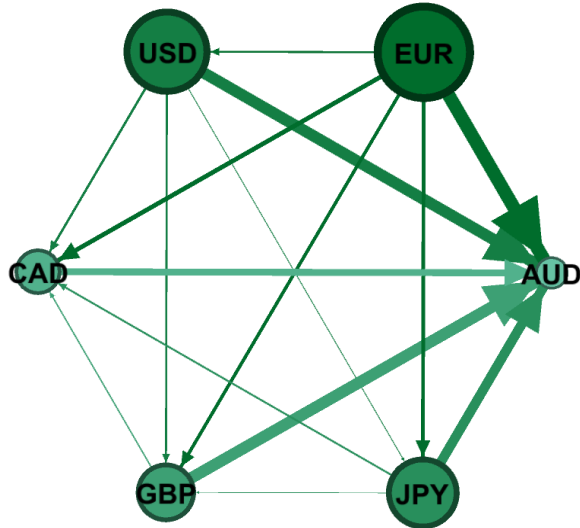
*Note:* series, daily. Dates on the x-axis indicate the start of the year, and ticks are quarterly.

Figure C.12 Directional-volatility connectedness network, 22/05/2015



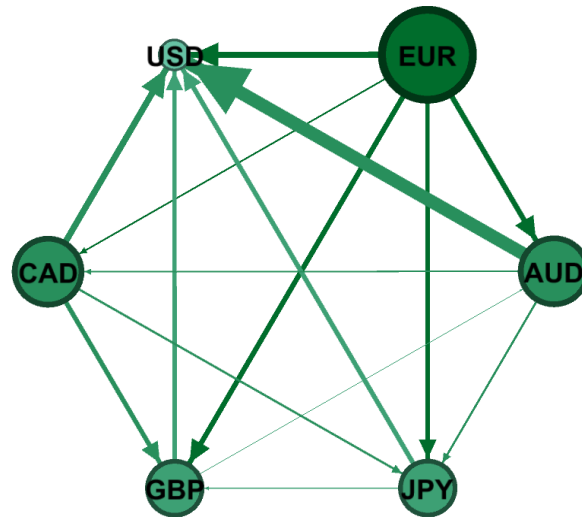
*Note:* The Nodes are the bitcoin markets and the link between two nodes (edge) is given by net pairwise directional connectedness. The edge size shows the magnitude of the net contribution of bitcoin markets in terms of net pairwise directional connectedness.

Figure C.13 Directional-volatility connectedness network, 15/02/2016



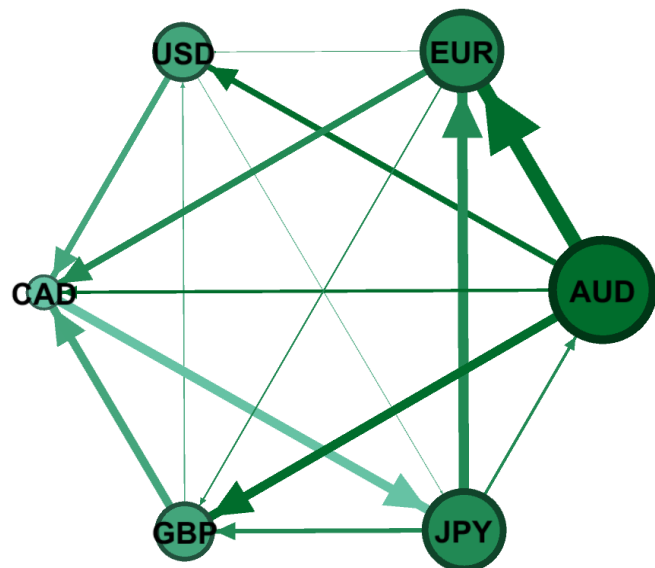
*Note:* The Nodes are the bitcoin markets and the link between two nodes (edge) is given by net pairwise directional connectedness. The edge size shows the magnitude of the net contribution of bitcoin markets in terms of net pairwise directional connectedness.

Figure C.14 Directional-volatility connectedness network, 13/10/2016



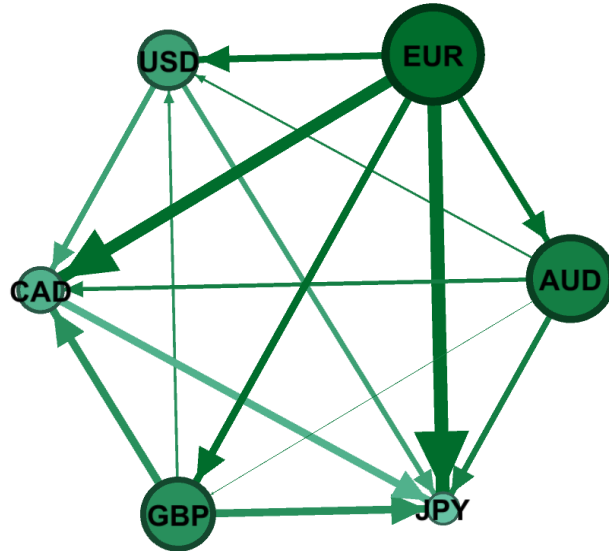
*Note:* The Nodes are the bitcoin markets and the link between two nodes (edge) is given by net pairwise directional connectedness. The edge size shows the magnitude of the net contribution of bitcoin markets in terms of net pairwise directional connectedness.

Figure C.15 Directional-volatility connectedness network, 26/04/2017



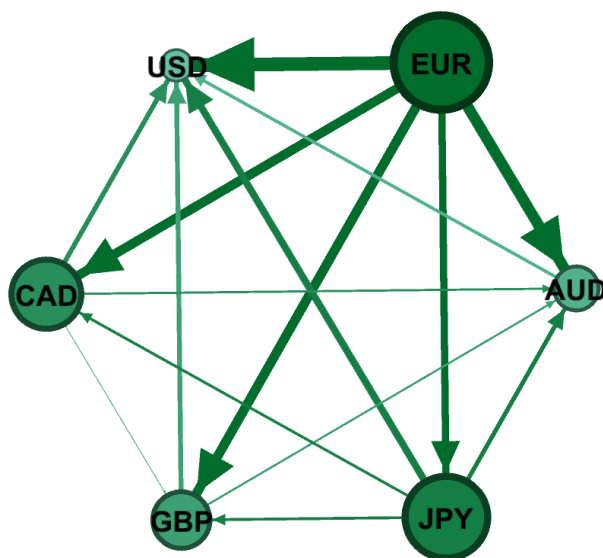
*Note:* The Nodes are the bitcoin markets and the link between two nodes (edge) is given by net pairwise directional connectedness. The edge size shows the magnitude of the net contribution of bitcoin markets in terms of net pairwise directional connectedness.

Figure C.16 Directional-volatility connectedness network, 17/05/2017



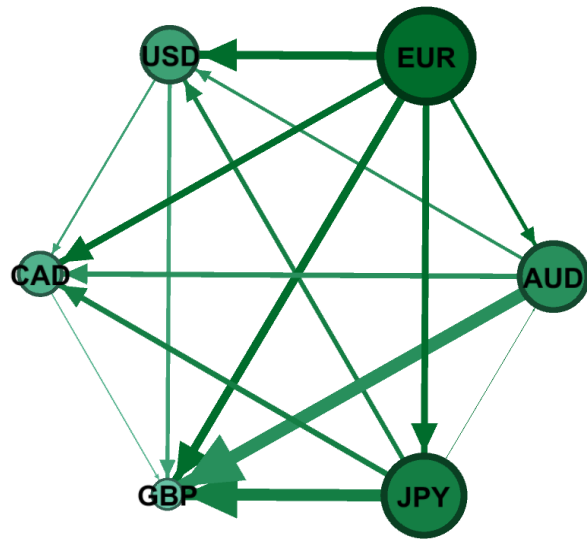
*Note:* The Nodes are the bitcoin markets and the link between two nodes (edge) is given by net pairwise directional connectedness. The edge size shows the magnitude of the net contribution of bitcoin markets in terms of net pairwise directional connectedness.

Figure C.17 Directional-volatility connectedness network, 18/12/2017



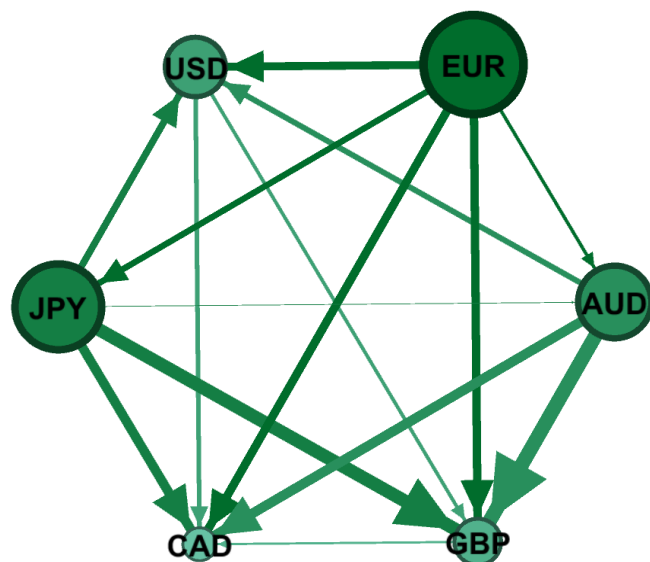
*Note:* The Nodes are the bitcoin markets and the link between two nodes (edge) is given by net pairwise directional connectedness. The edge size shows the magnitude of the net contribution of bitcoin markets in terms of net pairwise directional connectedness.

Figure C.18 Directional-volatility connectedness network, 26/12/2017



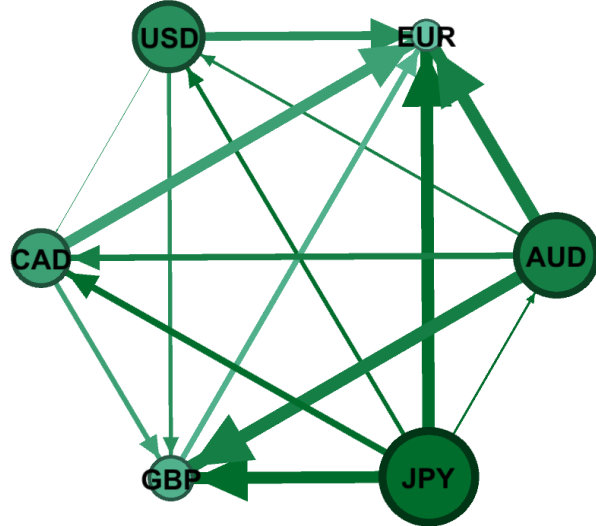
*Note:* The Nodes are the bitcoin markets and the link between two nodes (edge) is given by net pairwise directional connectedness. The edge size shows the magnitude of the net contribution of bitcoin markets in terms of net pairwise directional connectedness.

Figure C.19 Directional-volatility connectedness network, 07/01/2018



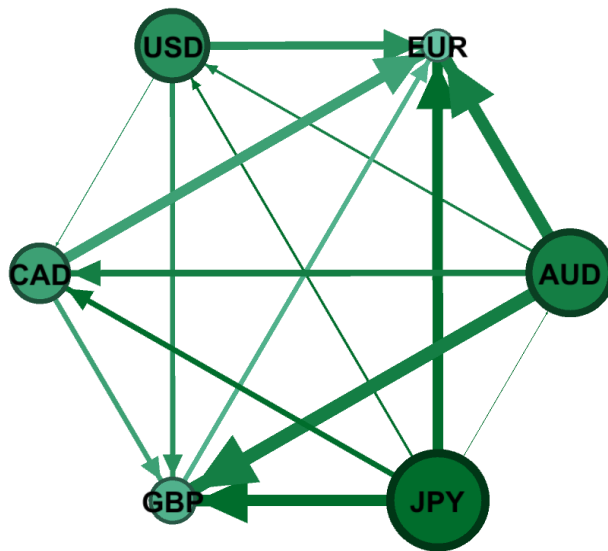
*Note:* The Nodes are the bitcoin markets and the link between two nodes (edge) is given by net pairwise directional connectedness. The edge size shows the magnitude of the net contribution of bitcoin markets in terms of net pairwise directional connectedness.

Figure C.20 Directional-volatility connectedness network, 15/02/2018



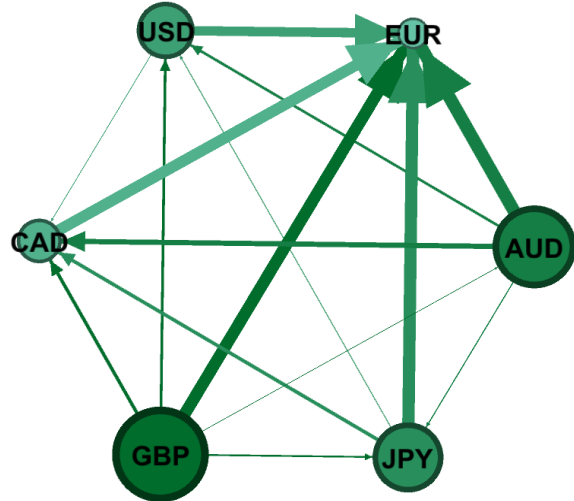
*Note:* The Nodes are the bitcoin markets and the link between two nodes (edge) is given by net pairwise directional connectedness. The edge size shows the magnitude of the net contribution of bitcoin markets in terms of net pairwise directional connectedness.

Figure C.21 Directional-volatility connectedness network, 04/03/2018



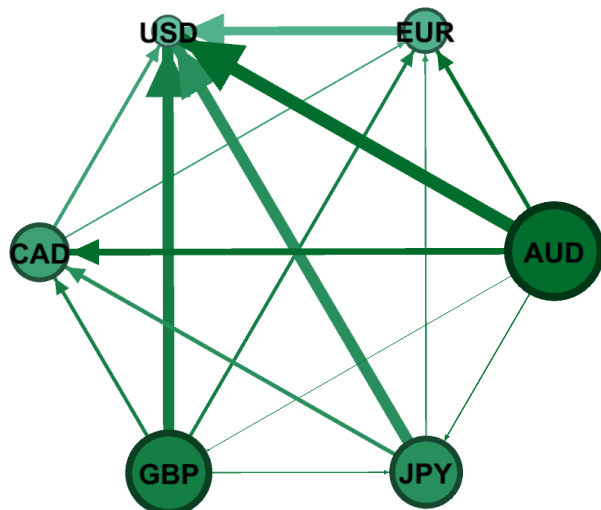
*Note:* The Nodes are the bitcoin markets and the link between two nodes (edge) is given by net pairwise directional connectedness. The edge size shows the magnitude of the net contribution of bitcoin markets in terms of net pairwise directional connectedness.

Figure C.22 Directional-volatility connectedness network, 12/04/2018



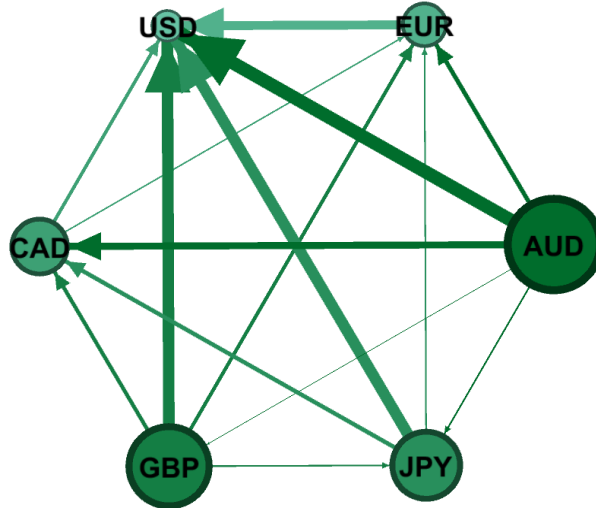
*Note:* The Nodes are the bitcoin markets and the link between two nodes (edge) is given by net pairwise directional connectedness. The edge size shows the magnitude of the net contribution of bitcoin markets in terms of net pairwise directional connectedness.

Figure C.23 Directional-volatility connectedness network, 21/12/2018



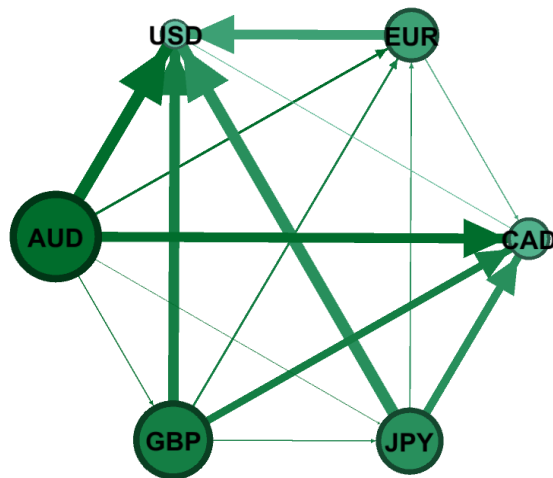
*Note:* The Nodes are the bitcoin markets and the link between two nodes (edge) is given by net pairwise directional connectedness. The edge size shows the magnitude of the net contribution of bitcoin markets in terms of net pairwise directional connectedness.

Figure C.24 Directional-volatility connectedness network, 27/12/2018



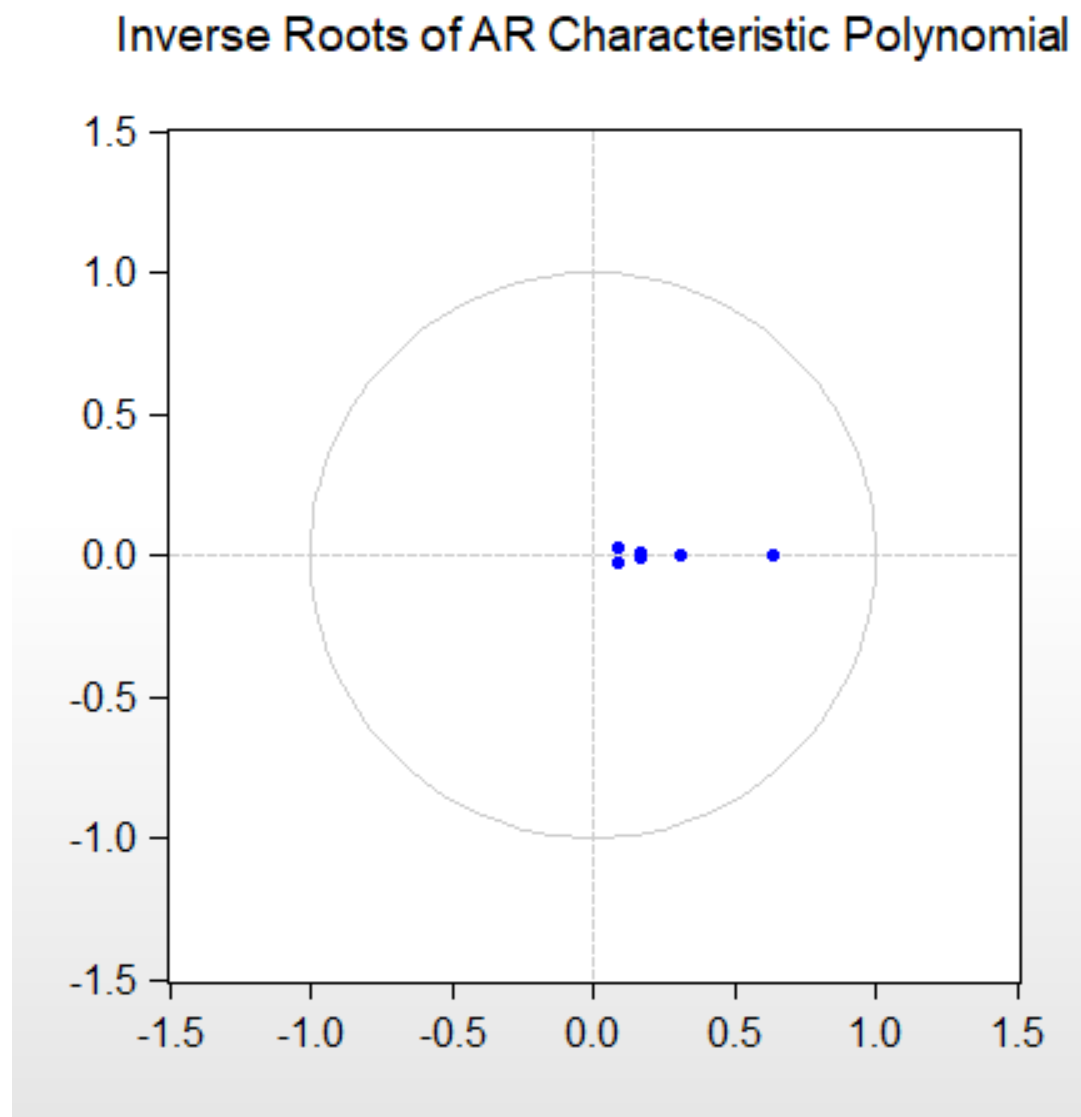
*Note:* The Nodes are the bitcoin markets and the link between two nodes (edge) is given by net pairwise directional connectedness. The edge size shows the magnitude of the net contribution of bitcoin markets in terms of net pairwise directional connectedness.

Figure C.25 Directional-volatility connectedness network, 26/01/2019



*Note:* The Nodes are the bitcoin markets and the link between two nodes (edge) is given by net pairwise directional connectedness. The edge size shows the magnitude of the net contribution of bitcoin markets in terms of net pairwise directional connectedness.

Figure C.26





# References

Abhishta, A., Joosten, R., Dragomiretskiy, S., & Nieuwenhuis, L. J. (2019). Impact of successful ddos attacks on a major crypto-currency exchange. In *2019 27th euromicro international conference on parallel, distributed and network-based processing (pdp)* (pp. 379–384).

Abiad, M. A. (2003). *Early warning systems: A survey and a regime-switching approach* (No. 3-32). International Monetary Fund.

Ahamad, S., Nair, M., & Varghese, B. (2013). A survey on crypto currencies. In *4th international conference on advances in computer science, aetacs* (pp. 42–48).

Alba, J. D. (1999). Are there systematic relationships between china's and southeast asia's exchange rates? evidence from dailydata. *Asian Economic Journal*, 13(1), 73-92. Retrieved from <https://onlinelibrary.wiley.com/doi/abs/10.1111/1467-8381.00075> doi: 10.1111/1467-8381.00075

Aldcroft, D. H., & Fearon, P. (1972). *British economic fluctuations, 1790-1939*. Springer.

Alexander, C., & Dakos, M. (2020). A critical investigation of cryptocurrency data and analysis. *Quantitative Finance*, 20(2), 173–188.

Alizadeh, S., Brandt, M. W., & Diebold, F. X. (2002). Range-based estimation of stochastic volatility models. *The Journal of Finance*, 57(3), 1047–1091.

Almukaynizi, M., Paliath, M., V. and Shah, Shah, M., & Shakarian, P. (2018). Finding cryptocurrency attack indicators using temporal logic and darkweb data. In *2018 ieee international conference on intelligence and security informatics (isi)* (pp. 91–93).

Alvarez-Ramirez, J., Rodriguez, E., & Ibarra-Valdez, C. (2018). Long-range correlations and asymmetry in the Bitcoin market. *Physica A: Statistical Mechanics and its Applications*, 492(C), 948-955.

Al-Yahyaee, K. H., Mensi, W., & Yoon, S.-M. (2018). Efficiency, multifractality, and the long-memory property of the bitcoin market: A comparative analysis with stock, currency, and gold markets. *Finance Research Letters*, 27, 228 - 234. Retrieved from <http://www.sciencedirect.com/science/article/pii/S1544612318300242> doi: <https://doi.org/10.1016/j.frl.2018.03.017>

Andersen, T. G., & Bollerslev, T. (1997). Intraday periodicity and volatility persistence in financial markets. *Journal of Empirical Finance*, 4(2), 115 - 158. Retrieved from <http://www.sciencedirect.com/science/article/pii/>

S0927539897000042 (High Frequency Data in Finance, Part 1) doi: [https://doi.org/10.1016/S0927-5398\(97\)00004-2](https://doi.org/10.1016/S0927-5398(97)00004-2)

Andersen, T. G., Bollerslev, T., Diebold, F. X., & Labys, P. (2001). The distribution of realized exchange rate volatility. *Journal of the American statistical association*, 96(453), 42–55.

Andersen, T. G., Davis, R. A., Kreiß, J.-P., & Mikosch, T. V. (2009). *Handbook of financial time series*. Springer Science & Business Media.

Antonakakis, N. (2008). Exchange rate volatility comovements and spillovers before and after the introduction of euro: A multivariate garch approach. *Department of Economics, Business School, University of Strathclyde*.

Antonakakis, N. (2012). Exchange return co-movements and volatility spillovers before and after the introduction of euro. *Journal of International Financial Markets, Institutions and Money*, 22(5), 1091-1109. Retrieved from <https://ideas.repec.org/a/eee/intfin/v22y2012i5p1091-1109.html> doi: 10.1016/j.intfin.2012.06.

Bai, J. (1994). Least squares estimation of a shift in linear processes. *Journal of Time Series Analysis*, 15(5), 453–472.

Bai, J., & Perron, P. (1998). Estimating and testing linear models with multiple structural changes. *Econometrica*, 47–78.

Bai, J., & Perron, P. (2003). Computation and analysis of multiple structural change models. *Journal of applied econometrics*, 18(1), 1–22.

Baillie, R. T. (1996). Long memory processes and fractional integration in econometrics. *Journal of econometrics*, 73(1), 5–59.

Baillie, R. T., & Bollerslev, T. (1991). Intra-day and inter-market volatility in foreign exchange rates. *The Review of Economic Studies*, 58(3), 565–585. Retrieved from <http://www.jstor.org/stable/2298012>

Baillie, R. T., Bollerslev, T., & Redfearn. (1993). Bear squeezes, volatility spillovers and speculative attacks in the hyperinflation 1920s foreign exchange. *Journal of International Money and Finance*, 12(5), 511 - 521. Retrieved from <http://www.sciencedirect.com/science/article/pii/026156069390037C> doi: [https://doi.org/10.1016/0261-5606\(93\)90037-C](https://doi.org/10.1016/0261-5606(93)90037-C)

Balcilar, M., Gupta, R., & Jooste, C. (2016). Analyzing south africa's inflation persistence using an arfima model with markov-switching fractional differencing parameter. *The Journal of Developing Areas*, 50(1), 47–57.

Bariviera, A. F. (2017). The inefficiency of bitcoin revisited: A dynamic approach. *Economics Letters*, 161, 1–4.

Bariviera, A. F., Basgall, M. J., Hasperué, W., & Naiouf, M. (2017). Some stylized facts of the bitcoin market. *Physica A: Statistical Mechanics and its Applications*, 484, 82–90.

Baruník, J., & Křehlík, T. (2018). Measuring the frequency dynamics of financial connectedness and systemic risk\*. *Journal of Financial Econometrics*, 16(2), 271-296.

Baruník, J., Kočenda, E., & Vacha, L. (2016). Asymmetric connectedness on the u.s. stock market: Bad and good volatility spillovers. *Journal of Financial Markets*, 27(C), 55-78.

Baur, Hong, K., & Lee, A. D. (2018). Bitcoin: Medium of exchange or speculative assets? *Journal of International Financial Markets, Institutions and Money*, 54, 177–189.

Baur, D., & Dimpfl, T. (2017). Realized bitcoin volatility. *SSRN*, 2949754, 1–26.

Bauwens, L., Hafner, C. M., & Laurent, S. (2012). *Handbook of volatility models and their applications* (Vol. 3). John Wiley & Sons.

Bauwens, L., Laurent, S., & Rombouts, J. V. (2006). Multivariate garch models: a survey. *Journal of applied econometrics*, 21(1), 79–109.

Bazdresch, S., & Werner, A. (2005). Regime switching models for the mexican peso. *Journal of International Economics*, 65(1), 185–201.

Beckers, S. (1983). Variances of security price returns based on high, low, and closing prices. *Journal of Business*, 97–112.

Bennett, C., & Gil, M. A. (2012). *Measuring historical volatility* (Tech. Rep.). Santander Global Banking: & Markets. (Equity Derivatives Division Technical Note)

Beran, J., & Terrin, N. (1994). Estimation of the long-memory parameter, based on a multivariate central limit theorem. *Journal of Time Series Analysis*, 15(3), 269–278.

Berkes, I., Horváth, L., Kokoszka, P., & Shao, Q.-M. (2006). On discriminating between long-range dependence and changes in mean. *The annals of statistics*, 34(3), 1140–1165.

Billio, M., & Monfort, A. (1998). Switching state-space models likelihood function, filtering and smoothing. *Journal of Statistical Planning and Inference*, 68(1), 65–103.

Billio, M., Monfort, A., & Robert, C. P. (1999). Bayesian estimation of switching arma models. *Journal of econometrics*, 93(2), 229–255.

Böhme, R., Christin, N., Edelman, B., & Moore, T. (2015). Bitcoin: Economics, technology, and governance. *Journal of Economic Perspectives*, 29(2), 213–38.

Bollerslev, T. (1986). Generalized autoregressive conditional heteroskedasticity. *Journal of econometrics*, 31(3), 307–327.

Bollerslev, T., Chou, R. Y., & Kroner, K. F. (1992). Arch modeling in finance: A review of the theory and empirical evidence. *Journal of econometrics*, 52(1-2), 5–59.

Bollerslev, T., & Hodrick, R. J. (2017). Financial market efficiency tests. In *Handbook of applied econometrics volume 1: Macroeconomics* (p. 361-399). Wiley-Blackwell. Retrieved from <https://onlinelibrary.wiley.com/doi/abs/10.1111/b.9780631215585.1999.00010.x> doi: 10.1111/b.9780631215585.1999.00010.x

Bouchaud, J.-P., Gefen, Y., Potters, M., & Wyart, M. (2004). Fluctuations and response in financial markets: the subtle nature of ‘random’price changes. *Quantitative finance*, 4(2), 176–190.

Bouri, E., Das, M., Gupta, R., & Roubaud, D. (2018). *Spillovers between bitcoin and other assets during bear and bull markets* (Working Papers No. 201812). University of Pretoria, Department of Economics.

Bouri, E., Gil-Alana, L. A., Gupta, R., & Roubaud, D. (2019). Modelling long memory volatility in the bitcoin market: Evidence of persistence and structural breaks. *International Journal of Finance & Economics*, 24(1), 412–426.

Box, G. E., & Jenkins, G. M. (1970). *Time series analysis: forecasting and control*. San Francisco: Holden-Day.

Brauneis, A., & Mestel, R. (2018). Price discovery of cryptocurrencies: Bitcoin and beyond. *Economics Letters*, 165, 58–61.

Brooks, C. (2014). *Introductory econometrics for finance*. Cambridge university press.

Bubák, V., Kočenda, E., & Žikeš, F. (2011). Volatility transmission in emerging european foreign exchange markets. *Journal of Banking & Finance*, 35(11), 2829–2841.

Cai, F., Howorka, E., & Wongswan, J. (2008). Informational linkages across trading regions: Evidence from foreign exchange markets. *Journal of International Money and Finance*, 27(8), 1215–1243.

Caporale, G. M., Gil-Alana, L., & Plastun, A. (2018). Persistence in the cryptocurrency market. *Research in International Business and Finance*.

Caporale, G. M., Kang, W.-Y., Spagnolo, F., & Spagnolo, N. (2019). Non-linearities, cyber attacks and cryptocurrencies. *Finance Research Letters*, 101297. Retrieved from <http://www.sciencedirect.com/science/article/pii/S1544612319309377> doi: <https://doi.org/10.1016/j.frl.2019.09.012>

Chaim, P., & Laurini, M. P. (2018). Volatility and return jumps in bitcoin. *Economics Letters*, 173, 158 - 163. Retrieved from <http://www.sciencedirect.com/science/article/pii/S0165176518304245> doi: <https://doi.org/10.1016/j.econlet.2018.10.011>

Charfeddine, L., & Guégan, D. (2012). Breaks or long memory behavior: An empirical investigation. *Physica A: Statistical Mechanics and its Applications*, 391(22), 5712–5726.

Charfeddine, L., & Maouchi, Y. (2019). Are shocks on the returns and volatility of cryptocurrencies really persistent? *Finance Research Letters*, 28, 423–430.

Charles, A., & Darné, O. (2018). *Volatility estimation for bitcoin: Replication and extension*. Manuscript.

Cheah, E.-T., & Fry, J. (2015). Speculative bubbles in Bitcoin markets? an empirical investigation into the fundamental value of Bitcoin. *Economics Letters*, 130, 32 - 36.

Cheah, E.-T., Mishra, T., Parhi, M., & Zhang, Z. (2018). Long memory interdependency and inefficiency in bitcoin markets. *Economics Letters*, 167, 18–25.

Chen, & Lin. (2000). Modelling business cycles in taiwan with time-varying markov-switching models. *Academia Economic Papers*, 28(1), 17–42.

Chen, & Tsay, W.-J. (2011). A markov regime-switching arma approach for hedging

stock indices. *Journal of Futures Markets*, 31(2), 165–191.

Cheung, Y.-W., & Ng, L. K. (1996). A causality-in-variance test and its application to financial market prices. *Journal of Econometrics*, 72(1-2), 33–48.

Chou, R. Y., Chou, H., & Liu, N. (2010). Range volatility models and their applications in finance. In *Handbook of quantitative finance and risk management* (pp. 1273–1281). Springer.

Chu, J., Chan, S., Nadarajah, S., & Osterrieder, J. (2017). Garch modelling of cryptocurrencies. *Journal of Risk and Financial Management*, 10(4), 17.

Chuen, D. L. K. (2015). *Handbook of digital currency: Bitcoin, innovation, financial instruments, and big data*. Academic Press.

Chyžhmar, K., Paterylo, I., Alieksieienko, I., & Shevchenko, S. (2019). Problem of protection against cyber crimes in the field of cryptocurrency circulation. *Journal of Legal, Ethical and Regulatory Issues*.

Cioczek-Georges, R., & Mandelbrot, B. B. (1995). A class of micropulses and antipersistent fractional brownian motion. *Stochastic processes and their applications*, 60(1), 1–18.

Claessens, S., & Forbes, K. (2013). *International financial contagion*. Springer Science & Business Media.

Claeys, P., & Vašíček, B. (2014). Measuring bilateral spillover and testing contagion on sovereign bond markets in europe. *Journal of Banking & Finance*, 46, 151–165.

Cochrane, J. H. (2005). Time series for macroeconomics and finance. *Manuscript, University of Chicago*.

Coli, M., Fontanella, L., & Granturco, M. (2005). Parametric estimation for arfima models via spectral methods. *Statistical Methods and Applications*, 14(1), 11–27.

Comte, F., & Renault, E. (1998). Long memory in continuous-time stochastic volatility models. *Mathematical finance*, 8(4), 291–323.

Conti, M., Kumar, E. S., Lal, C., & Ruj, S. (2018). A survey on security and privacy issues of bitcoin. *IEEE Communications Surveys & Tutorials*, 20(4), 3416–3452.

Corbet, S., Cumming, D. J., Lucey, B. M., Peat, M., & Vigne, S. A. (2020). The destabilising effects of cryptocurrency cybercriminality. *Economics Letters*, 191, 108741.

Corbet, S., Lucey, B., Urquhart, A., & Yarovaya, L. (2019). Cryptocurrencies as a financial asset: A systematic analysis. *International Review of Financial Analysis*, 62, 182–199.

Corbet, S., Meegan, A., Larkin, C., Lucey, B., & Yarovaya, L. (2018). Exploring the dynamic relationships between cryptocurrencies and other financial assets. *Economics Letters*, 165, 28–34.

Cox, D. R. (1961). Prediction by exponentially weighted moving averages and related methods. *Journal of the Royal Statistical Society. Series B (Methodological)*, 414–422.

Crato, N., & Rothman, P. (1994). A reappraisal of parity reversion for uk real exchange rates. *Applied Economics Letters*, 1(9), 139–141.

Dacorogna, M. M., Müller, U. A., Nagler, R. J., Olsen, R. B., & Pictet, O. V. (1993). A geographical model for the daily and weekly seasonal volatility in the foreign exchange market. *Journal of International Money and Finance*, 12(4), 413–438.

Damianov, D. S., & Elsayed, A. H. (2020). Does bitcoin add value to global industry portfolios? *Economics Letters*, 108935.

Dickey, D. A., & Fuller, W. A. (1979). Distribution of the estimators for autoregressive time series with a unit root. *Journal of the American Statistical Association*, 74(366), 427–431.

Diebold, & Inoue, A. (2001). Long memory and regime switching. *Journal of econometrics*, 105(1), 131–159.

Diebold, & Yilmaz, K. (2009). Measuring financial asset return and volatility spillovers, with application to global equity markets. *The Economic Journal*, 119(534), 158–171.

Diebold, & Yilmaz, K. (2012). Better to give than to receive: Predictive directional measurement of volatility spillovers. *International Journal of Forecasting*, 28(1), 57 - 66. (Special Section 1: The Predictability of Financial Markets Special Section 2: Credit Risk Modelling and Forecasting)

Diebold, F., & Rudebusch, G. (1990). A nonparametric investigation of duration dependence in the american business cycle. *Journal of political Economy*, 98(3), 596–616.

Diebold, F., & Yilmaz, K. (2014). On the network topology of variance decompositions: Measuring the connectedness of financial firms. *Journal of Econometrics*, 182(1), 119–134.

Diebold, F. X., Husted, S., & Rush, M. (1991). Real exchange rates under the gold standard. *Journal of Political Economy*, 99(6), 1252–1271.

Diebold, F. X., Lee, J.-H., & Weinbach, G. C. (1994). Regime switching with time-varying transition probabilities. *Business Cycles: Durations, Dynamics, and Forecasting*, 1, 144–165.

Diebold, F. X., Rudebusch, G., & Sichel, D. (1993). Further evidence on business-cycle duration dependence. In *Business cycles, indicators and forecasting* (pp. 255–284). University of Chicago Press.

Dwyer, G. P. (2015). The economics of bitcoin and similar private digital currencies. *Journal of Financial Stability*, 17, 81–91.

Dyhrberg, A. H. (2016). Bitcoin, gold and the dollar—a garch volatility analysis. *Finance Research Letters*, 16, 85–92.

Enders, W. (2008). *Applied econometric time series*. John Wiley & Sons.

Engle. (1982). Autoregressive conditional heteroscedasticity with estimates of the variance of united kingdom inflation. *Econometrica: Journal of the Econometric Society*, 987–1007.

Engle, Ito, T., & Lin, W.-L. (1990). Meteor showers or heat waves? heteroskedastic intra-daily volatility in the foreign exchange market. *Econometrica*, 58(3), 525-42.

Engle, & Kroner, K. F. (1995). Multivariate simultaneous generalized arch. *Econometric theory*, 11(1), 122–150.

Engle, & Susmel, R. (1993). Common volatility in international equity markets. *Journal of Business & Economic Statistics*, 11(2), 167–176.

Engle, R. F., & Gau, Y.-F. (1997). *Conditional volatility of exchange rates under a target zone*. Graduate School of International Relations and Pacific Studies.

Fama, E. F. (1970). Efficient capital markets: A review of theory and empirical work. *The journal of Finance*, 25(2), 383–417.

Fama, E. F. (1976). Efficient capital markets: reply. *The Journal of Finance*, 31(1), 143–145.

Fama, E. F. (1991). Efficient capital markets: II. *The journal of finance*, 46(5), 1575–1617.

Farmer, J. D., Gerig, A., Lillo, F., & Mike, S. (2006). Market efficiency and the long-memory of supply and demand: is price impact variable and permanent or fixed and temporary? *Quantitative finance*, 6(02), 107–112.

Fernández-Rodríguez, F., Gómez-Puig, M., & Sosvilla-Rivero, S. (2016). Using connectedness analysis to assess financial stress transmission in EMU sovereign bond market volatility. *Journal of International Financial Markets, Institutions and Money*, 43, 126 - 145.

Fiess, N., & Shankar, R. (2009). Determinants of exchange rate regime switching. *Journal of International Money and Finance*, 28(1), 68–98.

Fleming, M. J., & Lopez, J. A. (1999). Heat waves, meteor showers, and trading volume: an analysis of volatility spillovers in the us treasury market. federal reserve bank of new york staff reports. *Federal Reserve Bank of New York Staff Reports*.

Fofana, S., Diop, A., & Hili, O. (2014). Nonstationarity and long memory: Regime switching arfima-garch model. *Middle East Journal of Scientific Research*, 22(2), 180–192.

Ford, A. (1969). British economic fluctuations, 1870-1914 1. *The Manchester School*, 37(2), 99–130.

Ford, A. (1981). The trade cycle in britain 1860-1914. *The economic history of Britain since*, 2, 27-49.

Frickey, E. (1947). Production in the usa, 1860–1914. *Harvard University Press*.

Gabriel, V. J., & Martins, L. F. (2004). On the forecasting ability of arfima models when infrequent breaks occur. *The Econometrics Journal*, 7(2), 455–475.

Gandal, N., Hamrick, J., Moore, T., & Oberman, T. (2018). Price manipulation in the Bitcoin ecosystem. *Journal of Monetary Economics*.

Garcia, R. (1998). Asymptotic null distribution of the likelihood ratio test in markov switching models. *International Economic Review*, 763–788.

Garcia, R., & Perron, P. (1996). An analysis of the real interest rate under regime shifts. *The Review of Economics and Statistics*, 78(1), 111–125. Retrieved from <http://www.jstor.org/stable/2109851>

Garman, M. B., & Klass, M. J. (1980). On the estimation of security price volatilities from historical data. *Journal of business*, 67–78.

Ghimire, S., & Selvaraj, H. (2018). A survey on bitcoin cryptocurrency and its mining. In *2018 26th international conference on systems engineering (icseng)* (pp. 1–6).

Gillaizeau, M., Jayasekera, R., Maaitah, A., Mishra, T., Parhi, M., & Volokitina, E. (2019). Giver and the receiver: Understanding spillover effects and predictive power in cross-market bitcoin prices. *International Review of Financial Analysis*.

Glosten, L. R., Jagannathan, R., & Runkle, D. E. (1993). On the relation between the expected value and the volatility of the nominal excess return on stocks. *The journal of finance*, 48(5), 1779–1801.

Goldfeld, S. M., & Quandt, R. E. (1973). A markov model for switching regressions. *Journal of econometrics*, 1(1), 3–15.

Granger, C. W. (1980). Long memory relationships and the aggregation of dynamic models. *Journal of econometrics*, 14(2), 227–238.

Granger, C. W., & Ding, Z. (1996). Varieties of long memory models. *Journal of econometrics*, 73(1), 61–77.

Granger, C. W., & Hyung, N. (2004). Occasional structural breaks and long memory with an application to the s&p 500 absolute stock returns. *Journal of empirical finance*, 11(3), 399–421.

Granger, C. W., & Joyeux, R. (1980). An introduction to long-memory time series models and fractional differencing. *Journal of time series analysis*, 1(1), 15–29.

Gray, S. F. (1996). Modeling the conditional distribution of interest rates as a regime-switching process. *Journal of Financial Economics*, 42(1), 27–62.

Haldrup, N., Nielsen, F. S., & Nielsen, M. Ø. (2010). A vector autoregressive model for electricity prices subject to long memory and regime switching. *Energy Economics*, 32(5), 1044–1058.

Haldrup, N., & Nielsen, M. Ø. (2006). A regime switching long memory model for electricity prices. *Journal of econometrics*, 135(1-2), 349–376.

Hamao, Y., Masulis, R. W., & Ng, V. (1991). The effects of the 1987 stock crash on international financial integration.

Hamilton, J. D. (1989). A new approach to the economic analysis of nonstationary time series and the business cycle. *Econometrica: Journal of the Econometric Society*, 357–384.

Hamilton, J. D. (1994). *Time series analysis* (Vol. 2). Princeton university press Princeton, NJ.

Hamilton, J. D., & Raj, B. (2013). *Advances in markov-switching models: applications in business cycle research and finance*. Springer Science & Business Media.

Hammoudeh, S., & Li, H. (2008). Sudden changes in volatility in emerging markets: the case of gulf arab stock markets. *International Review of Financial Analysis*, 17(1), 47–63.

Hansen, B. E. (1990). Lagrange multiplier tests for parameter instability in non-linear

models. *University of Rochester*.

Hansen, B. E. (1992a). The likelihood ratio test under nonstandard conditions: testing the markov switching model of gnp. *Journal of applied Econometrics*, 7(S1), S61–S82.

Hansen, B. E. (1992b). Testing for parameter instability in linear models. *Journal of policy Modeling*, 14(4), 517–533.

Hansen, B. E. (1996). Erratum: The likelihood ratio test under nonstandard conditions: Testing the markov switching model of gnp. *Journal of Applied econometrics*, 195–198.

Hansen, B. E. (2001). The new econometrics of structural change: dating breaks in us labour productivity. *Journal of Economic perspectives*, 15(4), 117–128.

Hassan, Nassir, & Mohamad. (2006). The heat waves or meteor showers hypothesis: Test on selected asian emerging and developed stock markets. *Investment Management and Financial Innovations*, 3(1).

Hauser, M. A., Pötscher, B. M., & Reschenhofer, E. (1999). Measuring persistence in aggregate output: Arma models, fractionally integrated arma models and nonparametric procedures. *Empirical economics*, 24(2), 243–269.

Hidalgo, J., & Robinson, P. M. (1996). Testing for structural change in a long-memory environment. *Journal of Econometrics*, 70(1), 159–174.

Hodrick, R. J., & Prescott, E. C. (1997). Postwar us business cycles: an empirical investigation. *Journal of Money, credit, and Banking*, 1–16.

Hoffman, W. G. (1955). British industry, 1700-1950, trans. *W. O. Henderson and WH Chaloner* (New York, 1955), table facing, 330.

Hogan Jr, K. C., & Melvin, M. T. (1994). Sources of meteor showers and heat waves in the foreign exchange market. *Journal of International Economics*, 37(3-4), 239–247.

Holt, C. C. (2004). Forecasting seasonals and trends by exponentially weighted moving averages. *International journal of forecasting*, 20(1), 5–10.

Hong, Y. (2001). A test for volatility spillover with application to exchange rates. *Journal of Econometrics*, 103(1), 183 - 224. Retrieved from <http://www.sciencedirect.com/science/article/pii/S0304407601000434> (Studies in estimation and testing) doi: [https://doi.org/10.1016/S0304-4076\(01\)00043-4](https://doi.org/10.1016/S0304-4076(01)00043-4)

Hosking, J. R. (1981). Fractional differencing. *Biometrika*, 68(1), 165–176.

Hsieh, D. A. (1991). Chaos and nonlinear dynamics: application to financial markets. *The journal of finance*, 46(5), 1839–1877.

Hsieh, D. A. (1993). Implications of nonlinear dynamics for financial risk management. *Journal of Financial and quantitative Analysis*, 28(1), 41–64.

Hsieh, D. A. (1995). Nonlinear dynamics in financial markets: evidence and implications. *Financial Analysts Journal*, 51(4), 55–62.

Huang, B.-N., & Yang, C. W. (2002). Volatility of changes in g-5 exchange rates and its market transmission mechanism. *International Journal of Finance & Economics*, 7(1), 37–50.

Inagaki, K. (2007). Testing for volatility spillover between the british pound and

the euro. *Research in International Business and Finance*, 21(2), 161-174. Retrieved from <https://EconPapers.repec.org/RePEc:eee:riibaf:v:21:y:2007:i:2:p:161-174>

Ito, T., Engle, R. F., & Lin, W.-L. (1992). Where does the meteor shower come from?: The role of stochastic policy coordination. *Journal of International Economics*, 32(3-4), 221–240.

Ito, T., & Roley, V. V. (1987). News from the us and japan: which moves the yen/dollar exchange rate? *Journal of Monetary Economics*, 19(2), 255–277.

Jeanne, O., & Masson, P. (2000). Currency crises, sunspots and markov-switching regimes. *Journal of international economics*, 50(2), 327–350.

Jiang, Y., Nie, H., & Ruan, W. (2018). Time-varying long-term memory in bitcoin market. *Finance Research Letters*, 25, 280–284.

Johansen, S., & Nielsen, M. Ø. (2012). Likelihood inference for a fractionally cointegrated vector autoregressive model. *Econometrica*, 80(6), 2667–2732.

Katsiampa, P. (2017). Volatility estimation for bitcoin: A comparison of garch models. *Economics Letters*, 158, 3–6.

Kavli, H., & Kotzé, K. (2014). Spillovers in exchange rates and the effects of global shocks on emerging market currencies. *South African Journal of Economics*, 82(2), 209–238.

Kearney, C., & Patton, A. J. (2000). Multivariate garch modeling of exchange rate volatility transmission in the european monetary system. *Financial Review*, 35(1), 29–48.

Khuntia, S., & Pattanayak, J. (2018). Adaptive market hypothesis and evolving predictability of bitcoin. *Economics Letters*, 167, 26–28.

Kilian, L. (1999). Finite-sample properties of percentile and percentile-t bootstrap confidence intervals for impulse responses. *Review of Economics and Statistics*, 81(4), 652–660.

Kim, C.-J. (1994). Dynamic linear models with markov-switching. *Journal of Econometrics*, 60(1-2), 1–22.

Kim, C.-J., & Nelson, C. R. (1998). Business cycle turning points, a new coincident index, and tests of duration dependence based on a dynamic factor model with regime switching. *Review of Economics and Statistics*, 80(2), 188–201.

Kim, C.-J., & Nelson, C. R. (1999). State-space models with regime switching: classical and gibbs-sampling approaches with applications. *MIT Press Books*, 1.

King, M. A., & Wadhwani, S. (1990). Transmission of volatility between stock markets. *The Review of Financial Studies*, 3(1), 5–33.

Kirikos, D. G. (2000). Forecasting exchange rates out of sample: random walk vs markov switching regimes. *Applied Economics Letters*, 7(2), 133–136.

Kitamura, Y. (2010). Testing for intraday interdependence and volatility spillover among the euro, the pound and the swiss franc markets. *Research in International Business and Finance*, 24(2), 158-171. Retrieved from <https://EconPapers.repec.org/>

RePEc:eee:riibaf:v:24:y:2010:i:2:p:158-171

Klößner, S., & Wagner, S. (2014). Exploring all var orderings for calculating spillovers? yes, we can!—a note on diebold and yilmaz (2009). *Journal of Applied Econometrics*, 29(1), 172–179.

Kogias, E. K., Jovanovic, P., Gailly, N., Khoffi, I., Gasser, L., & Ford, B. (2016). Enhancing bitcoin security and performance with strong consistency via collective signing. In *25th {USENIX} security symposium ({USENIX} security 16)* (pp. 279–296).

Koop, G., & Korobilis, D. (2016). Model uncertainty in panel vector autoregressive models. *European Economic Review*, 81, 115–131.

Koop, G., Pesaran, M., & Potter, S. M. (1996). Impulse response analysis in nonlinear multivariate models. *Journal of Econometrics*, 74(1), 119 - 147.

Koutmos, D. (2018). Return and volatility spillovers among cryptocurrencies. *Economics Letters*, 173, 122–127.

Kuan, C.-M. (2002). Lecture on the markov switching model. *Institute of Economics Academia Sinica*, 1–30.

Kunsch, H. R. (1987). Statistical aspects of self-similar processes. In *Proceedings of the first world congress of the bernoulli society, 1987* (Vol. 1, pp. 67–74).

Kurka, J. (2017, December). *Do Cryptocurrencies and Traditional Asset Classes Influence Each Other?* (Working Papers IES No. 2017/29). Charles University Prague, Faculty of Social Sciences, Institute of Economic Studies. Retrieved from [https://ideas.repec.org/p/fau/wpaper/wp2017\\_29.html](https://ideas.repec.org/p/fau/wpaper/wp2017_29.html)

Kwaitkowski, D., Phillips, P. C., Schmidt, P., & Shin, Y. (1992). Testing the null hypothesis of stationarity against the alternative of a unit root. *Journal of econometrics*, 54(1), 159–178.

Kyriazis, N. A. (2019a). A survey on efficiency and profitable trading opportunities in cryptocurrency markets. *Journal of Risk and Financial Management*, 12(2), 67.

Kyriazis, N. A. (2019b). A survey on empirical findings about spillovers in cryptocurrency markets. *Journal of Risk and Financial Management*, 12(4), 170.

Lahaye, J., & Neely, C. (2018). The role of jumps in volatility spillovers in foreign exchange markets: meteor shower and heat waves revisited. *Journal of Business & Economic Statistics*(just-accepted), 1–31.

Lam, P.-s. (1990). The hamilton model with a general autoregressive component: estimation and comparison with other models of economic time series: Estimation and comparison with other models of economic time series. *Journal of Monetary Economics*, 26(3), 409–432.

Leser, C. (1961). A simple method of trend construction. *Journal of the Royal Statistical Society. Series B (Methodological)*, 91–107.

Li, Wang, X., & Miao, B. (2010). The dynamic characteristics of real effective exchange rate of rmb and policy inspiration [j]. *Journal of University of Science and Technology of China*, 6, 566–571.

Li, H., & Hong, Y. (2011). Financial volatility forecasting with range-based autoregressive volatility model. *Finance Research Letters*, 8(2), 69–76.

Lin, W.-L., Engle, R. F., & Ito, T. (1994). Do bulls and bears move across borders? international transmission of stock returns and volatility. *Review of Financial Studies*, 7(3), 507–538.

Liow, K. H. (2015). Volatility spillover dynamics and relationship across g7 financial markets. *The North American Journal of Economics and Finance*, 33, 328 - 365. Retrieved from <http://www.sciencedirect.com/science/article/pii/S1062940815000509> doi: <https://doi.org/10.1016/j.najef.2015.06.003>

Liu, K., Chen, Y., & Zhang, X. (2017). An evaluation of arfima (autoregressive fractional integral moving average) programs. *Axioms*, 6(2), 16.

Lobato, I. N., & Savin, N. E. (1998). Real and spurious long-memory properties of stock-market data. *Journal of Business & Economic Statistics*, 16(3), 261–268.

Louzis, D. (2015, December). Measuring spillover effects in Euro area financial markets: a disaggregate approach. *Empirical Economics*, 49(4), 1367-1400. Retrieved from <https://ideas.repec.org/a/spr/empeco/v49y2015i4p1367-1400.html> doi: 10.1007/s00181-010-0384-5

Lucey, B. M., Larkin, C., & O'Connor, F. (2014). Gold markets around the world - who spills over what, to whom, when? *Applied Economics Letters*, 21(13), 887-892.

Maravall, A., & del Río, A. (2007). Temporal aggregation, systematic sampling, and the hodrick–prescott filter. *Computational Statistics & Data Analysis*, 52(2), 975–998.

Marella, V., Lindman, J., Rossi, M., & Tuunainen, V. (2017). Bitcoin: A social movement under attack. *Scandinavian IRIS Association*.

Martens, M., De Pooter, M., & Van Dijk, D. J. (2004). Modeling and forecasting s&p 500 volatility: Long memory, structural breaks and nonlinearity.

McMillan, D. G., & Speight, A. E. (2010). Return and volatility spillovers in three euro exchange rates. *Journal of Economics and Business*, 62(2), 79-93. Retrieved from <https://EconPapers.repec.org/RePEc:eee:jebusi:v:62:y::i:2:p:79-93>

Melvin, M., & Melvin, B. P. (2003). The global transmission of volatility in the foreign exchange market. *Review of Economics and Statistics*, 85(3), 670–679.

Melvin, M., & Yin, X. (2000). Public information arrival, exchange rate volatility, and quote frequency. *The Economic Journal*, 110(465), 644–661.

Mensi, W., Al-Yahyaee, K. H., & Kang, S. H. (2018). Structural breaks and double long memory of cryptocurrency prices: A comparative analysis from bitcoin and ethereum. *Finance Research Letters*.

Mensi, W., Lee, Y.-J., Al-Yahyaee, K. H., Sensoy, A., & Yoon, S.-M. (2019). Intraday downward/upward multifractality and long memory in bitcoin and ethereum markets: An asymmetric multifractal detrended fluctuation analysis. *Finance Research Letters*.

Mills, T. C. (2016). Trends, cycles, and structural breaks in cliometrics. *Handbook of Cliometrics*, 509–534.

Morgan, M. S. (1990). *The history of econometric ideas*. Cambridge University Press.

Mukhopadhyay, U., Skjellum, A., Hambolu, O., Oakley, J., Yu, L., & Brooks, R. (2016). A brief survey of cryptocurrency systems. In *2016 14th annual conference on privacy, security and trust (pst)* (pp. 745–752).

Nakamoto, S. (2008). Bitcoin: A peer-to-peer electronic cash system.

Narayan, P. K., & Popp, S. (2010). A new unit root test with two structural breaks in level and slope at unknown time. *Journal of Applied Statistics*, 37(9), 1425–1438.

Nelson, & Foster. (1994). Asymptotic filtering theory for univariate arch models. *Econometrica*, 62(1), 1–41. Retrieved from <http://www.jstor.org/stable/2951474>

Nikkinen, J., Sahlström, P., & Vähämaa, S. (2006). Implied volatility linkages among major european currencies. *Journal of International Financial Markets, Institutions and Money*, 16(2), 87–103.

Pachal, S., & Ruj, S. (2019). Rational mining of bitcoin. In *2019 11th international conference on communication systems & networks (comsnets)* (pp. 1–8).

Parkinson, M. (1980). The extreme value method for estimating the variance of the rate of return. *The Journal of Business*, 53(1), 61–65.

Patnaik, A. (2013). A study of volatility spillover across select foreign exchange rates in india using dynamic conditional correlations. *Journal of Quantitative Economics*, 11(1&2).

Pesaran, H., & Shin, Y. (1998). Generalized impulse response analysis in linear multivariate models. *Economics Letters*, 58(1), 17 - 29.

Phillips, P. C. B., & Perron, P. (1988). Testing for a unit root in time series regression. *Biometrika*, 75(2), 335–346.

Qu, Z., & Perron, P. (2007). Estimating and testing structural changes in multivariate regressions. *Econometrica*, 75(2), 459–502.

Quandt, R. E. (1972). A new approach to estimating switching regressions. *Journal of the American statistical association*, 67(338), 306–310.

Raggi, D., & Bordignon, S. (2012). Long memory and nonlinearities in realized volatility: a markov switching approach. *Computational Statistics & Data Analysis*, 56(11), 3730–3742.

Ravn, M. O., & Uhlig, H. (2002). On adjusting the hodrick-prescott filter for the frequency of observations. *Review of economics and statistics*, 84(2), 371–376.

Ray, B. K., & Tsay, R. S. (2002). Bayesian methods for change-point detection in long-range dependent processes. *Journal of Time Series Analysis*, 23(6), 687–705.

Reschenhofer, E. (2000). Modification of autoregressive fractionally integrated moving average models for the estimation of persistence. *Journal of Applied Statistics*, 27(1), 113–118.

Reyes, M. G. (2001). Asymmetric volatility spillover in the tokyo stock exchange. *Journal of Economics and Finance*, 25(2), 206–213.

Rogers, L. C. G., & Satchell, S. E. (1991). Estimating variance from high, low and closing prices. *The Annals of Applied Probability*, 504–512.

Schaller, H., & Norden, S. V. (1997). Regime switching in stock market returns. *Applied Financial Economics*, 7(2), 177–191.

Scott, L. O. (1991). Financial market volatility: a survey. *Staff Papers*, 38(3), 582–625.

Shalini, S., & Santhi, H. (2019). A survey on various attacks in bitcoin and cryptocurrency. In *2019 international conference on communication and signal processing (iccs)* (pp. 0220–0224).

Shephard, N. (1994). Partial non-gaussian state space. *Biometrika*, 81(1), 115–131.

Shi, Y. (2015). Can we distinguish regime switching from long memory? a simulation evidence. *Applied Economics Letters*, 22(4), 318–323.

Shi, Y., & Ho, K.-Y. (2015). Long memory and regime switching: A simulation study on the markov regime-switching arfima model. *Journal of Banking & Finance*, 61, S189–S204.

Shimotsu, K. (2010). Exact local whittle estimation of fractional integration with unknown mean and time trend. *Econometric Theory*, 26(2), 501–540.

Shimotsu, K., & Phillips, P. C. (2005). Exact local whittle estimation of fractional integration. *The Annals of Statistics*, 33(4), 1890–1933.

Sims, C. A. (1980). Macroeconomics and reality. *Econometrica: Journal of the Econometric Society*, 1–48.

Sitohang, Y. O., & Darmawan, G. (2017). The accuracy comparison between arfima and singular spectrum analysis for forecasting the sales volume of motorcycle in indonesia. In *Aip conference proceedings* (Vol. 1868, p. 040011).

Soriano, P., & Climent, F. J. (2005). Volatility transmission models: A survey.

Speight, A. E., & McMillan, D. G. (2001). Volatility spillovers in east european black-market exchange rates. *Journal of International Money and Finance*, 20(3), 367–378.

Stock, J. H., & Watson, M. W. (2001). Vector autoregressions. *Journal of Economic perspectives*, 15(4), 101–115.

Subagyo, A., & Sugiarto, T. (2016). Application markov switching regression (ar). *Global Journal of Pure and Applied Mathematics*, 12(3), 2411–2421.

Symitsi, E., & Chalvatzis, K. J. (2018). Return, volatility and shock spillovers of bitcoin with energy and technology companies. *Economics Letters*, 170, 127–130.

Taylor, S. (1986). Modelling financial time series. *John Wiley & Sons*.

Teräsvirta, T. (2009). An introduction to univariate garch models. In *Handbook of financial time series* (pp. 17–42). Springer.

Tsay, W.-J. (2008). Analysing inflation by the arfima model with markov-switching fractional differencing parameter. *The Institute of Economics*.

Tsay, W.-J., & Härdle, W. K. (2009). A generalized arfima process with markov-switching fractional differencing parameter. *Journal of Statistical Computation and Simulation*, 79(5), 731–745.

Urquhart, A. (2016). The inefficiency of Bitcoin. *Economics Letters*, 148, 80 - 82.

Urquhart, A., Gebka, B., & Hudson, R. (2015). How exactly do markets adapt? evidence

from the moving average rule in three developed markets. *Journal of International Financial Markets, Institutions and Money*, 38, 127–147.

Urquhart, A., & Zhang, H. (2019). Is bitcoin a hedge or safe haven for currencies? an intraday analysis. *International Review of Financial Analysis*, 63, 49–57.

Vidal-Tomás, D., & Ibañez, A. (2018). Semi-strong efficiency of bitcoin. *Finance Research Letters*, 27, 259 - 265. Retrieved from <http://www.sciencedirect.com/science/article/pii/S1544612318300461> doi: <https://doi.org/10.1016/j.frl.2018.03.013>

Wang, S., Zhao, Q., & Li, Y. (2019). Testing for no-cointegration under time-varying variance. *Economics Letters*, 182, 45–49.

Wei, W. C. (2018). Liquidity and market efficiency in cryptocurrencies. *Economics Letters*, 168, 21 - 24. Retrieved from <http://www.sciencedirect.com/science/article/pii/S0165176518301320> doi: <https://doi.org/10.1016/j.econlet.2018.04.003>

Wiggins, J. B. (1991). Empirical tests of the bias and efficiency of the extreme-value variance estimator for common stocks. *Journal of Business*, 417–432.

Wiggins, J. B. (1992). Estimating the volatility of s&p 500 futures prices using the extreme-value method. *Journal of Futures Markets*, 12(3), 265–273.

Xin, Y. (2013). Ms-ar model based dynamic identification of rmb appreciation pressure. In *Management science and engineering (icmse), 2013 international conference on* (pp. 1633–1638).

Yang, D., & Zhang, Q. (2000). Drift-independent volatility estimation based on high, low, open, and close prices. *The Journal of Business*, 73(3), 477–492.

Yarovaya, L., Brzeszczyński, J., & Lau, C. K. M. (2016). Intra- and inter-regional return and volatility spillovers across emerging and developed markets: Evidence from stock indices and stock index futures. *International Review of Financial Analysis*, 43, 96 - 114.

Zhang, J., Fan, M., & Yu, X. (2008). On spillover effect of rmb exchange rate volatility. In *Business and information management, 2008. isbim'08. international seminar on* (Vol. 2, pp. 441–444).

Zięba, D., Kokoszczyński, R., & Śledziewska, K. (2019). Shock transmission in the cryptocurrency market. is bitcoin the most influential? *International Review of Financial Analysis*, 64, 102–125.